

1984

Oxidative Addition To Platinum(ii) Complexes

Patrick Kevin Monaghan

Follow this and additional works at: <https://ir.lib.uwo.ca/digitizedtheses>

Recommended Citation

Monaghan, Patrick Kevin, "Oxidative Addition To Platinum(ii) Complexes" (1984). *Digitized Theses*. 1391.
<https://ir.lib.uwo.ca/digitizedtheses/1391>

This Dissertation is brought to you for free and open access by the Digitized Special Collections at Scholarship@Western. It has been accepted for inclusion in Digitized Theses by an authorized administrator of Scholarship@Western. For more information, please contact tadam@uwo.ca, wlsadmin@uwo.ca.

The author of this thesis has granted The University of Western Ontario a non-exclusive license to reproduce and distribute copies of this thesis to users of Western Libraries. Copyright remains with the author.

Electronic theses and dissertations available in The University of Western Ontario's institutional repository (Scholarship@Western) are solely for the purpose of private study and research. They may not be copied or reproduced, except as permitted by copyright laws, without written authority of the copyright owner. Any commercial use or publication is strictly prohibited.

The original copyright license attesting to these terms and signed by the author of this thesis may be found in the original print version of the thesis, held by Western Libraries.

The thesis approval page signed by the examining committee may also be found in the original print version of the thesis held in Western Libraries.

Please contact Western Libraries for further information:

E-mail: libadmin@uwo.ca

Telephone: (519) 661-2111 Ext. 84796

Web site: <http://www.lib.uwo.ca/>

CANADIAN THESES ON MICROFICHE

I.S.B.N.

THESES CANADIENNES SUR MICROFICHE



National Library of Canada
Collections Development Branch

Canadian Theses on
Microfiche Service

Ottawa, Canada
K1A 0N4

Bibliothèque nationale du Canada
Direction du développement des collections

Service des thèses canadiennes
sur microfiche

NOTICE

The quality of this microfiche is heavily dependent upon the quality of the original thesis submitted for microfilming. Every effort has been made to ensure the highest quality of reproduction possible.

If pages are missing, contact the university which granted the degree.

Some pages may have indistinct print especially if the original pages were typed with a poor typewriter ribbon or if the university sent us a poor photocopy.

Previously copyrighted materials (journal articles, published tests, etc.) are not filmed.

Reproduction in full or in part of this film is governed by the Canadian Copyright Act, R.S.C. 1970, c. C-30. Please read the authorization forms which accompany this thesis.

**THIS DISSERTATION
HAS BEEN MICROFILMED
EXACTLY AS RECEIVED**

AVIS

La qualité de cette microfiche dépend grandement de la qualité de la thèse soumise au microfilmage. Nous avons tout fait pour assurer une qualité supérieure de reproduction.

S'il manque des pages, veuillez communiquer avec l'université qui a conféré le grade.

La qualité d'impression de certaines pages peut laisser à désirer, surtout si les pages originales ont été dactylographiées à l'aide d'un ruban usé ou si l'université nous a fait parvenir une photocopie de mauvaise qualité.

Les documents qui font déjà l'objet d'un droit d'auteur (articles de revue, examens publiés, etc.) ne sont pas microfilmés.

La reproduction, même partielle, de ce microfilm est soumise à la Loi canadienne sur le droit d'auteur, SRC 1970, c. C-30. Veuillez prendre connaissance des formules d'autorisation qui accompagnent cette thèse.

**LA THÈSE A ÉTÉ
MICROFILMÉE TELLE QUE
NOUS L'AVONS REÇUE**

OXIDATIVE ADDITION TO PLATINUM(II) COMPLEXES

by

Patrick Kevin Monaghan

Department of Chemistry

Submitted in partial fulfillment of
the requirements for the degree of
Doctor of Philosophy

Faculty of Graduate Studies
The University of Western Ontario
London, Ontario

©

Patrick Kevin Monaghan 1984

DEDICATION

This thesis is dedicated to my dear, deceased Mother, my Father,
my sister Margaret, and to my brothers.

ABSTRACT

This thesis describes the oxidative addition of alcohols, water and organic halides to dimethyl(2,2-bipyridine)platinum(II) (complex (I)) and to dimethyl(1,10-phenanthroline)platinum(II) (complex (II)). The work has involved characterising the reaction products and investigating the mechanism of oxidative addition. Up to now very little mechanistic work has been done for oxidative addition at platinum(II) centres.

Complexes (I) and (II) react with methanol, ethanol and isopropanol to produce the first series of platinum(IV) alkoxides of general formula $[\text{PtMe}_2(\text{OR})(\overline{\text{N N}}\text{H}_2\text{O})^+][\text{OH}]^-$ ($\overline{\text{N N}}$ = bipy or phen; R = Me, Et, ^iPr). Characterisation was achieved by ^1H nmr, ^{13}C nmr and elemental analysis. In an analogous reaction with water the product was a platinum(IV) hydroxo complex.

Primary organic halides reacted cleanly with complex (II) to produce complexes of general formula $[\text{PtXMe}_2(\text{R})(\text{phen})]$ ($\text{X} = \text{I}$ or Br ; R = Me, Et, ^nPr , ^nBu). The reactions proceed via an $\text{S}_{\text{N}}2$ mechanism.

The reaction of complex (II) with methylene dihalides is believed to proceed via the intermediacy of free-radicals. The reaction of CH_2X_2 ($\text{X} = \text{Cl}$, Br or I) with (II) produced a mixture of *cis*- and *trans*-isomers of general formula $[\text{PtXMe}_2(\text{CH}_2\text{X})(\text{phen})]$. Complex (II) reacted with CH_2ClI producing a mixture of platinum(IV) complexes, which involved halogen scrambling.

The reaction of $\text{X}(\text{CH}_2)_2\text{X}$ ($\text{X} = \text{I}$ or Br) with (II) is thought to proceed via competing radical chain and radical non-chain mechanisms.

The novel binuclear complexes $[\text{Pt}_2\text{X}_2\text{Me}_4\{(\text{CH}_2)_2\}(\text{phen})_2]$ were isolated from these reactions.

The reaction of (II) with an excess of the α,ω -diiodoalkanes $\text{I}(\text{CH}_2)_n\text{I}$ ($n = 3-5$) produced mononuclear complexes of general formula $[\text{PtIME}_2\{(\text{CH}_2)_n\text{I}\}(\text{phen})]$. The reaction proceeds *via* an $\text{S}_{\text{N}}2$ mechanism; These mononuclear complexes reacted further with (II), also *via* an $\text{S}_{\text{N}}2$ mechanism to produce the binuclear bridging polymethylene complexes, $[\text{Pt}_2\text{I}_2\text{Me}_4\{(\text{CH}_2)_n\}(\text{phen})_2]$. The rate-constants for these reactions could be measured and indicate a neighbouring atom effect for the reaction of the complexes, $[\text{PtIME}_2\{(\text{CH}_2)_n\text{I}\}(\text{phen})]$, with (II). In deoxygenated solvent isopropyl iodide reacted with (II) to form $[\text{PtIME}_2(\text{}^i\text{Pr})(\text{phen})]$. However, in the presence of dioxygen the major product was $[\text{PtIME}_2(\text{}^i\text{PrOO})(\text{phen})]$. This is the first platinum(IV)peroxo complex to be isolated and a single crystal x-ray structure was performed for this complex. The photoinitiated reaction of isopropyl iodide with (II) is believed to proceed *via* a free-radical chain mechanism. *tert*-Butyl iodide gave similar results in its reaction with (II) in oxygenated solvent.

Complex (II) reacts with $\text{}^i\text{PrI}$ or $\text{}^t\text{BuI}$, in the presence of the α,β -unsaturated olefins, CH_2CHX , ($\text{X} = \text{CN}, \text{CHO}, \text{COMe}$) to produce complexes of general formula $[\text{PtIME}_2(\text{CHXCH}_2\text{R})(\text{phen})]$ ($\text{R} = \text{}^i\text{Pr}; \text{}^t\text{Bu}$). This reaction proceeds *via* a free-radical chain mechanism and can be used to measure the rate constant for the attack of isopropyl radicals at platinum in (II).

The reaction of (II) with isopropyl bromide occurs *via* an $\text{S}_{\text{N}}2$ mechanism, to produce $[\text{PtBrMe}_2(\text{}^i\text{Pr})(\text{phen})]$.

This thesis presents data for the proposed mechanisms of oxidative addition, and compares and contrasts the mechanism of oxidative addition of organic halides to a platinum(II) centre.

"Just like that!"

Tommy Cooper (d. 1984)

ACKNOWLEDGEMENTS

I would like to express my sincere thanks to Dr. Richard J. Puddephatt for the excellent guidance and supervision he has given me during my research. I also wish to thank him and his wife for their hospitality on my arrival in Canada.

Special thanks are due to my typist, Anne Donovan, and to Anita Elworthy who prepared the figures in this thesis. Both have done excellent work and shown great patience towards me.

I would like to acknowledge all the secretaries and technical staff for their help and friendliness during my stay at Western. Special thanks must be given to Susan Wilson and Heather Schroeder for the proton nmr service they have given me.

Thanks are also given for the assistance from the faculty in the Chemistry Department and for the friendship of the other graduate students.

Finally I wish to thank Anne for her patience and kindness towards me over the past three years.

TABLE OF CONTENTS

	Page
CERTIFICATE OF EXAMINATION	ii
ABSTRACT	iv
ACKNOWLEDGEMENTS	vii
TABLE OF CONTENTS	viii
LIST OF TABLES	xvi
LIST OF FIGURES	xviii
CHAPTER 1 - INTRODUCTION	1
1. Historical Background to Organotransition-Metal Chemistry ...	1
2. Chemistry of Platinum	2
2.1 Oxidation States of Platinum	2
2.1.1 Platinum(0)	4
2.1.2 Platinum(I)	4
2.1.3 Platinum(II)	5
2.1.4 Platinum(III)	6
2.1.5 Platinum(IV)	6
2.1.6 Platinum(V)	7
2.1.7 Platinum(VI)	7
2.2 Platinum Compounds Containing Platinum-Carbon σ -Bonds ..	7
2.2.1 Platinum(II)-Carbon σ -Bonded Complexes	7
2.2.1.1 Preparation of Platinum(II)-Carbon	
σ -Bonded Complexes	8
2.2.1.2 Bonding in Platinum(II) Alkyl and Aryl	
Complexes	9
2.2.1.3 Stability of Platinum(II)-Carbon	
σ -Bonds	9
2.2.1.4 Chemical Reactions of Alkyl Complexes ..	10
2.2.2 Platinum(IV) Alkyl Complexes	11
2.2.2.1 Preparation of Platinum(IV) Alkyl	
Complexes	11
2.2.2.2 Structure of Platinum(IV) Alkyl	
Complexes	12
2.2.2.3 Reactions of Platinum(IV) Alkyl	
Complexes	12
3. Oxidative Addition	13
3.1 Mechanism of Oxidative Addition	14
3.2 Oxidative Addition Reactions of Platinum Complexes	16
References	19
CHAPTER 2 - OXIDATIVE ADDITION OF WATER AND ALCOHOLS TO DIMETHYL- PLATINUM(II) COMPLEXES	22
1. Introduction	22
2. Literature Survey	23
2.1 Survey of Known Platinum Alkoxides and Hydroxides	23

	Page
2.1.1 Alkoxides	23
2.1.2 Alcohols and Alkoxides in Synthetic and Catalytic Systems	27
2.2 Review of Platinum Hydroxides and Their Chemistry	29
2.2.1 Hydroxides	29
2.2.2 Chemistry of Platinum Hydroxides	32
2.3 Results and Discussion	33
2.3.1 Reactions with Alcohols	33
2.3.2 Rates of Reactions with Alcohols	46
2.3.3 Reactions with Water	49
2.3.4 Conclusions	50
References	52
CHAPTER 3 - OXIDATIVE ADDITION OF PRIMARY ORGANIC MONOHALIDES TO A DIMETHYLPLATINUM(II) COMPLEX	57
1. Introduction	57
2. Literature Survey	57
3. Results and Discussion	63
3.1 Introduction	63
3.2 Elemental Analysis	64
3.3 ¹ H NMR Data	64
3.4 Kinetic Studies	66
3.5 Reaction of Cyclopropylcarbinyl Bromide with (II)	70
3.6 Reaction of Methyl and Ethyl Iodide with a Mixture of (II) and CH ₂ = CHX	72
3.7 Conclusion	72
CHAPTER 4 - FORMATION OF MONONUCLEAR AND BINUCLEAR PLATINUM(IV) COMPLEXES USING METHYLENE HALIDES AND α,ω-DIHALOGENO- ALKANES AS REAGENTS	78
1. Introduction	78
2. Literature Precedents	78
2.1 Mononuclear Complexes	79
2.2 Binuclear Complexes	83
3. Results and Discussion	88
3.1 Reaction of [PtMe ₂ (phen)] with Methylene Dihalides	88
3.1.1 Preparation and Characterisation	88
3.1.2 Kinetic and Mechanistic Studies	95
3.1.3 Conclusions	100
3.2 Reaction of [PtMe ₂ (phen)] with I(CH ₂) _n I to Form Iodoalkylplatinum(IV) Complexes	104
3.2.1 Preparation and Characterisation	104
3.2.2 Kinetic and Mechanistic Studies	109
3.2.3 Conclusions	115
3.3 Reaction between [PtMe ₂ (phen)] and X(CH ₂) ₂ X	117
3.3.1 Analysis of the Gaseous Product from the Reaction of I(CH ₂) ₂ I with (II)	118
3.3.2 Pyrolysis of [Pt ₂ I ₂ Me ₄ {(CH ₂) ₂ }(phen)]	118
3.3.3 Kinetic and Mechanistic Studies for the Reaction between (II) and I(CH ₂) ₂ I	119
3.3.4 Mass Balance Experiment	123
3.3.5 Reaction of I(CH ₂) ₂ I with (II) in the Presence of Acrylonitrile	126
3.3.6 Conclusion	126

	Page
3.4 Formation of Bridging Polymethylene Platinum(IV) Complexes	127
3.4.1 Preparation and Characterisation	127
3.4.2 Pyrolysis of $[Pt_2I_2Me_n\{(CH_2)_n(phen)_2\}]$	132
3.4.3 Determination of the Second-Order Rate Constant for the Formation of the Binuclear Complexes	137
3.4.4 Conclusions	137
3.4.5 Reaction of α,α' -Dibromo-o-xylene with (II)	141
References	145

CHAPTER 5 - OXIDATIVE ADDITION OF SECONDARY AND TERTIARY ORGANIC HALIDES TO A DIMETHYLPLATINUM(II) COMPLEX

1. Introduction	149
2. Literature Survey	149
2.1 Oxygen-Transfer Reactions Using Transition-Metal Complexes	150
2.2 Isolated Transition-Metal Peroxo Complexes	155
3. Results and Discussions	158
3.1 Results from Reaction of 1PrI with (II)	159
3.1.1 Products from the Reaction of (II) with 1PrI	159
3.1.2 Characterisation of Complexes (XVI), (XXX)-(XXXII)	159
3.1.3 X-ray Crystal Structure of $[PtIME_2(^1PrOO)(phen)]$	165
3.1.4 Kinetic and Mechanistic Studies	168
3.1.5 Product Ratios for Different Reaction Conditions, in the Reaction between (II) and 1PrI	176
3.1.6 Conclusions for the Reaction between (II) and 1PrI	176
3.2 Reaction of <i>tert</i> -Butyl Iodide with (II)	180
3.2.1 Products from the Reaction	180
3.2.2 Characterisation of the Products from the Reaction of (II) with tBuI	181
3.2.3 Kinetic and Mechanistic Studies for the Reaction of (II) with tBuI	183
3.3 Reaction of 1PrBr with (II), in Acetone	184
3.3.1 Products from the Reaction of 1PrBr with (II)	184
3.3.2 Effect of Irradiation on the Reaction between 1PrBr and (II)	186
3.3.3 Competition Reactions of $^{10}PrBr$ and 1PrBr with (II)	186
3.3.4 Determination of the Rate Constant for the Reaction of a Mixture of $^{10}PrBr$ and 1PrBr with (II)	187
3.4 Conclusions	191
References	193

CHAPTER 6 - RADICAL TRAPPING BY ALKENES AS A ROUTE TO ORGANO-PLATINUM(IV) COMPLEXES AND AS A TEST OF THE MECHANISM OF OXIDATIVE ADDITION

1. Introduction	196
2. Results for the Reaction of 1PrI with (II) in the Presence of α,β -Unsaturated Olefins	196
2.2 Characterisation of Complexes (XXXV)	198

	Page
2.3 Kinetic Studies for the Reaction of ^1PrI with (II) in the Presence of Acrylonitrile	202
2.4 Product Ratio, (XXXVa) to (XXX), in the Reaction of ^1PrI and (II) in the Presence of Varying Concentrations of Acrylonitrile	204
3. Results for the Reaction of ^tBuI with (II) in the Presence of Alkene	209
3.1 Products from the Reaction	209
3.2 Characterisation of Complexes (XXXVI)	210
3.3 Competition Reaction of ^tBuI and ^1PrI with (II) in the Presence of Acrylonitrile	210
4. General Conclusions for Chapters 5 and 6	212
References	217
 CHAPTER 7 - INSTRUMENTATION AND PREPARATIVE WORK	 218
1. Instrumentation	218
1.1 Vacuum Line	218
1.2 Reaction Vessels	218
1.3 Photolysis	218
1.4 Nuclear Magnetic Resonance Spectroscopy	218
1.5 Gas-Liquid Chromatography	219
1.6 Mass Spectroscopy	219
1.7 Infra-red Spectroscopy	219
1.8 Ultra-violet and Visible Spectroscopy	220
1.9 Quantitative Analysis	220
2. Preparative Work	220
2.1 Preparation of General Compounds	220
2.1.1 $[\text{PtCl}_2(\text{SMe}_2)_2]$	220
2.1.2 $[\text{Pt}_2\text{Me}_4(\mu\text{-SMe}_2)_2]$	221
2.1.3 $[\text{PtMe}_2(\text{bipy})]$	222
2.1.4 $[\text{PtMe}_2(\text{phen})]$	222
2.2 Preparative Work and Experimental Details for Reactions of Chapter 2	222
2.2.1 Preparative Work and Experimental Details for the Work with $[\text{PtMe}_2(\text{bipy})]$	222
2.2.1.1 Drying Methanol and Ethanol	222
2.2.1.2 $[\text{PtMe}_2(\text{OMe})(\text{bipy})(\text{OH}_2)][\text{OH}]$	222
2.2.1.3 $[\text{PtMe}_2(\text{OEt})(\text{bipy})(\text{OH}_2)][\text{OH}] \cdot \text{H}_2\text{O}$	223
2.2.1.4 $[\text{PtMe}_2(\text{OH})(\text{bipy})(\text{OH}_2)][\text{OH}]$	223
2.2.1.5 Reaction of D_2O with $[\text{PtMe}_2(\text{bipy})]$	223
2.2.1.6 $[\text{PtMe}_2(\text{OMe})(\text{bipy})(\text{OH}_2)][\text{PF}_6]$	224
2.2.1.7 $[\text{PtMe}_2(\text{OMe})(\text{bipy})(\text{OH}_2)][\text{ClO}_4] \cdot 2\text{H}_2\text{O}$	224
2.2.1.8 $[\text{PtMe}_2(\text{OMe})(\text{bipy})(\text{OH}_2)][\text{BPh}_4] \cdot \text{H}_2\text{O}$	224
2.2.1.9 $[\text{PtMe}_2(\text{OH})(\text{bipy})(\text{OH}_2)][\text{PF}_6]$	224
2.2.1.10 Attempted Crystallisation	225
2.2.1.11 Detection of CH_4 by Gas Chromatography in the Reaction between $[\text{PtMe}_2(\text{bipy})]$ and MeOH	225
2.2.1.12 Detection of C_2H_6 by Gas Chromatography in the Reaction between $[\text{PtMe}_2(\text{bipy})]$ and EtOH	227
2.2.1.13 Conductivity Measurements for Reaction between $[\text{PtMe}_2(\text{bipy})]$ and Methanol	227

	Page
2.2.2 Preparative Work and Experimental Details for the Work with $[\text{PtMe}_2(\text{phen})]$	228
2.2.2.1 $[\text{PtMe}_2(\text{OMe})(\text{phen})(\text{OH}_2)][\text{OH}]$	228
2.2.2.2 $[\text{PtMe}_2(\text{OEt})(\text{phen})(\text{OH}_2)][\text{OH}] \cdot \text{H}_2\text{O}$	228
2.2.2.3 $[\text{PtMe}_2(\text{O}^i\text{Pr})(\text{phen})(\text{OH}_2)][\text{OH}]$	228
2.2.2.4 Reaction of $t\text{BuOH}$ with $[\text{PtMe}_2(\text{phen})]$	228
2.2.2.5 Reaction of PhCH_2OH with $[\text{PtMe}_2(\text{phen})]$..	229
2.2.2.6 $[\text{PtMe}_2(\text{OH})(\text{phen})(\text{OH}_2)][\text{OH}]$	229
2.2.2.7 $[\text{PtMe}_2(\text{OMe})\text{Cl}(\text{phen})]$	229
2.2.2.8 Gas Chromatography on Gaseous Products of Reaction between MeOH and $[\text{PtMe}_2(\text{phen})]$..	230
2.2.2.9 ^2H NMR of Sample from Reaction between CH_3OD and $[\text{PtMe}_2(\text{phen})]$	230
2.2.2.10 Potentiometric Titration of $[\text{PtMe}_2(\text{OEt})(\text{phen})(\text{OH}_2)][\text{OH}]$ with HCl	230
2.2.2.11 Calculation of the Molar Extinction Coefficient of $[\text{PtMe}_2(\text{phen})]$ in Acetone ..	231
2.2.2.12 Kinetic Measurements for the Reaction between $[\text{PtMe}_2(\text{phen})]$ and MeOH , and EtOH	232
2.2.2.13 Reaction of D_2O with $[\text{PtMe}_2(\text{phen})]$	232
2.3 Preparative Work and Experimental Details for Work in Chapter 3	232
2.3.1 $[\text{PtIme}_2(\text{phen})]$	232
2.3.2 $[\text{PtIme}_2(\text{Et})(\text{phen})]$	233
2.3.3 $[\text{PtBrme}_2(\text{Et})(\text{phen})]$	233
2.3.4 $[\text{PtIme}_2(^n\text{Pr})(\text{phen})]$	233
2.3.5 $[\text{PtBrme}_2(^n\text{Pr})(\text{phen})]$	233
2.3.6 $[\text{PtIme}_2(^n\text{Bu})(\text{phen})]$	234
2.3.7 Preparation of $\text{CH}_2\text{CH}_2\text{CH}-\text{CH}_2\text{Br}$	234
2.3.8 $[\text{PtBrme}_2(\text{CH}_2-\text{CHCH}_2\text{CH}_2)(\text{phen})]$	234
2.3.9 $[\text{PtIme}_2\{\text{CH}_3-(\text{CH}_2)_4\}(\text{phen})]$	234
2.3.10 $[\text{PtI}(\text{Me}_2)\{\text{CH}_3-(\text{CH}_2)_6\}(\text{phen})]$	235
2.3.11 Kinetics for the Reaction of MeI with $[\text{PtMe}_2(\text{phen})]$	235
2.3.12 Kinetics of the Reaction between $[\text{PtMe}_2(\text{phen})]$ and $\text{C}_2\text{H}_5\text{I}$, $\text{C}_3\text{H}_7\text{I}$, $\text{C}_4\text{H}_9\text{I}$, and $\text{C}_5\text{H}_{11}\text{I}$	236
2.4 Preparative Work and Experimental Details for the Work in Chapter 4	236
2.4.1 Simple Preparative Work	236
2.4.1.1 $[\text{PtI}_2\text{Me}_2(\text{phen})]$	236
2.4.1.2 $[\text{PtClIme}_2(\text{CH}_2\text{Cl})(\text{phen})]$	237
2.4.1.3 $[\text{PtClIme}_2(\text{CD}_2\text{Cl})(\text{phen})]$	237
2.4.1.4 $[\text{PtBrme}_2(\text{CH}_2\text{Br})(\text{phen})]$	237
2.4.1.5 Reaction between CH_2ClI and $[\text{PtMe}_2(\text{phen})]$..	237
2.4.1.6 Reaction between $[\text{PtMe}_2(\text{phen})]$ and CH_2ClBr	238
2.4.1.7 Reaction between $\text{I}(\text{CH}_2)_2\text{I}$ and $[\text{PtMe}_2(\text{phen})]$	238
2.4.1.8 Reaction between $\text{Br}(\text{CH}_2)_2\text{Br}$ and $[\text{PtMe}_2(\text{phen})]$	238
2.4.1.9 $[\text{PtIme}_2(\text{CH}_2\text{CH}_2\text{CH}_2\text{I})(\text{phen})]$	239

	Page	
2.4.1.10	[PtMe ₂ {(CH ₂) ₄ I}(phen)]	239
2.4.1.11	[PtMe ₂ {(CH ₂) ₅ I}(phen)]	239
2.4.1.12	[Pt ₂ I ₂ Me ₄ {(CH ₂) ₃ }(phen) ₂]	239
2.4.1.13	[Pt ₂ I ₂ Me ₂ {(CH ₂) ₄ }(phen)]	240
2.4.1.14	[Pt ₂ I ₂ Me ₂ {(CH ₂) ₅ }(phen)]	240
2.4.1.15	[PtBrMe ₂ (C ₆ H ₅ Br)(phen)]	240
2.4.1.16	Reaction of [PtMe ₂ (phen)] with [PtBrMe ₂ (C ₆ H ₅ Br)(phen)]	241
2.4.2	Other Experimental Procedures from Chapter 4	241
2.4.2.1	Reaction of CH ₂ I ₂ with [PtMe ₂ (phen)] followed on the Varian T60 NMR Instrument	241
2.4.2.2	Following the Effect of Galvinoxyl on the Reaction of CH ₂ I ₂ with [PtMe ₂ - (phen)], by Use of NMR	241
2.4.2.3	Reaction of CH ₂ I ₂ with [PtMe ₂ (phen)] in the Presence of Galvinoxyl and Diffuse Light	242
2.4.2.4	[PtMe ₂ (phen)] with Excess CH ₂ I ₂ in the Dark and in Diffuse Daylight	242
2.4.2.5	Reaction between a 1:1 Mole Ratio of CH ₂ I ₂ and [PtMe ₂ (phen)] in the Dark and in Diffuse Daylight	242
2.4.2.6	Reaction between a 1:1 Mole Ratio of CH ₂ I ₂ and [PtMe ₂ (phen)] in CH ₂ Cl ₂	243
2.4.2.7	Isomerisation of <i>cis</i> -[PtIME ₂ (CH ₂ I)- (phen)] in the Presence of LiCl	243
2.4.2.8	Analysis of the Gaseous Products from the Reaction between I(CH ₂) ₂ I and [PtMe ₂ (phen)], Using Gas Chromatography	243
2.4.2.9	Analysis of the Gaseous Products from Pyrolysis of [Pt ₂ I ₂ Me ₄ {(CH ₂) ₂ }(phen) ₂] Using Gas Chromatography	244
2.4.2.10	Analysis of Gaseous Products from Pyrolysis of [Pt ₂ I ₂ Me ₄ {(CH ₂) ₃ }(phen) ₂], Using Mass Spectrometry and Gas Chromatography	245
2.4.2.11	Analysis of the Gaseous Products from Pyrolysis of [Pt ₂ I ₂ Me ₄ {(CH ₂) ₄ }(phen) ₂], Using Mass Spectrometry and Gas Chromatography	245
2.4.2.12	Analysis of the Gaseous Products from Pyrolysis of [Pt ₂ I ₂ Me ₄ {(CH ₂) ₅ }(phen) ₂], Using Mass Spectrometry and Gas Chromatography	245
2.4.2.13	Kinetic Studies of the Reaction between CH ₂ I ₂ and [PtMe ₂ (phen)], Using UV/ Visible Spectroscopy	245
2.4.2.14	Kinetics for the Formation of [PtIME ₂ {(CH ₂) _n I}(phen)]	247
2.4.2.15	Kinetics for the Formation of [Pt ₂ I ₂ Me ₄ {(CH ₂) ₃ }(phen) ₂]	247

	Page
2.4.2.16 Kinetics for the Formation of [Pt ₂ I ₂ Me ₄ {(CH ₂) ₄ }(phen) ₂]	248
2.4.2.17 Kinetics for the Formation of [Pt ₂ I ₂ Me ₄ {(CH ₂) ₅ }(phen) ₂]	248
2.4.2.18 The Effects of Irradiation and Glavinoyl on the Rate of Reaction between I(CH ₂) ₃ I and [PtMe ₂ (phen)]	249
2.4.2.19 UV/Visible Spectrum for Reaction between I(CH ₂) ₅ I and [PtMe ₂ (phen)]	250
2.4.2.20 Reaction between I(CH ₂) ₂ I and [PtMe ₂ (phen)] Followed by UV/Visible Spectroscopy	250
2.4.2.21 Isomerisation of the Products in the Reaction between [PtMe ₂ (phen)] and CH ₂ ClBr	251
2.5 Preparative Work and Experimental Details of the Work in Chapter 5	252
2.5.1 Simple Preparative Work	252
2.5.1.1 [PtIME ₂ (¹ Pr)(phen)]	252
2.5.1.2 [PtIIME ₂ (¹ Pr)(bipy)]	252
2.5.1.3 [PtIME ₂ (¹ PrOO)(bipy)]	253
2.5.1.4 [PtIME ₂ (¹ PrOO)(phen)]	253
2.5.1.5 [PtBrMe ₂ (¹ Pr)(phen)]	255
2.5.1.6 Reaction between [PtIME ₂ (¹ Pr)(phen)] and Ag ₂ O	255
2.5.1.7 Reaction between ^t BuOOH and [PtMe ₂ - (phen)]	256
2.5.1.8 [PtIME ₂ (^t BuOO)(phen)]	256
2.5.2 Experimental Procedures from Chapter 5	258
2.5.2.1 Reaction between ¹ PrI and [PtMe ₂ (phen)] in Acetone-d ₆	258
2.5.2.2 Reaction between [PtMe ₂ (phen)] and ¹ PrI in a Solvent Mixture of Water and Acetone	258
2.5.2.3 Crystallisation of [PtIME ₂ (¹ PrOO)(phen)]	259
2.5.2.4 Pyrolysis of [PtIME ₂ (¹ PrOO)(phen)] and Analysis of Products by Gas Chromatography	259
2.5.2.5 Reaction between ¹ PrI and [PtMe ₂ (phen)] in THF	260
2.5.2.6 Attempt to Observe C.I.D.N.P. Effects in the Reaction between ¹ PrI and [PtMe ₂ - (phen)]	260
2.5.2.7 Investigation of the Product Ratios in the Reaction between ¹ PrI and [PtMe ₂ - (phen)] with Variation of Concentration of Reagents	261
2.5.2.8 Qualitative Test for the Peroxide Linkage in [PtIME ₂ (¹ PrOO)(phen)]	262
2.5.2.9 Reaction between ^t BuI and [PtMe ₂ (phen)] Followed by ¹ H NMR	263
2.5.2.10 Decomposition of [PtIME ₂ (^t BuOO)(phen)] in Solution, Followed by ¹ H NMR	263

	Page
2.5.2.11 Kinetics of the Reaction between ^1PrI and $[\text{PtMe}_2(\text{phen})]$	263
2.5.2.12 Irradiation of the Reaction between $^1\text{PrBr}$ and $[\text{PtMe}_2(\text{phen})]$, Followed by UV/Visible Spectroscopy	265
2.5.2.13 Kinetic Experiments for the Reaction between ^tBuI and $[\text{PtMe}_2(\text{phen})]$	266
2.6 Preparative Work and Experimental Details of the Work in Chapter 6	267
2.6.1 Preparative Work	267
2.6.1.1 $[\text{PtIME}_2\{\text{CH}(\text{CHO})\text{CH}_2^1\text{Pr}\}(\text{phen})]$	267
2.6.1.2 $[\text{PtIME}_2\{\text{CH}(\text{CN})\text{CH}_2^1\text{Pr}\}(\text{phen})]$	267
2.6.1.3 $[\text{PtIME}_2\{\text{CH}(\text{COMe})\text{CH}_2^1\text{Pr}\}(\text{phen})]$	268
2.6.1.4 Reaction between ^1PrI , Styrene and $[\text{PtMe}_2(\text{phen})]$	268
2.6.1.5 Reaction between Methyl Methacrylate ^1PrI and $[\text{PtMe}_2(\text{phen})]$	269
2.6.1.6 $[\text{PtIME}_2\{\text{CH}(\text{CN})\text{CH}_2^t\text{Bu}\}(\text{phen})]$	269
2.6.1.7 $[\text{PtIME}_2\{\text{CH}(\text{CHO})\text{CH}_2^t\text{Bu}\}(\text{phen})]$	269
2.6.1.8 Reaction between $\text{CH}_2\text{CH}(\text{CN})$ and $[\text{PtMe}_2(\text{phen})]$	269
2.6.2 Other Experimental Details of the Work in Chapter 6	270
2.6.2.1 Competition Experiment for the Reaction ^tBuI and ^1PrI , in the Presence of $\text{CH}_2\text{CH}(\text{CN})$, with $[\text{PtMe}_2(\text{phen})]$	270
2.6.2.2 Competition Reaction between $[\text{PtMe}_2(\text{phen})]$ and Methyl Vinyl Ketone for ^1Pr Radicals	270
2.6.2.3 Reaction of CH_2I_2 , and $[\text{PtMe}_2(\text{phen})]$ in the Presence of Acrolein	270
2.6.2.4 Reaction of CH_2I_2 and $[\text{PtMe}_2(\text{phen})]$ in the Presence of Acrylonitrile	271
2.6.2.5 Reaction of $\text{I}(\text{CH}_2)_2\text{I}$ and $[\text{PtMe}_2(\text{phen})]$ in the Presence of Acrylonitrile	271
2.6.2.6 Ratio of the Products Formed by the Reaction of $[\text{PtMe}_2(\text{phen})]$ with ^1PrI and $\text{CH}_2\text{CH}(\text{CN})$	271
2.6.2.7 Kinetics of the Reaction between ^1PrI , $[\text{PtMe}_2(\text{phen})]$ and $\text{CH}_2\text{CH}(\text{CN})$	272
VITA	304

LIST OF TABLES

Table	Description	Page
1.1	Usual Coordination Number and Stereochemistries of Platinum Compounds in Common Oxidation States	3
2.1	Observed First-Order Rate Constants for Reaction of I or II with Alcohols at 21°C	48
3.1	Second-Order Rate Constants for Reactions of (II) in Acetone at 25°C	69
3.2	Average Relative Rates for S _N 2 Displacement of Alkyl Systems	73
4.1	Product Ratio for the Reaction between (II) and CH ₂ I ₂ at 20°C	103
4.2	Observed First-Order Rate Constants (k _{obs}) for Reaction between [PtMe ₂ (phen)] and I(CH ₂) ₂ I in Acetone at 25°C	121
4.3	Second-Order Rate Constants for Reactions of (II) in Acetone at 25°C	139
5.1	Structural Parameters of Complex (XXXI)	167
5.2	Product Ratio for the Reaction of (II) with Isopropyl Iodide, in Acetone	177
6.1	Products Formed from the Reaction of (II) with ¹ PrI and CH ₂ = CHCN in Acetone at 20°C	208
7.1	¹ H NMR Data for Complexes in Chapter 2	274
7.2	¹³ C- ¹ H NMR Data for Complexes in Chapter 4	277
7.3	¹ H NMR Data for Complexes in Chapter 3	279
7.4	¹ H NMR Data for Complexes (XIII)-(XV), (XVII) and (XVIII)	281
7.5	¹ H NMR Data for Complexes (XXIV)-(XXVI)	284
7.6	¹³ C ¹ H NMR Data for [PtIME ₂ {(CH ₂) ₅ I}(phen)]	286

LIST OF TABLES

Table	Description	Page
7.7	$^{13}\text{C}\{^1\text{H}\}$ NMR Data for Binuclear Complexes	287
7.8	^1H NMR Data for Complexes, $[\text{PtXMe}_2\{(\text{CH}_2)\text{X}\}(\text{phen})]$	288
7.9	^1H NMR Data for $[\text{PtIME}_2(^i\text{Pr})(\text{phen})]$	291
7.10	$^{13}\text{C}\{^1\text{H}\}$ NMR Data for $[\text{PtIME}_2\{(\text{CH}_3)_2\text{CH}\}(\text{phen})]$	292
7.11	^1H NMR Data for Alkylperoxoplatinum(IV) Complexes	293
7.12	$^{13}\text{C}\{^1\text{H}\}$ NMR Data for Alkylperoxoplatinum(IV) Complexes	294
7.13	^1H NMR Data for Complexes, $[\text{PtIME}_2(\text{CHXCH}_2\text{R})(\text{phen})]$	295
7.14	$^{13}\text{C}\{^1\text{H}\}$ NMR Data for Complexes, $[\text{PtIME}_2(\text{CHXCH}_2\text{R})(\text{phen})]$	297
7.15	Elemental Analysis for Complexes in Chapter 2	299
7.16	Elemental Analysis for Complexes in Chapter 3	300
7.17	Elemental Analysis for Complexes in Chapter 4	301
7.18	Elemental Analysis for Complexes in Chapter 5 and 6	302
7.19	Mass Spectral Data	303

LIST OF FIGURES

Figure	Description	Page
2.1	^1H NMR Spectrum of $[\text{PtMe}_2(\text{OMe})(\text{bipy})(\text{H}_2\text{O})][\text{OH}]$.	36
2.2	^1H NMR Spectrum of $[\text{PtMe}_2(\text{OEt})(\text{phen})(\text{H}_2\text{O})][\text{OH}]$.	38
2.3	$^{13}\text{C}\{^1\text{H}\}$ NMR Spectrum of $[\text{PtMe}_2(\text{OEt})(\text{phen})(\text{H}_2\text{O})][\text{OH}]$.	39
2.4	UV/Visible Spectra of $[\text{PtMe}_2(\text{bipy})]$.	40
2.5	Molar Conductivity of a Solution of $[\text{PtMe}_2(\text{bipy})]$ in Methanol as a Function of Time.	41
2.6	Plot of pH <i>versus</i> Volume of Acid for the Titration of $[\text{PtMe}_2(\text{OEt})(\text{phen})(\text{H}_2\text{O})][\text{OH}]$ with Aqueous HCl.	43
2.7	Plot of $\text{Log} (A_t - A_\infty)$ <i>versus</i> Time for the Reaction between (II) with Methanol.	47
3.1	^1H NMR Spectrum of $[\text{PtIEtMe}_2(\text{phen})]$.	65
3.2	Plot of $\text{Log} \frac{(A_t - A_\infty)}{(A_0 - A_\infty)}$ <i>versus</i> Time for the Reaction of (II) with EtI.	67
3.3	Plot of k_{obs} <i>versus</i> Concentration of Iodide for the Reaction of EtI and MeI with (II).	68
4.1	^1H NMR Spectrum of <i>cis</i> - and <i>trans</i> - $[\text{PtClMe}_2(\text{CH}_2\text{Cl})(\text{phen})]$.	92
4.2	^1H NMR Spectrum of <i>cis</i> - and <i>trans</i> - $[\text{PtBrMe}_2(\text{CH}_2\text{Cl})(\text{phen})]$.	94
4.3	Decay of the MLCT Band in the UV/Visible Spectrum in the Reaction between (II) and CH_2I_2 .	96
4.4	The Effect of Galvinoxyl on the Rate of Reaction between (II) and CH_2I_2 .	97
4.5	The Effect of Irradiation on the UV/Visible Spectrum of a Reaction Mixture of (II) and CH_2I_2 .	99
4.6	^1H NMR Spectrum of <i>trans</i> - $[\text{PtIme}_2\{(\text{CH}_2)_5\text{I}\}(\text{phen})]$.	106

Figure	Description	Page
4.7	$^{13}\text{C}\{^1\text{H}\}$ NMR Spectrum of $[\text{PtI Me}_2\{(\text{CH}_2)_5\text{I}\}(\text{phen})]$	108
4.8	Change in the UV/Visible Spectrum for the Reaction between (II) and 1,5-diiodopentane	110
4.9	Plot of $\text{Log} \frac{(A_t - A_\infty)}{(A_0 - A_\infty)}$ Versus Time, for the Reaction of (II) with $\text{I}(\text{CH}_2)_4\text{I}$ for Varying Concentrations of $\text{I}(\text{CH}_2)_4\text{I}$	112
4.10	Plot of Observed First-Order Rate Constants (k_{obs}) Versus Concentration of $\text{I}(\text{CH}_2)_4\text{I}$, for the Reaction of (II) with $\text{I}(\text{CH}_2)_4\text{I}$	113
4.11	The Effect of Galvinoxyl and Irradiation on the Reaction between (II) and $\text{I}(\text{CH}_2)_3\text{I}$	114
4.12	The Effect of Galvinoxyl on the Reaction between (II) and $\text{I}(\text{CH}_2)_3\text{I}$	116
4.13	Plot of $\text{Log} (A_t - A_\infty)$ Versus Time for the Reaction of (II) with $\text{I}(\text{CH}_2)_2\text{I}$	120
4.14	A Plot of k_{obs} Versus $[\text{I}(\text{CH}_2)_2\text{I}]$ for the Reaction of (II) with $\text{I}(\text{CH}_2)_2\text{I}$	122
4.15	The Effect of Irradiation on the Reaction between (II) and $\text{I}(\text{CH}_2)_2\text{I}$	124
4.16	The Effect of Galvinoxyl on the Rate of Reaction between (II) and $\text{I}(\text{CH}_2)_2\text{I}$	125
4.17	^1H NMR Spectrum of $[\text{Pt}_2\text{I}_2\text{Me}_4\{(\text{CH}_2)_5\}(\text{phen})_2]$	131
4.18	$^{13}\text{C}\{^1\text{H}\}$ NMR Spectrum of $[\text{Pt}_2\text{I}_2\text{Me}_4\{(\text{CH}_2)_5\}(\text{phen})_2]$	133
4.19	Gas Chromatography Trace of the Gaseous Products from the Pyrolysis of $[\text{Pt}_2\text{I}_2\text{Me}_4\{(\text{CH}_2)_3\}(\text{phen})_2]$	134
4.20	Gas Chromatography Trace of the Gaseous Products from the Pyrolysis of $[\text{Pt}_2\text{I}_2\text{Me}_4\{(\text{CH}_2)_4\}(\text{phen})_2]$	136
4.21	Plot of $\text{Log} \frac{(A_t - A_\infty)}{(A_0 - A_\infty)}$ Versus Time for the Reaction of (II) with $[\text{PtI Me}_2\{(\text{CH}_2)_5\text{I}\}(\text{phen})]$ for Varying Concentrations of (XIX)	138
5.1	^1H NMR Spectrum of $[\text{PtI Me}_2(^1\text{Pr})(\text{phen})]$	160
5.2	^1H NMR Spectrum of $[\text{PtI Me}_2(^1\text{PrOO})(\text{phen})]$	162
5.3	$^{13}\text{C}\{^1\text{H}\}$ NMR Spectrum of $[\text{PtI Me}_2(^1\text{Pr})(\text{phen})]$	163

Figure	Description	Page
5.4	ORTEP Drawing of the Molecule [PtIME ₂ (¹ PrOO)(phen)]	166
5.5	Newman Projection of the Molecule [PtIME ₂ (¹ PrOO)(phen)] Viewed Along the O(1)-Pt Bond	169
5.6	Change in the UV/Visible Spectrum for the Reaction between (II) and ¹ PrI	170
5.7	Plot of Log (A _t -A _∞) Versus Time for the Reaction between (II) and ¹ PrI	172
5.8	Plot of Log (A _t -A _∞) Versus Time for the Reaction between (II) and ¹ PrI	174
5.9	The Effect of Irradiation on the Reaction between (II) and ¹ PrI Followed by Monitoring the Decay of the Band at 473 nm in the UV/Visible Spectrum	175
5.10	¹³ C{ ¹ H} NMR Spectrum of [PtIME ₂ (^t BuOO)(phen)]	182
5.11	The Change in the UV/Visible Spectrum during the Reaction between (II) and ^t BuI	185
5.12	Plot of Relative Concentrations of ⁿ PrBr and ¹ PrBr Versus the Relative Concentration of Products in the Reaction of Mixtures of ⁿ PrBr/ ¹ PrBr with (II)	188
5.13	Plot of the Pseudo-First-Order Rate Constants (k _{obs}) Versus Concentration of ⁿ PrBr for the Reaction of Mixtures of ⁿ PrBr/ ¹ PrBr with (II)	189
6.1	The ¹ H NMR Spectrum of [PtIME ₂ (CHCNCH ₂ ¹ Pr)(phen)]	199
6.2	¹³ C{ ¹ H} NMR Spectrum of [PtIME ₂ (CHCNCH ₂ ¹ Pr)(phen)]	200
6.3	2-D Heteronuclear ¹ H- ¹³ C Chemical Shift Correlated NMR of [PtIME ₂ (CHCNCH ₂ ¹ Pr)(phen)]	201
6.4	Plot of Absorbance Versus Time for the Reaction of (II) with ¹ PrI and CH ₂ CHCN	203
6.5	A Plot of Log (A _t -A _∞) Versus Time for the Reaction of (II) with ¹ PrI and CHCNCH ₂	205
6.6	¹ H NMR Spectrum of [PtIME ₂ (CHCNCH ₂ ^t Bu)(phen)]	211
6.7	High Field Region of the ¹ H NMR Spectrum of the Products from the Reaction of (II) with Mixtures of ¹ PrI/ ^t BuI and CHCNCH ₂	213
7.1	Apparatus for Collecting Gases for Gas Chromatography Analysis	226

KEY ABBREVIATIONS

X	=	Halogen
R	=	Alkyl or Aryl group
Ph	=	Phenyl
Me	=	Methyl
Et	=	Ethyl
ⁱ Pr	=	Isopropyl
^t Bu	=	<i>tert</i> -Butyl
bipy	=	2,2'-bipyridine
phen	=	1,10-phenanthroline
nmr	=	Nuclear Magnetic Resonance
cod	=	cyclooctadiene
$\overline{\text{N N}}$	=	phen or bipy
ppm	=	Parts per million
Hz	=	Hertz
nm	=	Nanometers
L	=	Ligand
A_t	=	Absorbance at time t
A_∞	=	Absorbance at completion of reaction
A_0	=	Absorbance at time = 0
UV	=	Ultra-violet
diphos	=	Chelating diphosphine
diphoe	=	1,2-bis(diethylphosphino)ethane
M	=	Metal Centre
cp	=	Cyclopentadienyl

CHAPTER 1

INTRODUCTION

1. HISTORICAL BACKGROUND TO ORGANOTRANSITION-METAL CHEMISTRY

The first organometallic compound to be synthesised was tetramethyl diarsine in 1760 by Cadet de Gassicourt. The compound was characterised by Bunsen. Much of the early impetus in organometallic chemistry came from the synthesis in 1849 of diethylzinc, by Frankland. A comprehensive review of the development of organometallic chemistry has been presented by Thayer.¹

The first organotransition-metal compound to be synthesised was by Zeise in 1827. The complex was not fully understood or appreciated for more than a century. It is in fact a platinum-olefin complex $K[(C_2H_4)PtCl_3]$, known as Zeise's salt.

The first transition-metal alkyl and aryl complexes were prepared in 1907, by Pope and Peachey,² and again these were platinum compounds, trimethyl platinum complexes, $[PtMe_3X]_4$. At about the same time Hoffmann and von Nambutt prepared a platinum complex of dicyclopentadiene in alcohol,³ which was recognised by Chatt, *et al.*⁴ as the first example of a platinum(II) alkyl, in which the platinum complex was an alkoxydicyclopentadienylplatinum chloride dimer, $[(C_{10}H_{12}OMe)PtCl]_2$.

A landmark event in organotransition-metal chemistry was the discovery⁵ in 1951 of ferrocene.

The use of organotransition-metal complexes as catalysts has received much attention. Much of the early stimulation in this field

came from the discovery of the cobalt-catalysed oxo process,⁶ by Roelen in 1938, and from the earlier work by Fischer and Tropsch on the reductive polymerisation of carbon monoxide.

At the present time a huge variety of organotransition-metal complexes are known, containing both σ - and π - bonds. The following sections will review some of the general chemistry of platinum. Platinum has a very wide and interesting chemistry and emphasis will be placed only on those areas which pertain to the work presented in this thesis.

2. CHEMISTRY OF PLATINUM

Ever since the synthesis of Zeise's salt, platinum has been an important element in organometallic chemistry. It is able to form a wide range of complexes that are kinetically sufficiently inert to enable them to be isolated and characterised. Several comprehensive texts are available on the chemistry of platinum.⁷⁻⁹

In its compounds, platinum shows a distinct preference for three oxidation states, zero, +2 and +4. Recently an increasing number of compounds in which platinum is in the +1 oxidation state have been described. Compounds in the +3 and +5 oxidation states are rare and compounds in the +6 oxidation state are known only for platinum surrounded by oxygen or fluorine ligands.

Platinum undergoes facile two-electron oxidations or reductions between its three main oxidation states, and oxidation of platinum(II) to platinum(IV) forms the basis of this thesis.

2.1 Oxidation States of Platinum

The most common oxidation states for platinum are zero, +2 and +4. Table 1.1 summarises the usual coordination numbers and

TABLE 1.1: Usual Coordination Number and Stereochemistries of Platinum Compounds in Common Oxidation States

Oxidation State	Coordination Number	Geometry	Examples	Reference
$0, d^{10}$	2	linear	$[\text{Pt}(\text{PRh}^t\text{Bu})_2]_2$	10
	3	trigonal planar	$[\text{Pt}(\text{PPh}_3)_3]$	8
	4^a	tetrahedral	$[\text{Pt}(\text{PPh}_3)_3\text{GO}]$	
	4^a	square planar	$[\text{Pt}(\text{PPh}_2\text{Et})_2(\text{CO})_2]$	7
$+2, d^8$	4^a	square planar	K_2PtCl_4	8
	5	trigonal bipyramidal	$[\text{Pt}(\text{SnCl}_3)_5]^{3-}$	8
	6	octahedral	$[\text{Pt}(\text{NO})\text{Cl}_5]^{2-}$	8
$+4, d^6$	6^a	octahedral	$\text{K}_2 \text{ fac-}[\text{Pt}(\text{NO}_2)_3\text{Cl}_3]$	9

^aMost common

stereochemistries for these oxidation states.

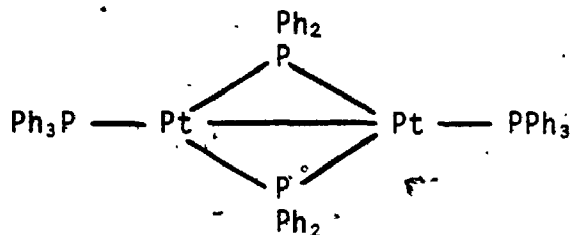
2.1.1 Platinum(0)

Platinum(0) has a $5d^{10}$ electronic configuration. The most common coordination numbers for this oxidation state are four, three and two. With four neutral ligands bonded to the metal, the complex is coordinatively saturated. The first zerovalent platinum complexes to be synthesised were by Malatesta¹¹ and contained tertiary aryl phosphine ligands. The phosphine complexes have been the most widely investigated for the platinum(0) oxidation state. The stabilisation of zerovalent platinum complexes is associated with strong σ -donors that are also capable of some π -acceptance.⁸ Replacement of strong π -accepting, weaker σ -donating CO by the fairly strongly σ -donating tertiary phosphines markedly enhances the strength of the platinum-carbonyl bond, so that $[\text{Pt}(\text{PR}_3)_3\text{CO}]$ and $[\text{Pt}(\text{PR}_3)_2(\text{CO})_2]$ can be prepared and are thermally stable at room temperature whilst $[\text{Pt}(\text{PR}_3)(\text{CO})_3]$ is only stable under high pressure of CO and $[\text{Pt}(\text{CO})_4]$ is only stable at low temperature.

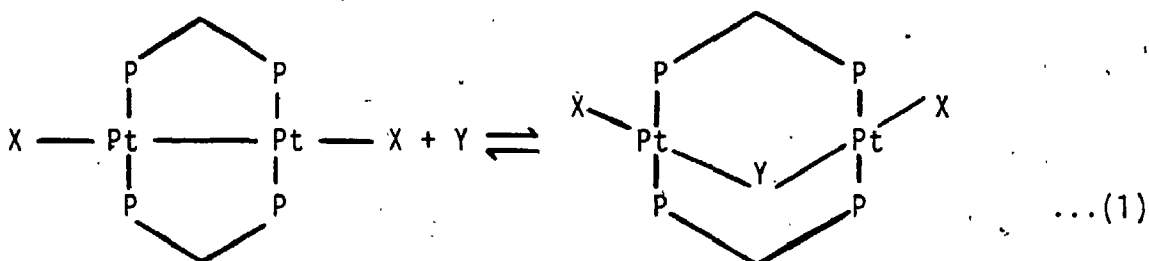
2.1.2 Platinum(I)

It is only in the last ten years or so that platinum compounds in the +1 and +3 oxidation states have been adequately characterised.¹²

Most compounds of the odd oxidation states of platinum exist as binuclear metal-metal bonded species. They are remarkable for the variety of bridging groups which have been characterised. A particularly common structural feature is the nearly linear $\text{R}_3\text{PPtPtPR}_3$ unit which is often found with two bridging groups. One such complex is shown below.¹³

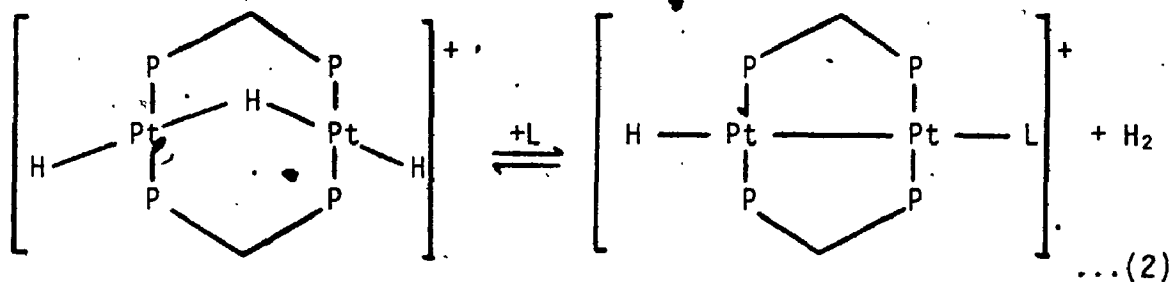


One unusual feature of some of these molecules is the facile, sometimes reversible insertion of small molecules into the metal-metal bond as shown in equation 1. The small molecule Y may be carbon monoxide, an



isocyanide, sulphur dioxide or a methylene group.

The formation of a platinum(I) binuclear complex has been achieved¹⁴ by the reductive elimination of dihydrogen from a binuclear platinum(II) complex shown in equation 2.



2.1.3 Platinum(II)

This is by far the most common oxidation state for platinum. Most platinum(II) complexes have a square planar stereochemistry and will be 16 electron complexes. They are therefore coordinatively unsaturated and can be readily oxidised to octahedral platinum(IV).

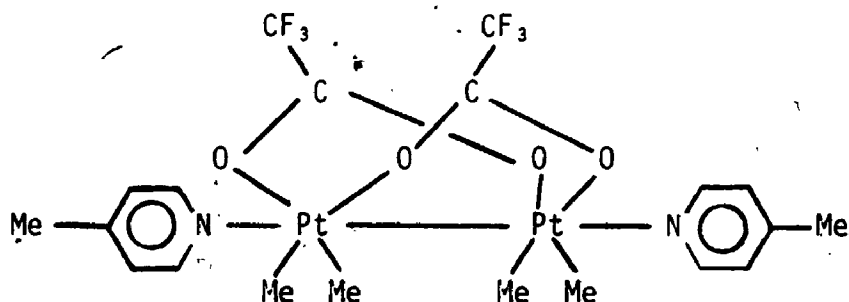
Platinum(II) shows a marked preference for nitrogen, halogens, cyanide and heavy donor atoms (P, As, S, Se) in the formation of complexes,

and exhibits a good deal less affinity for oxygen and fluorine. This is related to the soft nature of the platinum(II) metal centre.^{15,16}

A large range of platinum(II) alkyl, olefin and hydride complexes are also known. The platinum(II) alkyl complexes will be discussed in more detail later in this chapter.

2.1.4 Platinum(III)

The +3 oxidation state for platinum is very rare, and only binuclear platinum(III) complexes have been characterised. Those that have been characterised by x-ray diffraction all fit into a common structural pattern in which each platinum is bound to five ligands and to the other platinum atom in a roughly octahedral arrangement. One such molecule $[\text{Pt}(\text{O}_2\text{CCF}_3)(\text{CH}_3)_2(\gamma\text{-picoline})]_2$ is shown below.



2.1.5 Platinum(IV)

Platinum(IV) has a $5d^6$ electronic configuration and its complexes are diamagnetic. All the platinum(IV) complexes have an octahedral or almost octahedral arrangement of ligands around the metal. They tend to be kinetically inert but can undergo reactions such as reductive elimination as well as electrophilic and nucleophilic substitution reactions.

2.1.6 Platinum(V)

Platinum(V) has a $5d^5$ electronic configuration, and complexes in this oxidation state are paramagnetic, with a single unpaired electron. Compounds such as $[\text{PtF}_5]$ and $[\text{PtOF}_3]$ are known,⁸ as well as a series of hexafluoroplatinates(V). All the platinum(V) compounds of which the structures are known have octahedral coordination about the platinum atom.

2.1.7 Platinum(VI)

The best known platinum(VI) compound is $[\text{PtF}_6]$, which is an extremely reactive, thermally unstable compound. It is produced by electronically heating a platinum wire in fluorine whilst in close contact with a surface cooled by liquid nitrogen.

2.2 Platinum Compounds Containing Platinum-Carbon σ -Bonds

2.2.1 Platinum(II)-Carbon σ -Bonded Complexes

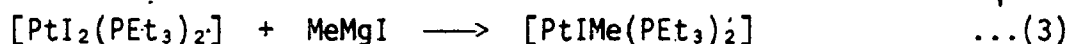
The first platinum(II)-carbon σ -bonded complex was prepared by Hoffmann and von-Narbutt³ and later characterised by Chatt.⁴ The preparation of this complex is described in Section 1.

The first report⁴ of a complex containing a platinum(II)-methyl σ -bond was for *trans*- $[\text{PtIME}(\text{PPh}_3)_2]$. This was prepared by oxidative addition of methyl iodide to $[\text{Pt}(\text{PPh}_3)_3]$.

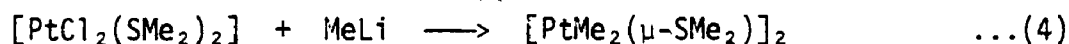
Several preparative methods can be used to synthesise platinum(II)-carbon σ -bonded complexes. A comprehensive review of these methods is given in reference 7. A brief discussion of some of these methods is given below.

2.2.1.1 Preparation of Platinum(II)-Carbon σ -Bonded Complexes

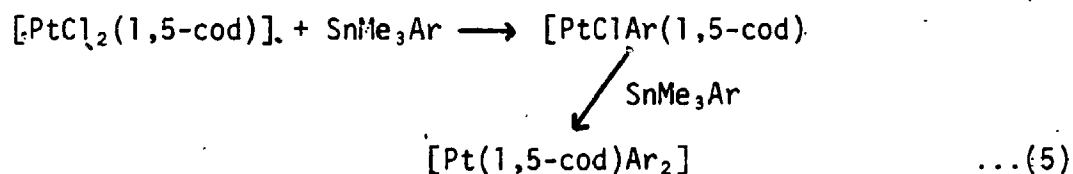
Treatment of a halometal complex with an anionic alkylating agent such as a Grignard or organolithium reagent is the most widely used method. The use of a Grignard reagent is shown in equation 3.



If *cis* or *trans*- $[\text{PtCl}_2(\text{SMe}_2)_2]$ is treated with methyl lithium the product is a platinum(II) dimer (equation 4), containing bridging dimethyl sulphide ligands.



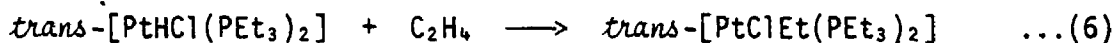
Organotin reagents such as $[\text{SnMe}_3\text{Ar}]$ have been found to very useful for the preparation of platinum(II)-carbon σ -bonded complexes. The number of aryl groups introduced into the platinum(II) complex depends on the number of equivalents of $[\text{SnMe}_3\text{Ar}]$ used.¹⁸ This is illustrated in equation 5.



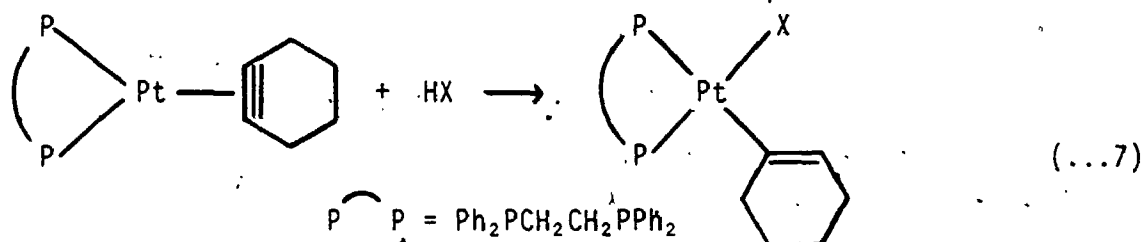
One very versatile method for forming platinum(II)-carbon σ -bonds is by oxidative addition of organic halides to platinum(0) complexes. Platinum(0) phosphine complexes have been the most widely used. This reaction will be discussed in more detail shortly.

The insertion of unsaturated organic compounds into platinum-hydrogen bonds provides a further preparative method. For example¹⁹ ethene reacts with *trans*- $[\text{PtHCl}(\text{PEt}_3)_2]$ to produce a platinum(II) alkyl

complex (equation 6).



A σ -vinyl complex is formed when platinum(0)-cyclohexyne complexes²⁰ are treated with a range of compounds HX, where X = CH₂NO₂, CH₂COMe, CH₂COPh, CH(CN)Ph, OH, and OMe (equation 7).



2.2.1.2 Bonding in Platinum(II) Alkyl and Aryl Complexes

In platinum(II)-alkyl complexes the σ -bond from the alkyl group to the platinum is formed by overlap of a filled sp^3 hybrid orbital on the alkyl carbon with an empty $sp_X d_{X^2-y^2}$ hybrid orbital on platinum (the platinum-carbon bond is taken as the x-axis).

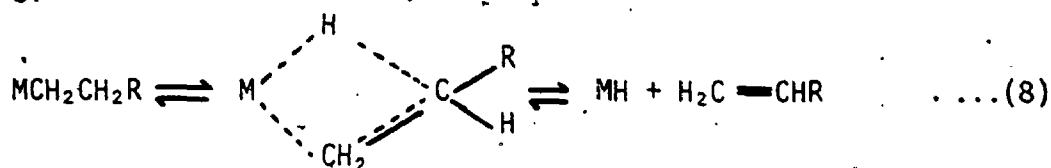
In platinum(II)-aryl complexes the σ -bonds are formed by overlap of a filled sp^2 hybrid orbital on the carbon with an empty $sp_X d_{X^2-y^2}$ hybrid orbital. In the case of platinum(II)-aryl complexes some back π -bonding is possible and this accounts for the increased stability of such complexes compared to alkyl complexes.²¹

2.2.1.3 Stability of Platinum(II)-Carbon σ -Bonds

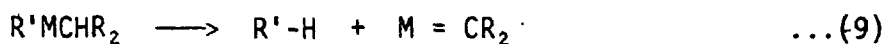
It is believed that the stability of platinum-carbon σ -bonds is of a kinetic rather than a thermodynamic origin.⁷

The cleavage of platinum-carbon σ -bonds is believed to be a concerted process involving more than one site on the metal. Thus β -elimination can occur whereby a substituent on the β -carbon of the alkyl moiety can become directly bonded to the metal.²² This is shown in

equation 8:



α -Elimination often involves elimination of two fragments, one bonded to the metal and one bonded to the α -carbon of a substituent, the latter usually being a proton. Equation 9 illustrates this.



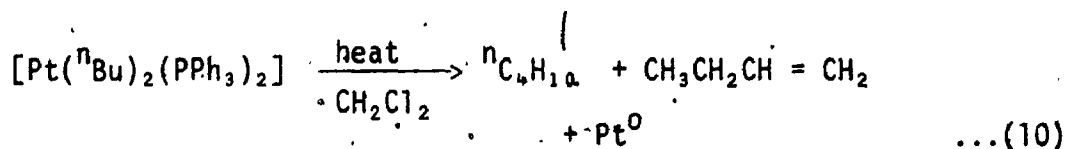
It is currently believed that the stability of platinum(II)-carbon σ -bonded complexes depends on the blocking of these concerted mechanisms.²³⁻²⁵

2.2.1.4 Chemical Reactions of Alkyl Complexes

Most of the chemical reactions of alkyl complexes fall into one of three categories: a) cleavage reactions, in which the platinum(II)-carbon bond is split; b) insertion reactions, in which a reagent is 'inserted' into the platinum(II)-carbon bond; c) replacement reactions, in which either the alkyl ligand or one of the other ligands bound to platinum(II) is replaced.

The cleavage reactions may be induced thermally, photochemically or by the attack of electrophiles. One example of thermal cleavage is the decomposition of $[\text{Pt}(\text{}^n\text{Bu})_2(\text{PPh}_3)_2]$ in hot methylene chloride solution.²²

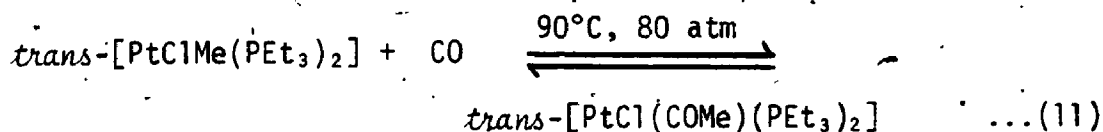
The decomposition is intramolecular and is shown in equation 10.



The photolysis of the same complex produces butane 54%, butene 3% and octane < 1%. This reaction is believed to proceed *via* intermediate butyl radicals.

Platinum(II) alkyl groups are sensitive to cleavage by electrophiles. Thus *cis*-[PtMe₂(PEt₃)₂] reacts with two equivalents of HCl to produce *cis*-[PtCl₂(PEt₃)₂] and methane. The mechanism has been investigated²⁶ and may proceed *via* an oxidative addition/reductive elimination reaction, to be discussed later.

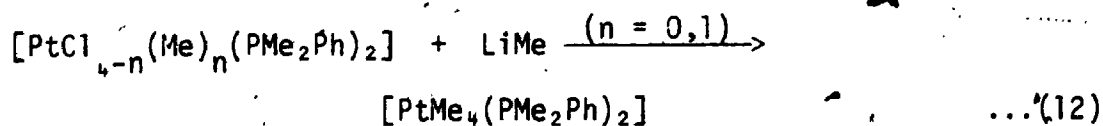
A number of unsaturated molecules can insert into platinum(II)-carbon σ -bonds. These include carbon monoxide, sulphur dioxide, isocyanides, olefins, acetylenes and carbenes. One such insertion is shown in equation 11 for carbon monoxide.



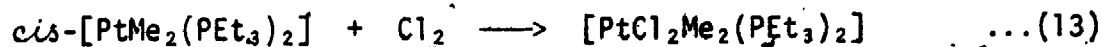
2.2.2 Platinum(IV) Alkyl Complexes

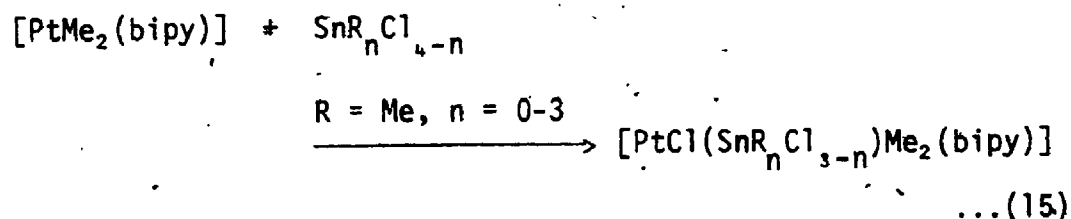
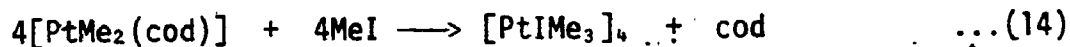
2.2.2.1 Preparation of Platinum(IV) Alkyl Complexes

Platinum(IV) alkyl complexes can be prepared using both Grignard and alkyllithium reagents. One such reaction is shown in equation 12.

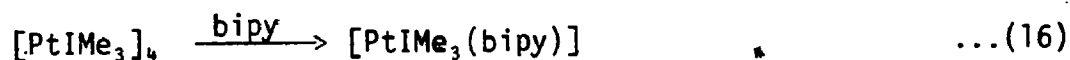


A very versatile preparative method is the oxidative addition of halogens,²⁷ alkyl and acyl halides²⁸ or metal halides²⁹ to platinum(II) alkyl complexes. Examples of each are shown in equations 13-15.





The complex $[\text{PtIME}_3]_4$ has been widely used to form platinum(IV) complexes.³⁰⁻³³ Equation 16 shows one such reaction.



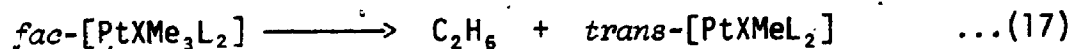
2.2.2.2 Structure of Platinum(IV) Alkyl Complexes

Single-crystal x-ray structure determinations on a large number of platinum(IV) alkyl complexes show that the platinum atom is octahedrally coordinated. The complexes $[\text{PtXMe}_3]_4$ (X = I, Cl, OH) are all tetrameric, with the platinum atoms located at opposite corners of a cube.

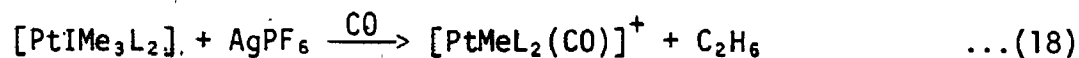
2.2.2.3 Reactions of Platinum(IV) Alkyl Complexes

Platinum(IV) alkyl complexes are often quite stable. Their main reaction is reductive elimination, which may be promoted thermally, photochemically or by addition of other ligands.

Thus, when *fac*- $\text{Pt}^{\text{IV}}\text{Me}_3$ complexes are heated they eliminate ethane³⁴ as shown in equation 17.

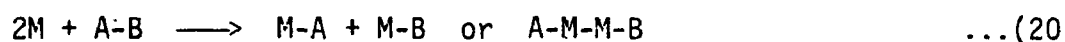
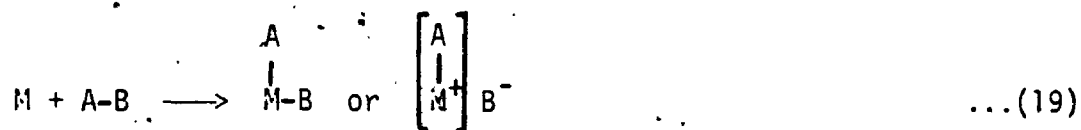


Reductive elimination of ethane from $[\text{PtIME}_3\text{L}_2]$ ($\text{L} = \text{PMe}_2, \text{Ph}, \text{py}$) occurs if AgPF_6 is added to the complex in acetone, or if CO is present (equation 18).



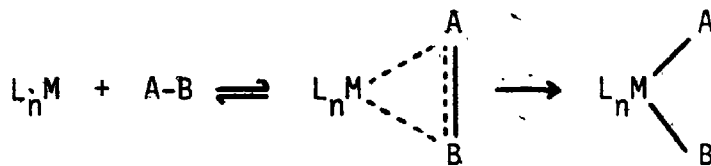
3. OXIDATIVE ADDITION

Oxidative addition is used to describe a class of reactions in which a group A-B , adds to and oxidises a metal complex, M . Both one- and two-electron oxidative additions are recognized and these are shown in equations 19 and 20.



For each reaction the oxidation number and coordination number of the metal increases. The reverse reactions are known as reductive eliminations and both these reaction types are important in many reactions catalysed by transition-metal complexes. Several reviews are available dealing with oxidative addition.³⁵⁻³⁷

Oxidative addition is facilitated by high electron density at the metal centre. Generally the reactivity of group 8 metals towards oxidative addition increases in going from right to left in the periodic table, in going down a given group in the table and in decreasing the initial oxidation state of the metal.



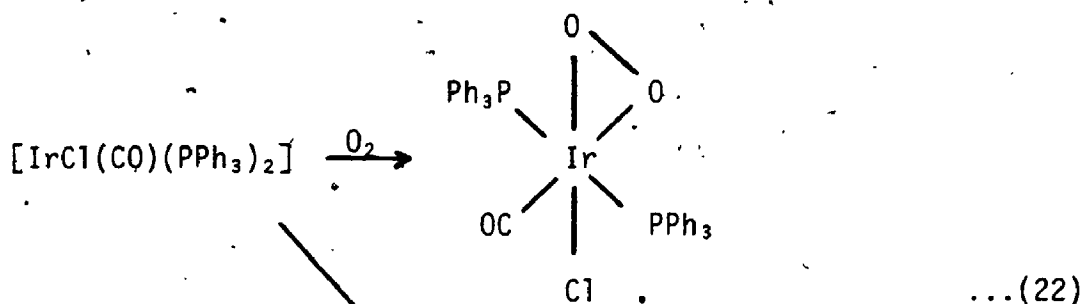
SCHEME 2

Concerted Mechanism of Oxidative Addition

Such a mechanism operates for the addition of silanes³⁸ to metal complexes as shown by equation 21.

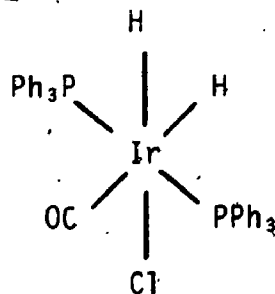


The oxidative addition of dioxygen, and hydrogen to metal centres also proceeds in this way as illustrated below in their reaction with Vaska's Complex.



... (22)

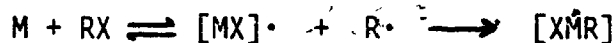
H₂



... (23)

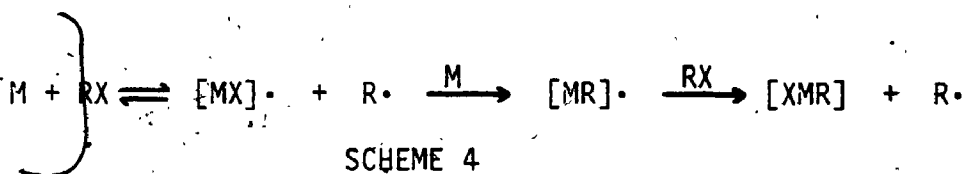
c) Radical Mechanisms

Two mechanisms have been proposed involving radicals.⁴⁰⁻⁴² One is a non-chain radical mechanism (Scheme 3) and the other a radical chain mechanism (Scheme 4)



SCHEME 3

Radical Non-chain Mechanism of
Oxidative Addition



SCHEME 4

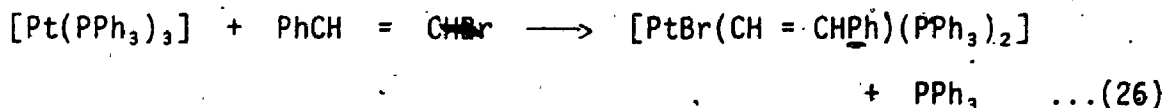
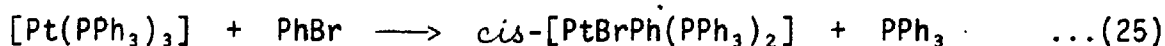
Radical Chain Mechanism of
Oxidative Addition

3.2 Oxidative Addition Reactions of Platinum Complexes

Oxidative addition to platinum(0) and platinum(II) complexes has proved a versatile method for synthesising new platinum complexes and the reaction can proceed *via* various mechanisms.

a) Oxidative Addition to Platinum(0) Complexes

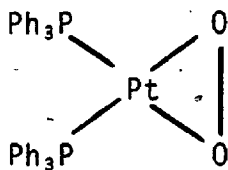
Equations 24-26 indicate some of the oxidative addition reactions of $[Pt(PPh_3)_3]$ with organic halides.



Complex $[Pt(PPh_3)_3]$ is very susceptible to oxidative addition due to the high electron density on the metal centre and due to the coordinatively unsaturated nature of the complex. In general the less sterically demanding the phosphine ligands, the greater the rate of oxidative

addition. Furthermore the more basic the phosphine the greater its ability to promote oxidative addition: $\text{PMe}_3 > \text{PMe}_2\text{Ph} > \text{PMePh}_2 > \text{PPh}_3$.

In the oxidative addition reactions of platinum(0) phosphine complexes each of the mechanisms discussed in the previous section has been observed. A concerted mechanism operates⁴³ in the reaction between $[\text{Pt}(\text{PPh}_3)_3]$ and dioxygen to give the product shown below.

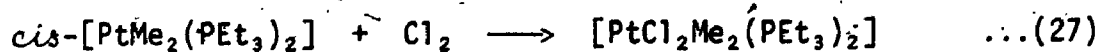


The reaction of benzyl chloride with $[\text{Pt}(\text{PEt}_3)_3]$ to produce $[\text{PtBr}(\text{PEt}_3)_2(\text{PhCH}_2)]$ proceeds *via* the $\text{S}_{\text{N}}2$ mechanism,⁴¹ whilst the reaction using benzyl bromide is believed to proceed *via* competing $\text{S}_{\text{N}}2$ and radical non-chain pathways. Not as many examples exist for radical chain mechanisms of these platinum(0) complexes. There is a report⁴⁴ however that the optically active α -bromoester, $\text{CH}_3\text{CHBrCOOC}_2\text{H}_5$, reacts with $[\text{Pt}(\text{PPh}_3)_2(\text{C}_2\text{H}_4)]$ *via* such a mechanism. This was inferred from total loss of optical activity and inhibition of the reaction by galvinoxyl.

b) Oxidative Addition Reactions of Platinum(II) Complexes

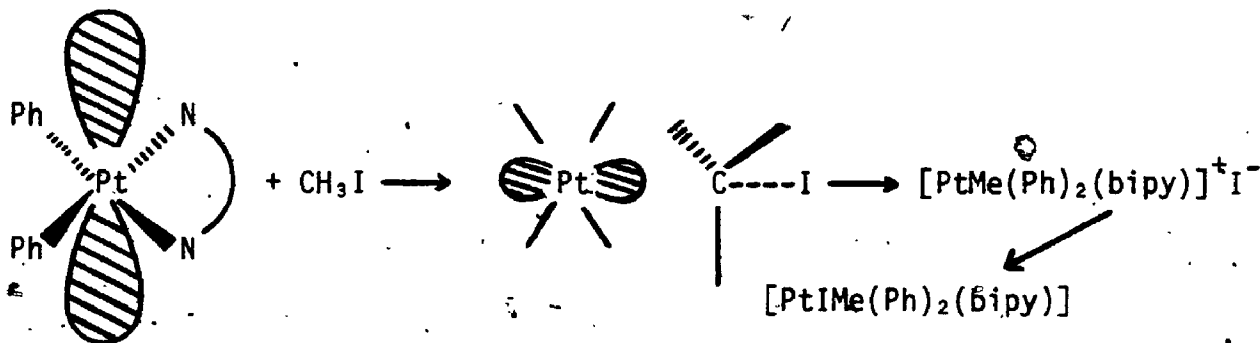
Although there are numerous examples of oxidative addition to platinum(II) complexes, very little mechanistic work has been done.

Platinum(II) alkyl, aryl, σ -vinyl and acetylide complexes are readily oxidised by halogens,^{21,27,44} producing the platinum(IV) complexes (equation 27).



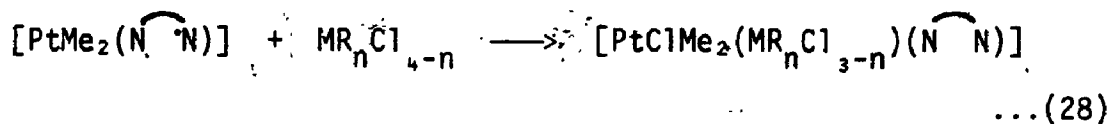
Methyl iodide can oxidatively add to platinum(II) complexes and provides a good method for the preparation of platinum(IV) methyl complexes. The

mechanism of this reaction with $[\text{PtPh}_2(\text{bipy})]$ has been studied⁴⁵ and is believed to proceed by an $\text{S}_{\text{N}}2$ mechanism. The non-bonding electrons in the d_{z^2} orbital of the platinum attack the carbon atom displacing the iodine atom which subsequently coordinates to the platinum. This is shown in Scheme 5.



$\text{S}_{\text{N}}2$ Mechanism of Oxidative Addition to Platinum(II)

Metal-metal bonds can be formed in the oxidative addition of tin and lead alkyl chlorides to platinum(II)²⁹ as shown in equation 28.



M = Pb, n = 2,3

M = Sn, n = 0-3

N N = bipy or phen.

REFERENCES

1. Thayer, J.S.; Adv. Organomet. Chem., 1975, 13, 1.
2. Pöpe, W.; Peachey, S.J.; Proc. Chem. Soc., 1907, 23, 86.
3. Hoffmann, K.A.; von Narbutt, J.; Chem. Ber., 1908, 41, 1625.
4. Chatt, J.; Vallarino, L.M.; Venanzi, L.M.; J. Chem. Soc., 1957, 2496.
5. Kealy, T.J.; Pauson, P.J.; Nature (London), 1951, 168, 1039.
6. Roelen, O.; DRP849548 (1938) and Angew. Chem., 1948, 60, 62.
7. Hartley, F.R.; "Comprehensive Organometallic Chemistry", Wilkinson, G.; Stone, F.G.A.; Abel, E.W.; Eds.; 1982, Vol 6, Pergamon Press, Toronto.
8. Hartley, F.R.; "The Chemistry of Platinum and Palladium", 1973, Applied Science, London.
9. Belluco, A.; "Organometallic and Coordination Chemistry of Platinum", 1974, Academic Press, London and New York.
10. Otsuka, S.; Yoshida, T.; Matsumoto, M.; Nakatsu, K.; J. Am. Chem. Soc., 1976, 98, 5850.
11. Malatesta, L.; Angoletta, M.; J. Chem. Soc., 1957, 1186.
12. Balch, A.L.; Comments Inorg. Chem., 1984, 3, 51.
13. Taylor, N.S.; Chieh, P.C.; Carty, A.J.; J. Chem. Soc. Chem. Comm., 1975, 448.
14. Brown, M.P.; Fischer, J.R.; Hill, R.H.; Puddephatt, R.J.; Seddon, K.R.; Inorg. Chem., 1981, 20, 3516.
15. Pearson, R.G.; J. Am. Chem. Soc., 1963, 85, 3533.
16. Davies, J.A.; Hartley, F.R.; Chem. Rev., 1981, 81, 79.
17. Schagen, J.D.; Overbeek, A.R.; Scheuk; Inorg. Chem., 1978, 17, 1938.

18. Eaborn, C.; Odell, K.; Pidcock, A.; *J. Organomet. Chem.*, 1975, 96, C38.
19. Chatt, J.; Shaw, B.L.; *J. Chem. Soc.*, 1962, 5075.
20. Bennett, M.A.; Robertson, G.B.; Whimp, P.O.; Yoshida, T.; *J. Am. Chem. Soc.*, 1973, 95, 3028.
21. Chatt, J.; Shaw, B.L.; *J. Chem. Soc.*, 1959, 705.
22. Whitesides, G.M.; Gaasch, J.F.; Stedronsky, E.R.; *J. Am. Chem. Soc.*, 1972, 94, 5258.
23. Wilkinson, G.; *Pure Appl. Chem.*, 1972, 30, 627.
24. Davidson, P.J.; Lappert, M.F.; Pearce, R.; *Chem. Rev.*, 1976, 76, 219.
25. Braterman, P.S.; Cross, R.J.; *J. Chem. Soc. Dalton Trans.*, 1972, 657.
26. Jawad, J.K.; Puddephatt, R.J.; *Inorg. Chim. Acta.*, 1978, 31, L391.
27. Hall, J.R.; Swile, G.A.; *J. Organomet. Chem.*, 1974, 76, 257.
28. Appleton, T.G.; Clark, H.C.; Manzer, L.E.; *J. Organomet. Chem.*, 1974, 65, 275.
29. Kuyper, J.; *Inorg. Chem.*, 1977, 16, 2171.
30. Lile, W.J.; Menzies, R.C.; *J. Chem. Soc.*, 1949, 1168.
31. Kite, K.; Truter, M.R.; *J. Chem. Soc. (A)*, 1966, 207.
32. Gilman, H.; Lichtenwalter, M.; *J. Am. Chem. Soc.*, 1938, 60, 3085.
33. Kite, K.; Smith, J.A.S.; Wilkins, E.J.; *J. Chem. Soc. (A)*, 1966, 1744.
34. Brown, M.P.; Puddephatt, R.J.; Upton, C.E.E.; *J. Chem. Soc. Dalton Trans.*, 1974, 2457.
35. Collman, J.P.; Hegedus, L.S.; "Principles and Applications of Organotransition Metal Chemistry", 1980, Chap. 4. University Science Books, California.
36. Stille, J.K.; Lau, K.S.Y.; *Acc. Chem. Res.*, 1977, 10, 434.
37. Collman, J.P.; Roper, W.R.; *Adv. Organomet. Chem.*, 1968, 7, 53.

38. Keim, W.; J. Organomet. Chem., 1968, 14, 179.
39. Oliver, A.J.; Graham, W.A.G.; Inorg. Chem., 1970, 9, 243.
40. Labinger, J.A.; Osborn, J.A.; Inorg. Chem., 1980, 19, 3230.
41. Kramer, A.V.; Osborn, J.A.; J. Am. Chem. Soc., 1974, 96, 7832-
42. Hall, T.L.; Lappert, M.F.; Lednor, P.W.; J. Chem. Soc. Dalton Trans., 1980, 1448.
43. Cook, C.D.; Jauhal, G.S.; Can. J. Chem., 1967, 45, 301.
44. Ruddick, J.D.; Shaw, B.L.; J. Chem. Soc. (A), 1969, 2964.
45. Jawad, J.K.; Puddephatt, R.J.; J. Organomet. Chem., 1976, 113, 297.

CHAPTER 2
OXIDATIVE ADDITION OF WATER AND ALCOHOLS TO
DIMETHYLPLATINUM(II) COMPLEXES

1. INTRODUCTION

As early as 1846 some alkoxy derivatives of silicon and boron had been described^{1,2} but only from about 1950 has the field of alkoxide chemistry seen rapid development. Bradley's book³ provides an excellent text on the subject, along with the review by Mehrotra.⁴

It is clear from these latter two publications that not many platinum metal alkoxides have been synthesised, and the same can be said of platinum metal hydroxides. Both the alkoxide and hydroxide ligands are classified^{5,6} as being 'hard' bases whilst Pt^{2+} and Pt^{4+} are classified as 'soft' acids.⁷ An alternative terminology⁸ is class a) acids ('hard') and class b) acids ('soft'). Pearson has suggested a simple rule for predicting the stability of complexes formed between acids and bases: Hard acids prefer to bind to hard bases and soft acids prefer to bind to soft bases. Thus it is not expected that platinum will form stable alkoxides or hydroxides. The hard species, both acids and bases tend to be small and not very polarisable whilst the soft species tend to be larger and more polarisable. For a more detailed discussion, the reader is referred to Huheey's book.⁷

A possible explanation for the strength of early-transition-metal alkoxide bonds has been put forward by Navrotsky⁹ and Rothwell.¹⁰ The alkoxy group can π -donate to the metal and this is associated with

large M-O-C angles. As the electron deficiency of the metal decreases (to the right of the d block) then so also does the number and stability of metal alkoxides.

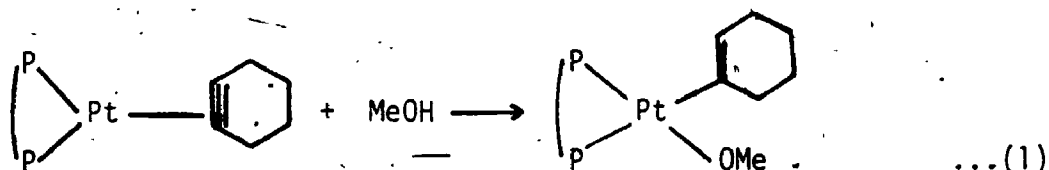
2. LITERATURE SURVEY

2.1 Survey of Known Platinum Alkoxides and Hydroxides

2.1.1 Alkoxides

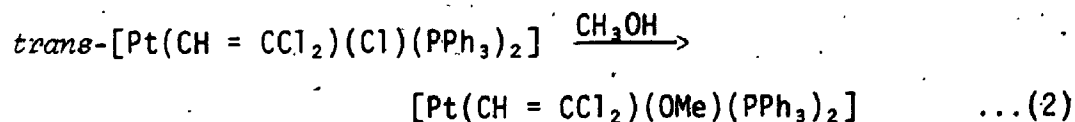
The first report¹¹ of a platinum alkoxide was in 1958, but this platinum(IV) complex $[\text{PtMe}_3(\text{OMe})]_4$ was incompletely characterised. It is believed that the series of platinum(IV) alkoxides discussed later in this chapter are the first to be fully characterised.

The first alkoxoplatinum(II) complexes were prepared¹² by the reaction between the cyclohexyne complex $[\text{Pt}(\text{C}_6\text{H}_8)(\text{diphos})]$ and methanol (eq. 1, $\text{P} \sim \text{P} = \text{Ph}_2\text{PCH}_2\text{CH}_2\text{PPh}_2$).

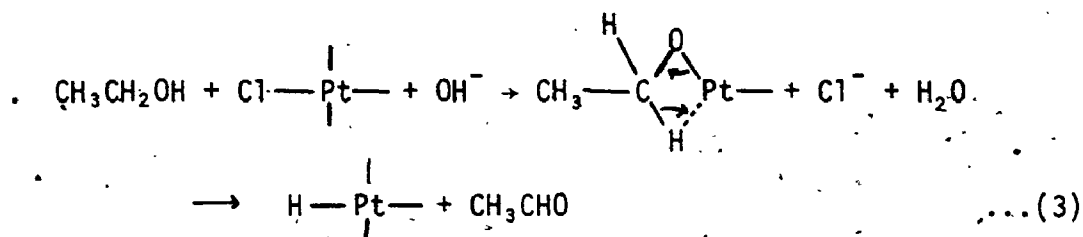


This was the first non-ionic methoxo-complex of platinum(II). The methoxide can be converted to the hydroxide by traces of water. The methoxide does not undergo β -elimination to form a hydride.

Otsuka *et al.* synthesised¹³ a series of platinum(II) methoxides by the metathesis of $[\text{PtR}(\text{Cl})(\text{PPh}_3)_2]$ with NaOMe in methanol (eq. 2).

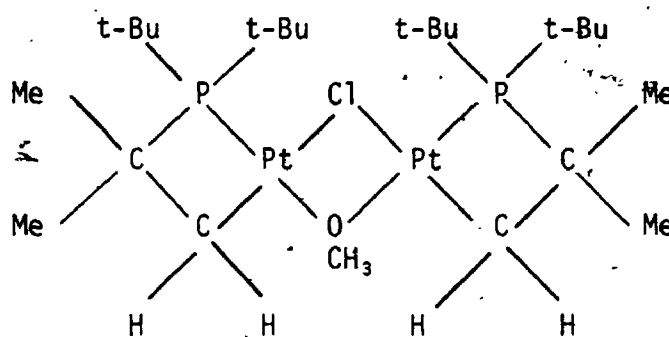


In these sorts of reactions, it is possible to see β -elimination with formation of a platinum hydride¹⁴ (eq. 3)

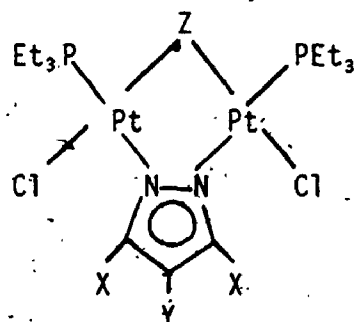


The first alkoxo-bridged platinum complex was prepared by Clark and co-workers¹⁵ by treating $[\text{Pt}_2\text{Cl}_2(\text{t-Bu}_2\text{PCMe}_2\text{CH}_2)_2]$ with NaOH in methanol.

The novelty of this complex is increased by the presence of mixed alkoxo- and chloro-bridges between two platinum atoms. This is shown below.



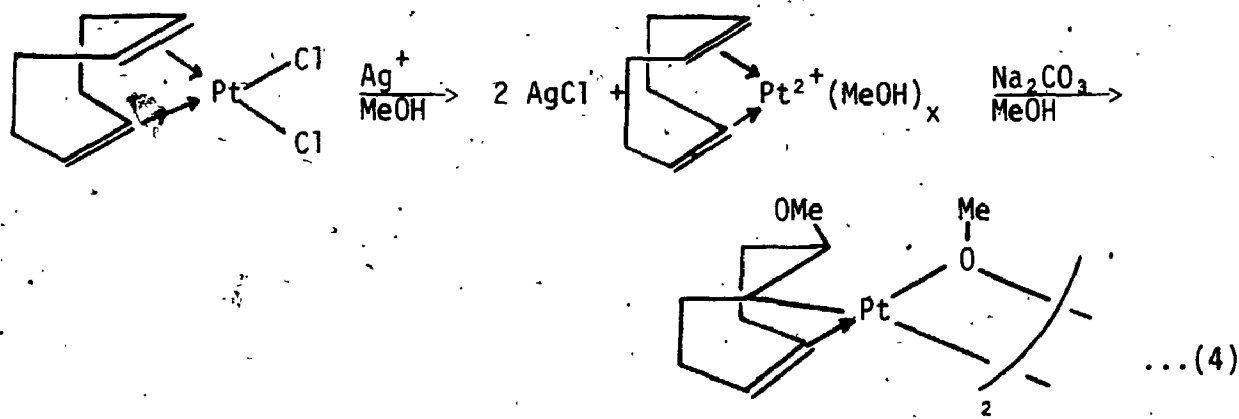
The palladium analogue was later synthesised by Goel.¹⁶ A further mixed methoxy-bridged platinum(II) complex was synthesised by Clark¹⁷ in which the second bridging group is the bidentate pyrazolato-N,N' ligand (see below).



Z = Cl, OMe
X = H, Me
Y = H, Br

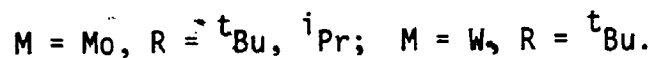
A series of platinum(II) hydroxo- and alkoxo-complexes were prepared by Ros and co-workers¹⁸ using the metathesis technique,¹³ described above. In this case NaOMe was used. The products were $[\text{Pt}(\text{OMe})(\text{R}_\text{x})\text{L}_2]$ ($\text{L}_2 = \text{cis} - \text{Ph}_2\text{PCH} = \text{CHPh}_2$, or 2PPh_3 , $\text{R}_\text{x} = \text{CF}_3$, CH_2CN). The electronegative R_x groups increase the effective positive charge on the metal, and consequently the electron density on the OMe group will decrease, increasing the covalency of the Pt-OMe bond. Alternatively the greater the formal charge on platinum the more it resembles a class a) acid. These methoxo-complexes react with CO to give methoxycarbonyl derivatives $[\text{Pt}(\text{COOCH}_3)(\text{R}_\text{x})(\text{Ph}_2\text{PCH} = \text{CHPh}_2)]$. Similar insertions were performed using CS_2 and SO_2 . This work is relevant since alkoxy carbonyl complexes of Pd have been postulated as intermediates in carbonylation reactions of alcohols.

In 1981 two groups published independently the structure of a platinum(II) methoxo-complex.^{19,20} This bridging methoxo-complex was prepared from $[\text{PtCl}_2(\text{COD})]$ (COD = cyclooctadiene) (eq. 4).

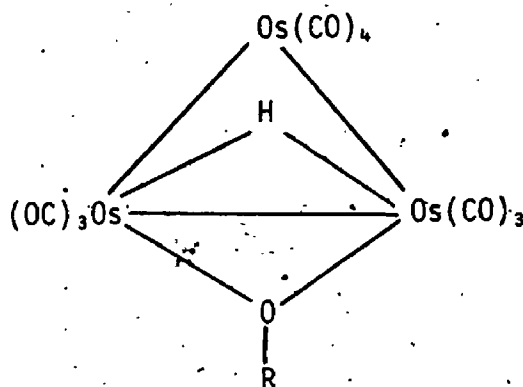


Apart from the work of Bennett¹² there does not appear to be any report in the literature of the formation of alkoxides of the platinum metals by direct interaction with alcohols. The report of such reactions given later in this chapter represents an unusual synthetic route.

There has been much interest in the activation of alcohols with transition metal complexes. Chisholm and co-workers have investigated the reaction of alcohols with tungsten and molybdenum dialkylamide complexes²¹ (eq. 5).



Only a few examples of the addition of ROH to a metal centre as OR and H are reported in the literature. Wilkinson²² has isolated $[WH_3(OMe)(PMe_3)_4]$ from the reaction between $[WH_2(PMe_3)_5]$ and dry methanol. Deeming²³ was successful in synthesising a series of triosmium clusters containing bridging hydrido- and alkoxo-ligands derived from the alcohol. The structure is shown below.



R = Me, Ph, 2-naphthyl, CHMe₂, CH₂Ph, CHMePh,
CMe₂Ph.

The starting complex in each case was $[Os_3(CO)_{12}]$.

A palladium(II) methoxide containing bis(hexafluoroacetyl-acetonate) was prepared by Siedle.²⁴ $[Pd(F_6acac)_2]$ in methanol

deposited at room temperature, crystals of $[\text{Pd}_2(\mu\text{-CH}_3\text{O})_2(\text{F}_6\text{acac})_2]$. If methoxide salts were used, decomposition was observed. The presence of the electron-withdrawing (F_6acac) ligands is part of the reason for the stability of these alkoxides. Siedle points out that the relative ease of hydrogen transfer to late second- and third-row metals may account for the paucity of their alkoxide chemistry. Attempts to prepare homologues of the methoxo-complex failed, presumably due to hydrogen abstraction.

The photoinduced reaction²⁵ between $[(\eta\text{-C}_5\text{H}_5)_2\text{WH}_2]$ and methanol produced $[(\eta\text{-C}_5\text{H}_5)_2\text{WH}(\text{OMe})]$ along with $[(\eta\text{-C}_5\text{H}_5)_2\text{WMe}(\text{OMe})]$. The reaction is believed to go via a 'tungstenocene' intermediate which inserts into the O-H bond of methanol.

2.1.2 Alcohols and Alkoxides in Synthetic and Catalytic Systems

Alkoxyplatinum complexes have been invoked as probable intermediates in the preparation of various hydridoplatinum complexes. Chatt and Shaw¹⁴ in preparing the hydrido-complex $\text{trans-}[\text{PtH}(\text{Cl})(\text{PEt}_3)_2]$ by reduction of $\text{cis-}[\text{PtCl}_2(\text{PEt}_3)_2]$ with KOH in ethanol proposed an ethoxyplatinum complex as intermediate, which by hydride transfer would then produce the final hydride (eq. 3).

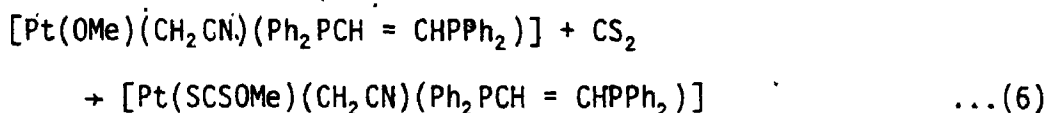
Isopropyl alcohol reacted in a similar fashion producing acetone. Alcoholic KOH has been a widely used reducing agent in the preparation of hydrido-(carbonyl) complexes^{26,27} of metals such as Ru, Rh, Os and Ir.

Otsuka²⁸ has prepared stable dihydride complexes $\text{trans-}[\text{PtH}_2\text{L}_2]$ ($\text{L} = \text{PPh}(\text{tBu})_2, \text{PCy}_3, \text{P}(\text{iPr})_3$). The reaction was carried out in neat methanol using PtL_2 .

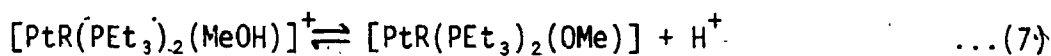
A series of platinum complexes have been prepared by insertion of small molecules into the Pt-OR bond. Bennett²⁸ reacted 1,2-bis-(diphenylphosphino)ethane cyclohexyneplatinum(0) with methanol in the

presence of CO. The product was the methoxycarbonyl $[\text{Pt}(\text{CO}_2\text{CH}_3)(\text{C}_6\text{H}_9)\text{-}(\text{dppe})]$.

Ros¹⁸ and co-workers successfully inserted CO, SO₂, COS, and CS₂ into a series of Pt-OR bonds (e.g. eq. 6)

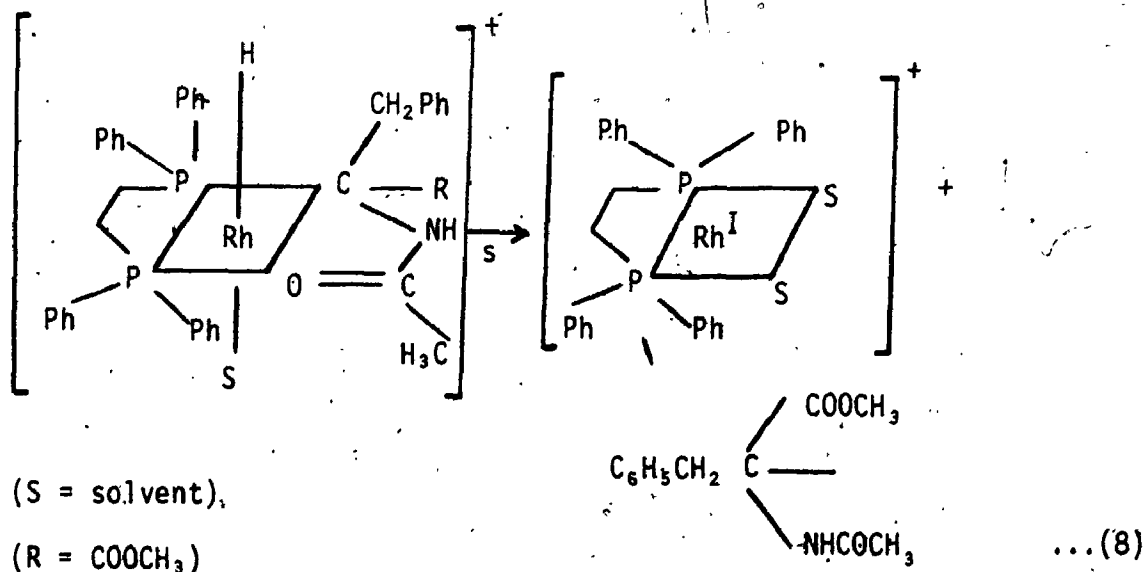


Methanol, used as solvent, has been shown to have a marked effect on the rate of hydrogenation of olefins.²⁹ This rate enhancement is explained in terms of the following equilibrium:

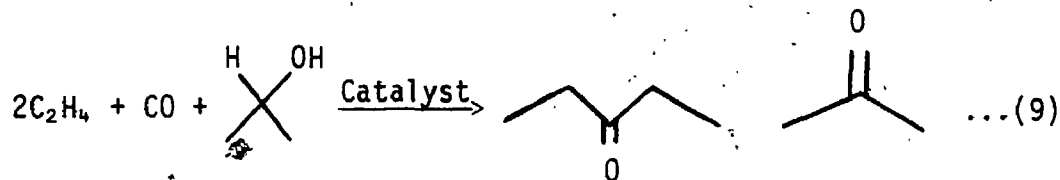


The high electron density donated by methoxide ligands enables the complex to undergo oxidative addition with H₂ more readily.

The hydrogenation of methyl(Z)- α -acetamidocinnamate in methanol is catalysed⁶⁸ by $[\text{Rh}(\text{diphos})(\text{CH}_3\text{OH})_2]^+$. The rate-determining step of the reaction is the product-forming intramolecular reductive elimination process corresponding to eq. 8



Alcohols have been found to be sources of hydrogen in the synthesis of ketones from olefin-CO mixtures. Ruthenium complexes have been used as catalysts (eq. 9).



The catalytic carbonylation of methanol to produce acetic acid is a very important industrial process. It was in 1968 that Paulik and Roth of Mosanto Company announced the discovery of a low-pressure system for carbonylation of methanol.^{31,32} An iodide-promoted Rh or Ir catalyst is used.

2.2 Review of Platinum Hydroxides and Their Chemistry

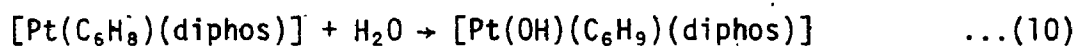
2.2.1 Hydroxides

It is clear from the literature that there are not many stable hydroxides of the platinum metals. In 1911, Werner³³ determined the relative basic strength of a series of platinum hydroxides. The older literature³⁴ contains references to a number of platinum(II) and palladium(II) hydroxo-complexes. The first more modern study was the characterisation of $[Pt_2(OH)_2(PPh_2O)_2(PEt_3)_2]$ by Chatt and Heaton.³⁵ The hydroxide was formed in the reaction between KOH and $cis-[PtCl_2(PPh_2Cl)(PEt_3)]$. The hydroxo-groups are bridging which appears to be a more favourable bonding mode for OH. Shaw recently reported⁶⁷ the first bridging-hydroxo A-frame complex, $[Pt_2Me_2(\mu-OH)(\mu-dppm)_2][BF_4]$. This was formed in the reaction between $[Pt_2Me_2(\mu-dppm)_2][BF_4]$ and NaOH in acetone. The latter complex reacted with methanol to give the hydride-bridged A-frame complex $[Pt_2Me_2(\mu-H)(\mu-dppm)][BF_4]$.

One of the more common routes to hydroxo-complexes of platinum

is the displacement of chloro-ligands by AgBF_4 in some moist solvent. The cationic complex $[\text{Pt}_2(\mu\text{-OH})_2\text{L}_4]^+$ ($\text{L} = \text{PEt}_3, \text{PPh}_3, \text{py}$) was prepared in this way.³⁶ These workers were not successful in producing terminal hydroxo-complexes.

The first nonionic mononuclear hydroxo-complexes of platinum(II) were prepared by Bennett¹² *et al.* (eq. 10)

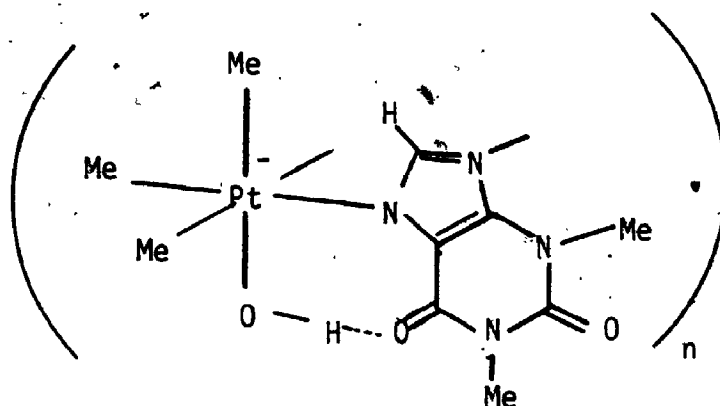


The same group have also synthesised^{37,38} terminal hydroxo-complexes using $[\text{PtCl}(\text{diphos})\text{Me}]$. AgBF_4 is added to this platinum complex. The reaction mixture is evaporated to dryness and then treated with $\text{NaOH}/\text{CH}_3\text{OH}$. The product is $[\text{Pt}(\text{OH})(\text{diphos})\text{Me}]$. They observed that ν_{PtP} trans to OH was unexpectedly low, which the authors attributed to a larger *trans*-influence for OH than previously believed.

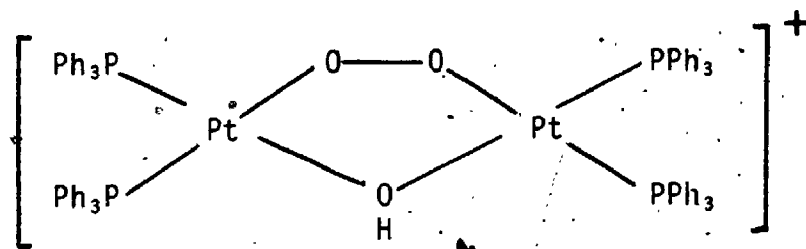
The monomeric hydroxo-complexes *cis*- $[\text{Pt}(\text{OH})\{(\text{CH}_2)_n\text{CN}\}\text{L}_2]$ ($\text{L}_2 = 2\text{PPh}_3, \text{Ph}_2\text{PCH} = \text{CHPPh}_2, n = 1,3$) were shown³⁹ to be intermediates in the synthesis of $[\text{PtH}\{(\text{CH}_2)_n\text{CN}\}\text{L}_2]$. Pure monomeric hydroxo-complexes were obtained for $n = 1$. The same group extended this work,¹⁸ varying the alkyl groups bonded to platinum.

Lock and co-workers⁴⁰ have published the crystal structure of a number of platinum(II) hydroxo-complexes. They point out, that like other transition metals, platinum prefers bridging-hydroxo-complexes. Their interest in compounds such as $[\text{PtCl}_2(\text{NH}_3)_2(\text{OH})_2]$ stems from the antitumor activity associated with such compounds. Lock *et al.* have published the crystal structures of this platinum(IV) hydroxo-complex.⁴¹ It is one of the few crystallographic determinations for a platinum hydroxo-complex. Hall and co-workers,⁴² also interested in the antitumor

compounds, have synthesised the oligomeric complex shown below.

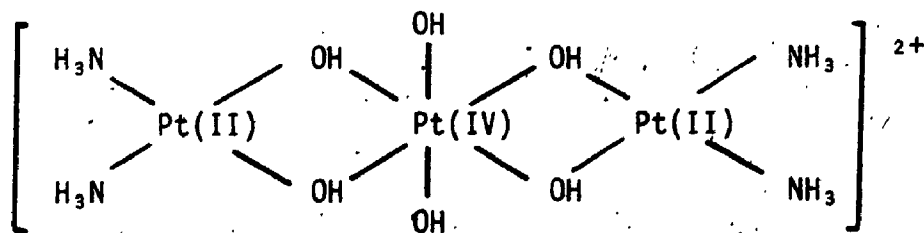


The crystal structure of an interesting mixed bridging-complex of platinum⁴³ was published in 1978. It consists of bridging peroxo- and hydroxo-ligands. This is shown below.



It can be converted into the dihydroxo-bridged complex, $[\text{Pt}_2(\text{OH})_2(\text{PPh}_3)_4]^+$, by treating with aqueous HClO_4 .

The irradiation⁴⁴ of aerated aqueous solutions containing *cis*- $[\text{Pt}(\text{NH}_3)_2(\text{H}_2\text{O})_2]^{2+}$ gave rise to the formation of a blue product identified as a mixed valence (Pt(II):Pt(IV) = 2) hydroxo-bridged trinuclear cationic complex shown below.

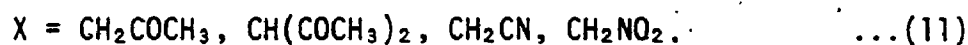
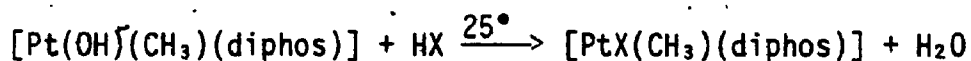


Otsuka and co-workers have investigated the oxidative addition of water to platinum(0) phosphine complexes. Their incentive arises from the current problem of water-mediated energy conversion and from the possible application of the (PtHOH) species for organic synthesis. They originally synthesised ¹³C hydroxo-complexes using the method of Bennett and Appleton,³⁷ described earlier. The authors point out that the greater the *trans*-influence of the ligand *trans* to OH the more ionic the OH would be, through the inductive effect. This is borne out by the increased shielding of the hydroxy hydrogen in the ¹H nmr as the *trans*-influence of the ligand increases. The Japanese workers believed that water (pKa = 15.7) being more acidic than methanol (pKa = 17.7) which shows facile oxidative addition to a range of platinum(0) phosphino-complexes,⁴⁵ would oxidatively add to the same platinum(0) complexes. They isolated the σ -hydrido hydroxo compound [PtH(OH)(PⁱPr₃)₂] from the system [Pt(PⁱPr₃)₂]/H₂O. The OH signal was not detected in the ¹H nmr. They failed to isolate this product from the system, [Pt(PⁱPr₃)₃]/H₂O. Otsuka's group⁴⁶⁻⁴⁸ has also investigated oxidative addition of water to rhodium(I). Oxidative addition of water to [RhH(PⁱPr₃)₃] took place at room temperature in pyridine to give [RhH₂(py)₂(PⁱPr₃)₂][OH]. This *cis*-dihydride was isolated as its BPh₄ salt.

2.2.2 Chemistry of Platinum Hydroxides

The hydroxides of platinum have been found useful in a number of synthetic systems.

These hydroxo-complexes have been found to undergo condensation reactions^{18,28,37,39,49} with weakly acidic hydrocarbon compounds, e.g. acetone, acetylacetone, acetonitrile, or nitromethane (eq. 11).



The reversibility of these reactions enables hydroxoplatinum(II) complexes to catalyse⁴⁵ hydrogen-deuterium exchange with D₂O and activated methyl and methylene carbon atoms. These hydroxo-complexes are strong bases and pH values of 11.93 and 11.82 have been measured⁴⁹ for $[\text{Pt}(\text{OH})\text{Ph}(\text{P}^t\text{BuMe}_2)_2]$ and $[\text{Pt}(\text{OH})\text{Ph}(\text{P}^t\text{BuMe}_2)_2]$ respectively.

Otsuka has investigated⁴⁵ the H-D exchange reaction and has shown that the system $\text{PtL}_3/\text{H}_2\text{O}$ ($\text{L} = \text{PEt}_3, \text{P}^i\text{Pr}_3$) is an efficient catalyst for exchange at activated C-H bonds in ketones, aldehydes, sulfones, sulfoxides, and nitroalkanes. Furthermore these $\text{Pt}^0/\text{H}_2\text{O}$ systems have been used as catalysts for the hydration of nitriles and olefins (eq. 12).



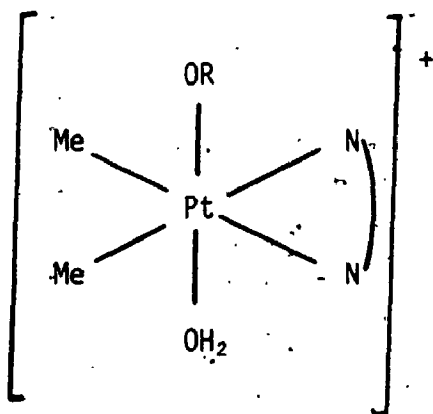
Insertion into the Pt-O bond of these hydroxo-complexes have been investigated by Bennett,³⁷ and Ros.¹⁸ The Pt-O bond undergoes facile insertion of CO, COS, CS₂ and SO₂ in a similar fashion as alkoxo-platinum complexes (eq. 6).

2.3 Results and Discussion

2.3.1 Reactions with Alcohols

The complexes $[\text{PtMe}_2(\text{bipy})]$, (I), and $[\text{PtMe}_2(\text{phen})]$, (II), are red solids, the colour being due to the presence of a metal to ligand charge transfer band (MLCT) in the visible region of the spectrum.⁵⁰ The ¹H nmr spectra of I and II can be interpreted unambiguously. For I the resonances due to MePt and bipy protons are in the ratio 6:8 as expected.

The high field region shows a singlet due to the MePt protons, with satellites due to coupling of the protons with ^{195}Pt ($I = 1/2$, 33.8% nat. abundance). The $^2J_{\text{PtMe}}$ coupling is 86 Hz. The two aromatic rings are equivalent as shown from the symmetrical pattern at low-field. There is some coupling between ^{195}Pt and the proton in position C6, with $^3J_{\text{PtH}}$ equal to 22 Hz. The ^1H nmr of (II) is very similar. The complexes are electron-rich and are among the most reactive of noble-metal complexes in oxidative addition reactions.⁵¹⁻⁵² A solution of $[\text{PtMe}_2(\text{bipy})]$ in methanol was initially yellow-orange in colour but the colour slowly faded to very pale yellow. Evaporation of the solution gave a pale yellow oil, from which a tan solid could be obtained, with difficulty, by precipitation from CH_2Cl_2 solution with pentane. The complex was hygroscopic and we have been unable to grow crystals, despite many attempts. Similar compounds were formed in ethanol and 2-propanol as solvents, and $[\text{PtMe}_2(\text{phen})]$ reacted in the same way. The complexes were not easy to characterise and the evidence for the structure proposed, $[\text{PtMe}_2(\text{OR})(\overset{\curvearrowright}{\text{N}}\text{N})(\text{OH}_2)]^+\text{OH}^-$, is discussed below ($R = \text{Me}, \text{Et}, \text{}^i\text{Pr}$). These ionic complexes consist of an octahedral platinum(IV) cation shown below.



III) $\overset{\curvearrowright}{\text{N}}\text{N} = \text{bipy}$

IIIa) $R = \text{Me}$; b) $R = \text{Et}$; c) $R = \text{}^i\text{Pr}$

IV) $\overset{\curvearrowright}{\text{N}}\text{N} = \text{phen}$

IVa) $R = \text{Me}$; b) $R = \text{Et}$; c) $R = \text{}^i\text{Pr}$

All elemental analysis, ^1H , ^{13}C nmr and mass spectral data for the complexes in this chapter are given at the end of Chapter 7.

i) Elemental analysis (Experimental Section) was consistent with this formula. In some cases, a better agreement was obtained by including extra water of crystallisation. Formulae giving the best fit with experimental analyses are given in Table 7.15 (Chap. 7), but the number of water molecules present is difficult to determine unambiguously, given the hygroscopic nature of the compounds.

ii) The ^1H nmr spectra of complexes (IIIa) - (IVc) give very clear indication as to the stereochemistry of these complexes (Table 7.1). For IIIa) the ^1H nmr gave resonances due to MePt, MeO and bipy protons in the ratio 6:3:8 as expected. The coupling constant $^2\text{J}(\text{PtH})$ for the MePt groups decreased from 86 Hz in (I) to 73 Hz in (IIIa), as expected on oxidation from Pt(II) to Pt(IV).⁵¹ The spectra show that the two MePt groups and the two aromatic rings of the bipy ligand are equivalent and hence that the *cis*-[PtMe₂N₂] structure is retained in (IIIa). The assignments of bipy protons were straightforward using literature precedents on similar compounds⁵³⁻⁵⁷ and were confirmed by homonuclear decoupling experiments.

Figure 2.1 shows the ^1H nmr spectrum of IIIa). The presence of the methoxy ligand in (IIIa) was demonstrated by the observation of ^{195}Pt coupling in both the ^1H and $^{13}\text{C}\{^1\text{H}\}$ nmr spectra (Table 7.2) [$\delta(\text{CH}_3\text{OPt})$ 2.75 ppm, $^3\text{J}(\text{PtH})$ 41 Hz; $\delta(\text{CH}_3\text{OPt})$ 57.3 ppm, $^2\text{J}(\text{PtC})$ 18 Hz]. No exchange was observed when the complex was dissolved in CD_3OD or in D_2O , since the methoxy signal with ^{195}Pt coupling was still observed in the ^1H nmr spectrum. Remarkably, the D_2O solution could be made 0.1 M in HClO_4 and the MeOPt group was still present as evidenced by an unchanged ^1H nmr spectrum.

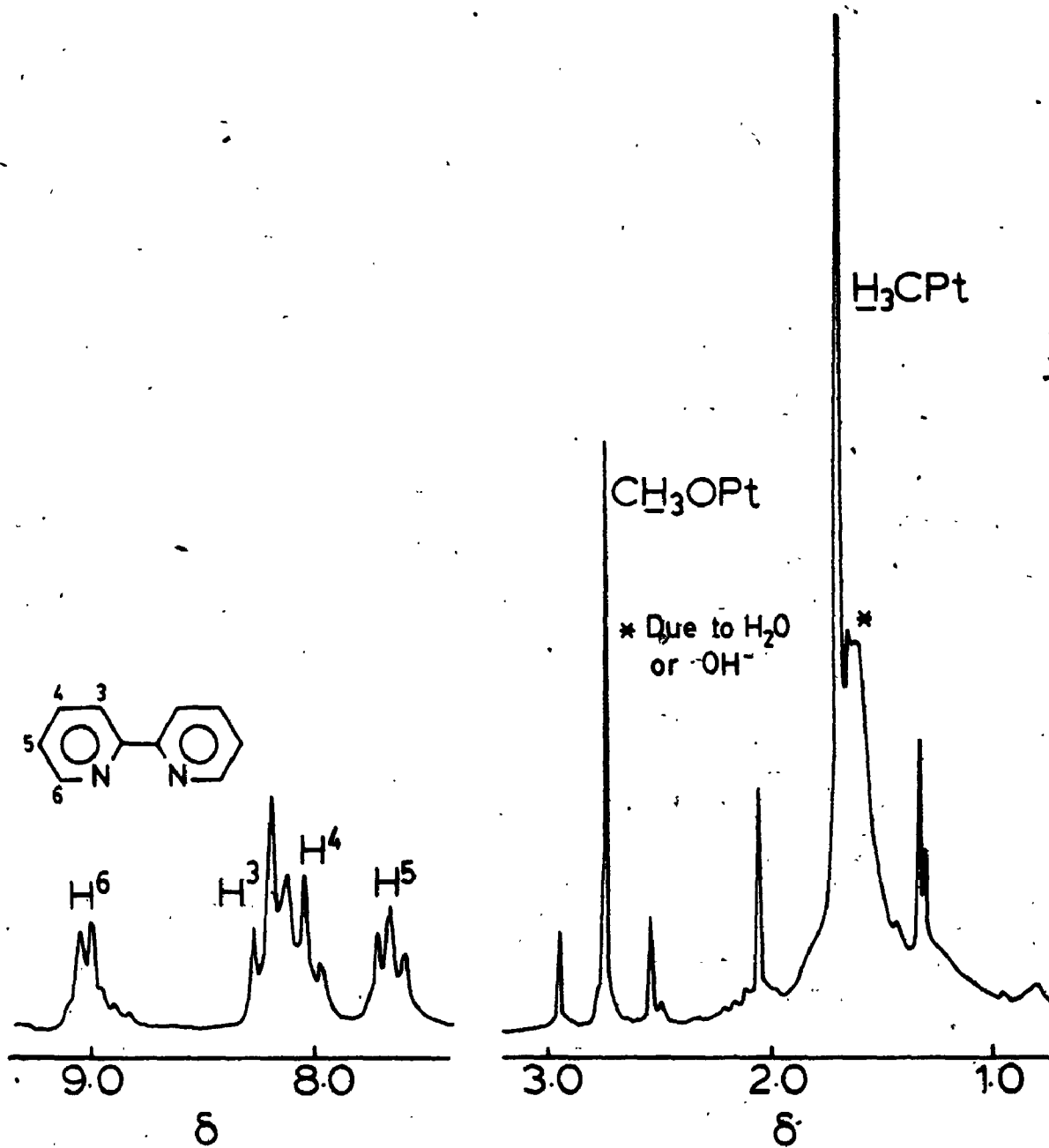


FIGURE 2.1: ^1H NMR Spectrum (100 MHz) of $[\text{PtMe}_2(\text{OMe})(\text{bipy})(\text{H}_2\text{O})][\text{OH}]$ in CD_2Cl_2 .

The ^1H nmr spectrum of the ethoxo-complex (IVb) shows the triplet due to $-\text{CH}_3$ at 0.59 ppm and a quartet due to $-\text{OCH}_2$ at 2.85 ppm with ^{195}Pt satellites. This is shown in Fig. 2.2. The $^{13}\text{C}\{^1\text{H}\}$ nmr of (IVb) is shown in Fig. 2.3. The ^1H and ^{13}C nmr data for complexes (IIIa) - (IVc), given in Tables 7.1 and 7.2, are straightforward and confirm the structural conclusions discussed above.

The presence of $-\text{OH}$ groups in the products was indicated by broad resonances of varying chemical shift in the ^1H nmr spectra of solutions in CDCl_3 or CD_2Cl_2 , but these gave no structural information. In CD_3OD or D_2O solutions, the presence of $-\text{OH}$ groups was demonstrated by increased intensity of the solvent $-\text{OH}$ resonances indicating H for D exchange with solvent.

A simple oxidative addition of alcohol RO-H groups should lead to formation of Pt-H groups, but no high-field resonances were seen in the ^1H nmr spectra (or the ^2H nmr spectra on the product of reaction of (II) with CH_3OD). The absence of Pt-H groups was also indicated by the ir spectra which contained no peaks in the 2000 cm^{-1} region.

The ir spectra of these complexes were not very instructive. The $\nu(\text{C-O})$ band could be tentatively assigned²⁸ as follows: (IIIa), 1073; (IIIb), 1055; (IVa), 1058; (IVb), 1050 cm^{-1} . Ir spectra of the complexes were run as CsI pellets.

iii) The uv/visible spectra of these complexes contain no MLCT band in the region 350-500 nm, confirming oxidation of platinum(II) to platinum(IV) has occurred⁵⁰⁻⁵¹ (Fig. 2.4). The d orbitals of the platinum(IV) are too low in energy for any MLCT in the visible region.

iv) The ionic nature of the products was first demonstrated by conductivity measurements. The conductivity of a 10^{-3} M solution of (I) in methanol increased as reaction occurred (Fig. 2.5) to a limiting

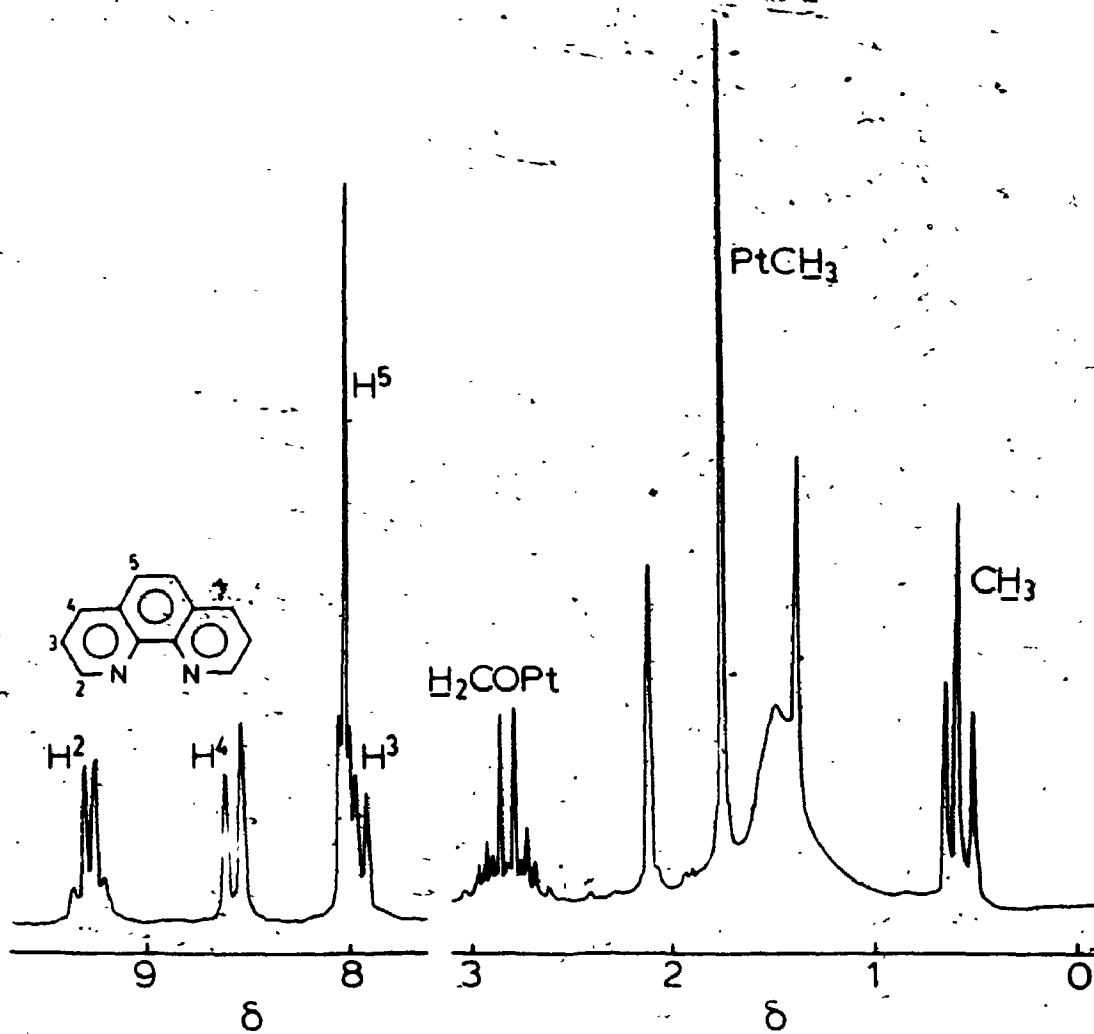


FIGURE 2.2: ^1H NMR Spectrum (100 MHz) of $[\text{PtMe}_2(\text{OEt})(\text{phen})(\text{H}_2\text{O})][\text{OH}]$ in CD_2Cl_2 .

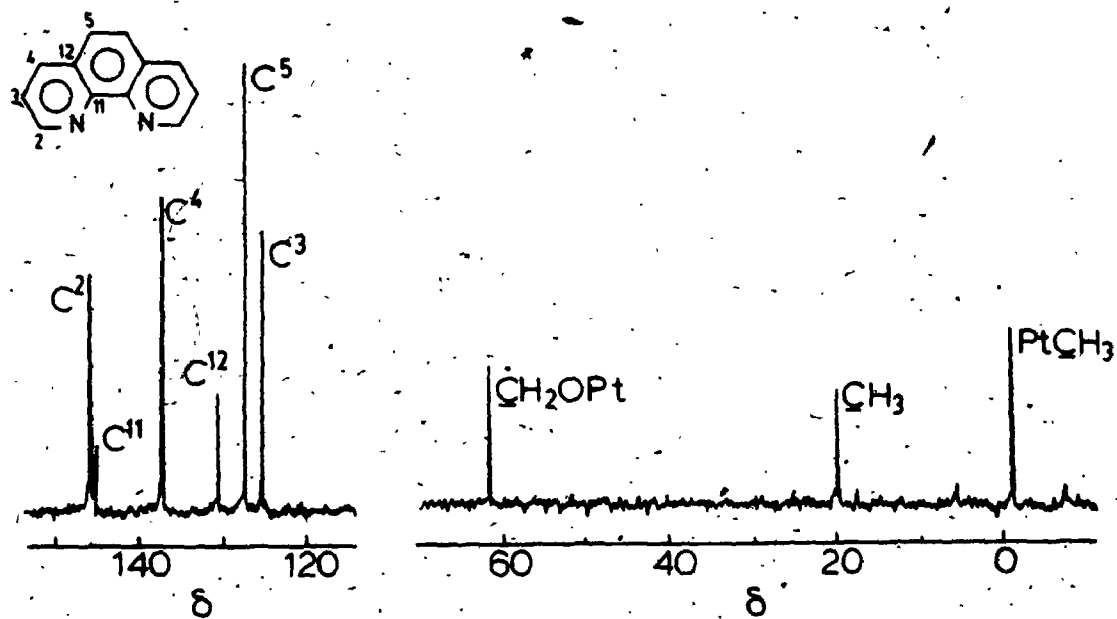


FIGURE 2.3: $^{13}\text{C}\{^1\text{H}\}$ NMR Spectrum (50 MHz) of $[\text{PtMe}_2(\text{OEt})(\text{phen})(\text{H}_2\text{O})][\text{OH}]$ in CD_2Cl_2 .

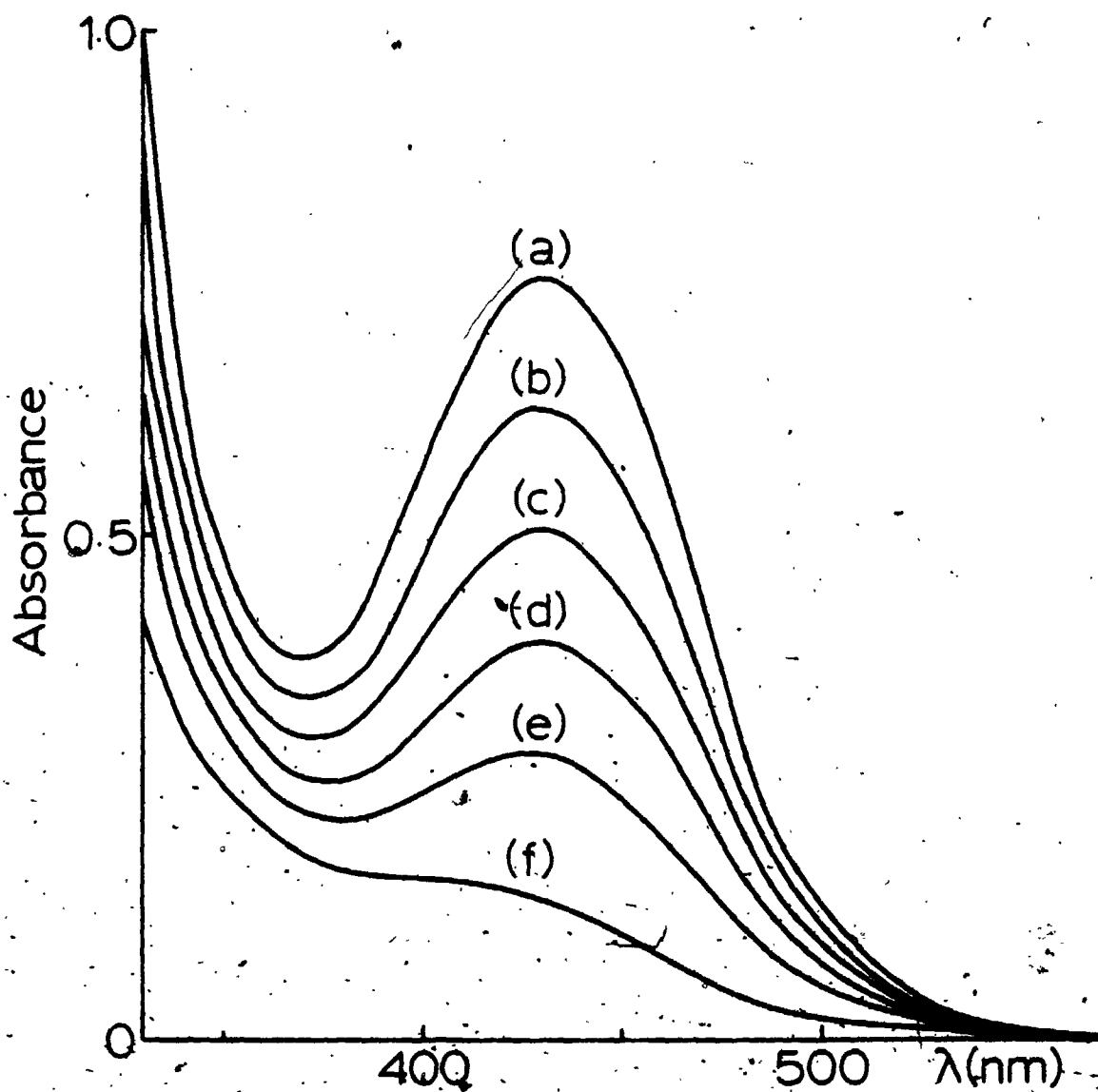


FIGURE 2.4: UV/Visible Spectra of $[PtMe_2(bipy)]$ (10^{-6} M) in Ethanol at 21°C.
a) $t = 0$; b) $t = 23$ min; c) $t = 48$ min;
d) $t = 78$ min; e) $t = 119$ min;
f) $t = 280$ min.

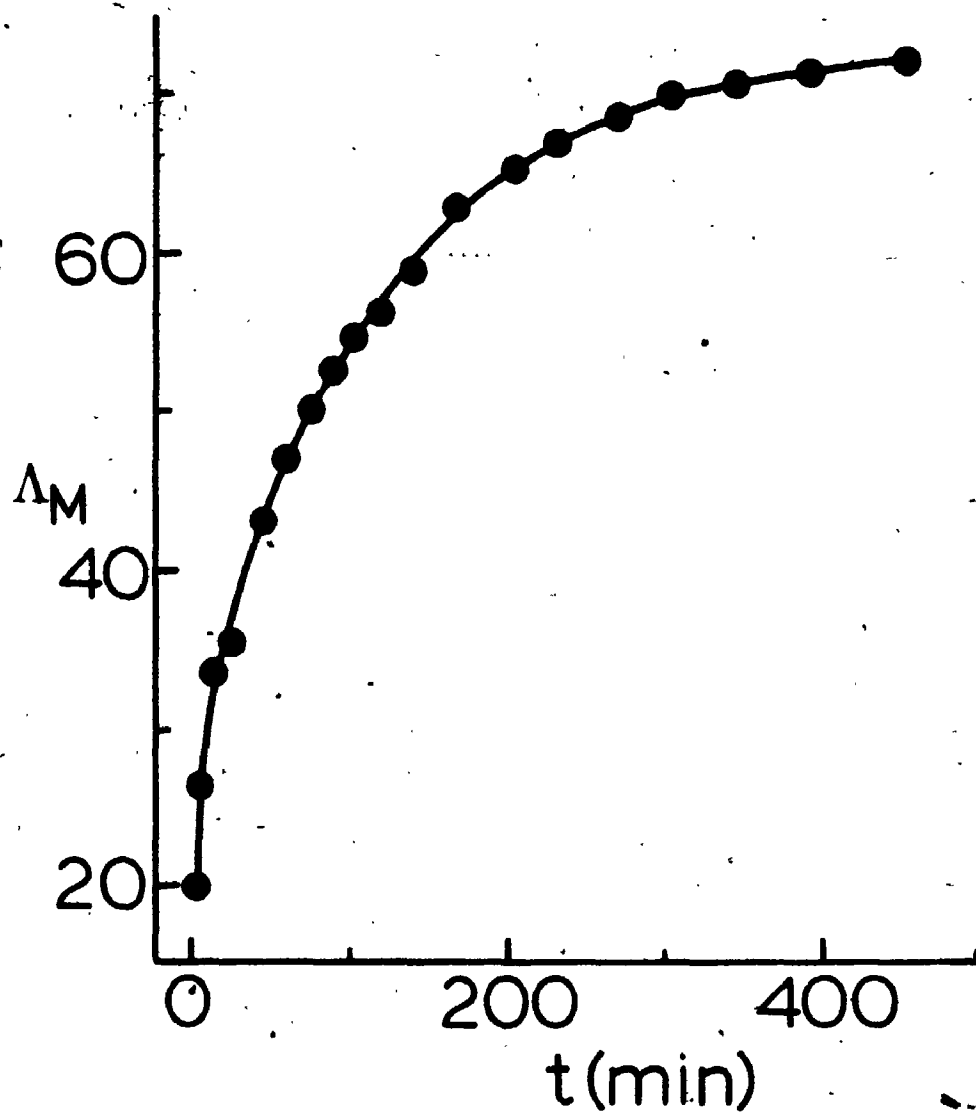
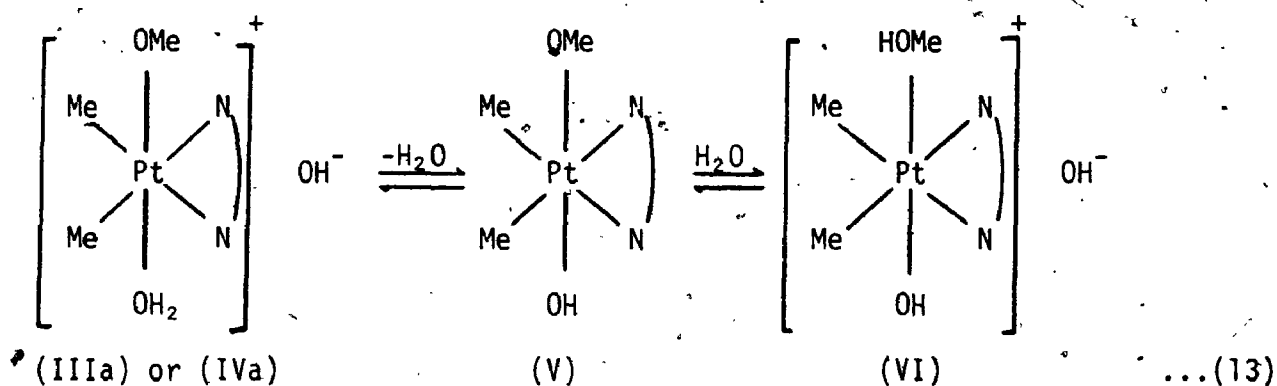


FIGURE 2.5: Molar Conductivity ($\bar{\Lambda}_M$, $\text{cm}^2 \Omega^{-1} \text{mol}^{-1}$) of a Solution of $[\text{PtMe}_2(\text{bipy})]$ (10^{-3} M) in Methanol as a Function of Time.

value of $\Lambda_M \cong 76.5 \text{ cm}^2 \Omega^{-1} \text{ mol}^{-1}$, in the range (though towards the low end) expected for a 1:1 electrolyte.⁵⁸ For example, LiCl (10^{-3} M) gave $\Lambda_M = 88 \text{ cm}^2 \Omega^{-1} \text{ mol}^{-1}$ in methanol. The complex $[\text{PtMe}_2(\text{OMe})(\text{bipy})\text{H}_2\text{O}][\text{OH}]$ was reacted with a series of non-coordinating anions (ClO_4^- , BPh_4^- , PF_6^-). The ^1H nmr spectra of the isolated products were the same as the starting material, within experimental error. The incorporation of the non-coordinating anions was clearly shown by the ir spectra.

An equilibrium of the form shown in equation (13) might be expected, but the isomeric form (IIIa) must be favoured.



If (VI) were formed, exchange of co-ordinated MeOH with CD_3OD or D_2O would be expected in (IIIa), but was not observed. However, the equilibrium $(\text{IIIa}) \rightleftharpoons (\text{V})$ may explain why the conductivity is somewhat lower than a typical 1:1 electrolyte. It follows from the proposed equilibrium (III) or $(\text{IV}) \rightleftharpoons (\text{V})$ that complexes (IIIa)-(IIIc) or (IVa)-(IVc) should act as bases. This was confirmed. A 10^{-2} M solution of (IVb) in ethanol had $\text{pH} = 10.3$ indicating that it is a somewhat stronger base than sodium acetate ($\text{pH} = 9.3$ at 10^{-2} M). The solution of (IVb) could be titrated in a 1:1 molar ratio with dilute HCl solution. Figure 2.6 shows a plot of pH versus volume of HCl(aq) added. A blank was run in which the HCl was titrated against pure ethanol. The pH change of the EtOH was dramatic for a very small initial volume of HCl added. An inflection occurs in

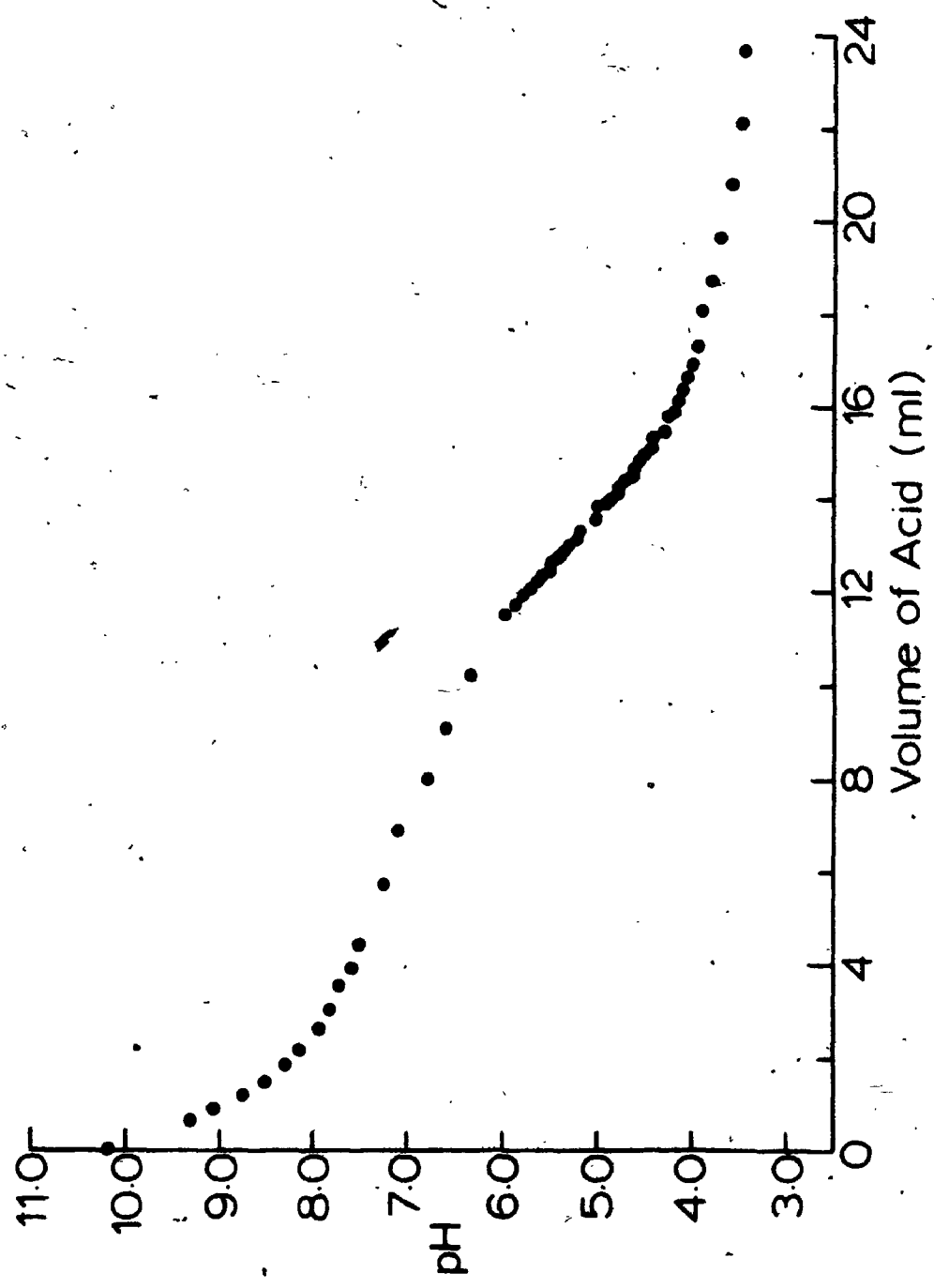
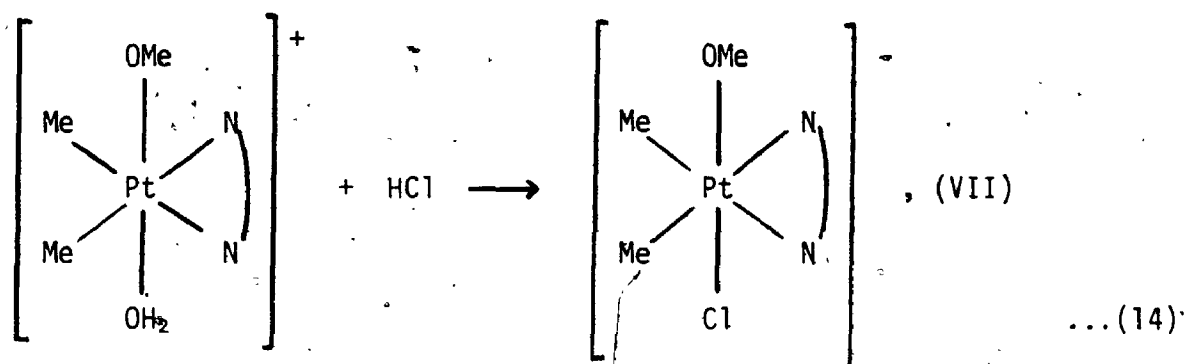


FIGURE 2.6: Plot of pH Versus Volume of Acid (mL) for the Titration of $[\text{PtMe}_2(\text{OEt})(\text{phen})(\text{H}_2\text{O})][\text{OH}]$ (0.01 M) with Aqueous HCl (0.02 M).

the portion of the curve (12-14 mL) where the equivalence point would be expected for a 1:1 molar ratio reaction.

v) The chief problem in characterisation at this stage was to confirm the presence of the H_2O or HO^- ligand on platinum. This is difficult to do directly, as already shown by others.^{12,28,45,48} The most direct evidence came from a reaction of (IVa) in methanol with an equimolar amount of anhydrous HCl , giving the reaction of equation 14.

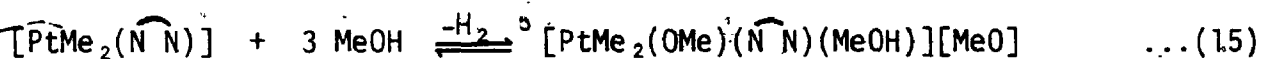


The product (VII) was sufficiently volatile to give a parent ion in the electron impact mass spectrum. The m/e values for the ^{195}Pt , ^{35}Cl isotopomers are given in Table 7.19. From the natural abundance of the isotopes of Pt, Cl, C and H the intensities of the signals can be calculated. The experimental intensities are given below with the calculated intensities in parentheses; 468, 0.02 (0.02); 470, 0.82 (0.78); 471, 0.94 (0.84); 472, 1.00 (1.00); 473, 0.41 (0.42); 474, 0.42 (0.42); 475, 0.07 (0.07); 475, 0.06 (0.06); 477, 0.01 (0.01). Except for complex (IVa), which showed a parent ion at $m/e = 454$ (^{195}Pt , ^{35}Cl isotopomer) the rest of the alkoxo-complexes gave fragmentation patterns in the mass spectra which gave no structural information. The ^1H nmr spectrum of (VII) (Table 7), was very similar to that of (IVa) except that the coupling $^3\text{J}(\text{PtH}) = 58$ Hz, associated with the $^{\text{Me}}\text{OPt}$ group was higher than for (IVa), with $^3\text{J}(\text{PtH}) = 41$ Hz, due to the lower *trans*-influence of chloride.⁴⁹

Treatment of (IIIa) or (IVa) with lithium chloride in methanol or with aqueous HCl solution gave mixtures of complexes which could not be separated.

Since the chloride ligand in (VII) is definitely present, it follows that there must be a ligand OH_2 or OH^- *trans* to the methoxo group in complexes (III) and (IV).

vi) The stoichiometry of the reaction requires that hydrogen should be formed, and this was confirmed, for the reaction of (II) with methanol, by g.c. analysis. Thus the initial reactions are described by equation 15.



^1H nmr spectra of products obtained by removing solvent from crude reaction mixtures, show additional methoxo-resonances which are not present after purification by repeated precipitations. We suggest that the coordinated MeOH and free methoxide undergo rapid exchange with adventitious water to give complexes (IIIa) or (IVa), during the work-up procedure.

The isopropoxo-complexes of (I) and (II) were characterised by the ^1H nmr spectra and by elemental analysis. Complex (II) was reacted with $t\text{BuOH}$ in acetone. The reaction was slow but eventually oxidation of platinum(II) to platinum(IV) occurred, as indicated by the colour change from red to yellow and by the new MePt peak in the ^1H nmr spectrum at $\delta 1.2$ with $^2\text{J}(\text{PtMe})$ equal to 62 Hz. It was not possible, however, to characterise the mixture of products.

The reaction between benzyl alcohol and (II) was also slow. A yellow solution was produced after several days. It was not easy to

remove the product due to the high boiling point of the alcohol. The product was not fully characterised. There does appear, however, to be at least two products. The ^1H nmr spectrum contains two MePt peaks at 1.86 ppm and 1.80 ppm with $J(\text{PtH})$ equal to 73 Hz in each case. This is clear indication of oxidation of platinum(II) to platinum(IV). A peak at 4.00 ppm could be assigned to the $-\text{CH}_2$ group of the phenylmethoxy-group. The signal has ^{195}Pt satellites with $^3J_{\text{PtH}}$ of 51 Hz. This coupling is however considerably larger than for the $-\text{CH}_2$ group of (IIIb) and (IVb), and the $-\text{CH}_3$ group of (IIIa) and (IVb). There is a complex resonance pattern in the low field region which may be due to the phenyl ring of the phenylmethoxy-complex.

2.3.2 Rates of Reactions with Alcohols

Complexes (I) and (II) are coloured due to a MLCT band in the visible region. For (II), in methanol, λ_{max} is at 416 nm and in methanol λ_{max} is at 423 nm.

A solution of $[\text{PtCl}_2(\text{phen})]$ in methanol (10^{-4} M) was prepared and part of the solution immediately transferred to a 1 cm quartz cuvette in the cell compartment of the spectrophotometer. The decay of the absorption at 416 nm was measured with time. A plot of $\log(A_t - A_\infty)$ versus time (where A_t is absorbance at time t , A_∞ = absorbance at completion of reaction) gave a good straight line plot (Fig. 2.7), from which the observed rate constant (Table 2.1) was calculated. The same method was used to obtain the results in Table 2.1. It can be seen that complexes (I) and (II) are very similar in reactivity and that the reactivity of the alcohols follows the series $\text{MeOH} > \text{EtOH} > \text{PrOH}$. This is the same as the series of acidities, $\text{p}K_a$, of the alcohols. ⁵⁹ The

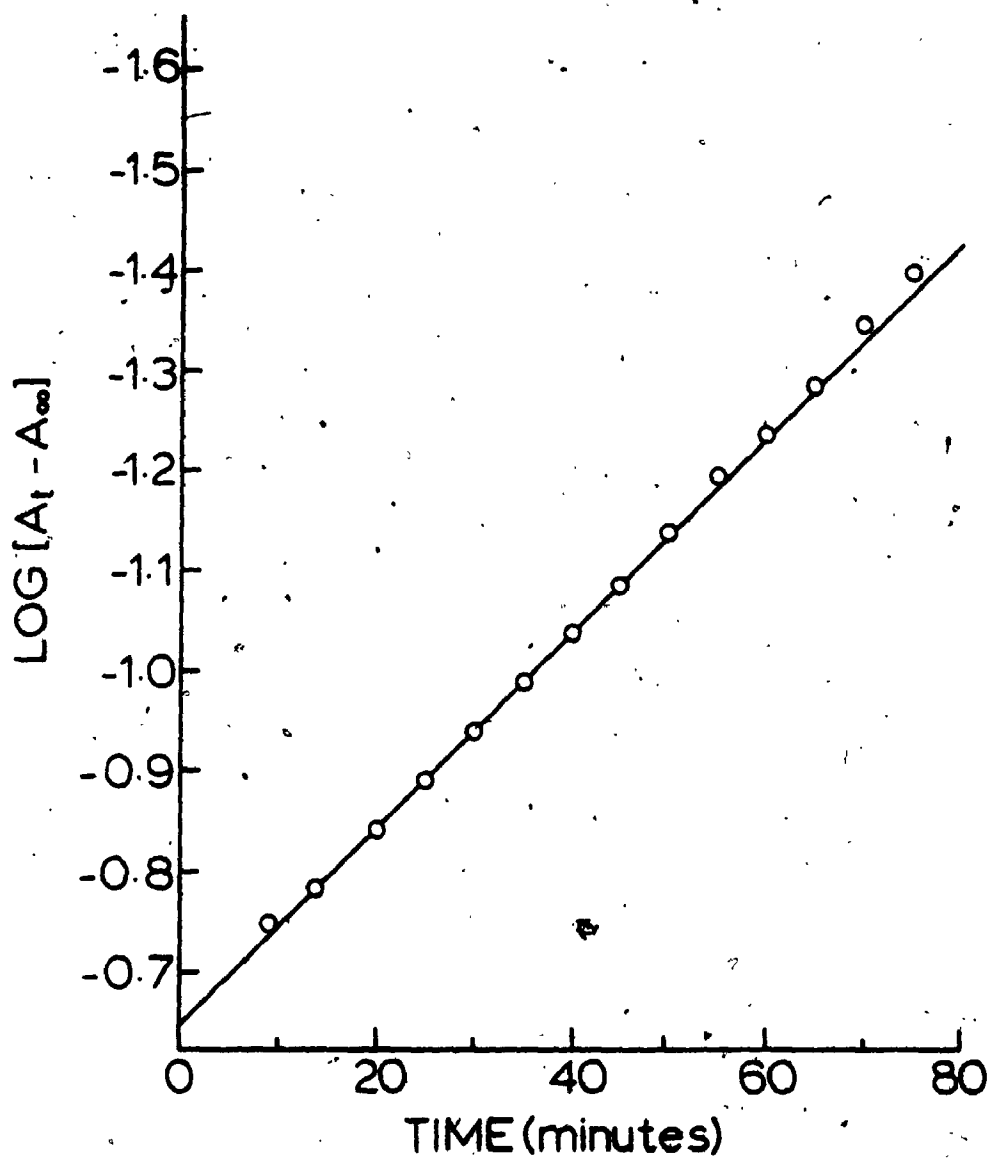


FIGURE 2.7: Plot of $\text{Log}(A_t - A_\infty)$ Versus Time (Min) for the Reaction between (II) (1×10^{-4} M) with Methanol, at 21°C .

TABLE 2.1: Observed First-Order Rate Constants for Reaction of I or II with Alcohols at 21°C^a

Complex	Alcohol	λ/nm^b	$10 k_{\text{obsd}}/s^{-1}c$
I	MeOH	430	3.3
I	EtOH	430	1.6
I	iPrOH	430	0.45
II	MeOH	416	3.85
II	EtOH	423	1.8

^aUsing alcohols as solvent.

^bWavelength used to monitor reactions.

^cObserved first-order rate constants.

rate of reaction of $[\text{PtMe}_2(\text{bipy})]$ with methanol was not affected by the presence of NaI ($4 \times 10^{-2} \text{ M}$) or LiCl ($2 \times 10^{-2} \text{ M}$). It was thought that prior coordination of I^- to (I) would activate the platinum centre towards attack on MeOH . This is shown not to be the case, nor was any iodo-complex found in the reaction product.

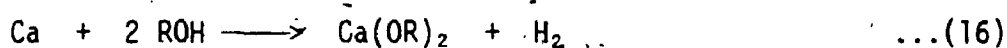
2.3.3 Reactions with Water

When a solution of (I) or (II) in acetone was treated with distilled water the colour of the solution became pale yellow. After standing for several hours a pale yellow product was extracted in each case. The complexes analysed as $[\text{PtMe}_2(\text{OH})(\widehat{\text{N N}})(\text{OH}_2)][\text{OH}]$ (VIII, $\widehat{\text{N N}} = \text{bipy}$; IX, $\widehat{\text{N N}} = \text{phen}$) and, by analogy with the alcohol reactions described above, they are formulated in this way. The ^1H nmr of (VIII) shows a MePt signal at 1.84 with $^2J_{\text{PtH}}$ equal to 70 Hz. It is clear that the methyl groups are still equivalent and that oxidative addition has occurred. Similar conclusions can be drawn for (IX). A broad peak occurs for (IX) at 1.07 ppm which could be assigned to an OH group. The derivative $[\text{PtMe}_2(\text{OH})(\text{bipy})(\text{OH}_2)][\text{PF}_6]_3$ (X), was prepared and the ^1H nmr was identical to that of (VIII). It is significant that there are none of the typical broad signals in the high field region of the spectrum of (X), a good indication that these are due to the OH^- ion.

Complex (II) was reacted with D_2O and its ^2H nmr spectrum shows a broad resonance at 1.1 ppm. This is most likely the OD group analogous to the OH in (IX) since deuterium chemical shifts, in ppm, are essentially the same as those of the analogous ^1H isotope.⁶⁰

2.3.4 Conclusions

The platinum(IV) alkoxides described here are the first to be synthesised and characterised. They possess several unusual features. Oxidative addition of alcohols to platinum(II) would normally be expected to result in protonation of the metal with alkoxide as either weakly bonded or present as the counterion.¹² Certainly, oxidative addition of water to platinum(0) gives this sort of product.⁴⁵ If a platinum hydride were to form, elimination of CH₄ would be expected. Little or no CH₄ was detected by g.c. in the reaction between (I) and methanol. It should be noted that treatment of [PtMe₂(N N)] with acids leads to formation of CH₄ from an intermediate thought to be formed by oxidative addition,⁶¹ [PtMe₂H(N N)]⁺. Another alternative is that the alkoxo-hydride, [PtMe₂(OR)H(N N)], does form followed by rapid reaction of the hydridic Pt-H group with protic solvent. However, there is an obvious parallel with the reactions of alkali and alkaline earth metals with alcohols (e.g. equation 16), and it is also possible that a similar electron transfer mechanism operates.⁶²



Perhaps most remarkable is the inertness of the Pt-OR bond in the products (III) and (IV). This group fails to undergo exchange with free alcohol and is also inert to hydrolysis by water or by dilute perchloric acid. These properties are extremely unusual in metal alkoxides, and must be attributed to the general kinetic inertness of platinum(IV) complexes. It was considered that alcohol might attack at the N N ligand, rather than at the metal, as suggested by Gillard,⁵⁴ but challenged by others.⁶³⁻⁶⁵ However the nmr data are not consistent with this formation. In reactions with CD₃OD, no H-D exchange between the

bipy, phen and alcohol was observed.⁶⁶

The platinum(IV) hydroxo-complexes are among the few that have been synthesised and characterised,^{40,41} and as far as we know, the first to be prepared directly from water. It is unusual that a hydrido-hydroxo complex could not be isolated, but instead an aquo-(hydroxo)complex.

The detailed mechanisms of the reactions discussed in this chapter are not fully understood. In the case of the alcohols, it would appear that their relative acidity (i.e. ease of loss of proton) is an important factor in determining the rate of reaction.

REFERENCES

1. Ebelman, J.J.; Bouquet, M., *Ann. Chim. Phys.*, 1846, 17, 54.
2. Ebelman, J.J.; *Ann. Chim. Phys.*, 1846, 57, 331.
3. Bradley, D.C.; Mehrota, R.C.; Gaur, D.P., "Metal Alkoxides", 1978, Academic Press, London, New York, San Francisco.
4. Mehrota, R.C., *Advances Inorg. Chem. and Radiochem.*, 1983, 26, 269.
5. Pearson, R.G.; *J. Am. Chem. Soc.*, 1963, 85, 3533.
6. Davies, J.A.; Hartley, F.R.; *Chem. Rev.*, 1981, 81, 79.
7. Huheey, J.E.; "Inorganic Chemistry", 1978, 2nd Edition, Harper and Row, New York, Hagerstown, San Francisco, London.
8. Aholand, S.; Chatt, J.; Davies, N.R.; *Quart. Rev. Chem. Soc.*, 1958, 12, 265.
9. Navrotsky, A.; "M.T.P. International Review of Sciences", Series Two; Sharp, D.W.A.; Ed., University Park Press: Baltimore, 1975; Vol. 5, Chapter 2.
10. Coffindaffer, T.W.; Rothwell, I.P.; Huffman, J.C.; *Inorg. Chem.*, 1983, 22, 2906.
11. Ivanova, O.M.; Gellman, A.D.; *Zhur. Neorg. Khim.*, 1958, 3, 1334.
12. Bennett, M.A.; Robertson, G.B.; Whimp, P.O.; Yoshida, T., *J. Am. Chem. Soc.*, 1973, 95, 3028.
13. Yoshida, T.; Okano, T.; Otsuka, S.; *J. Chem. Soc., Dalton Trans.*, 1976; 993.
14. Chatt, J.; Shaw, B.L.; *J. Chem. Soc.*, 1962, 5075.
15. Clark, H.C.; Goel, A.B.; *J. Organomet. Chem.*, 1979, 178, C27.

16. Goel, A.B.; Goel, S.; *Trans. Met. Chem.*, 1980, 5, 378.
17. Bonatt, F.; Clark, H.C.; Wong, C.S.; *Can. J. Chem.*, 1980, 58, 1435.
18. Michelin, R.A.; Massimo, N.; Ros, R.; *J. Organomet. Chem.*, 1979, 175, 239.
19. Giordano, F.; Vitagliano, A.; *Inorg. Chem.*, 1981, 20, 633.
20. Goel, A.B.; Goel, S.; Vanderveer, G.D.; *Inorg. Chim. Acta.*, 1981, 54, L169.
21. Akiyama, M.; Chisholm, M.H.; Cotton, F.A.; Estine, M.W.; Haitko, D.A.; Leonelli, J.; Little, D.; *J. Am. Chem. Soc.*, 1981, 103, 779.
22. Chiu, K.W.; Jones, R.A.; Wilkinson, G.; Galas, A.M.R.; Hursthouse, M.B.; Abdul Malik, M.K.; *J. Chem. Soc., Dalton Trans.*, 1981, 1204.
23. Azam, K.A.; Deeming, A.J.; Kimber, R.E.; Shukla, P.R.; *J. Chem. Soc., Dalton Trans.*, 1976, 1853.
24. Siedle, A.R.; Pignolet, L.H.; *Inorg. Chem.*, 1982, 21, 3090.
25. Farrugia, L.; Green, M.L.H.; *J. Chem. Soc. Chem. Comm.*, 1975, 416.
26. Chatt, J.; Shaw, B.L.; *Chem. Ind.*, 1960, 931; 1961, 290.
27. Vaska, L.; *J. Am. Chem. Soc.*, 1961, 83, 756.
28. Bennett, M.A.; Yoshida, T.; *J. Am. Chem. Soc.*, 1978, 100, 1750.
29. Clark, H.C.; Billard, C.; Wong, C.S.; *J. Organomet. Chem.*, 1979, 173, 34.
30. Isnard, P.; Denise, B.; Sneed, R.P.A.; Cognion, J.M.; Dural, P.; *J. Organomet. Chem.*, 1982, 240, 169 and references therein.
31. Paulik, F.E.; Roth, J.F.; *J. Chem. Soc. Chem. Comm.*, 1968, 1578.
32. Forster, D.; *Advan. Organomet. Chem.*, 1979, 17, 255.
33. Werner, A.; "New Ideas on Inorganic Chemistry", Longmans, Green and Co., London, 1911.
34. *Gmelins Handbuch der Anorganische Chemie*, 1942, Vol. 65, and 1957, Vol. 68.

35. Chatt, J.; Heaton, B.T.; J. Chem. Soc., A, 1968, 2745.
36. Bushnell, G.W.; Dixon, K.R.; Hunter, R.G.; McFarland, J.J.; Can. J. Chem., 1972, 50, 3694.
37. Appleton, J.G.; Bennett, M.A.; J. Organomet. Chem., 1973, 55, C88.
38. Appleton, J.G.; Bennett, M.A.; Inorg. Chem., 1978, 17, 738.
39. Ros, R.; Michelin, R.A.; Bataillard, R.; Roulet, R.; J. Organomet. Chem., 1978, 161, 75.
40. Britten, J.F.; Lippert, B.; Lock, C.J.L.; Pilon, P.; Inorg. Chem., 1982, 21, 1936 and references therein.
41. Faggiani, R.; Lock-Howard, H.E.; Lock, C.J.L.; Lippert, B.; Rosenberg, B.; Can. J. Chem., 1982, 60, 529.
42. Agnew, N.H.; Appleton, T.G.; Hall, J.R.; Kilmister, G.F.; McMahon, I.J.; J. Chem. Soc. Chem. Comm., 1979, 324.
43. Bhaduri, S.; Raithby, R.R.; Zuccano, C.I.; Hursthouse, M.B.; Casella, L.; Ugo, R.; J. Chem. Soc. Chem. Comm., 1978, 991.
44. Bigozzi, C.A.; Bartocci, C.; Maldolti, A.; Carassiti, V.; Inorg. Chim. Acta., 1982, 62, 187.
45. Yoshida, T.; Matsuda, T.; Okano, T.; Kitani, T.; Otsuka, S.; J. Am. Chem. Soc., 1979, 101, 2027.
46. Yoshida, T.; Okano, T.; Saito, K.; Otsuka, S.; Inorg. Chim. Acta., 1980, 44, L135.
47. Yoshida, T.; Okano, T.; Otsuka, S.; J. Am. Chem. Soc., 1980, 102, 5967.
48. Yoshida, T.; Okano, T.; Otsuka, S.; J. Am. Chem. Soc., 1981, 103, 3411.
49. Arnold, D.P.; Bennett, M.A.; J. Organomet. Chem., 1980, 199, 119.
50. Chaudhury, N.; Puddephatt, R.J.; Organomet. Chem., 1975, 84, 105.

51. Jawad, J.K.; Puddephatt, R.J.; *J. Organomet. Chem.*, 1976, 117, 297;
ibid., *J. Chem. Soc., Dalton Trans.*, 1977, 1466.
52. Monaghan, P.K.; Puddephatt, R.J.; *Inorg. Chim. Acta.*, 1983, 76, L237.
53. Saito, T.; Aiki, M.; Uchida, Y.; Misono, A.; *J. Phys. Chem.*, 1967,
71, 2370.
54. Gillard, R.D.; Lyons, J.R.; *J. Chem. Soc. Chem. Comm.*, 1973, 585.
Bielli, E.; Gillard, R.D.; James, R.W.; *J. Chem. Soc., Dalton Trans.*,
1976, 1837. Bielli, E.; Gidney, P.M.; Gillard, R.D.; Heaton, B.T.;
J. Chem. Soc., Dalton Trans., 1974, 2133. Gillard, R.D.; Co-ord.
Chem. Rev., 1975, 16, 67. Al-Obaidi, K.H.; Gillard, R.D.; Kane-
Maguire, L.A.P.; Williams, P.A.; *Transition Met. Chem.*, 1977, 2, 64.
55. Farver, O.; Monsted, O.; Nord, G.; *J. Am. Chem. Soc.*, 1979, 101,
6118.
56. Wernberg, O.; Hazell, A.; *J. Chem. Soc., Dalton Trans.*, 1980, 973.
57. Konnecke, A.; Lippmann, E.; Mlochowski, J.; Silwa, W.; *Org. Mag.*
Res., 1979, 12, 696.
58. Geary, W.J.; *Co-ord. Chem. Rev.*, 1971, 7, 81.
59. Lowry, T.H.; Richardson, K.S.; "Mechanism and Theory in Organic
Chemistry", Harper and Row, New York, 1981, pp. 262-267. Hine, J.;
Hine, M.; *J. Am. Chem. Soc.*, 1952, 74, 5266.
60. Mantsch, H.H.; Saito, H.; Smith, I.C.P., *Prog. NMR Spectroscopy*,
1977, 11, 211.
61. Jawad, J.K.; Puddephatt, R.J.; *Inorg. Chim. Acta.*, 1978, 31, L391.
62. Hughes, G.; Lobb, C.R.; "Comprehensive Chemical Kinetics", 1976,
Vol. 18, Ch. 7; Ed. Bamford, C.H.; Tipper, C.F.H., Elsevier,
Amsterdam.
63. Farver, O.; Monsted, O.; Nord, G.; *J. Am. Chem. Soc.*, 1979, 101, 6118.

64. Wernberg, O.; Hazell, A.; J. Chem. Soc., Dalton Trans., 1980, 973.
65. Spellane, P.J.; Watts, R.J.; Inorg. Chem., 1981, 20, 356T.
66. Constable, E.C.; Seddon, K.R.; J. Chem. Soc., Chem. Comm., 1982, 34.
67. Hutton, A.T.; Shalbanzadeh, B.; Shaw, B.L.; J. Chem. Soc. Chem. Comm., 1983, 1053.
68. Halpern, J.; Acc. Chem. Res., 1982, 332.

CHAPTER 3

OXIDATIVE ADDITION OF PRIMARY ORGANIC MONOHALIDES TO A DIMETHYLPLATINUM(II) COMPLEX

1. INTRODUCTION

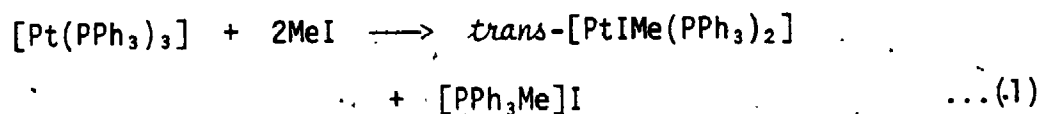
This chapter deals with the oxidative addition of primary organic monohalides, RX, to $[\text{PtMe}_2(\text{phen})]$, (II). The product in all cases was a platinum(IV) adduct $[\text{PtXMe}_2(\text{R})(\text{phen})]$, with the groups R and X *trans* to one another. The kinetics were found to be second order overall, corresponding to a rate expression

$$-\frac{d[\text{II}]}{dt} = k_2[\text{II}][\text{RX}]$$

The literature survey, presented below, will deal mainly with the oxidative addition of primary organic halides to transition-metal centres.

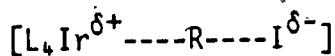
2. LITERATURE SURVEY

Since the late 1950's there has been extensive work in the area of oxidative addition of organic halides to transition-metal centres.¹⁻⁴ Oxidative addition has proven to be a very versatile method for forming metal-carbon bonds, and is an important step in catalytic cycles such as hydrogenation of olefins,³ and carbonylation of methanol to form acetic acid⁵ (Monsanto Process). Malatesta,⁶ who was the first to prepare platinum(0) complexes, used methyl iodide to prepare platinum(II) complexes, as shown in equation 1.

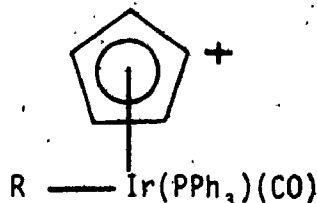


Chatt is responsible for a lot of the early synthetic work in preparing platinum(IV) complexes, by reacting methyl iodide with platinum(II) phosphine complexes.⁷ Since then, a series of low valent (Rh^{I} , Ir^{I} , Pt^{0}) transition-metal complexes have been reacted with similar primary organic halides, to give new metal-alkyl, and metal-allyl complexes.

The mechanism of oxidative addition has been the source of much debate. Currently three mechanisms are believed to be operative in oxidative addition reactions. The reaction can go *via* an $\text{S}_{\text{N}}2$ type attack of the nucleophilic metal at the carbon-halogen bond. This would lead to inversion of configuration at the carbon centre. This type of mechanism was first postulated by Halpern⁸ for the reaction of methyl iodide, and benzyl halides with Vaska's complex $[\text{IrX}(\text{CO})(\text{PPh}_3)_2]$. He proposed that the large negative entropies of activation and an increased rate in the more polar solvent indicates an increase in polarity in going from reactants to the transition state as shown below.

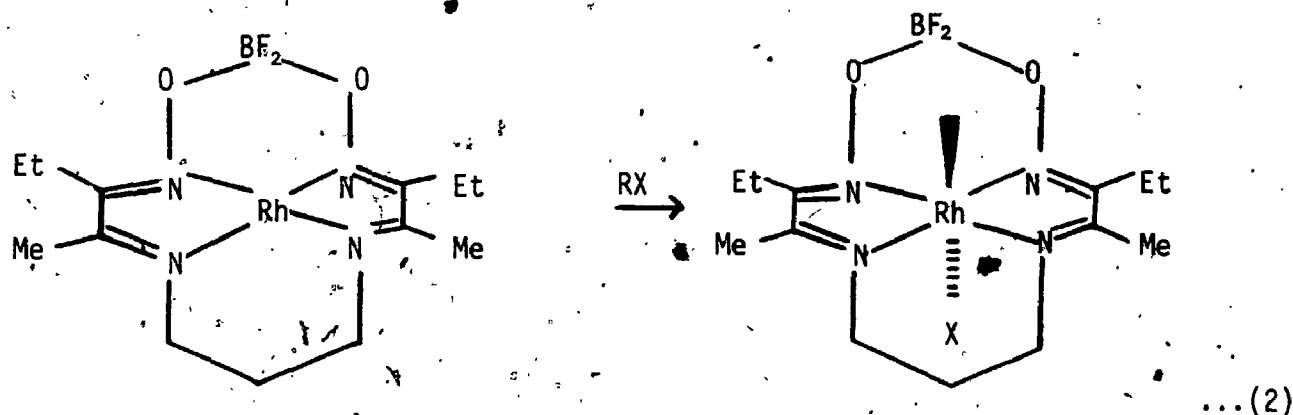


Additional support⁹ for the $\text{S}_{\text{N}}2$ displacement has been obtained from the isolation of ionic intermediates such as the one shown below.



$\text{R} = \text{CH}_3, \text{PhCH}_2.$

Collman has carried out a study¹⁰ on the structure-reactivity relationship on a rhodium complex showing orders of reactivity, $R = \text{CH}_3 > \text{CH}_3\text{CH}_2 > \text{secondary} > \text{cyclohexyl} > \text{adamantyl}$ and $X = \text{I} > \text{tosylate} \sim \text{Br} > \text{Cl}$ (eq. 2).



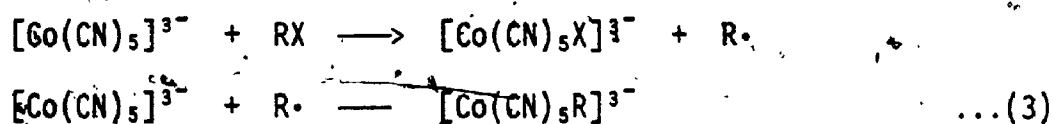
This implies an S_N2 attack by the rhodium centre at carbon.

A series of very elegant experiments has been reported by Stille¹¹⁻¹⁴ involving the use of optically active organic halides and their oxidative addition to palladium(0). The absolute configurations of the products of oxidative addition¹¹ of optically active benzyl-d-chloride and bromide to $[\text{Pd}(\text{PEt}_3)_3]$ were determined using a carbonylation and cleavage with Cl_2/MeOH to produce the corresponding methyl esters. In both cases inversion of configuration was observed.

A second mechanism whereby oxidative addition can take place is a concerted three-centred transition state. This would be expected to go with retention of configuration at the carbon. It has been argued¹⁵ that large negative entropies of activation and enhanced rates in polar solvent can equally well be due to a mechanism such as this. However, there do not appear to be any reports in the literature for organic halides, in which this mechanism has been shown to operate.

The intermediacy of free-radicals in oxidative addition was first suggested by Halpern¹⁶ for the reaction of a series of alkyl and

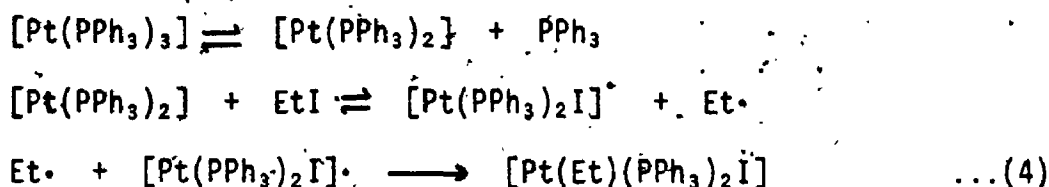
benzyl halides with $[\text{Co}(\text{CN})_5]^{3-}$. The mechanism of the reaction is shown in equation 3.



This can be described as a radical non-chain mechanism. The rate determining step is the abstraction of a halogen atom by $[\text{Co}(\text{CN})_5]^{3-}$ to generate an organic free-radical. Similar results were obtained by Kwiatek and Seyler.¹⁷

In 1972 Osborn¹⁸ published work on the oxidative addition of some primary halides to $[\text{IrCl}(\text{CO})(\text{PMe}_3)_2]$. He claimed that a free-radical chain path was operative. This was the first claim that oxidative addition for organic halides could go via such a mechanism. For methyl iodide an alternative mechanism was believed to exist, since radical inhibitors had no effect on its reaction rate with the iridium complex. In 1980 two important papers¹⁹ appeared in which Osborn discusses the various factors which can help to demonstrate the intermediacy of free-radicals - loss of stereochemistry at the carbon attacked, sensitivity to radical initiators and inhibitors, structural effects upon reactivity (tertiary > secondary > primary alkyl halide) and the trapping of radicals by acrylonitrile.

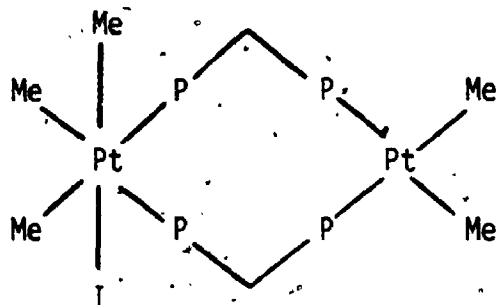
The alternative non-chain radical mechanism was proposed by Lappert²⁰ for the reaction of $[\text{Pt}(\text{PPh}_3)_n]$ ($n = 3$ or 4) with methyl and ethyl iodide. This conclusion was based on esr experiments in the presence of spin-traps. The proposed pathway is shown below for ethyl iodide (eq. 4).



The rate-determining step is believed to be the homolytic abstraction of the iodine atom by the platinum starting material. There has been much debate as to how this occurs. In some systems it is believed that the oxidative addition is initiated by electron transfer from the metal centre to the organic halide. Lappert presents this as a possibility in his work.²⁰ Connor^{21,22} has proposed such a transfer for the oxidative addition of benzyl bromide to *cis*-[Mo(CO)₂(Me₂PCH₂CH₂PMe₂)₂]. In a recent piece of work²³ a series of complexes have been isolated or detected in solution, of the general formula [IrH₂(RX)_n(PPh₃)₂]⁺ (RX = MeI, EtI, C₆H₄I₂, etc., n = 1 or 2) in which the halocarbon bonds to iridium through the halogen atom. Such complexes provide models for probable intermediates in oxidative addition of RX to metal centres in which halogen abstraction occurs (eq. 5).



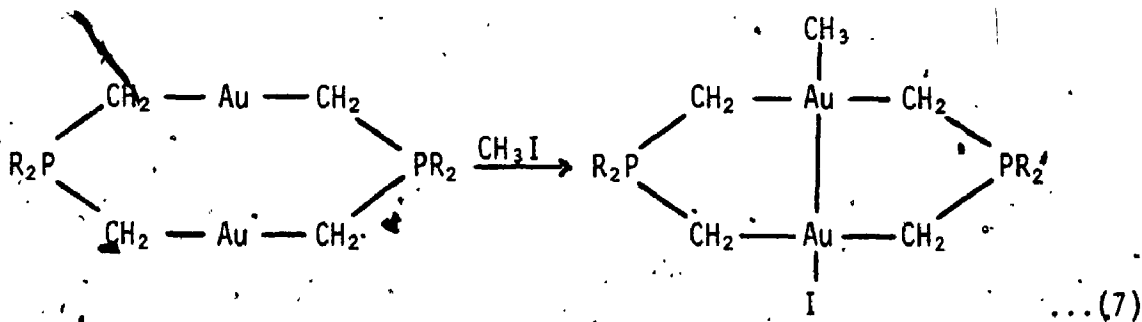
Oxidative addition to binuclear species has not been so extensively studied and the mechanistic features are not as well understood.^{24,25} Puddephatt²⁶ was able to synthesise a mixed Pt^{II}/Pt^{IV} bridging diplatinum complex by the oxidative addition of methyl iodide to [Me₂Pt(μ-dmpm)₂PtMe₂] (dmpm = Me₂PCH₂PMe₂) according to equation 6.



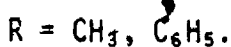
... (6)

Oxidative addition of methyl iodide to $[\text{Rh}_2(\mu\text{-S}^t\text{Bu})_2(\text{CO})_2(\text{PMe}_2\text{Ph})_2]$ ²⁷ likewise leads to oxidation of only one metal centre, the final product being the acetyl complex $[\text{Rh}_2(\mu\text{-S}^t\text{Bu})_2(\text{CO})(\text{PMe}_2\text{Ph})_2(\text{COCH}_3)\text{I}]$.

A one-electron oxidation²⁸ at each of the gold centres in a binuclear species has been achieved by the addition of MeI. A metal-metal bond is generated by this oxidation (eq. 7).



... (7)



Much of the work in the area of oxidative addition has involved the use of iridium(I), rhodium(I), and platinum(0) complexes. In the case of platinum(II), comparatively little work (particularly mechanistic) has been done. Nyholm²⁹ has synthesised some platinum(IV) complexes by the oxidative addition of Cl_2 to platinum(II) arsine complexes. Chatt⁷ has oxidatively added methyl iodide to $[\text{PtI}(\text{PEt}_3)_2]$ under rather vigorous conditions (100°C for 1 hr) to yield $[\text{PtI}_2\text{Me}_2(\text{PEt}_3)_2]$.

Puddephatt *et al.*³⁰ have looked at the oxidative addition of MeI.

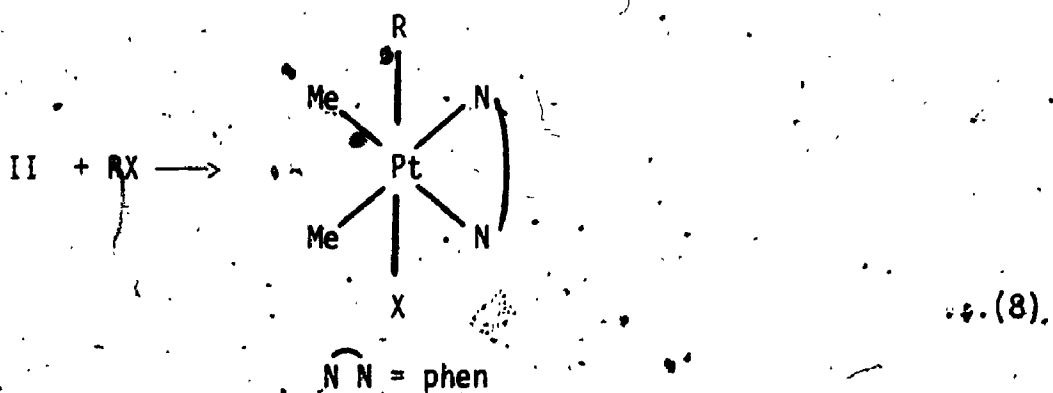
that for these complexes the MLCT band is at lower energy when there is higher electron density at the metal centre, and the reactivity towards oxidative addition is then greater. A solvent effect has also been noted by these authors³¹ for the reaction of MeI with $[\text{Pt}(\text{Ph})_2(\text{bipy})]$. The rate increases with increasing polarity of the solvent, suggesting a polar transition state for the reaction.

The reaction between $p\text{-MeC}_6\text{H}_4\text{SO}_2\text{Cl}$ and $\text{cis-}[\text{PtMe}_2(\text{PMe}_2\text{Ph})_2]$ is inhibited by the presence of a small amount of galvinoxyl, and Lappert²⁰ concludes that a radical-chain mechanism is operative.

3. RESULTS AND DISCUSSION

3.1 Introduction

Complex(II) reacted with a series of primary organic halides in acetone, producing pale yellow solutions. An excess of halide was used, the iodides reacting considerably faster than the bromides. The reactions proceeded in all cases with *trans* addition as shown in equation 8. The products were isolated as pale yellow solids.



XI	a)	R = Me	X = I	e)	R = ⁿ Pr	X = Br
	b)	R = Et	X = I	f)	R = ⁿ Bu	X = I
	c)	R = Et	X = Br	g)	R = CH ₃ (CH ₂) ₄	X = I
	d)	R = ⁿ Pr	X = I	h)	R = CH ₃ (CH ₂) ₆	X = I

A high yield of product was obtained in each case, and characterisation was achieved by elemental analysis and ^1H nmr. Full experimental details are given in Section 2.3 of Chapter 7.

3.2 Elemental Analysis

Good elemental analysis was obtained, consistent with the general formula $[\text{PtXMe}_2(\text{R})(\text{phen})]$. The data are shown in Table 7.16 of Chapter 7.

3.3 ^1H NMR Spectra

The stereochemistry at platinum was established by ^1H nmr spectroscopy. For example, for the complex $[\text{PtIEtMe}_2(\text{phen})]$, (XIb), only one MePt signal is observed (1.63 ppm) indicating that the two Me groups remain equivalent in the product (see Fig. 3.1). The coupling constant $^2J_{\text{PtMe}}$ has decreased from 86.5 Hz in (II) to 71.5 Hz in (XIb) consistent with oxidation of the platinum(II) to platinum(IV).^{30,33} Likewise the coupling between H2 of the phen ring and the platinum is reduced from 21.5 Hz in (II) to 18 Hz in (XIb). A similar change is noted for all the platinum(IV) complexes. The resonances due to the phen protons, although of different chemical shift to those in (II), maintain the same pattern, further indication that complex (XIb) still possesses a plane of symmetry. The methyl protons of the ethyl group show up as a triplet, upfield from the MePt signal. The position of this group above the plane of the aromatic ring results in more shielding.³² The $^3J_{\text{PtH}}$ value for this group is 68.4 Hz. The resonances due to the Pt-CH₂ unit are somewhat obscured by the PtMe signal, but part of the quartet, with its platinum satellites, can be seen. The ^1H nmr data for the EtBr analogue (XIc) are very similar. It was however more difficult to assign the peaks

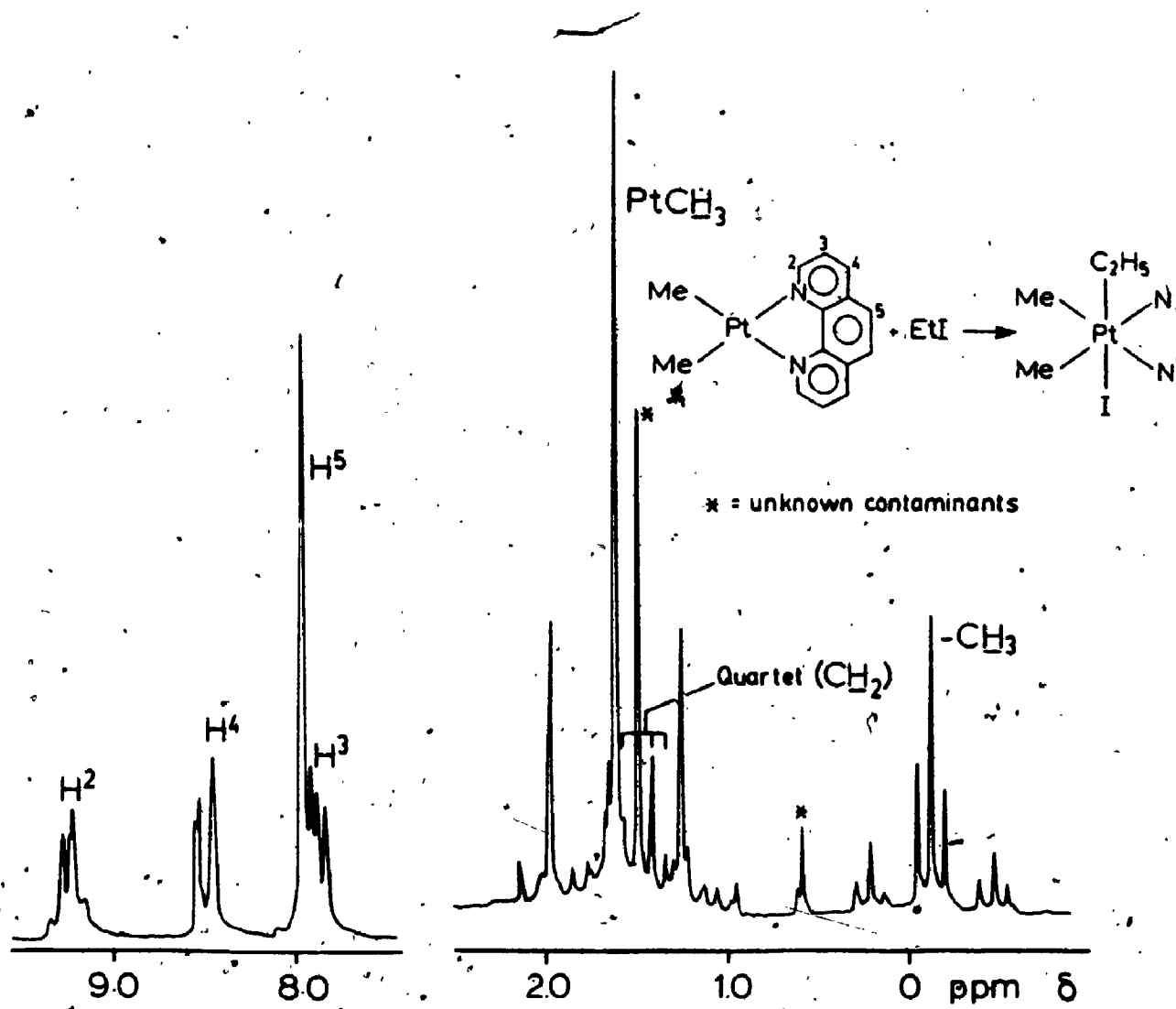


FIGURE 3.1: ^1H NMR Spectrum (100 MHz) of $[\text{PtI}(\text{EtMe}_2)(\text{phen})]$ in CD_2Cl_2 .

due to the PtCH₂ unit.

The ¹H nmr spectrum of (XIa) contains two MePt peaks in the ratio 2:1. The Me groups in the plane of the aromatic rings occur down-field from the Me group above the plane, as observed for similar trimethyl complexes.³³ As in the bipy analogue³³ the value of ²J_{PtMe} for the Me *trans* to iodide is greater than that for Me *trans* to phen.

For complexes with alkyl chains containing more than two carbon atoms it was not possible to assign all the peaks in the ¹H nmr spectra but those features consistent with a platinum(IV) complex formed by *trans* oxidative addition were present (Table 7.3).

3.4 Kinetic Studies

The rates of reaction of (II) with CH₃(CH₂)_nI (n = 0-4) were determined, using acetone as solvent, by monitoring the decay of the MLCT band at 472.7 nm of complex (II) as the reactions progressed. For each organic halide a series of runs were made, keeping the concentration of (II) constant, whilst varying the concentration of the halide. A large excess of the halide was used in each case. The absorbance (A_t) was recorded at regular intervals and a plot of $\log \frac{(A_t - A_\infty)}{(A_0 - A_\infty)}$ versus time was made for each concentration of the halide. Figure 3.2 shows the results obtained for ethyl iodide. From the slope of such plots the pseudo-first-order rate constants (k_{obs.}) were obtained and when plotted against concentration of the halide a straight line was produced. Figure 3.3 shows the results for ethyl iodide. The second-order rate constants (k₂), obtained from the slope of such plots, are recorded in Table 3.1

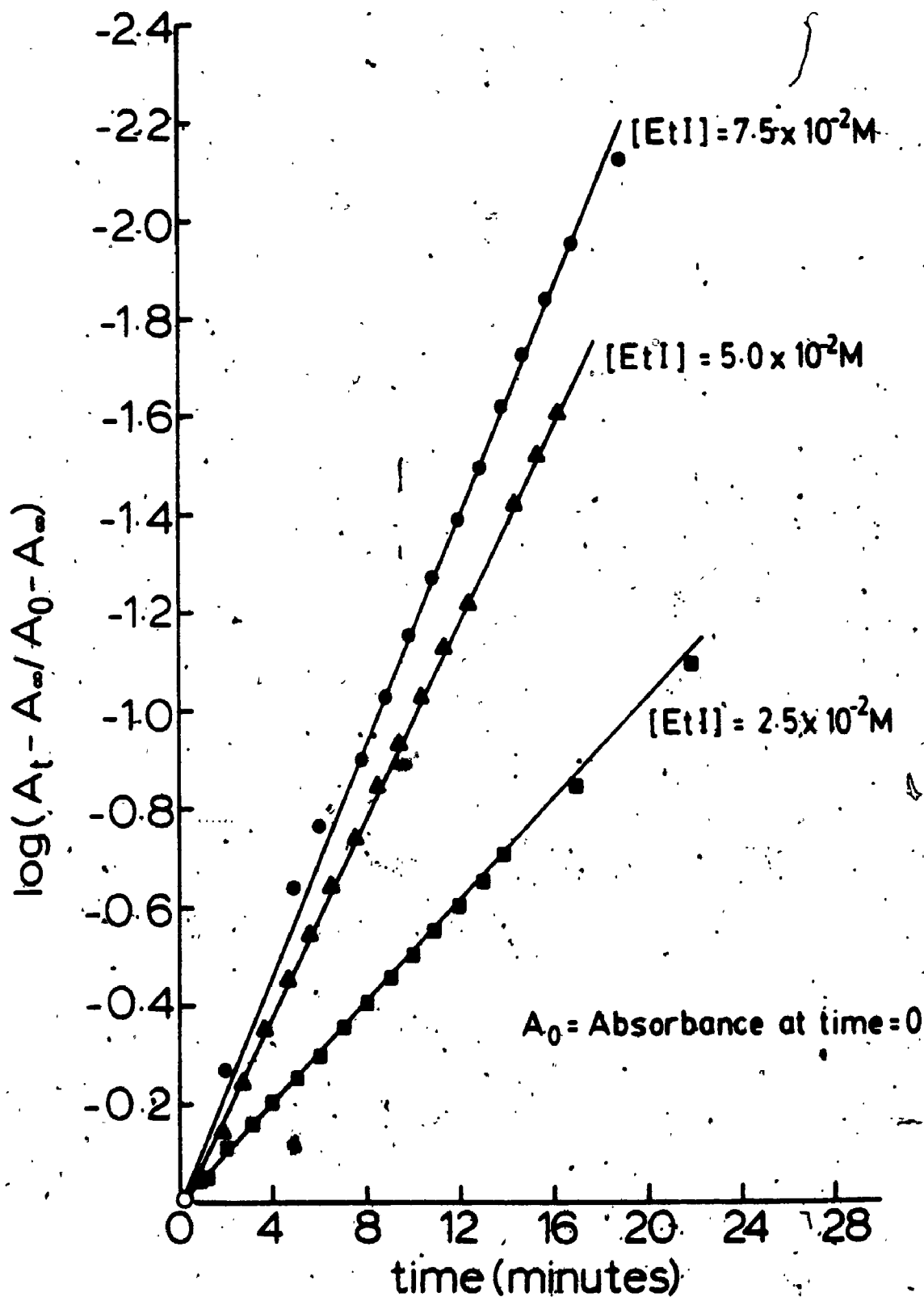


FIGURE 3.2: Plot of $\log \frac{(A_t - A_\infty)}{(A_0 - A_\infty)}$ Versus Time (Min) for the Reaction of (II) ($5.0 \times 10^{-4} M$) with EtI, in Acetone at $25^\circ C$. $A_0 =$ absorbance at time = 0.

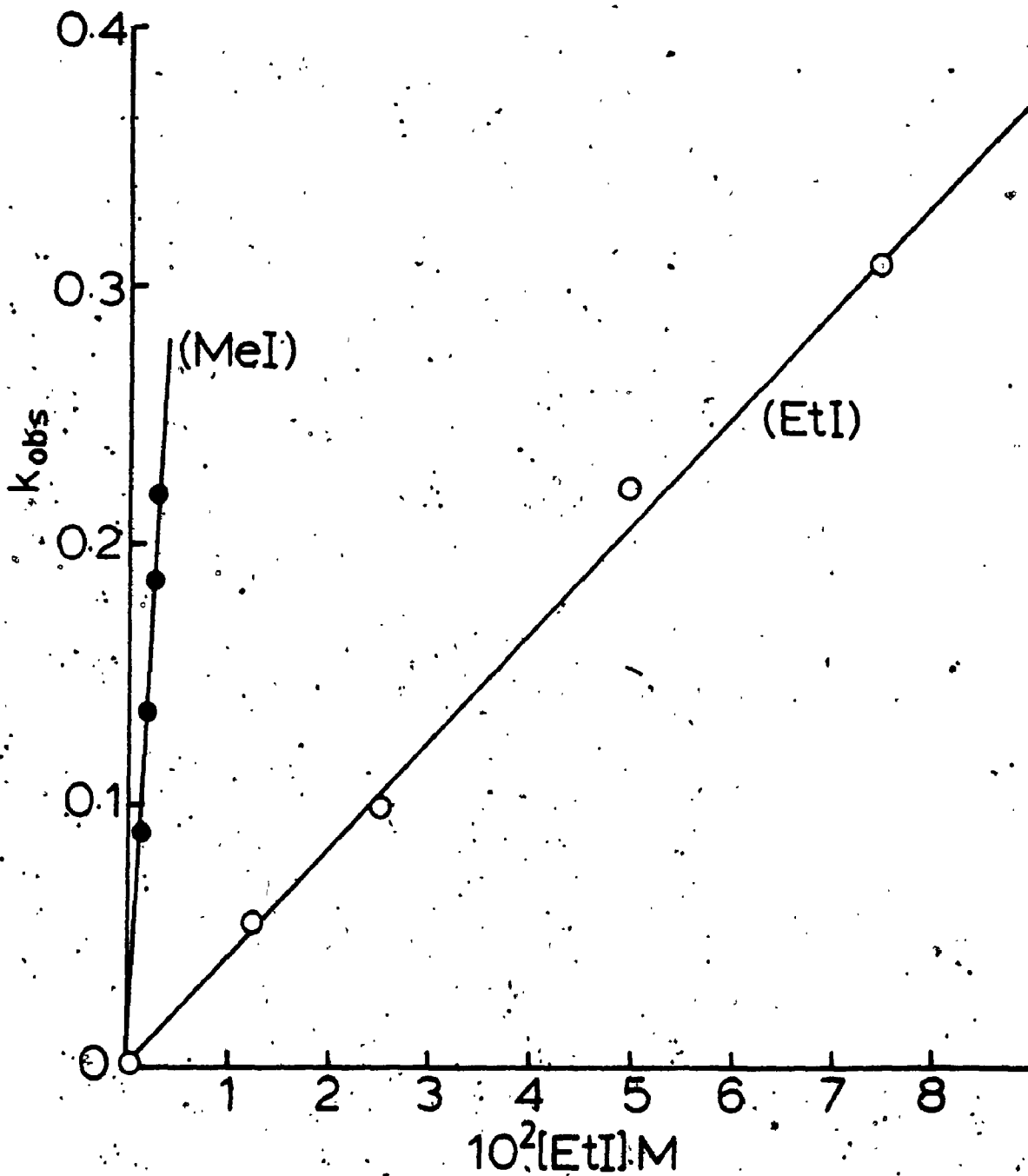


FIGURE 3.3: Plot of k_{obs} Versus Concentration of Iodide for the Reaction of EtI and MeI with (II), in Acetone, at 25°C.

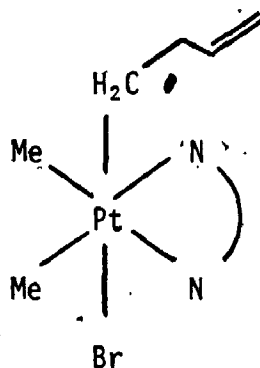
TABLE 3.1: Second-Order Rate Constants for Reactions of (II) in Acetone at 25°C

<u>Reagent</u>	$10^3 k_2$ (L.mol ⁻¹ .s ⁻¹)
MeI	69,000
EtI	69
n _{pr} I	34
n _{bu} I	39
CH ₃ (CH ₂) ₄ I	44

3.5 Reaction of Cyclopropylcarbonyl Bromide with (II)

In later chapters a full discussion is presented of complex (II) undergoing oxidative addition *via* free-radical pathways, and a number of techniques are available for probing such pathways.

A primary organic halide was chosen, cyclopropylcarbonyl bromide, which is known to react sometimes *via* the cyclopropylcarbonyl radical.³⁴ Furthermore, the homoallyl rearrangement which characterises the cyclopropylcarbonyl radical is a particularly well understood radical rearrangement.^{35,36} As a result of such a rearrangement, a complex as shown below would be expected.

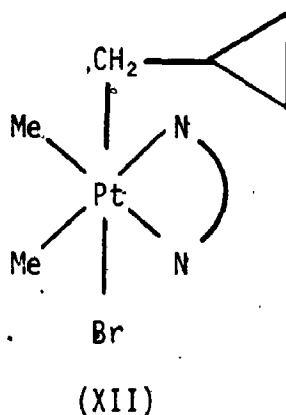


The butenyl group could also be *cis* to the bromide.

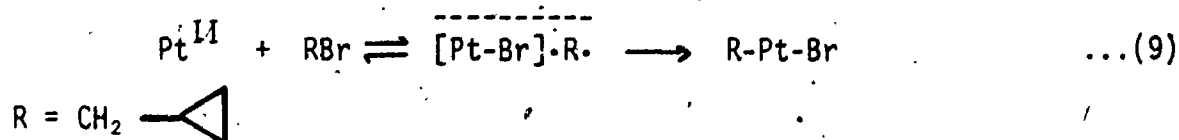
The cyclopropylcarbonyl bromide was prepared according to the literature method,³⁷ as described in Chapter 7. An excess of the ligand was reacted with $[\text{PtMe}_2(\text{phen})]$ in acetone, producing a pale yellow solution.

The ^1H nmr spectrum of the product from this reaction contains only one MePt signal at 1.66 ppm, with a $^2J_{\text{PtMe}}$ value of 71.5 Hz. This is clear evidence that the complex contains a plane of symmetry and that oxidation from platinum(II) to platinum(IV) has occurred. The resonances due to the aromatic rings possess the same pattern as for complex (II). A doublet occurs at 1.36 ppm, with platinum

satellites, showing a ${}^2J_{PtH}$ value of 70 Hz. The ratio of this doublet to the MePt singlet is very close to 3:1. It is assigned as the $-CH_2$ group of the cyclopropylcarbinyll bonded to platinum. The resonances due to the cyclopropyl protons occur at high field as two broad signals. There are no peaks in the region of the spectrum where olefinic protons occur. The 1H nmr data of this complex (XII) are consistent with the structure shown below.



This would indicate that the reaction does not proceed *via* the cyclopropylcarbinyll radical, since this would lead to some butenylplatinum(IV) product. However there is the possibility that a caged radical-pair collapses before rearrangement to give complex (XII) as shown in equation 9.



Rearrangement within the cage to form the butenyl radical is a slower process³⁴ ($k = 1.3 \times 10^8 s^{-1}$ at 25°C) than diffusion of the cyclopropylcarbinyll radical out of the cage. The absence of any butenylplatinum(IV) complex must therefore mean that any radical reaction must occur within the solvent cage. It is considered more probable that a non-radical mechanism operates.

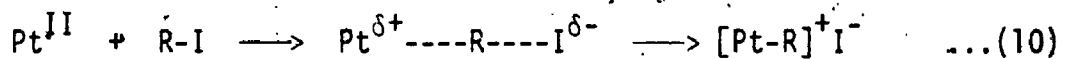
3.6 Reaction of Methyl and Ethyl Iodide with a Mixture of (II) and $\text{CH}_2 = \text{CHX}$ (X = CHO, or CN)

Reactions involving free-radicals, carried out in the presence of activated olefins, can lead to the polymerisation of the olefins.¹⁹

Methyl iodide was reacted with (II) in the presence of freshly distilled acrolein [$\text{CH}_2 = \text{CHC}(\text{O})\text{H}$]. The ^1H nmr spectrum of the product was identical to that of complex (XIa), and no peaks due to polymeric material were observed. A similar reaction with ethyl iodide and (II) in the presence of freshly distilled acrylonitrile produced complex (XIb) and no polymeric material.

3.7 Conclusion

The observed second-order rate law does not discriminate³⁸ between a classical $\text{S}_{\text{N}}2$ mechanism (eq. 10) and a radical non-chain mechanism.



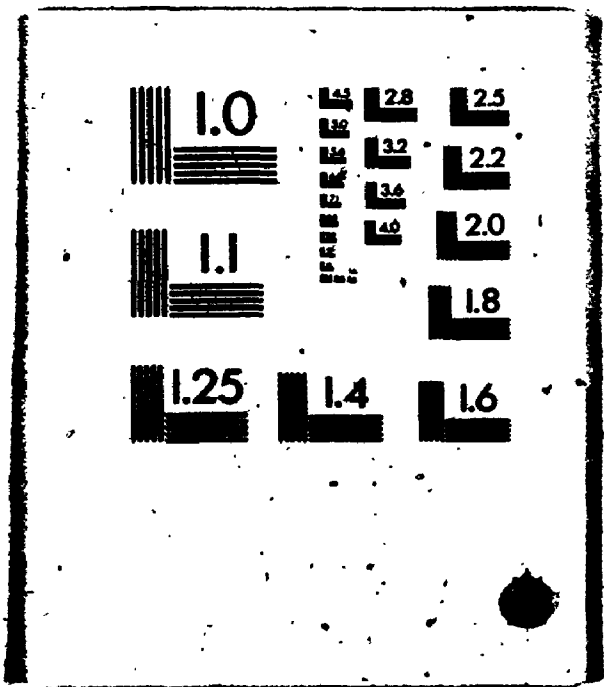
A radical-chain mechanism can be discounted, in part due to the fact that such *good* second-order kinetics are followed. Although approximate second-order kinetics can be observed for radical-chain reactions, this is unusual and more complex kinetics are usually observed. Typically there is an induction period followed by a fast reaction.²⁰

The failure to observe polymeric products when methyl and ethyl iodide react with (II) is good indication that free-radicals are not involved. Table 3.1 shows the second-order rate constants for the reaction of the organic halides with (II). A reversed trend would be expected if the reactions involved alkyl radicals.

TABLE 3.2: Average Relative Rates for S_N2 Displacement of Alkyl Systems

<u>Radical</u>	<u>Average Relative Rates for S_N2 Displacement</u>
Methyl	30
Ethyl	1.0
Propyl	0.4
Butyl	0.4

2



A radical non-chain mechanism would be expected to produce some $[\text{PtI}_2\text{Me}_2(\text{phen})]$ as one of the products. None of this complex is produced in any of the reactions discussed in this chapter.

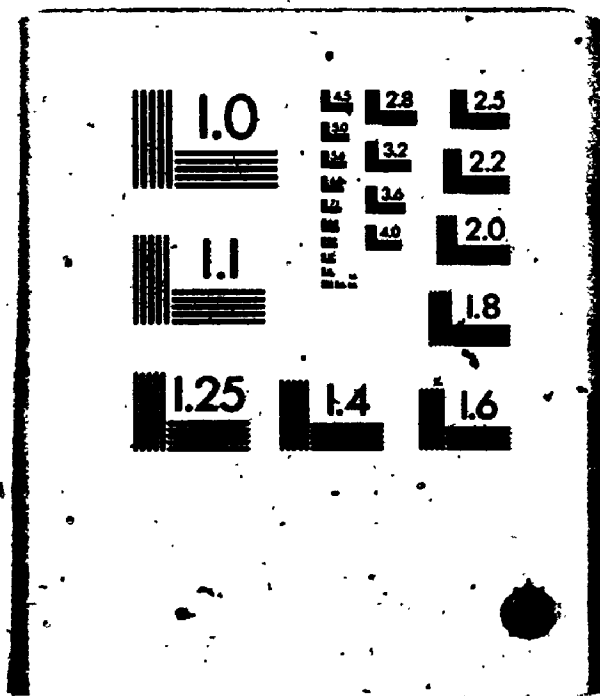
The production of the cyclopropylcarbonyl adduct, complex (XII), is further evidence that the $\text{S}_{\text{N}}2$ type mechanism is operative.

In a series of reactions between methyl iodide and a wide range of transition-metal nucleophiles Pearson³⁹ concludes that the $\text{S}_{\text{N}}2$ mechanism is operative in all cases. Indeed there has only been one report of methyl iodide reacting with a transition-metal complex through the intermediacy of free-radicals.²⁰

From a study⁴⁰ of the rates for $\text{S}_{\text{N}}2$ displacement reactions of alkyl systems a list of average relative rates has been proposed. These are shown in Table 3.2. A comparison with the rate constants in Table 3.1 shows that great selectivity exists in the reaction of (II) with methyl iodide. This is presumably due to steric effects. The data in Tables 3.1 and 3.2, for the remaining alkyl groups, are in good agreement for an $\text{S}_{\text{N}}2$ type oxidative addition of these halides to complex (II), and not for any radical type mechanism.

In conclusion, there is strong evidence that all the reactions discussed in this chapter, between primary halides and complex (II), proceed *via* an $\text{S}_{\text{N}}2$ mechanism.

2



A radical non-chain mechanism would be expected to produce some $[\text{PtI}_2\text{Me}_2(\text{phen})]$ as one of the products. None of this complex is produced in any of the reactions discussed in this chapter.

The production of the cyclopropylcarbinyl adduct, complex (XII), is further evidence that the $\text{S}_{\text{N}}2$ type mechanism is operative:

In a series of reactions between methyl iodide and a wide range of transition-metal nucleophiles Pearson³⁹ concludes that the $\text{S}_{\text{N}}2$ mechanism is operative in all cases. Indeed there has only been one report of methyl iodide reacting with a transition-metal complex through the intermediacy of free-radicals.²⁰

From a study⁴⁰ of the rates for $\text{S}_{\text{N}}2$ displacement reactions of alkyl systems a list of average relative rates has been proposed. These are shown in Table 3.2. A comparison with the rate constants in Table 3.1 shows that great selectivity exists in the reaction of (II) with methyl iodide. This is presumably due to steric effects. The data in Tables 3.1 and 3.2, for the remaining alkyl groups, are in good agreement for an $\text{S}_{\text{N}}2$ type oxidative addition of these halides to complex (II), and not for any radical type mechanism.

In conclusion, there is strong evidence that all the reactions discussed in this chapter, between primary halides and complex (II), proceed *via* an $\text{S}_{\text{N}}2$ mechanism.

REFERENCES

1. Collman, J.P.; Acc. Chem. Res., 1968, 1, 136.
2. Collman, J.P.; Roper, W.R.; Adv. Organometal. Chem., 1968, 7, 53.
3. Halpern, J.; Acc. Chem. Res., 1970, 3, 386.
4. Stille, J.K.; Lau, K.S.Y.; Acc. Chem. Res., 1977, 10, 434.
5. Forster, D.; Adv. Organometal. Chem., 1979, 17, 255.
6. Maletesta, L.; Caridello, S.; J. Chem. Soc. (A), 1958, 2323.
7. Chatt, J.; Shaw, B.L.; J. Chem. Soc., 1959, 705.
8. Chock, P.B.; Halpern, J.; J. Am. Chem. Soc., 1966, 88, 3511.
9. Kang, J.W.; Maitlis, P.M.; J. Organomet. Chem., 1971, 26, 393.
10. Collman, J.P.; MacLaury, M.R.; J. Am. Chem. Soc., 1974, 96, 3018;
Collman, J.P.; Murphy, D.W.; Dolcetti, G., *ibid.*, 1973, 95, 2687.
11. Stille, J.K.; Becker, Y.; J. Am. Chem. Soc., 1978, 100, 838.
12. Lau, K.S.Y.; Fries, R.W.; Stille, J.K.; J. Am. Chem. Soc., 1974, 96,
4983.
13. Wong, P.K.; Lau, K.S.Y.; Stille, J.K.; J. Am. Chem. Soc., 1974, 96,
5956.
14. Lau, K.S.Y.; Wong, P.K.; Stille, J.K.; J. Am. Chem. Soc., 1976, 98,
5832.
15. Ugo, R.; Pasini, A.; Fusi, A.; Cenine, S.; J. Am. Chem. Soc., 1972,,
94, 7364.
16. Halpern, J.; Maher, J.P.; J. Am. Chem. Soc., 1965, 87, 5361.
17. Kwiatek, J.; Seyler, J.K.; J. Organomet. Chem., 1965, 3, 421.
18. Bradley, J.S.; Connor, D.E.; Dolphin, D.; Labinger, J.A.; Osborn,
J.A.; J. Am. Chem. Soc., 1972, 94, 4043.

19. Labinger, J.A.; Osborn, J.A.; *Inorg. Chem.*, 1980, 19, 3230;
Labinger, J.A.; Osborn, J.A.; Coville, N.J.; *ibid.*, 1980, 19, 3236.
20. Hall, T.L.; Lappert, M.F.; Lednor, P.W.; *J. Chem. Soc., Dalton Trans.*, 1980, 1448.
21. Connor, J.A.; Riley, P.I.; *J. Chem. Soc. Chem. Comm.*, 1976, 634.
22. Connor, J.A.; Riley, P.I.; *J. Chem. Soc., Dalton Trans.*, 1979, 1318.
23. Crabtree, R.H.; Faber, J.W.; Mellea, M.F.; Quirk, J.M.; *Organometallics*, 1982, 1, 1361.
24. Sevin, A.; Hengtai, Y.; Chaquin, P.; *J. Organomet. Chem.*, 1984, 262, 391.
25. Halpern, J.; *Inorg. Chim. Acta.*, 1982, 62, 31.
26. Ling, S.; Puddephatt, R.J.; Manojlovic-Muir, L.; Muir, K.W.; *J. Organomet. Chem.*, 1983, 255, C11.
27. Mayanza, A.; Bonnet, J.-J.; Galy, J.; Kalck, P.; Poilblanc, R., *J. Chem. Res. (S)*, 1980, 146.
28. Fackler, J.P., Jr.; Basil, J.D.; *Organometallics*, 1982, 1, 871.
29. Nyholm, R.S.; *J. Chem. Soc.*, 1950, 843.
30. Jawad, J.K.; Puddephatt, R.J.; *J. Chem. Soc., Dalton Trans.*, 1977, 1466.
31. Jawad, J.K.; Puddephatt, R.J.; *J. Organomet. Chem.*, 1976, 117, 297.
32. Kuyper, J.; *Inorg. Chem.*, 1978, 17, 77.
33. Clegg, D.E.; Hall, J.R.; Swile, G.A.; *J. Organomet. Chem.*, 1972, 38, 403.
34. San Filippo, J., Jr., Silbermann, J.; Fagan, P.J.; *J. Am. Chem. Soc.*, 1978, 100, 4834.
35. Kochi, J.K.; Lousic, P.J.; Eaton, D.R., *J. Am. Chem. Soc.*, 1969, 91, 1877.

36. Wilt, J.W.; "Free Radicals", Kochi, J.K.; Ed., 1973, Vol. 1, Chap. 8, Wiley, New York.
37. Meek, J.S.; Rowe, G.W.; J. Am. Chem. Soc., 1955, 77, 6675.
38. Schrauzer, G.N.; Deutsch, E.; J. Am. Chem. Soc., 1969, 91, 3341.
39. Pearson, R.G.; Figdome, P.E.; J. Am. Chem. Soc., 1980, 102, 1541.
40. Streitwieser, A., Jr.; "Solvolytic Displacement Reactions", 1962, Chap. 1, McGraw-Hill, New York.

CHAPTER 4

FORMATION OF MONONUCLEAR AND BINUCLEAR PLATINUM(IV) COMPLEXES USING METHYLENE HALIDES AND α,ω -DIHALOGENOALKANES AS REAGENTS

1. INTRODUCTION

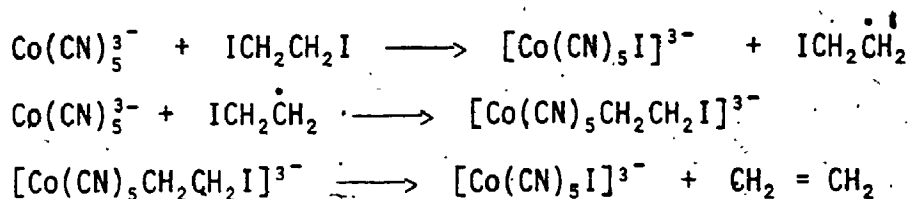
The reaction of $[\text{PtMe}_2(\text{phen})]$ with a series of α,ω -dihaloalkanes leads to the formation of either mononuclear or binuclear platinum(IV) complexes. In most cases the mononuclear complex could be isolated and converted into the corresponding binuclear complex. The kinetics of these reactions have been studied and the mechanism of the reactions is discussed.

2. LITERATURE PRECEDENTS

Fischer and Tropsch originally suggested the polymerisation of methylene groups on a metal surface to account for the formation of products in the Fischer-Tropsch reaction.¹ Recent evidence² has been found to be consistent with this proposal and this has resulted in considerable current interest in binuclear complexes containing bridging methylene or polymethylene groups. A possible route to such complexes is by the use of α,ω -haloalkanes, and the present survey will concentrate on complexes (mononuclear and binuclear) formed from such ligands as well as from methylene dihalides. Recently two very comprehensive reviews have appeared^{3,4} dealing with bridged hydrocarbyl binuclear transition-metal complexes.

2.1 Mononuclear Complexes

Halpern has done extensive work on the kinetics of oxidative addition of alkyl halides to $\text{Co}(\text{CN})_5^{3-}$. In the case of $\text{I}(\text{CH}_2)_2\text{I}$, the proposed mechanism^{5,6} is that shown in Scheme 1.

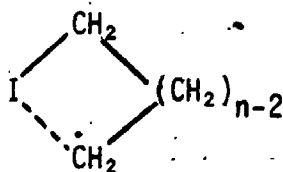


SCHEME 1

Proposed Mechanism for the Reaction of
 $[\text{Co}(\text{CN})_5]^{3-}$ with $\text{I}(\text{CH}_2)_2\text{I}$

A similar mechanism was proposed in the case of $\text{I}(\text{CH}_2)_3\text{I}$, with the formation of cyclopropane in the final step. The intermediate iodoalkylcobalt species were not isolated but the kinetics clearly indicated a two step mechanism.

The rate constants for the reaction of $\text{Co}(\text{CN})_5^{3-}$ with the diiodides were higher than with the corresponding monoiodides. Furthermore the rate constants exhibited an inverse dependence on 'n', the number of carbon atoms separating the two iodine atoms. Halpern considers this to be due to stabilisation of the iodoalkyl radical, $\text{CH}_2(\text{CH}_2)_{n-2}\dot{\text{C}}\text{H}_2\text{I}$, by the residual iodine substituent, possibly through cyclic bridging, i.e.



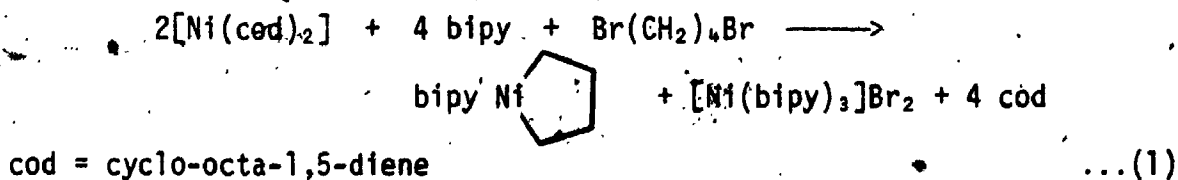
The oxidative addition of $\text{ICH}_2\text{CH}_2\text{I}$ to $[\text{Pt}(\text{PPh}_3)_2(\text{C}_2\text{H}_4)]$ does not yield

an iodoalkylplatinum complex, but the diiodoplatinum(II) complex $[\text{PtI}_2(\text{PPh}_3)_2]$, with the evolution of ethene. As will be discussed later in this chapter, an analogous reaction occurs between $[\text{PtMe}_2(\text{phen})]$ and $\text{ICH}_2\text{CH}_2\text{I}$.

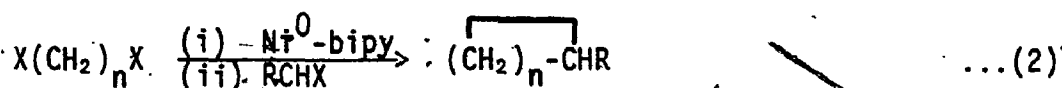
The reaction of gem-dihalides (RCHX_2) with transition-metal complexes often involves the intermediacy of free-radicals. In diffuse daylight $[\text{Pt}(\text{PPh}_3)_2(\text{C}_2\text{H}_4)]$ reacts⁷ with CH_2Cl_2 , acting as solvent, to produce *trans*- $[\text{PtCl}(\text{PPh}_3)_2(\text{CH}_2\text{Cl})]$. Addition of the radical scavenger duroquinone or conducting the reaction in the dark decreases the rate of reaction. This indicates that, at least in the light, free-radicals are involved. In a later study of the same platinum(0) complex, Lappert⁸ used a series of gem-dihalides (e.g. CH_2I_2 , CH_2ClI , CH_2BrCl) and isolated mixtures of *cis*- and *trans*- α -halogenoalkyls of platinum(II). For the mixed dihalide, CH_2ClI , halogen-scrambled products were obtained and the authors suggest a free-radical mechanism. Moss,¹⁹ using a shorter reaction time isolated *cis*- $[\text{PtI}(\text{PPh}_3)_2(\text{CH}_2\text{Cl})]$ as the sole product.

In an investigation of the mechanism of alkylation of dinitrogen, coordinated to molybdenum and tungsten, Leigh⁹ and co-workers detected the CH_2Br radical when CH_2Br_2 was used.

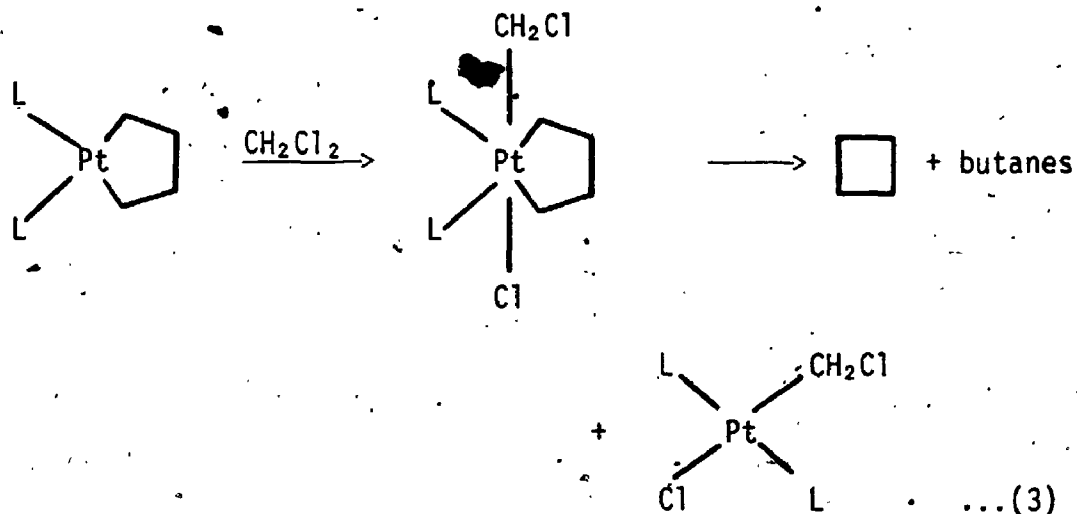
The synthesis of cycloalkanes using α,ω -dihalogenoalkanes has been demonstrated by Hagihara¹⁰ and co-workers. They used bis(cyclo-octa-1,5-diene)nickel and were able to isolate a nickelacyclopentane in a reaction with $\text{Br}(\text{CH}_2)_4\text{Br}$, as shown in equation 1.



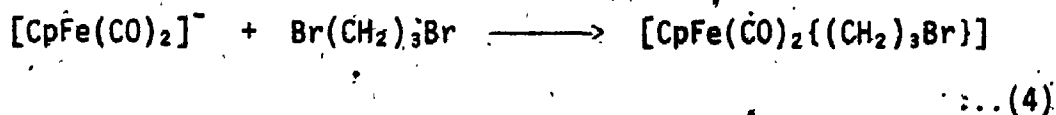
In reactions with α,ω -dihalogenoalkanes and gem-dihalides this nickel-acycloalkane produced a series of cycloalkanes according to equation 2.



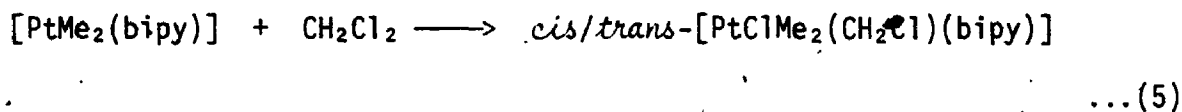
In a study of the thermal decomposition of platinacycloalkanes $[\text{L}_2\text{Pt}(\text{CH}_2)_n\text{CHR}]$ ($\text{L} = \text{}^n\text{Bu}_3\text{P}, \text{Et}_3\text{P}; \text{L}_2 = \text{bipy}$) in methylene chloride, Whitesides¹¹ has proposed oxidative addition of CH_2Cl_2 as the key step. Part of the proposed thermolysis scheme is shown in equation 3.



Binuclear complexes containing a polymethylene bridge have often been synthesised from the action of α,ω -dihalogenoalkanes on transition-metal carbonyl anions. Such binuclear species are believed to be formed from an intermediate haloalkyl complex. The first such haloalkyl complex derived from the anion $[\text{CpFe}(\text{CO})_2]^-$ ($\text{Cp} = \text{cyclopentadienyl}$) was synthesised by Moss.¹² Such complexes as $[\text{CpFe}(\text{CO})_2\{(\text{CH}_2)_3\text{Br}\}]$ were isolated in high yield according to equation 4.

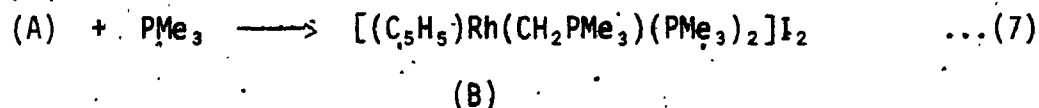
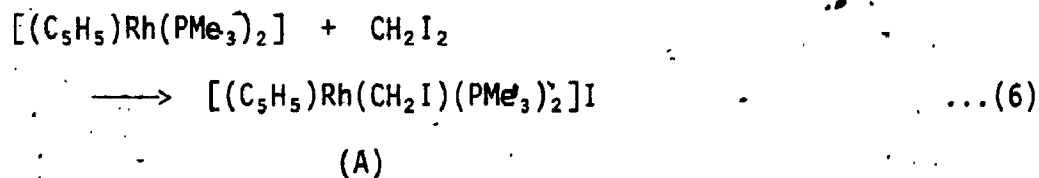


In the oxidative addition¹³ of CH_2Cl_2 to $[\text{PtMe}_2(\text{bipy})]$ the product was initially a mixture of the *cis*- and *trans*- adducts in a ratio of 2:1 (eq. 5). The *cis*- product slowly converted to the *trans*-isomer and after 2 weeks the composition remained unchanged, having a *cis/trans* ratio of 1:4.

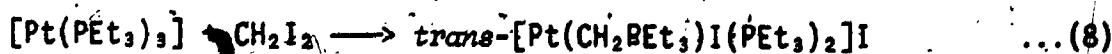


In an attempt to prepare haloalkyl transition-metal complexes CH_2ClI was reacted¹⁴ with $[\text{Pt}(\text{PPh}_3)_4]$. Instead of the expected oxidative addition reaction to yield a chloromethyl complex, the reaction produced a cationic ylide complex formulated as *cis*- $[\text{PtCl}(\text{PPh}_3)_2(\text{CH}_2\text{PPh}_3)]\text{I}$.

Metal halomethyl complexes (particularly iodomethyl) contain a labile carbon-halogen bond. This probably accounts for the reaction discussed in the previous paragraph. Werner¹⁵ has taken advantage of this lability to synthesise a dicationic methylenephosphorane complex (eq. 6 and 7).

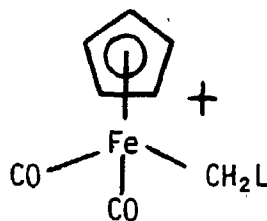


A similar result has been reported by Klein¹⁶ and Hammer for the reaction of $[\text{Co}(\text{PMe}_3)_4]$ with CH_2Cl_2 . Lappert⁸ has been able to synthesise a platinum(II) ylide by the action of CH_2I_2 on $[\text{Pt}(\text{PEt}_3)_3]$ (eq. 8).

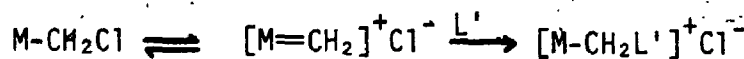


The reaction goes *via* the initial formation of an iodomethylplatinum complex. The mechanism¹⁷ for this reaction of an α -halogenomethylplatinum complex with a tertiary phosphine could be regarded as S_N2 , by analogy with the Menschutkin reaction¹⁸ ($RX + NR_3 \rightarrow [NR_4]X$).

In a very recent paper Moss²⁰ reports the reactions of some chloromethyl complexes of molybdenum, tungsten, rhenium, iron and ruthenium with some tertiary phosphines. Reaction of $[(Cp)Fe(CO)_2(CH_2Cl)]$ with tertiary phosphines gave cationic ylide complexes isolated as the $(BPh_4)^-$ salt, shown below.



$L = PPh_3, PMe_2Ph, PEt_2Ph, PMePh_2$. $[W(Cp)(CO)_3(CH_2Cl)]$, in a reaction with PPh_3 , gave $[(Cp)W(CO)_3(CH_2PPh_3)]^+$. The remaining metals did not give the methylenephosphorane ylides. The ylide formation is believed to go *via* a carbene intermediate, shown in Scheme 2.



$L' =$ phosphine ligand

SCHEME 2

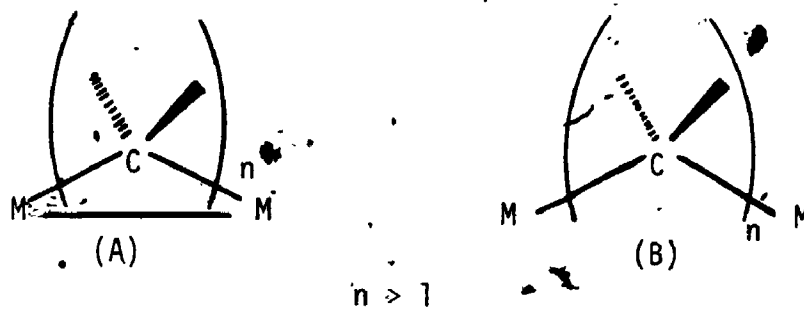
Proposed Mechanism for the Formation of Ylides

2.2 Bimuclear Complexes

There exists an abundance of complexes in which two metal centres are bridged by a hydrocarbyl ligand.^{3,4} For most cases a metal-metal bond exists between the centres. This review of μ -hydrocarbyl complexes will

Concentrate exclusively on alkanediyl compounds of type A and B in

Scheme 3.

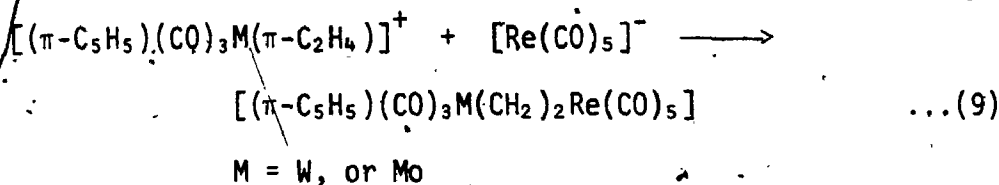


SCHEME 3

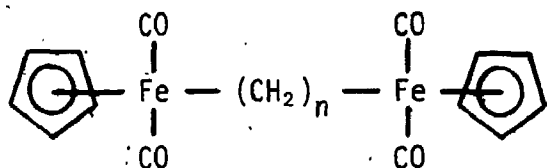
General Structures of Binuclear μ -Alkanediyl Complexes

Typical members of class B have been reported for $2 < n < 10$ but there is no reason to assume that the chain length has an upper limit.³

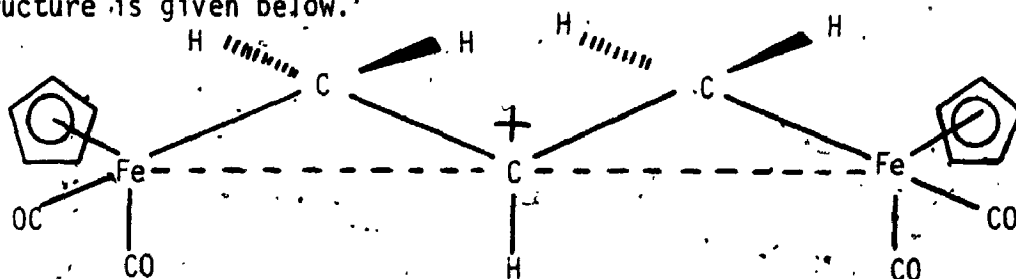
An early prediction²¹ claimed that the ethylene bridge ($n = 2$) was inherently unstable. In contrast to this view, Sinn^{22,23} *et al.* have prepared a series of μ -(C_2H_4) organometals, e.g. $(\mu-C_2H_4)[(\eta^5-C_5H_5)_2-Zr-Cl-AlEt_3]_2$. There is no metal-metal bond present and the carbon-carbon bond distance in the bridge is 15.5 pm which is typical of a single bond. In the rhenium compound $[(\mu-C_2H_4)-\{Re(CO)_5\}_2]$, reported by Beck,^{24,25} the C-C distance is much shorter than in the above zirconium complex. Such complexes are more or less ethane-derived organometals rather than ethylene-bridged systems. An interesting feature of Beck's work is the synthetic route used. It consists of the nucleophilic attack of metal carbonyl anions on coordinated ethylene in cationic complexes (eq. 9).



A very general method for preparation of polymethylene bridged complexes is the reaction of metal carbonyl anions with α,ω -dihaloalkanes. The reactions between $[\text{Fe}(\text{CO})_2(\eta^5\text{-C}_5\text{H}_5)]^-$ and $\text{Br}(\text{CH}_2)_n\text{Br}$ ($n = 3-6$) were investigated by King,^{26,27} and found to yield products of general formula $[(\text{CH}_2)_n\{\text{Fe}(\text{CO})_2(\eta^5\text{-C}_5\text{H}_5)\}_2]$ and with the structure given below.

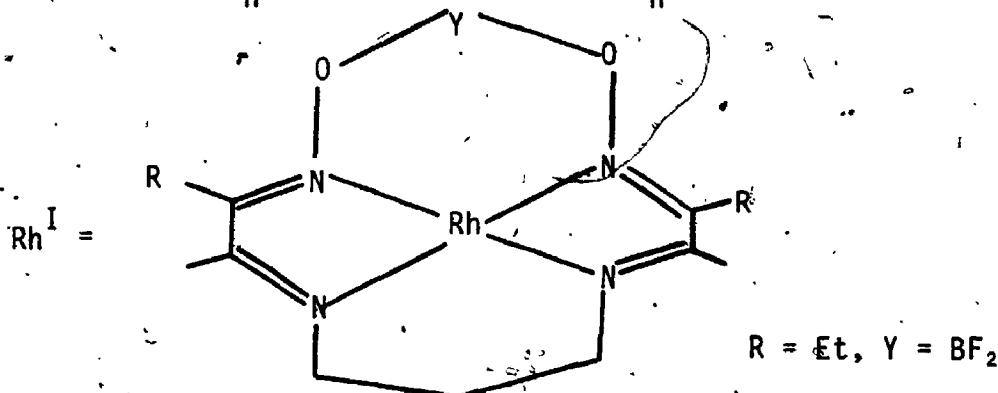
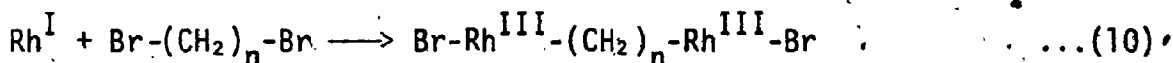


Different products were isolated for the reaction with $[\text{Mn}(\text{CO})_5]^-$. King and Bisette²⁸ showed that a hydride ion could be removed from the β - CH_2 group of $[(\mu\text{-CH}_2)_3\{\eta^5\text{-C}_5\text{H}_5\}\text{Fe}(\text{CO})_2\}_2]$ to yield a cation. The crystal structure of this cation was determined by Laing,²⁹ and the structure is given below.

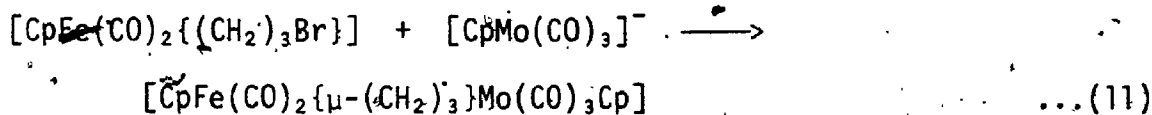


There is close contact between the iron centres and the β -carbon, which is undoubtedly responsible for the unexpected stability of this non-classically bonded carbonium ion.

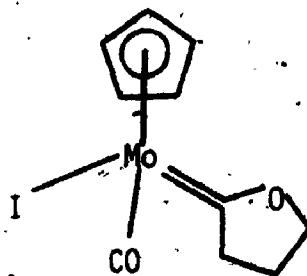
Collman has studied the reactivity of a macrocyclic rhodium(I) complex with a series of alkyl halides³⁰ (see Chapter 3). For $\text{Br}(\text{CH}_2)_n\text{Br}$ ($n = 2, 4, 6$) the sole product was a binuclear rhodium(III) complex (eq. 10).



It is thought that the reaction goes *via* a bromoalkyl intermediate and that the second oxidative addition is much faster than the first due to a neighbouring group effect. In order to synthesise mixed μ -alkanediyl complexes Moss¹² has used the strategy of reacting a haloalkyl complex of one metal with the anionic carbonyl complex of another (eq. 11).

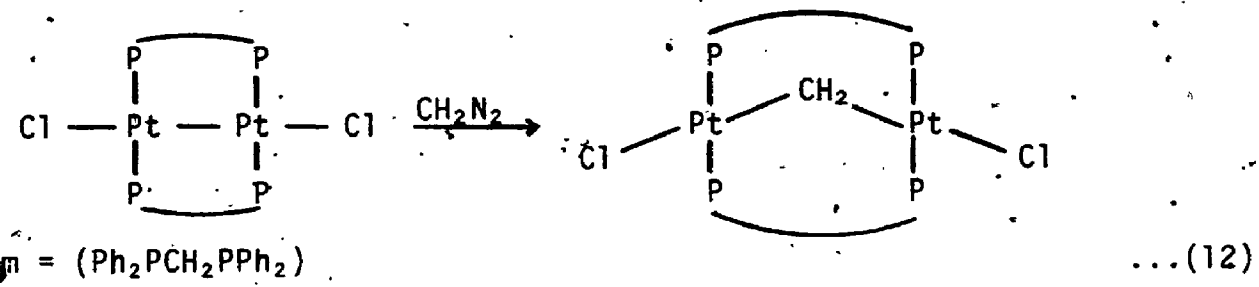


Winter's group has recently published a series of papers³¹⁻³³ on the reactions of iron, tungsten and molybdenum complexes with $\text{X}(\text{CH}_2)_3\text{X}$ ($\text{X} = \text{I}, \text{Br}$). Both halomethyl and μ -alkanediyl products were isolated. The complex $[\text{Mo}\{(\text{CH}_2)_3\text{I}\}(\text{CO})_3(\eta^5-\text{C}_5\text{H}_5)]$ if refluxed, forms a carbene complex by migration of the alkyl chain to an adjacent carbonyl group. The product is shown below.



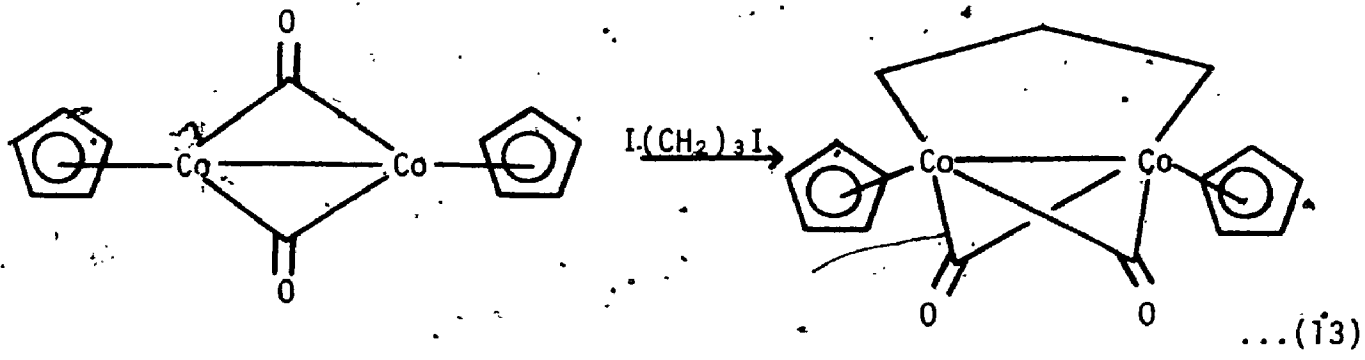
None of the complexes discussed so far contain a metal-metal bond. For bridging methylene complexes, the presence of a metal-metal bond appears

to be the rule. Exceptions do exist however and the first report of a bridging-methylene unit, in the absence of a metal-metal bond, was by Puddephatt³⁴ and co-workers. The reaction of diazomethane with $[\text{Pt}_2\text{Cl}_2(\mu\text{-dppm})_2]$ produced the A-frame complex shown in equation 12.



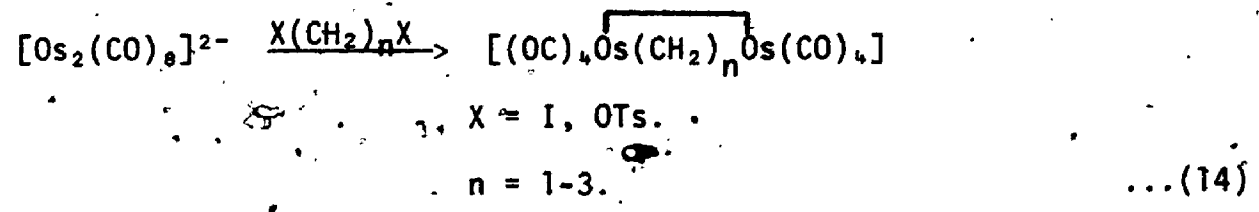
Other analogous complexes have been reported since.^{35,36,37}

For bridging-hydrocarbonyl complexes (with $n > 1$) most examples reported, do not have metal-metal bonds. Bergmann³⁸ has succeeded however in synthesising the propane-1,3-diyl cobalt derivative from the radical anion $[(\eta^5\text{-C}_5\text{H}_5)\text{Co}(\mu\text{-CO})]_2^-$ and 1,3-diiodopropane (eq. 13).

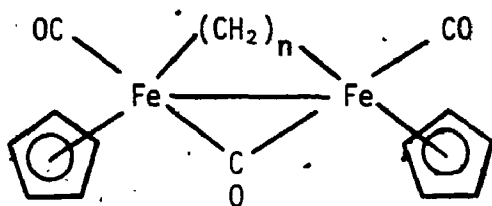


This compound is best described as a dimetallacyclopentane.

The first 1,2-dimetallacyclobutane was reported by Norton and Anderson³⁹ along with other metal-metal bonded μ -alkanediy complexes. The synthesis involved the reaction of $[\text{Os}_2(\text{CO})_6]^{2-}$ with $\text{X}(\text{CH}_2)_n\text{X}$ (eq. 14).



The thermal and photochemical decomposition of complexes such as $[(n-C_5H_5)(CO)_2Fe(\mu-CH_2)_nFe(CO)_2(n-C_5H_5)]$ ($n = 3-5$) is believed to go⁴⁰ via transient dimetallacycles of the type shown below.



In the case of metallocyclobutanes they are considered as intermediates in transition-metal catalysed metathesis of olefins.

It is clear then that there is much activity in the general area of bridging-hydrocarbyl complexes. In the subsequent discussion some of the kinetics and mechanism of their formation in the case of platinum(IV) will be presented.

3. RESULTS AND DISCUSSION

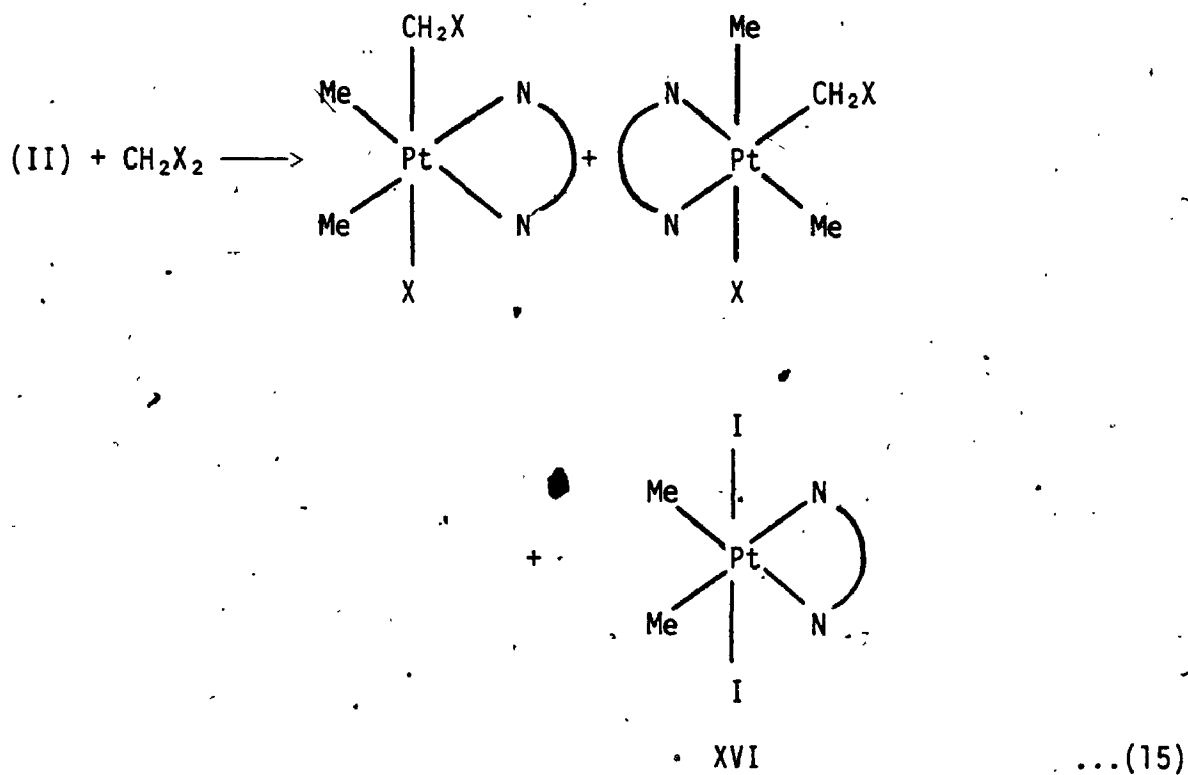
This section will be divided according to the work done with methylene dihalides and that done with $X(CH_2)_nX$ ($X = I, Br, n = 2-5$).

3.1 Reaction of $[PtMe_2(phen)]$ with Methylene Dihalides

3.1.1 Preparation and Characterisation

The methylene dihalides CH_2I_2 , CH_2Br_2 , CH_2BrCl , CH_2ClI , reacted with (II) in acetone. In the case of CH_2Cl_2 , the reaction was performed using CH_2Cl_2 as solvent, and took several hours to go to completion. The reactions with CH_2I_2 and CH_2ClI were very fast, whilst that with CH_2ClBr and CH_2Br_2 were considerably slower, taking several hours to go to completion. Each of the compounds produced was isolated as a pale yellow solid and preparative details are given in section 2.4 of Chapter 7,

along with results of elemental analysis and ^1H nmr data (see Tables 7.8 and 7.17). The product formed by oxidative addition in all cases was a mixture of *cis*- and *trans*-isomers, and for the reaction with CH_2ClI and CH_2I_2 some $[\text{PtI}_2\text{Me}_2(\text{phen})]$ was also produced. The products of the reactions and their stereochemistries are shown below.



a; *cis*

b; *trans* (denotes mode of CH_2X_2 addition)

XIIIa), X = I

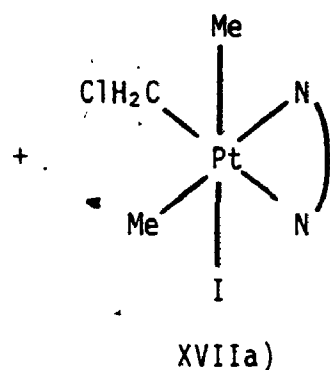
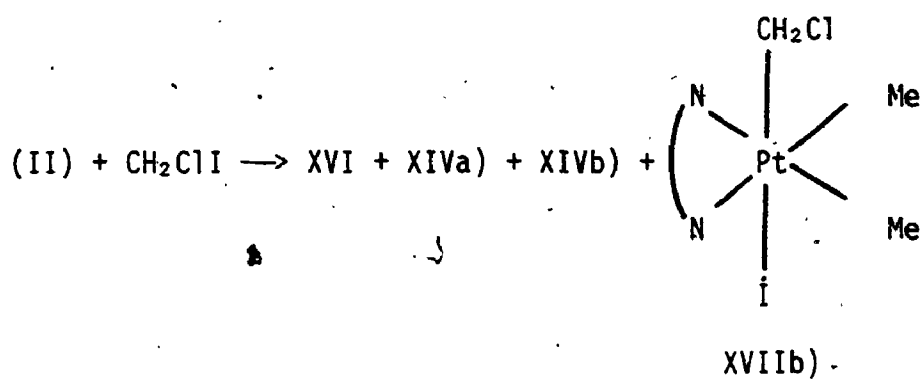
XIIIb), X = I

XIVa), X = Cl

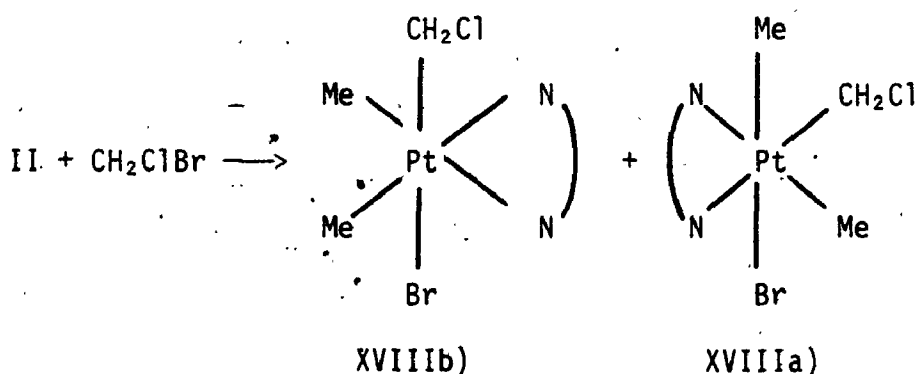
XIVb), X = Cl

XVa), X = Br

XVb), X = Br



... (16)



... (17)

This is the only series of organic halides encountered in this work for which oxidative addition yields the *cis*-isomer. If the products are left in solution, isomerisation takes place to form the *trans*-isomer. This will be discussed later. In an attempt to form a binuclear complex, the *trans*-isomer (XIIIb) was added to a solution of (II) in acetone (1:1 mole ratio). No reaction occurred.

The complexes were characterised by 1H nmr spectroscopy, and data previously published by Kuyper¹³ for *cis*- and *trans*-[PtClMe₂(CH₂Cl)(bipy)]

proved very helpful. The ^1H nmr spectrum of the products from the reaction of (II) with CH_2Cl_2 is shown in Fig. 4.1. The peak at 1.47 ppm is due to the protons of the MePt group of the *trans*-isomer (XIVb), with a $^2J_{\text{PtMe}}$ value of 69 Hz, characteristic of a platinum(IV) complex. The intensity of this peak relative to the one at 3.62 ppm, is 3:1. This, along with the presence of ^{195}Pt satellites for this low field peak, is clear indication that it can be assigned to PtCH_2Cl . The *cis*-isomer (XIVa) contains two non-equivalent methyl groups. The one above the plane of the aromatic rings will be more shielded¹³ and occurs at 0.81 ppm. A peak of equal intensity occurs at 1.55 ppm and is assigned to the MePt group *trans* to phen in (XIVa). The relative size of the $^2J_{\text{PtMe}}$ coupling constants are as expected for a methyl group *trans* to phen and *trans* to Cl^{41} respectively. Complex (XIVa) does not possess a plane of symmetry and, as a result, the methylene protons are not equivalent. This accounts for the AB pattern in the ^1H nmr spectrum at approximately 5 ppm. Signals due to both these methylene protons have ^{195}Pt satellites with considerably differing $^2J_{\text{PtCH}_2}$ values (91 and 39 Hz). In the *cis*-isomer (XIVa) the protons on the carbon adjacent to the nitrogen atoms are not equivalent. As a result a doublet of doublets is observed, due to one of them, at 9.75 ppm, whilst the signal due to the other is buried under the signal due to H^2 of the *trans*-isomer at 9.18 ppm - note the distortion of this signal.

To help confirm these assignments complex(II) was reacted with CD_2Cl_2 and the ^1H nmr spectrum of the product was found not to contain the AB pattern, nor the peak at 3.62 ppm.

The ^1H nmr spectra of the products from the reaction with CH_2Br_2 and CH_2I_2 (Table 7.8) were very similar to that in Figure 4.1. In the

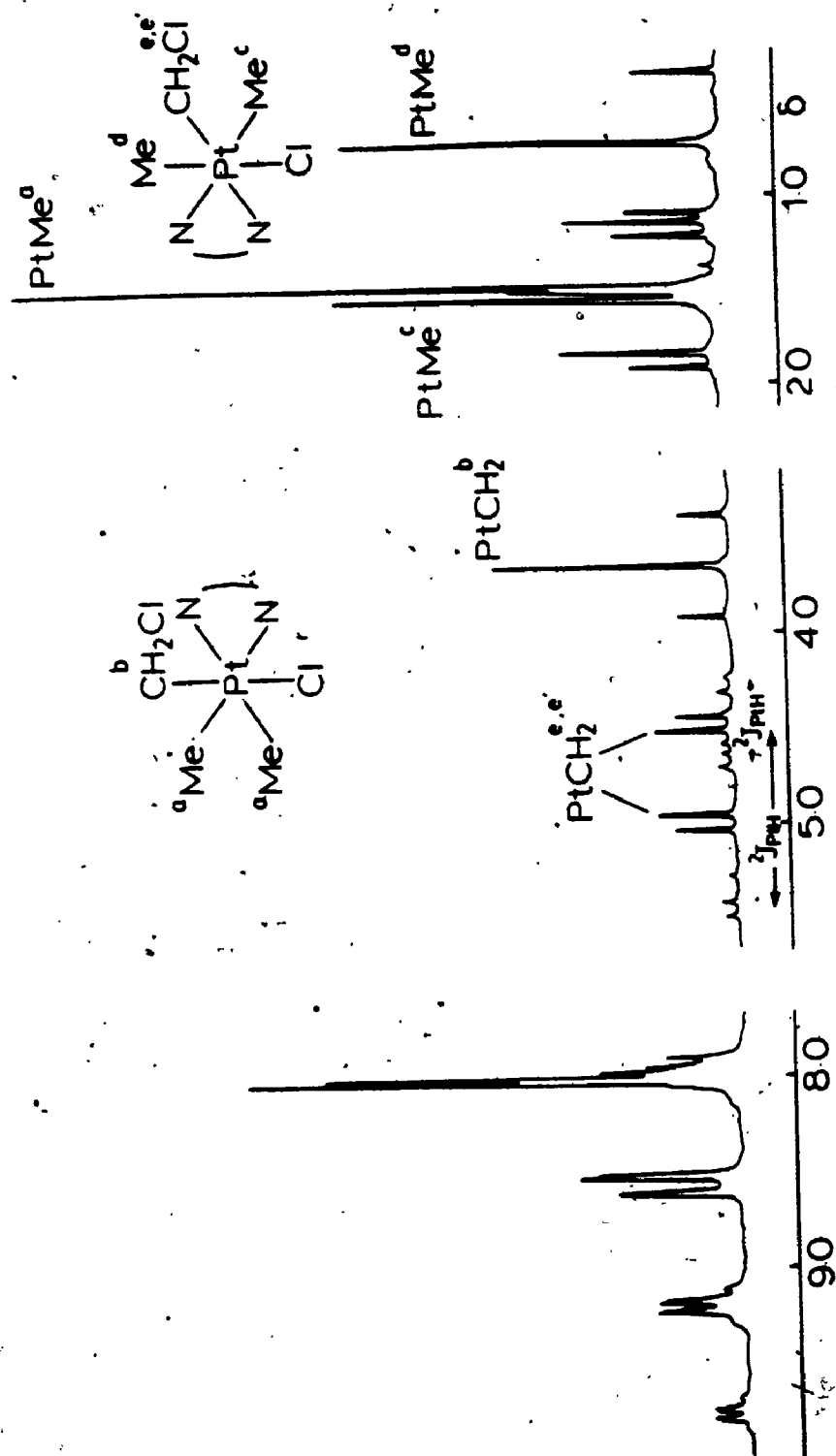


FIGURE 4.1: ^1H NMR Spectrum (100 MHz) of *cis-* and *trans-*
 $[\text{PtClMe}_2(\text{CH}_2\text{Cl})(\text{phen})]$ in CDCl_3 .

case of CH_2I_2 however, a peak at 2.53 ppm, with ^{195}Pt satellites, was present. This has been assigned to the MePt group of *trans*- $[\text{PtI}_2\text{Me}_2(\text{phen})]$ by comparison with an authentic sample.

For complexes (XIIIa), (XIVa) and (XVa) the $^2J_{\text{PtMe}}$ values of the MePt group *trans* to halide does not follow the usual trend.^{41,58} Normally the $^2J_{\text{PtMe}}$ values of the methyl *trans* to Cl and Br are very similar and larger than the value for methyl *trans* to I.

The ^1H nmr spectrum of the products from the reaction between (II) and CH_2ClBr , by comparison with those discussed above, clearly shows that a *cis*-adduct and *trans*-adduct were formed (Fig. 4.2). There exist two equally intense MePt peaks, one at 1.65 ppm and one at 0.81 ppm due to the *cis*-product (XVIIIa), and a peak at 1.55 ppm due to the MePt group of the *trans*-isomer (XVIIIb). A singlet at 3.58 ppm is assigned to $-\text{CH}_2-$ bonded to platinum, with a $^2J_{\text{PtCH}_2}$ value of 51.6 Hz. The familiar AB pattern is likewise present. None of the chemical shifts correspond to those of complexes (XIVa), (XIVb), (XVa) and (XVa). The problem is whether reaction takes place *via* rupture of the C-Cl bond or the C-Br bond. In line with previous work on oxidative addition of organic halides to metal centres, one would anticipate the latter.¹⁷ By comparing the trends in chemical shifts, and $^2J_{\text{PtMe}}$ values for a methyl group *trans* to Cl or Br, the assignments were made for addition *via* rupture of the C-Br bond (eq. 17). The ^1H nmr spectrum of the products from the reaction of CH_2ClI with (II) was very complicated. There were two AB patterns, and two signals assignable to PtCH_2X ($\text{X} = \text{Cl}$ or I). The assignments were made by comparison with the data already discussed and the products are shown in equation 16. Halogen scrambling, similar to the reactions studied by Lappert,¹⁷ must have occurred, indicative of a free-radical mechanism.

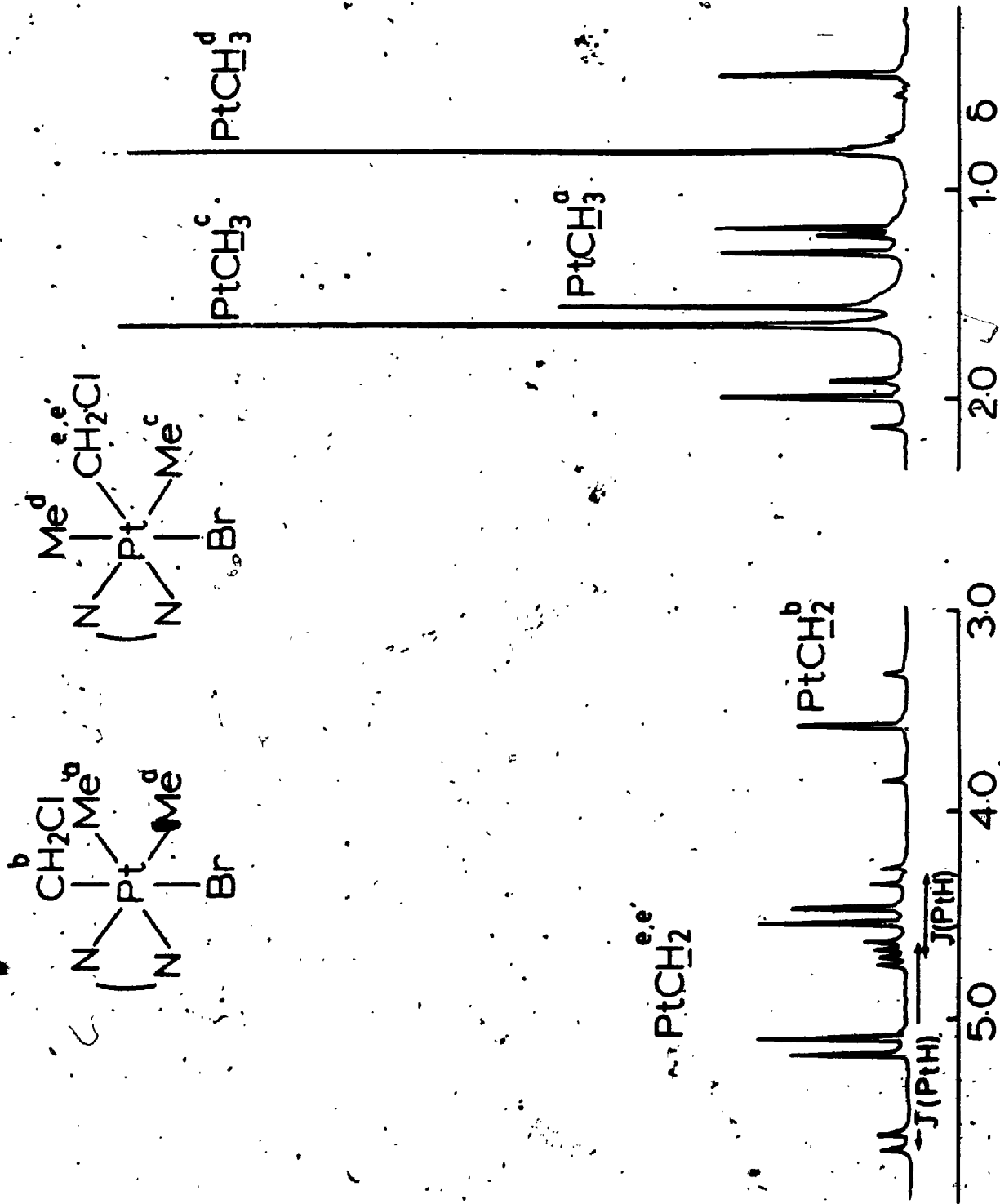


FIGURE 4.2: ^1H NMR Spectrum (100 MHz) of cis- and $\text{trans-}[\text{PtBrMe}_2\text{-CH}_2\text{Cl}](\text{phen})$ in CDCl_3 .

It is not clear if any dichloro-adduct $[\text{PtCl}_2\text{Me}_2(\text{phen})]$ is produced but a peak in the ^1H nmr spectrum at 2.35 ppm ($^2J_{\text{PtMe}}$, 72 Hz) may be due to this compound. Alternatively, this peak may be due to the protons of the MePt group in $[\text{Pt}(\text{Cl})(\text{I})\text{Me}_2(\text{phen})]$. Several unsuccessful attempts (at room temperature and at -60°C) were made to prepare the dichloroplatinum-(IV) complex. Each attempt resulted in a mixture of products.

3.1.2 Kinetic and Mechanistic Studies

The majority of the kinetic and mechanistic studies were carried out for CH_2I_2 reacting with (II). A number of different techniques were used and the results are presented here. Experimental details are given in section 2.4 of Chapter 7.

i) UV/Visible Spectrophotometry

The rate of the reaction between CH_2I_2 and (II) was monitored by the decay of the MLCT band in the uv/visible spectrum due to (II), as the reaction progressed. The solvent used was acetone and the work was done in diffuse daylight. A large excess of CH_2I_2 was used in the reactions. Figure 4.3 shows a plot of absorbance (at 473 nm) versus time for a typical run. There is a very obvious induction period followed by a rapid reaction. This is characteristic of a free-radical chain reaction. Such reactions are known⁴² to be inhibited by radical scavengers, such as galvinoxyl. The reaction between CH_2I_2 and (II) was again monitored as described above and once the reaction proceeded at a rapid rate a small volume of galvinoxyl solution (0.25 mL, 10% molar ratio) was added. Some retardation did occur, as shown in Figure 4.4.

The reaction does appear to go, at least in part, *via* a chain mechanism and such reactions can be initiated by photolysis. To confirm this a sample of the reaction mixture was placed in the spectrophotometer

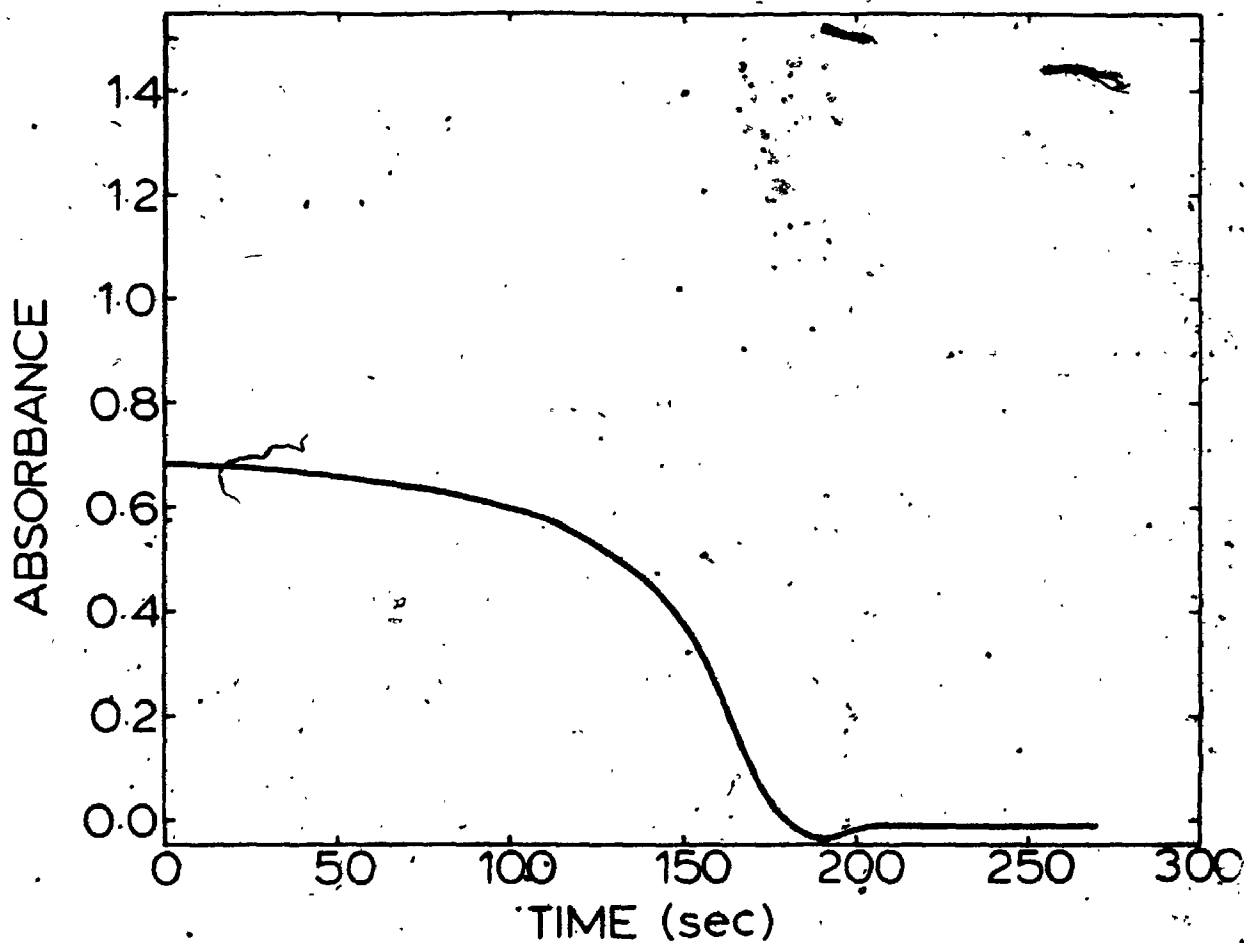


FIGURE 4.3: Decay of the MLCT Band in the UV/visible Spectrum, at 472.7 nm, Due to (II), in the Reaction between (I) (2.5×10^{-4} M) and CH_2I_2 (2.0×10^{-3} M). Solvent used was acetone.

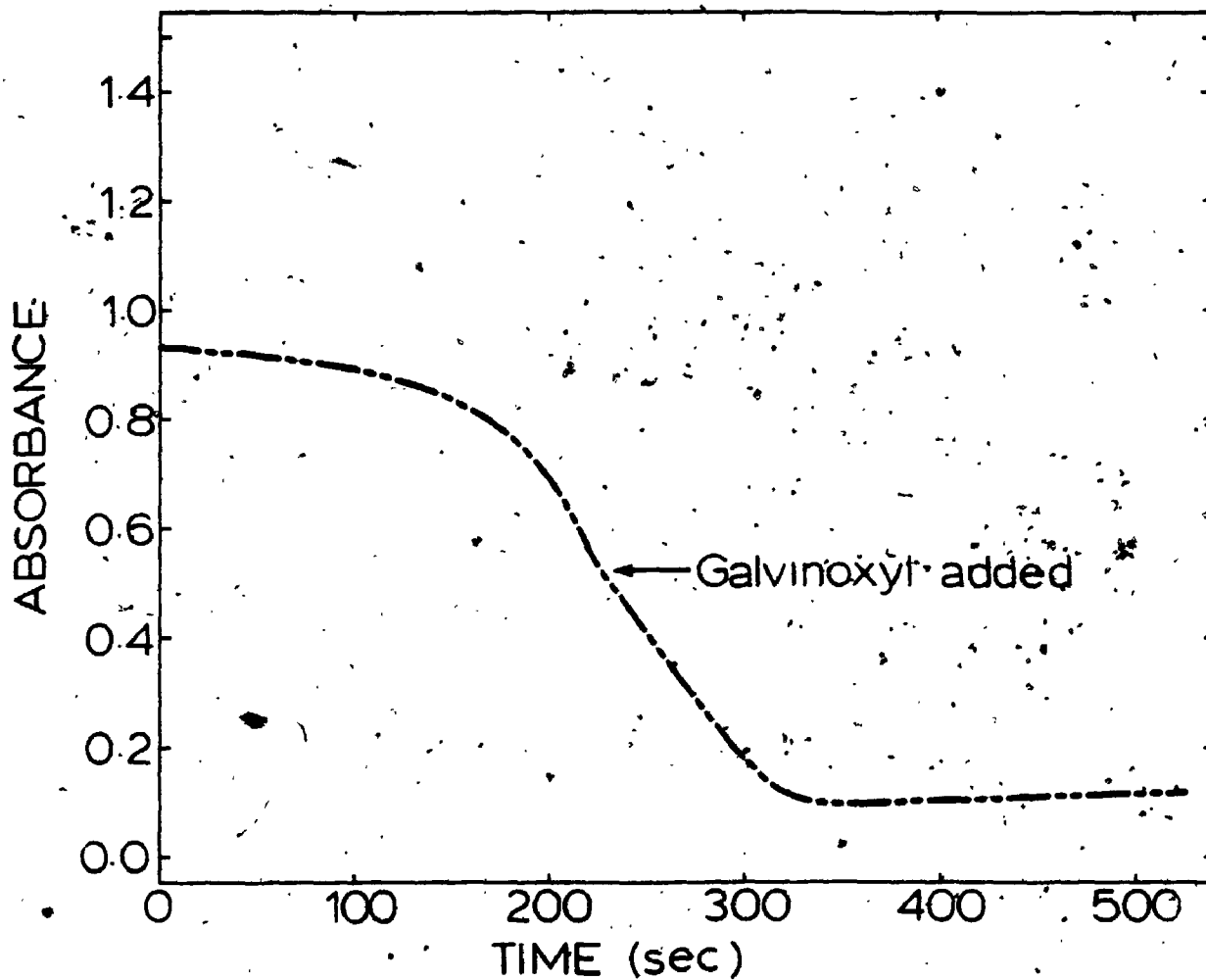


FIGURE 4.4: The Effect of Galvinoxyl (10% mole ratio) on the Rate of Reaction between (II) (10^{-4} M) and CH_2I_2 (4×10^{-3} M) Followed by Decay of the Absorbance at 472.7 nm in the UV/visible Spectrum.

and the absorbance from 600-325 nm was recorded with time. The absorbance at 473 nm decreases quite slowly. After a period of 15 minutes the sample was irradiated for 5 seconds producing a very rapid decrease in absorbance as shown in Fig. 4.5. Further proof that this is a light induced reaction came from comparing the rate of reaction for two identical reaction solutions, one of which was irradiated, the other not. The induction period and reaction time for the irradiated sample was approximately half that for the non-irradiated sample.

ii) ^1H NMR Spectroscopy

The reaction between CH_2I_2 and complex (II) in methylene chloride was followed by means of ^1H nmr. A 1:1 mole ratio of reagents was used. The initial product is that due to *cis*-addition, complex (XIVa) and this isomerises into the *trans*-isomer (XIVb). Under the conditions used, very little of the diiodide adduct (XVI) was formed, and during the isomerisation of (XIIIa) to (XIIIb) no increase in the amount of (XVI) was observed. No anomalous intensities, due to CIDNP, were observed for any of the signals.

The reaction was repeated using the same 1:1 mole ratio of reactants but in the presence of a small amount of galvinoxyl. The rate of disappearance of the starting material (II) in the presence of galvinoxyl was at least five times slower than in the absence of galvinoxyl, indicative of a radical chain-reaction.

The reaction between complex (II) and excess CH_2ClBr was monitored by ^1H nmr and again the initial product was the *cis*-isomer (XVIIIa) which isomerises to the *trans*-isomer (XVIIIb). No anomalous peak intensities due to CIDNP were observed in the spectrum.

iii) Product Ratios

The reaction of (II) with CH_2I_2 was performed under various conditions - in the dark and in diffuse daylight, with a 1:1 mole ratio

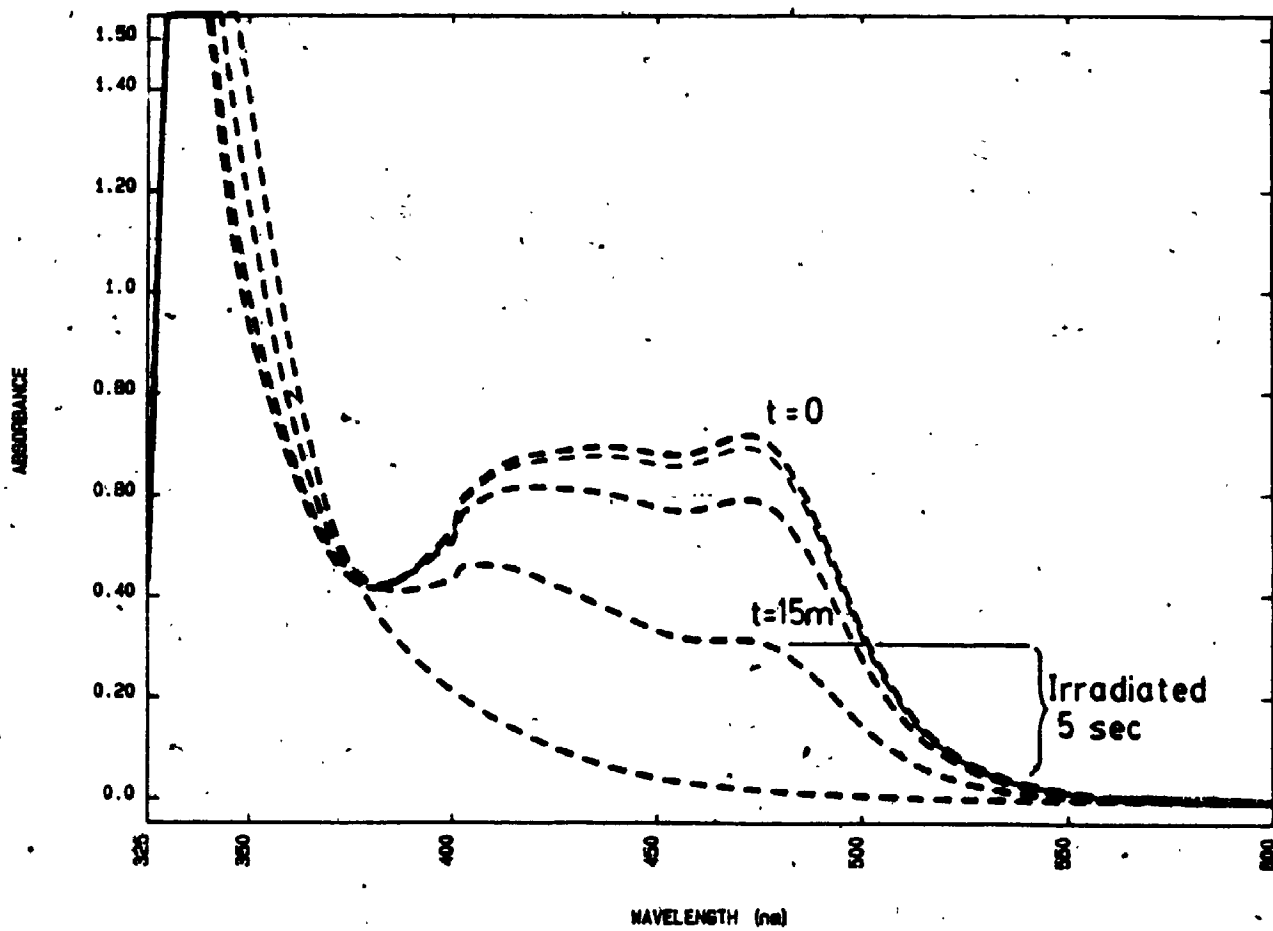


FIGURE 4.5: The Effect of Irradiation on the UV/visible Spectrum of a Reaction Mixture of [II] (5×10^{-4} M) and CH_2I_2 (4×10^{-2} M) in Acetone.

of reagents and with excess CH_2I_2 and in the presence of galvinoxyl. The main point of interest was the amount of complex (XVI) relative to the amount of the *cis*- and *trans*-isomers (XIII). This was calculated using the peak heights of the MePt signals in the ^1H nmr spectra and the results are shown in Table 4.1.

iv) Radical Trap Experiment

In Chapter 3, a short discussion was given concerning the use of α,β -unsaturated olefins to trap radical intermediates. Full experimental details are given in sections 2.6.2.3 and 2.6.2.4 of Chapter 7.

16
A solution of (II) was made up in acetone and to this was added freshly distilled acrolein. On addition of CH_2I_2 , the solution immediately turned pale yellow. The major product was complex (XVI), as indicated by a strong signal at 2.53 ppm in the ^1H nmr spectrum of the reaction product. None of the *cis*-isomer (XIIIa) was produced. Two broad peaks in the ^1H nmr spectrum at 1.5 ppm and 1.1 ppm may be due to the presence of polymer.

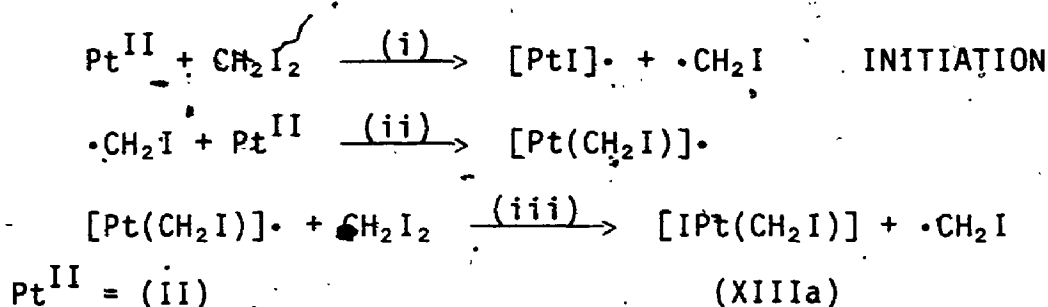
The reaction was repeated with the addition of freshly distilled acrylonitrile in place of acrolein. The ^1H nmr spectrum of the product shows that complex (XVI) was formed as the major product, together with some of complexes (XIIIa) and (XIIIb). The peaks due to the latter complexes are somewhat obscured by broad peaks, probably due to the presence of polymer in the reaction product. These results point to the intermediacy of free-radicals in the reaction between CH_2I_2 and (II).

3.1.3 Conclusions

The formation of a *cis*-isomer in the reactions discussed above is unique to the work discussed in this thesis, although *small* traces of

cis-isomer were observed for the reaction of (II) with $I(CH_2)_nI$ ($n = 3-5$). No studies have been made of the mechanism of the isomerisation of (XIIIb) to (XIIIa). Presumably pre-dissociation of a ligand from the octahedral complex (XIIa) would be necessary.⁴³

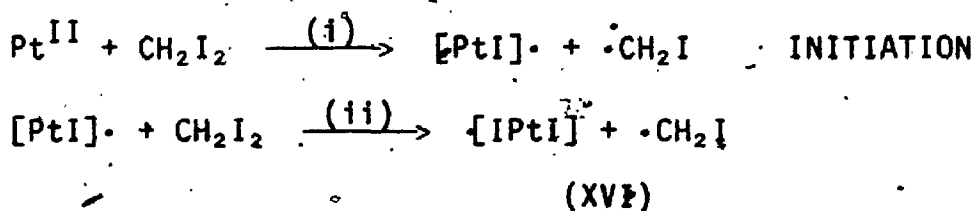
In the case of the reaction between CH_2I_2 and (II), the retardation by galvinoxyl, the long induction period, and the increased rate due to photolysis clearly point to a radical chain mechanism,⁴² as shown in Scheme 4.



SCHEME 4

Proposed Radical Chain Mechanism for the Reaction of (II) with CH_2I_2

The formation of complex (XVI) is most easily rationalised in terms of a competing non-chain mechanism. It has been shown that this complex is not formed during the isomerisation of (XIIIb) to (XIIIa). The non-chain mechanism is shown in Scheme 5.



SCHEME 5

Proposed Radical Non-Chain Mechanism for the Reaction of (II) with CH_2I_2

The initiation step in both Schemes 4 and 5 is believed to be the homolytic abstraction of iodine from CH_2I_2 , by complex (II). This can be induced photochemically, as discussed for the case of isopropyl iodide in Chapter 5. The reaction does proceed thermally in the dark, but more slowly, and, if this thermal reaction proceeds *via* the same initiation step, the relative amounts of complex (XVI) to complexes (XIIIa) and (XIIIb) should be the same. Table 4.1 shows, that within experimental error, this is the case. The presence of galvinoxyl has been shown to have some retarding effect on the reaction. This effect will be to slow down the chain pathway resulting in a larger yield of (XVI) relative to (XIIIa) and (XIIIb). This is borne out by the data in Table 4.1.

One point of interest is that, with methylene chloride as solvent, the relative amount of (XVI) formed decreases quite noticeably. This has not been investigated further and no convincing explanation can be offered.

No CIDNP effects were seen for those reactions followed by ^1H nmr. However, it is not uncommon that radical type reactions fail to show such effects.

In the reaction of (II) with CH_2Cl_2 , CH_2Br_2 and CH_2ClBr there is no formation of the complex $[\text{PtX}_2\text{Me}_2(\text{phen})]$ ($\text{X} = \text{Cl}, \text{Br}$). If these halides react in a fashion similar to CH_2I_2 formation of such a complex would be likely. However, if in Scheme 4 the rate for step ii) is much faster than step ii) in Scheme 5 little or no $[\text{PtX}_2\text{Me}_2(\text{phen})]$ would be formed. Ease of abstraction of halogens is known to follow the order $\text{I} > \text{Br} > \text{Cl}$. No kinetic studies were performed in the case of these halides and so conclusions concerning the mechanism cannot be made.

In the case of the reaction of CH_2ClI with (II), it has already been indicated that halogen scrambling occurs. This, along with the

TABLE 4.1: Product Ratio for the Reaction between (II) and CH_2I_2 at 20°C

Conditions	$10^3 [\text{PtMe}_2\text{phen}]$ M	$10^2 (\text{CH}_2\text{I}_2)$ M	Solvent	Product Ratio XIIIa,b/XVI
Excess CH_2I_2 Dark	8.2	20.6	Acetone	2.2
Excess CH_2I_2 Diffuse light	8.2	20.6	Acetone	2.3
1:1 mole ratio Dark	9.4	0.94	Acetone	1.2
1:1 mole ratio Diffuse light	9.4	0.94	Acetone	1.4
1:1 mole ratio Galvinoxyl present Diffuse light	5.8	0.58	Acetone	0.94
1:1 mole ratio Diffuse light	8.6	0.86	Methylene chloride	3.4

formation of significant amounts of $[\text{PtI}_2\text{Me}_2(\text{phen})]$, indicates the involvement of free-radicals. All four products from the reaction contain the (PtCH_2Cl) unit, implying that it is the C-I bond which is ruptured during the course of the reaction. If this is so then the product from a radical chain mechanism would be $[\text{PtIME}_2(\text{CH}_2\text{Cl})(\text{phen})]$, and this is indeed formed. The non-chain pathway would yield (XVI). It is not clear how complexes (XIVa) and XIVb) are formed, but similar results were observed by Lappert.¹⁷ No data are available on the mechanism for the formation of these two latter complexes.

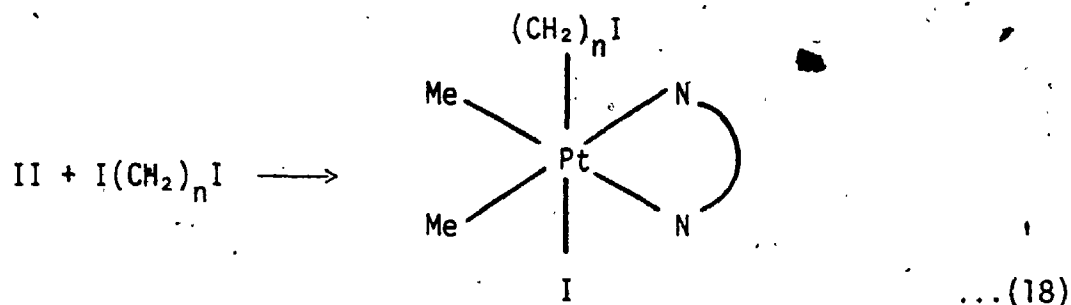
The data presented in this section is strong evidence that the reaction between CH_2I_2 and (II) proceeds *via* two competing pathways, radical chain and radical non-chain. There is also good evidence that the reaction with CH_2ClI involves free-radicals. The failure of (XIIIb) to react with (II) is almost certainly a result of steric hindrance. The binuclear complex, $[\text{Pt}_2\text{I}_2\text{Me}_4(\mu\text{-CH}_2)(\text{phen})_2]$, that would be formed, is not viable due to steric interactions between ligands on the different platinum atoms.

3.2 Reaction of $[\text{PtMe}_2(\text{phen})]$ with $\text{I}(\text{CH}_2)_n\text{I}$ ($n = 3-5$) to Form Iodoalkylplatinum(IV) Complexes

3.2.1 Preparation and Characterisation

A solution of complex (II), in acetone, reacted with excess of each of the α,ω -diiodoalkanes to form a pale yellow solution. The solid product was isolated by precipitation, using pentane. The full experimental details are given in section 2.4 of Chapter 7. If sufficiently large excess of the α,ω -diiodoalkanes is not used, some precipitation is observed, due to the formation of the insoluble binuclear complexes $[\text{Pt}_2\text{I}_2\text{Me}_4\{(\text{CH}_2)_n\}(\text{phen})_2]$. The new reactions are

shown in equation 18.



XVII $n = 3$, XVIII $n = 4$, XIX $n = 5$, for $\text{N} \text{---} \text{N} = \text{phen}$; XX $n = 3$, for $\text{N} \text{---} \text{N} = \text{bipy}$.

The product of each reaction is predominantly that for *trans*-addition of the α,ω -diiodides, but very small traces of the *cis*-isomers were observed.

Characterisation of the complexes was achieved by elemental analysis (Table 7.17), ^1H nmr spectroscopy (Table 7.4), mass spectroscopy (Table 7.19) and in the case of complex (XIX), ^{13}C nmr spectroscopy (Table 7.6). Figure 4.6 shows the high field region of the ^1H nmr spectrum of the product from the reaction of (II) with excess $\text{I}(\text{CH}_2)_5\text{I}$. The spectrum was recorded on a Bruker AM-250 spectrometer, with CD_2Cl_2 as solvent. The strong singlet at 1.60 ppm, with ^{195}Pt satellites, is assigned to protons of the MePt group of (XIX). The $^2J_{\text{PtMe}}$ value of 71.5 Hz is characteristic of a platinum(IV) complex.⁴¹ The presence of only one MePt signal indicates that the complex possesses a plane of symmetry, as expected for a product of *trans*-addition. The triplet at 2.90 ppm is assigned to the protons of the iodomethyl group.¹² These protons couple to H_δ , with a $^3J_{\text{HH}}$ value of 6.9 Hz and are downfield, relative to the other alkyl chain protons, due to deshielding by the iodine atom. The triplet due to the protons of the $-\text{CH}_2$ group bonded to platinum, by comparison with the assignment of PtCH_2 in $[\text{PtIME}_2(\text{C}_2\text{H}_5)\text{---}(\text{phen})]$ (Table 7.3), are expected to occur close to the MePt region. A

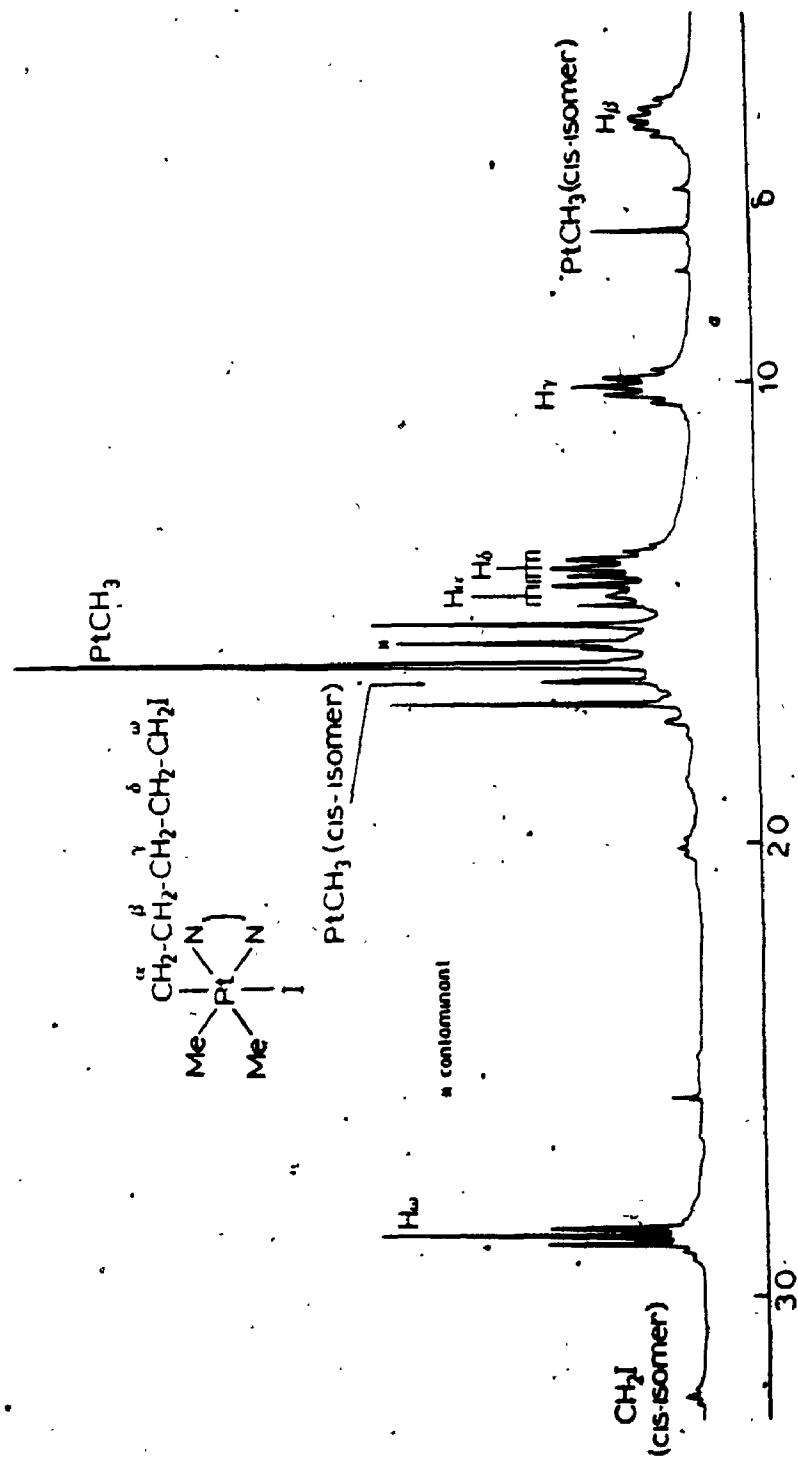


FIGURE 4.6: ^1H NMR Spectrum (400 MHz) of $\text{trans}[\text{Pt}(\text{Me})_2((\text{CH}_2)_5\text{I})]$ (phen) in CD_2Cl_2 .

distorted triplet, centred at 1.45 ppm, is assigned to this PtCH₂-group. The ¹⁹⁵Pt-satellites cannot be resolved. Three quintets are present in the ¹H nmr spectrum and these are due to the protons (H_β, H_γ, H_δ) of the remaining methylene groups. They are expected to occur upfield from the MePt signal, due to the shielding influence of the aromatic rings. The quintet at 0.40 ppm is broadened and this is attributed to coupling to ¹⁹⁵Pt (I = 1/2). On this basis, and due to its high field resonance, the quintet is assigned to the β-protons. The quintet due to the δ-protons relative to that due to the γ-protons, is expected to be at lower field as a result of its closer proximity to the iodine atom. The signal at 0.99 ppm is therefore attributed to the γ-protons and the quintet centred at 1.39 ppm, to the δ-protons. The small peaks at 0.65 ppm and 1.62 ppm (²J_{PtMe}, 71.5 Hz and 74 Hz, respectively) are due to the two inequivalent MePt groups of the *cis*-isomer. The triplet due to the protons of the iodomethylene group of this *cis*-isomer occurs at 3.22 ppm. The same characteristics are to be found in the ¹H nmr spectra (Table 7.4) of complexes (XVII), (XVIII) and (XX). The ¹³C nmr spectrum of the most soluble complex, (XIX), was recorded, and is shown in Figure 4.7. The high field peak at -5.41 ppm (¹J_{PtC}, 695.8 Hz) is assigned to the carbon of a MePt group, by comparison with similar complexes.⁴⁴ The presence of only one such signal also indicates the symmetrical stereochemistry of complex (XIX). ¹³C nmr data for α,ω-diiodoalkanes are presented in the text by Stothers.⁴⁵ This data is helpful in making assignments for the remaining carbons of the alkyl chain. Iodine tends to shield the carbon atom to which it is bonded and the high field peak at 7.34 ppm is therefore assigned to the ω-carbon atom. The peak at 26.14 ppm has ¹⁹⁵Pt satellites, with coupling to carbon of 662.8 Hz. This indicates direct

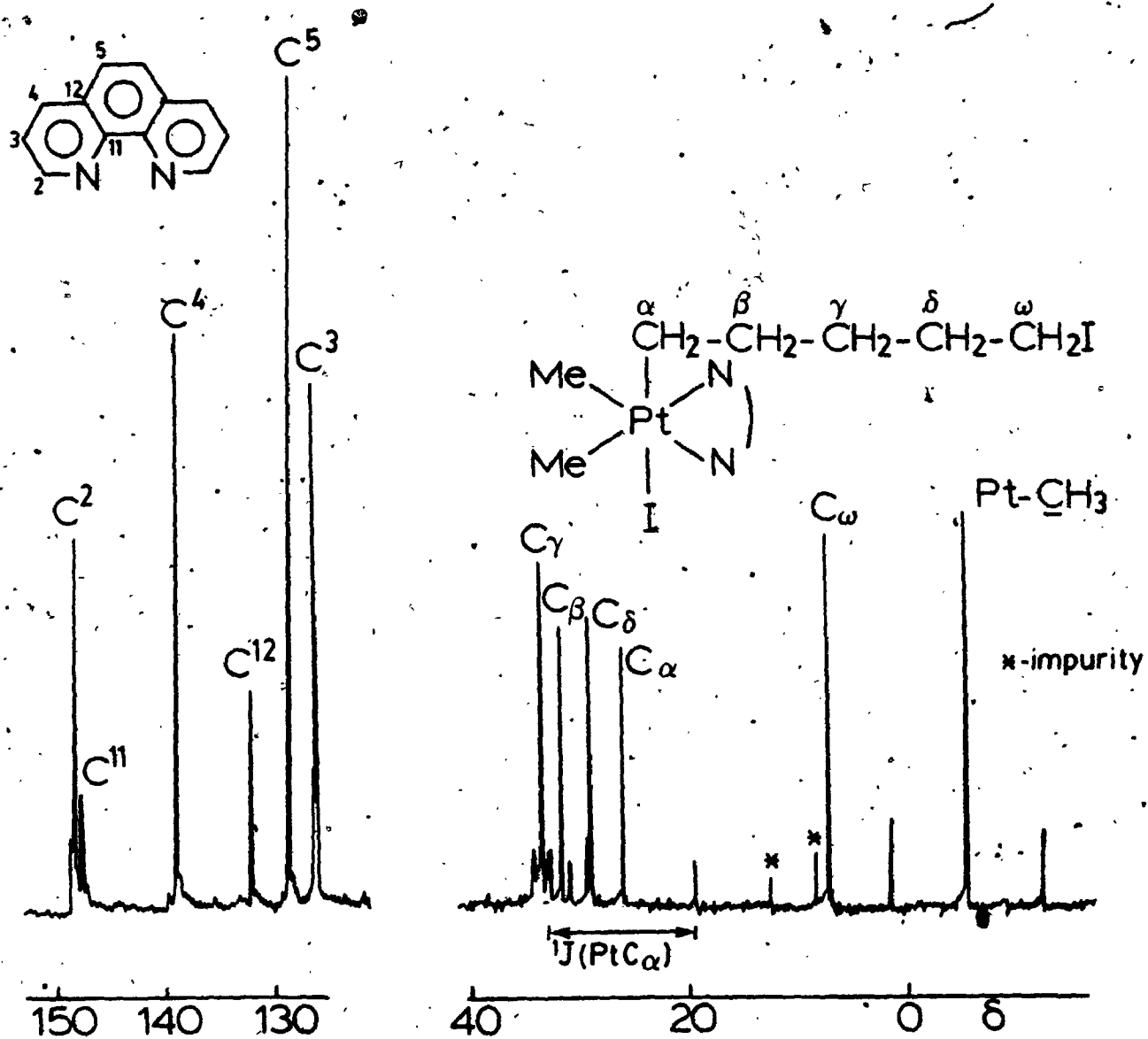


FIGURE 4.7: $^{13}\text{C}\{^1\text{H}\}$ NMR Spectrum (50 MHz) of $[\text{PtI Me}_2\{(\text{CH}_2)_5\text{I}\}-(\text{phen})]$ in CD_2Cl_2 .

bonding to platinum and the resonance is assigned to the α -carbon atom. The remaining assignments, for the alkyl chain, are made on the basis of the magnitude of ^{195}Pt -C coupling constants, assuming the coupling decreases the further the carbon atom is from the platinum. Thus the β -carbon signal occurs at 31.67 ppm, the γ -carbon at 33.39 ppm, and the δ -carbon at 29.07 ppm. The assignments for the phenanthroline ring were based on literature precedents.^{46,47} The low intensity of the peaks due to C^{11} and C^{12} is attributed to the absence of the Nuclear Overhauser Effect for these atoms.

Attempts to characterise these iodoalkylplatinum(IV) complexes by means of mass spectrometry, were not successful. No parent ion was observed in any of the spectra but peaks were observed, which are assigned to alkylplatinum fragments (Table 7.19, Chap. 7).

3.2.2 Kinetic and Mechanistic Studies

A series of kinetic experiments was performed (section 2.4, Chapter 7) for the reaction of these α,ω -diiodoalkanes with complex (II). These are discussed in this section.

i) Determination of Second-Order Rate Constants for Formation of $[\text{PtI Me}_2\{(\text{CH}_2)_n\text{I}\}(\text{phen})]$

The rates of reaction of (II), in acetone, with the α,ω -diiodoalkanes was determined by monitoring the decay of the MLCT band in the uv/visible spectrum of (II), as the reactions progressed. An excess of the diiodides was used in each case. The decay of this band for the reaction of $\text{I}(\text{CH}_2)_5\text{I}$ with (II) is shown in Figure 4.8.

A series of runs were made for different concentrations of the diiodide, keeping the concentration of (II) constant. The absorbance (A_t) at 472.7 nm was recorded at regular intervals, and a plot of $\log \frac{(A_t - A_\infty)}{(A_0 - A_\infty)}$

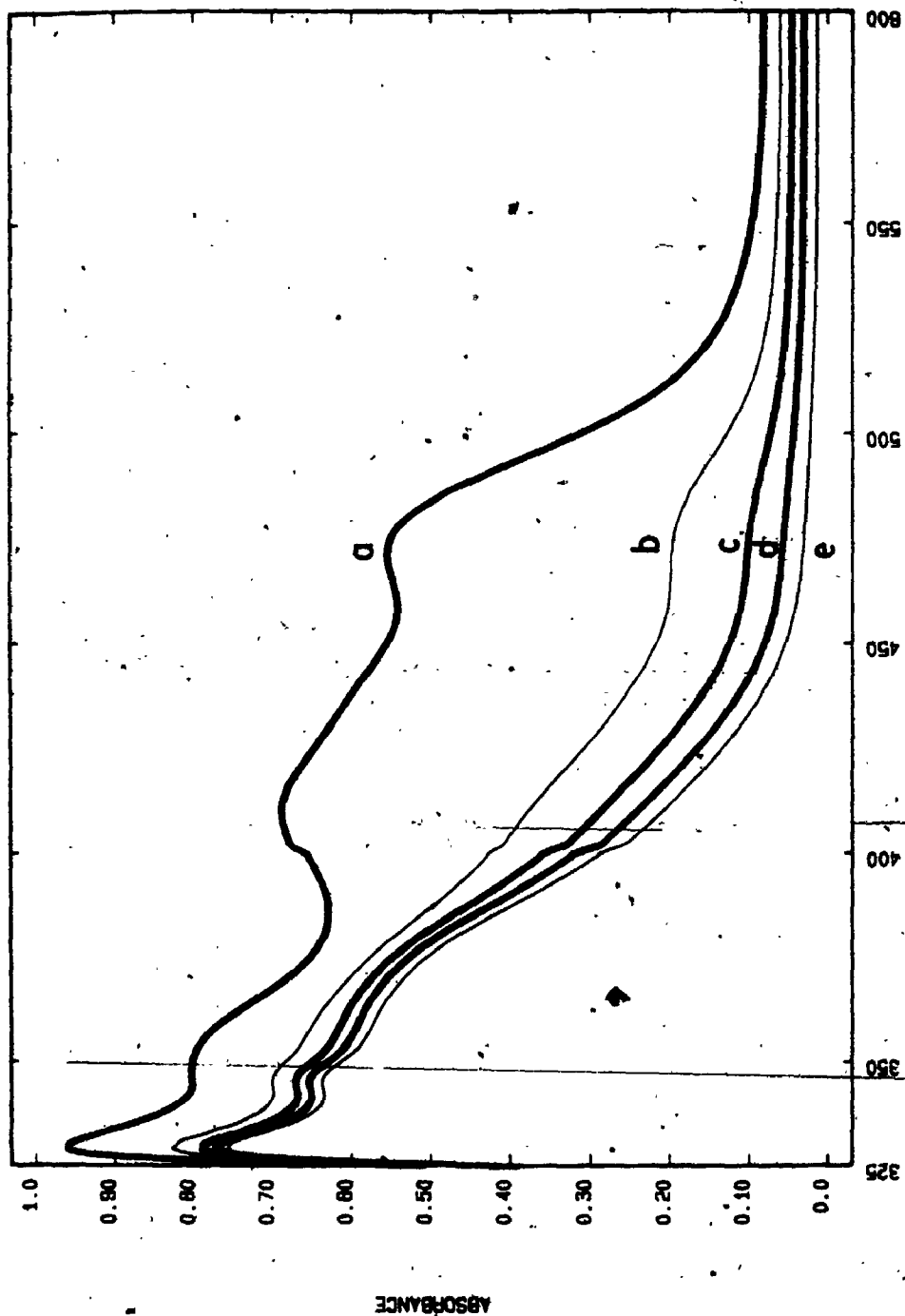


FIGURE 4.8: Change in the UV/visible Spectrum for the Reaction between (II) (5.0×10^{-4} M) and 1,5-diodopentane (2.0×10^{-1} M), in Acetone. Reaction in diffuse daylight: a) $t = 0$; b) 20 min; c) $t = 25$ min; d) $t = 30$ min; e) $t = 50$ min.

versus time was made for each concentration. The results for the reaction with $I(CH_2)_4I$ are shown in Figure 4.9. From such plots the pseudo-first-order rate constants (k_{obs}) were calculated and the graph of k_{obs} versus concentration of diiodide was plotted. A typical plot is shown in Figure 4.10 for the use of $I(CH_2)_4I$. From such plots the second-order rate constants for the reactions were obtained and are shown in Table 4.3 later in the chapter.

The 1H nmr spectra of the products from these kinetic experiments confirmed that the iodoalkylplatinum(IV) complexes were the sole products.

ii) Irradiation of Reaction Mixture

In section 3.1.2 of this chapter the effect of irradiation on the reaction between CH_2I_2 and (II) was described. An acceleration in the reaction rate was very clearly demonstrated. In a similar fashion the reaction between $I(CH_2)_3I$ and (II) was monitored, by following the decay of the MLCT band at 473 nm due to (II), whilst irradiating the sample. Figure 4.11 illustrates the result. The broken line represents the change in absorbance, with time, for the reaction performed in diffuse light. The unbroken line represents the change, using identical concentrations of reagents, for irradiation of the sample. The sample was irradiated from the 55 sec mark to the 280 sec mark. Furthermore a small volume of the radical scavenger, galvinoxyl (0.1 mL, 4% mole ratio) was added to the irradiated sample at the 160 sec mark. Comparison of the two plots shows that neither irradiation nor galvinoxyl have any significant effect on the reaction rate.

A further experiment was performed in which galvinoxyl was added to the reaction sample, whilst monitoring the absorbance (at 473 nm). The reaction was done in diffuse daylight. In order to obtain a faster rate of reaction a higher concentration of $I(CH_2)_3I$ was used compared to the

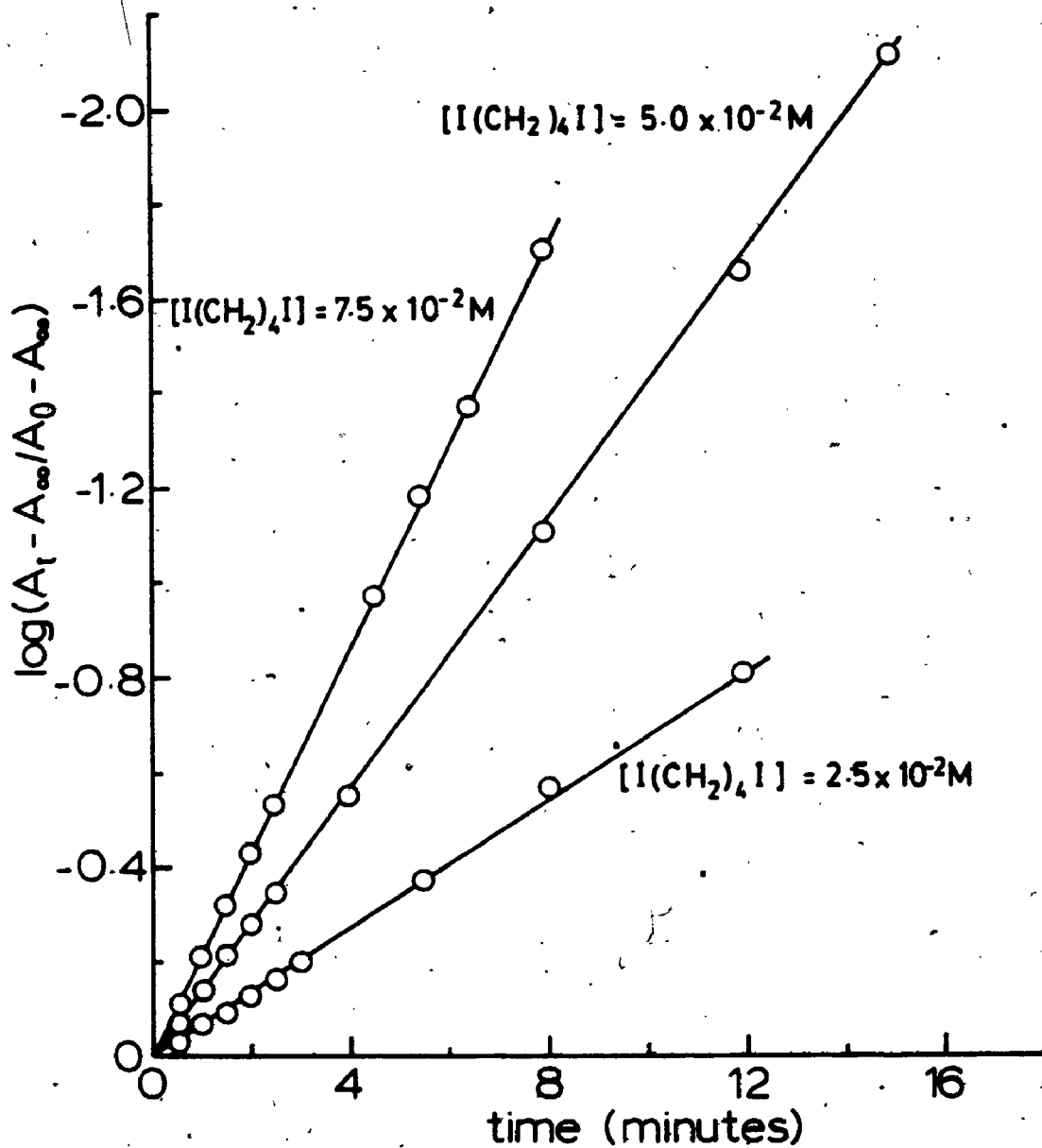


FIGURE 4.9: Plot of $\log \frac{(A_t - A_\infty)}{(A_0 - A_\infty)}$ Versus Time, for the Reaction of (II) (5.0×10^{-4} M) with $I(CH_2)_4I$, in Acetone at $25^\circ C$, for Varying Concentrations of $I(CH_2)_4I$.

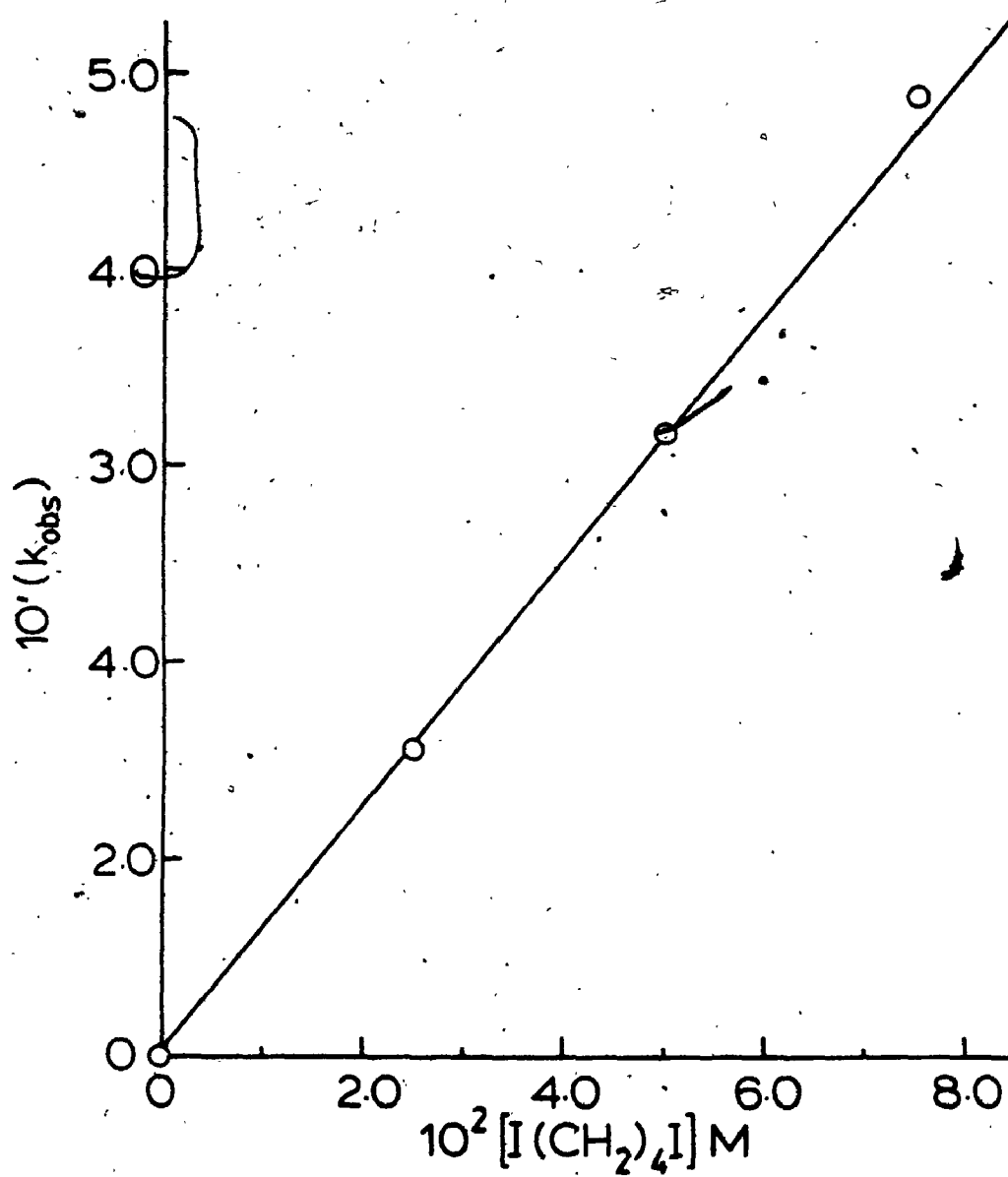


FIGURE 4.10: Plot of Observed First-Order Rate Constants (k_{obs}) Versus Concentration of $\text{I}(\text{CH}_2)_4\text{I}$, in Acetone at 25°C , for the Reaction of (II) with $\text{I}(\text{CH}_2)_4\text{I}$.

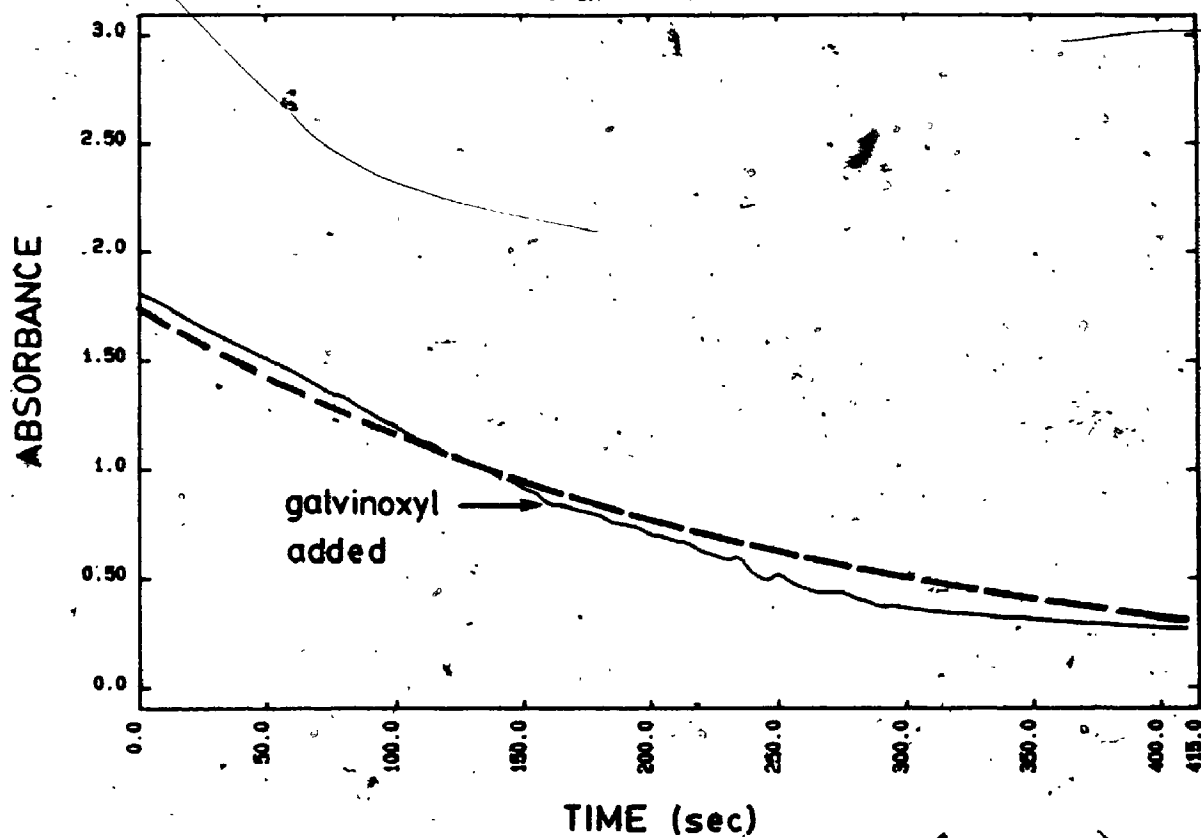


FIGURE 4.11: The Effect of Galvinoxyl and Irradiation on the Reaction between (II) and $I(CH_2)_3I$.
----- Diffuse Daylight; ——— Sample Irradiated and Galvinoxyl Added (λ , 473 nm).

experiment described in the previous paragraph. The result of this experiment is shown in Figure 4.12 and again the galvinoxyl has had no effect on the reaction rate. The discontinuity (at 100 sec) is due to the addition of the galvinoxyl.

A control experiment was performed, in which the absorbance from 325 nm to 600 nm of a mixture of $I(CH_2)_3I$ and galvinoxyl was monitored. Peaks at 578 nm (very weak) and 396 nm (strong) were observed. By comparison with an authentic sample the peaks are assigned to galvinoxyl. On irradiating this mixture for several minutes no change occurred in the spectrum.

3.2.3 Conclusions

All the reactions discussed in this section follow good second-order kinetics, which is strong evidence for an S_N2 type mechanism. The relative rates of reaction, as indicated by the rate constants in Table 4.3 (see Section 3.4.3), follow the trend expected for an S_N2 mechanism.

Irradiation of the reaction mixture would be expected to accelerate the rate if free-radicals were involved. No such effect was observed, thus discounting the intermediacy of free-radicals.

The results from the experiments with galvinoxyl must be treated more carefully. Galvinoxyl would be expected to retard a radical chain-mechanism, but not a radical non-chain mechanism. It is possible⁴⁸ that galvinoxyl does not *totally* inhibit a chain-mechanism but it is not thought that the reactions under discussion fall into this category. Thus, the failure of galvinoxyl to retard the reaction between (II) and $I(CH_2)_3I$ is further indication of an S_N2 mechanism.

The absence of any of complex (XVI), $[PtI_2Me_2(phen)]$, in any of the reaction products, is good indication that a radical non-chain mechanism is not operating.

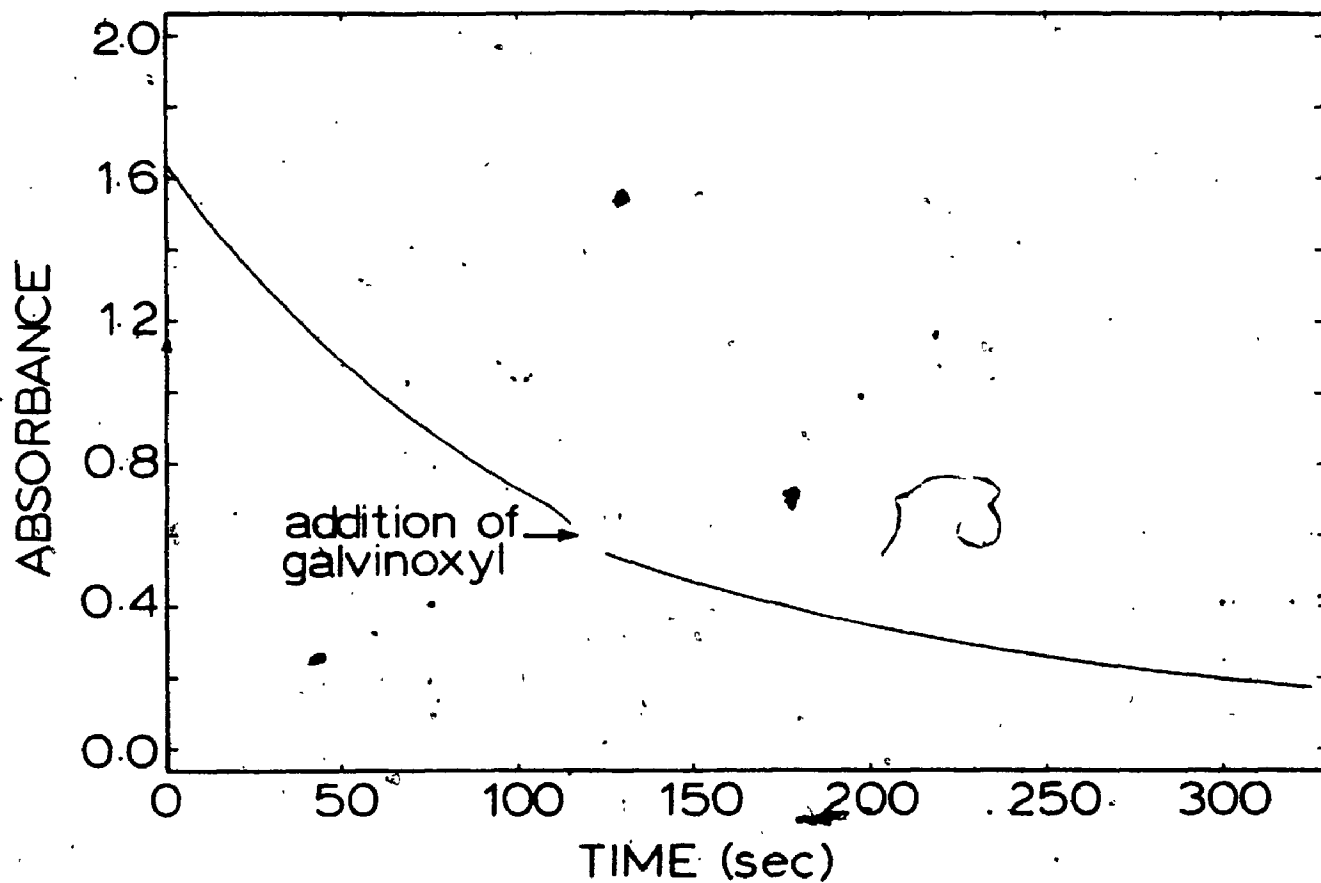


FIGURE 4.12: The Effect of Galvinoxyl (4% mole ratio) on the Reaction between (II) and $I(CH_2)_3I$, in Acetone. Reaction followed by decay of the band at 473 nm in the uv/visible spectrum.

The evidence presented in this section points very clearly to an S_N2 mechanism for the formation of these iodoalkylplatinum(IV) complexes (XVII-XX).

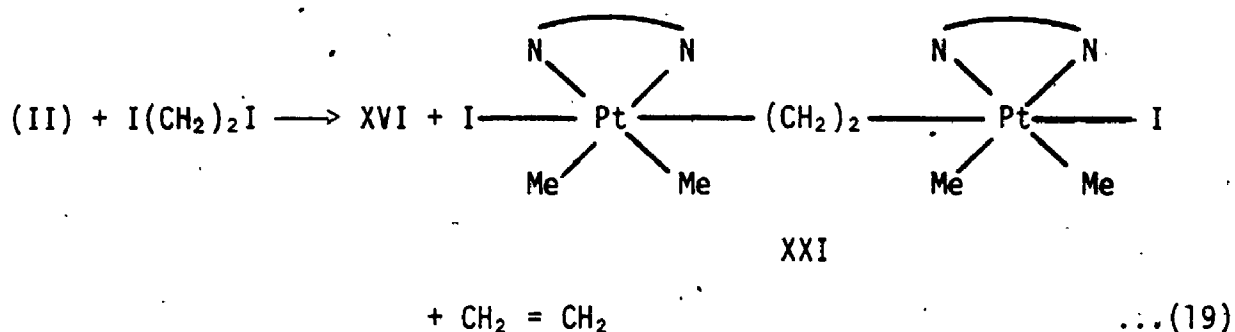
3.3 Reaction between $[PtMe_2(phen)]$ and $X(CH_2)_2X$ ($X = I, Br$)

In the reaction between complex (II) and $I(CH_2)_2I$ or $Br(CH_2)_2Br$, in acetone, an insoluble product was formed in both cases. The insoluble product for the reaction with $I(CH_2)_2I$ has been characterised as $[Pt_2I_2Me_4\{(CH_2)_2\}(phen)_2]$ (XXI). In the reaction with $Br(CH_2)_2Br$ the insoluble product is believed to be $[Pt_2Br_2Me_4\{(CH_2)_2\}(phen)_2]$ (XXII). Experimental details for this work are in section 2.4 of Chapter 7.

Due to the insolubility of these two complexes no nmr spectral data could be obtained. The elemental analyses (Table 7.17) of the complexes are however consistent with the general formula $[Pt_2X_2Me_4\{(CH_2)_2\}(phen)_2]$ ($X = Br, I$).

The reaction of (II) with these two α,ω -dihalogenoalkanes, not only produced the insoluble product, but a more soluble product was left in solution. In the reaction with $I(CH_2)_2I$ this more soluble product was identified as $[PtI_2Me_2(phen)]$ (XVI) by its 1H nmr spectrum. The product left in solution for the reaction of (II) with $Br(CH_2)_2Br$ was not completely identified. It proved insufficiently soluble to obtain a good 1H nmr spectrum. The elemental analysis data (C, 36.27%; H, 3.00%; N, 5.91%; Br, 13.24%) for this complex does not compare well with those calculated for $[PtBr_2Me(phen)]$ or the bromoalkyl complex $[PtBrMe_2\{(CH_2)_2Br\}(phen)]$. The data is however fairly consistent with that calculated for complex (XXII).

The new reaction of (II) with $I(CH_2)_2I$ is shown in equation 19.



3.3.1 Analysis of the Gaseous Product from the Reaction of I(CH₂)₂I with (II)

A solution of (II) in acetone was placed in the apparatus shown in Figure 7.1 of Chapter 7. The mixture was frozen and a solution of I(CH₂)₂I in acetone was added. The apparatus was sealed, evacuated and allowed to come to room temperature. On completion of the reaction a sample of the gas above the reaction mixture was analysed by gas chromatography. By comparison with the retention time of an authentic sample of ethene, the presence of a large amount of ethene in the gaseous product of the reaction was confirmed. A small volume of ethene was introduced into the reaction vessel and this new gaseous mixture was analysed by gas chromatography. The peak, believed to be due to ethene, increased significantly in intensity.

3.3.2 Pyrolysis of [Pt₂I₂Me₄{(CH₂)₂}(phen)₂]

A sample of complex (XXI) was pyrolysed in the apparatus shown in Figure 7.1 of Chapter 7. Experimental details are given in section 2.4.2.9 of Chapter 7. The gaseous products were analysed by gas chromatography. The major product was ethene. This was confirmed by comparing the retention time of this product with that of an authentic sample of ethene.

3.3.3 Kinetic and Mechanistic Studies for the Reaction between (II) and I(CH₂)₂I

The kinetics for the reaction between (II) and 1,2-diiodoethane proved more complex than for any system discussed thus far in this thesis. The results and conclusions are presented below.

i) Determination of the Rate Constant

The reaction between (II) and 1,2-diiodoethane, in acetone, was monitored by following the decay of the MLCT band in the uv/visible spectrum of II, as the reaction progressed. The 1,2-diiodoethane was purified before use, and an excess of the ligand was used. A series of runs were performed, keeping the concentration of (II) constant whilst varying the concentration of 1,2-diiodoethane. The absorbance (A_t) at 472.7 nm was recorded at regular intervals, and for each concentration of 1,2-diiodoethane a plot of $\log_{10} (A_t - A_\infty)$ versus time was made. A typical plot is shown in Figure 4.13. From such plots the pseudo-first-order rate constants (k_{obs} , Table 4.2) were calculated and plotted against the concentration of 1,2-diiodoethane. This is shown in Figure 4.14. The second-order rate constant was calculated from the slope of this line and was found equal to $11.7 \text{ L mol}^{-1} \text{ s}^{-1}$.

It is clear from Figure 4.13 that the reaction does not follow simple first-order kinetics with respect to (II) under the conditions of the experiment. Figure 4.13 indicates that an acceleration of the reaction rate occurs in the later stages of the reaction. The calculation of k_{obs} was made by using only the linear portion of such plots.

ii) UV/visible Spectrum of the Reaction Mixture

A solution of (II), in acetone, was added to a solution of 1,2-diiodoethane in acetone and the uv/visible spectrum of the mixture was monitored between 600 to 325 nm. An intense band formed immediately on

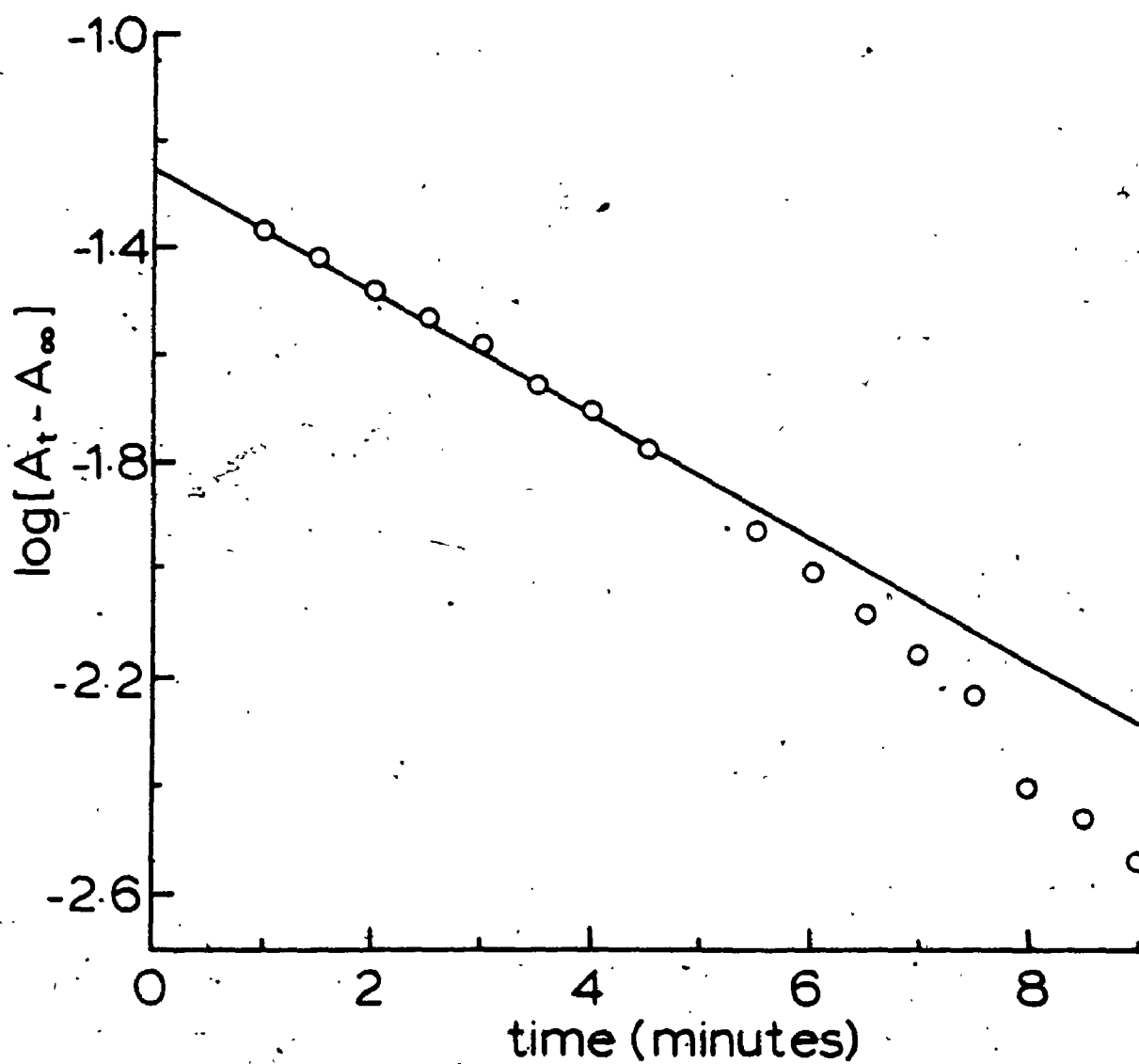


FIGURE 4.13: Plot of $\log(A_t - A_\infty)$ Versus Time (Min) for the Reaction of (II) (5.0×10^{-5} M) with $\text{I}(\text{CH}_2)_2\text{I}$ (4.0×10^{-4} M) in Acetone at 25°C .

TABLE 4.2: Observed First-Order Rate Constants (k_{obs}) for Reaction
 between $[\text{PtMe}_2(\text{phen})]$ (5.0×10^{-5} M) and $\text{I}(\text{CH}_2)_2\text{I}$ in
 Acetone at 25°C

$10^4 [\text{I}(\text{CH}_2)_2\text{I}]$	$10^3 k_{\text{obs}}/\text{S}^{-1}$
4.0	4.3
5.0	5.0
6.0	7.4

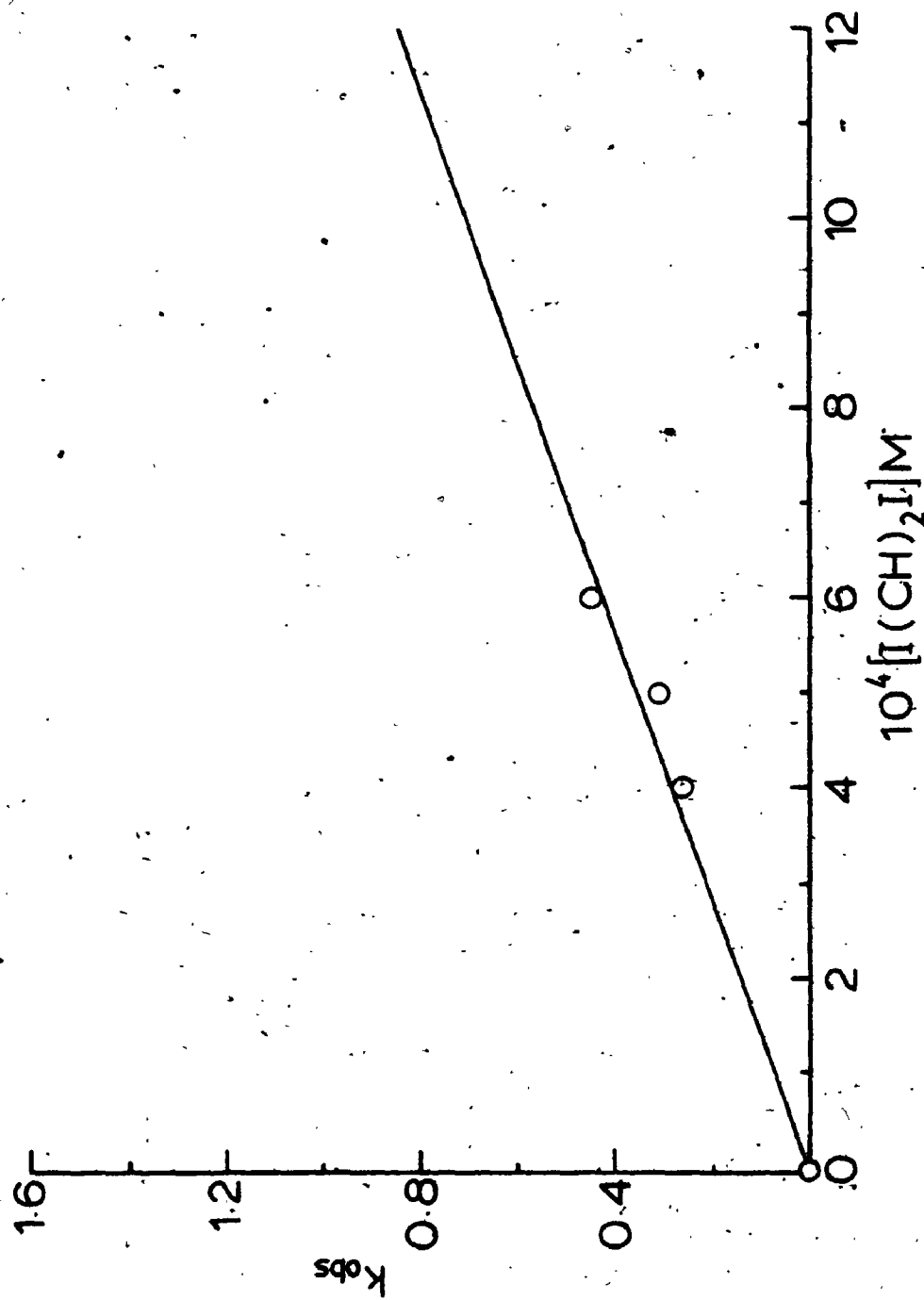


FIGURE 4.14: A Plot of k_{obs} (S^{-1}) Versus $[I(CH_2)_2I]$ for the Reaction of (II) ($5.0 \times 10^{-5} M$) with $I(CH_2)_2I$, in Acetone at $25^\circ C$.

mixing, centred at approximately 400 nm. This band gradually decayed but details of the decay were not studied.

iii) Effect of Irradiation and of Galvinoxyl on the Reaction Rate

To a solution of (II), in acetone (1.5×10^{-4} M), was added an equal volume of an acetone solution of 1,2-diiodoethane (9.0×10^{-3} M). The reaction was performed in diffuse daylight and the absorbance at 473 nm was recorded. The reaction mixture was irradiated after 2 m for a period of 1 m. A rapid increase in rate was observed. On removal of the irradiating source the reaction rate decreased. Figure 4.15 shows the results of this experiment.

Using a reaction mixture of identical reagent concentrations as described above, the effect of galvinoxyl on the rate of reaction was investigated. The absorbance (A_t) at 473 nm was measured as the reaction progressed, and a plot of A_t versus time was made. This is shown in Figure 4.16. In order to accelerate the reaction rate the solution was irradiated in the early part of the reaction. A small volume of galvinoxyl solution (0.5 mL, 10% mole ratio with respect to (II)) was added after 4 m. There was a very obvious inhibition of the reaction (Fig. 4.16).

3.3.4 Mass Balance Experiment

A known mass of (II) was reacted with an excess of $I(CH_2)_2I$, in acetone. The relative number of moles of (II) used to the moles of (XVI) and (XXI) produced was 4:2:1. This gives a good mass balance for platinum. These results indicate the stoichiometry shown in equation 20.

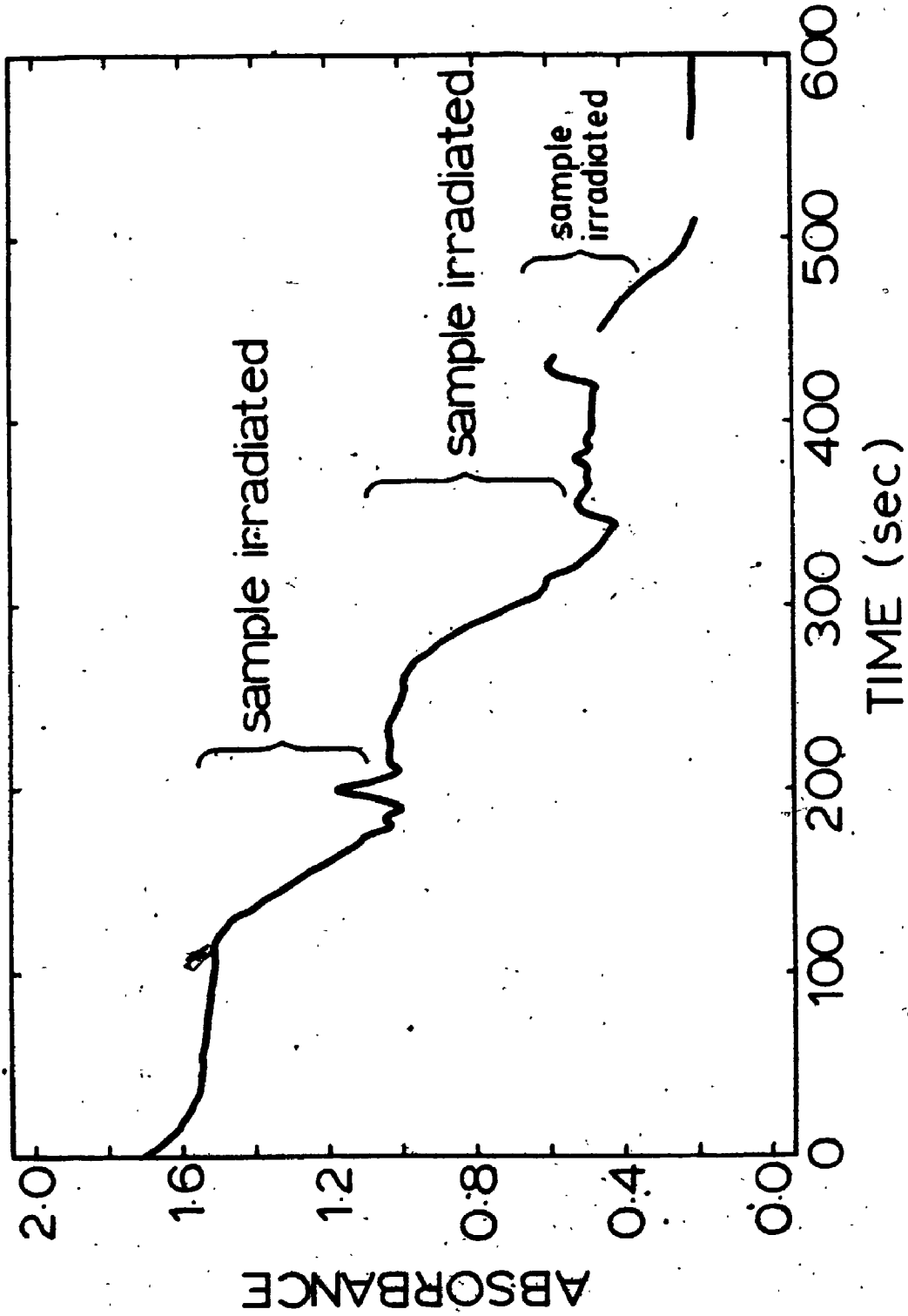


FIGURE 4.15: The Effect of Irradiation on the Reaction between (II) and $I(CH_2)_2I$. Reaction followed by decay of the band at 473 nm in the uv/visible spectrum.

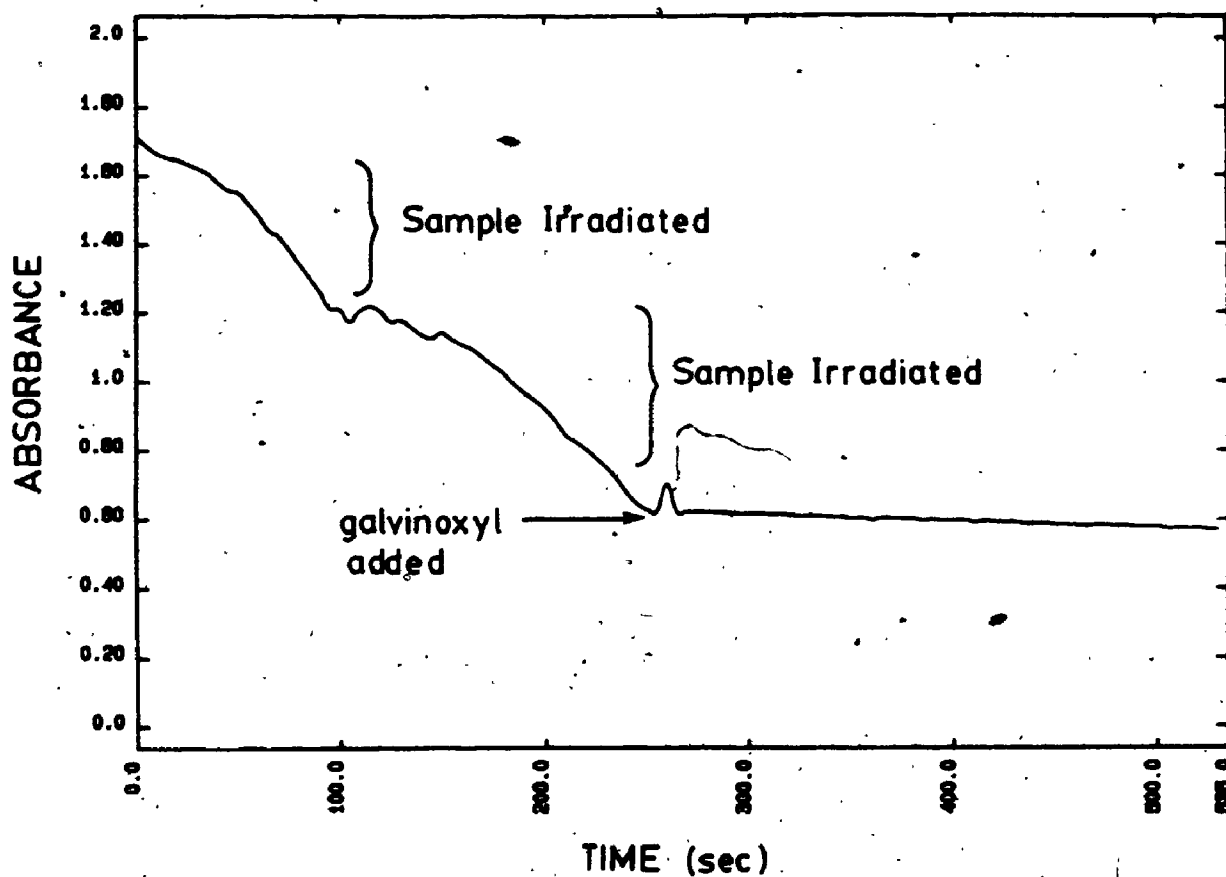
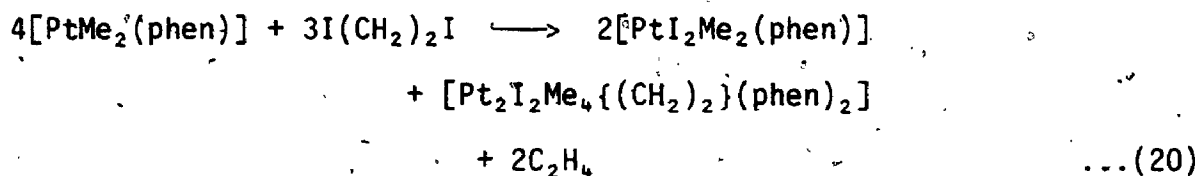


FIGURE 4.16: The Effect of Galvinoxyl (10% mole ratio) on the Rate of Reaction between (II) and $I(CH_2)_2I$. Reaction followed by decay of band at 472.7 nm in the uv/visible spectrum.



3.3.5 Reaction of $\text{I}(\text{CH}_2)_2\text{I}$ with (II) in the Presence of Acrylonitrile

The experimental details of this reaction are given in section 2.6.2.5 of Chapter 7. The products of the reaction were the binuclear complex (XXI) and the diiodide (XVI).

3.3.6 Conclusion

In section 3.1 of this chapter the reaction of methylene iodide with (II) was discussed and the mechanism proposed was that of a free-radical chain. The reaction of (II) with $\text{I}(\text{CH}_2)_n\text{I}$ ($n = 3-5$), to produce iodoalkylplatinum(IV) complexes, is believed to proceed *via* an $\text{S}_{\text{N}}2$ mechanism. The expected low reactivity of methylene iodide to nucleophilic attack⁴⁹ presumably accounts for it being forced to adopt the free-radical mechanism of oxidative addition.

The mechanism for the reaction of 1,2-diiodoethene with (II) is more complex and is not yet fully understood. The failure to obtain good second-order kinetics suggests that a simple $\text{S}_{\text{N}}2$ type mechanism is not operating. The involvement of radicals is clearly indicated by the very noticeable retardation of the reaction rate by galvinoxyl and by the light-induced nature of the reaction. The formation of complex (XVI) is best rationalised in terms of a radical non-chain mechanism, as discussed earlier for the reaction of methylene iodide with (II) (Scheme 5).

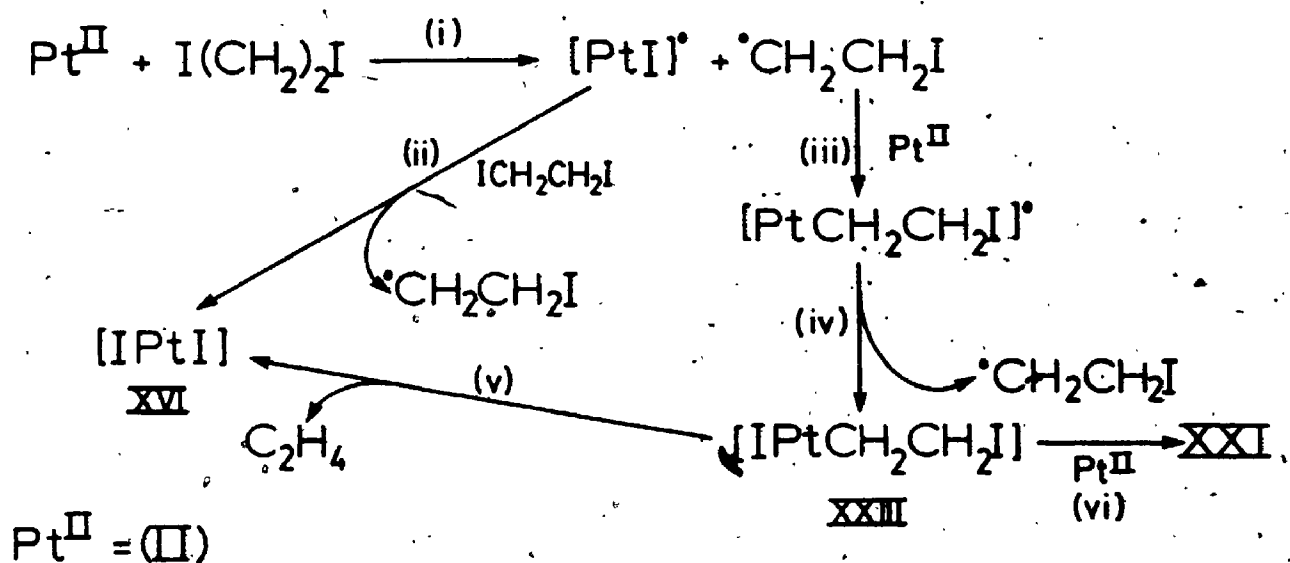
The very strong band that forms in the uv/visible spectrum, at approximately 400 nm, when 1,2-diiodoethane is added to (II), decays as the reaction proceeds. The nature of this intermediate is not known. In.

a related reaction⁵ of $[\text{Co}(\text{CN})_5]^{3-}$ with 1,2-diiodoethane to produce $[\text{Co}(\text{CN})_5\text{I}]^{3-}$ and ethene, Halpern has suggested that the reaction proceeds *via* the intermediate $[(\text{Co}(\text{CN})_5\text{CH}_2\text{CH}_2\text{I})]^{3-}$ species, with its subsequent decay to products. In the reaction of (II) with 1,2-diiodoethane the strong band in the uv/visible spectrum may be due to the intermediate iodoalkylplatinum(IV) complex $[\text{PtI}\text{Me}_2\{(\text{CH}_2)_2\text{I}\}(\text{phen})]$ (XXIII). This complex could then decompose to produce ethene and (XVI), or react with (II) to form the binuclear complex (XXI). This second oxidative addition is believed to be very fast. Scheme 6 summarises the proposed mechanism. Formation of (XXIII) is by a radical chain process. The chain-carrier radical, $\text{CH}_2\text{CH}_2\text{I}$, could be stabilised by formation of the bridged radical.^{5,50} Such stabilisation might lower the activation energy for the halogen abstraction in step (i) and may account for the high reactivity of the 1,2-diiodoethane with (II). Formation of (XXI) from the proposed complex (XXIII) could proceed *via* an $\text{S}_{\text{N}}2$ mechanism or *via* a radical process. No studies were made of this. Likewise the decomposition of (XXIII) to form (XVI) and ethene is not fully understood.

3.4 Formation of Bridging Polymethylene Platinum(IV) Complexes

3.4.1 Preparation and Characterisation

Experimental details for the preparation of these complexes, with general formula $[\text{Pt}_2\text{I}_2\text{Me}_4\{(\text{CH}_2)_n\}(\text{phen})_2]$ ($n = 3-5$) are given in sections 2.4.1.12, 2.4.1.13, and 2.4.1.14 of Chapter 7. For the formation of complexes with $n = 3$ and 4 a slight excess of the α,ω -diiodoalkane was reacted with (II) in acetone. This produced a pale yellow precipitate of the required binuclear complex and the corresponding iodoalkylplatinum(IV) complex (XVII or XVIII) was left in solution. Alternatively the reaction

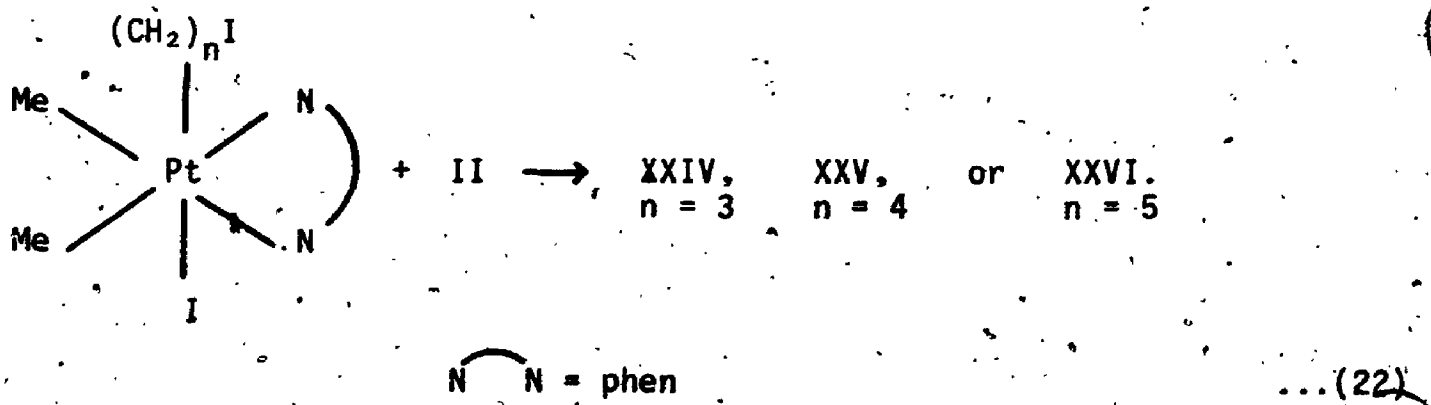
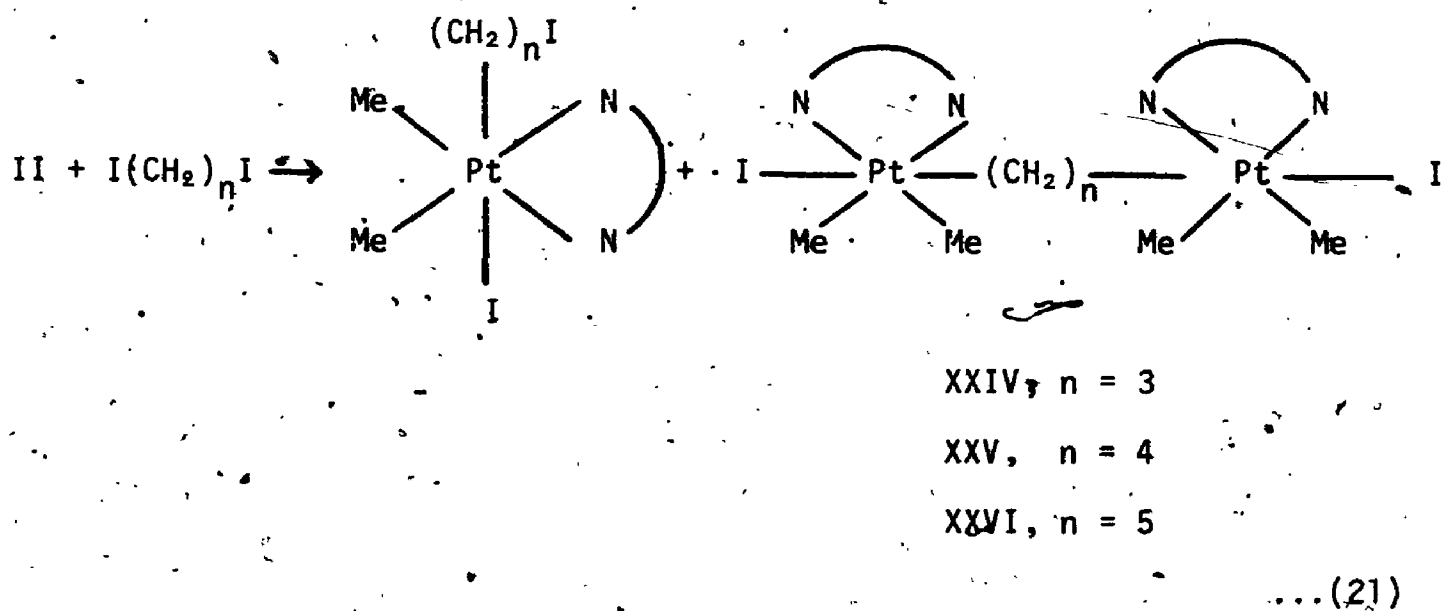


Scheme 6

Proposed Mechanism for the Reaction of 1,2-Diiodoethane with $[\text{PtMe}_2(\text{phen})]$.

can be carried out using a 1:1 mole ratio of complex (II) with the α,ω -diiodoalkane. Preparation of the binuclear complex with $n = 5$ was best carried out by reacting (II) with an acetone solution of $[\text{Pt}(\text{Me})_2\text{N}(\text{CH}_2)_5\text{I}(\text{phen})]$. This method can also be used for the preparation of the complexes with $n = 3$ and 4.

Each of these new binuclear complexes was isolated as a pale yellow solid and for $n = 3,4$ they were found to be quite insoluble in most common organic solvents. These new reactions are shown in equations 21 and 22.



The solubility of the binuclear complexes increases as 'n' increases and a good ^1H -nmr spectrum (Table 7.5) could be obtained only for (XXVI). The

spectrum was recorded on a Bruker AM-250 spectrometer and is shown in Figure 4.17. The very strong peak at 1.34 ppm is assigned to the MePt protons and is good evidence that complex (XXVI) retains the methyl groups *trans* to the phenanthroline ligand as shown on Figure 4.17. The protons (H_{α}) of the methylene group, directly bonded to platinum should appear as a triplet with ^{195}Pt satellites. The distorted triplet at 0.96 ppm is assigned to these protons with $^2J_{\text{PtH}}$ equal to 64 Hz. A somewhat similar distortion was observed for the signal due to the H_{α} protons of the mononuclear complex (XIX) (see Fig. 4.6). The protons of the two remaining methylene groups should appear as quintets. A broadened quintet occurs at -0.07 ppm (not shown on Fig. 4.17). This is assigned to the H_{β} protons on the grounds that these protons will couple to ^{195}Pt more than the H_{γ} protons, accounting for the signal broadening. The quintet due to the H_{γ} protons is seen at 0.4 ppm.

A small amount of the binuclear isomer (XXVII) is also present and its structure is illustrated in Figure 4.17. The singlet at 0.45 ppm ($^2J_{\text{PtMe}}$, 73 Hz) is assigned to the protons of the MePt group above the plane of the aromatic rings. The peak at 1.36 ppm ($^2J_{\text{PtMe}}$, 72 Hz), of equal intensity to that at 0.45 ppm, is assigned to the protons of the MePt group, *trans* to nitrogen, on the same platinum atom as the methyl group at 0.45 ppm. The remaining two MePt groups of (XXVII) are not equivalent and thus should produce two singlets, with ^{195}Pt satellites. If however their resonances are accidentally degenerate a peak twice the intensity of the one at 0.45 ppm would be observed. The peak at 1.64 ppm is believed to be due to these two MePt groups, but is of rather low intensity. A small amount of unreacted *trans*-monomer (XIX) is present in the reaction product and the MePt protons of this complex appear as a

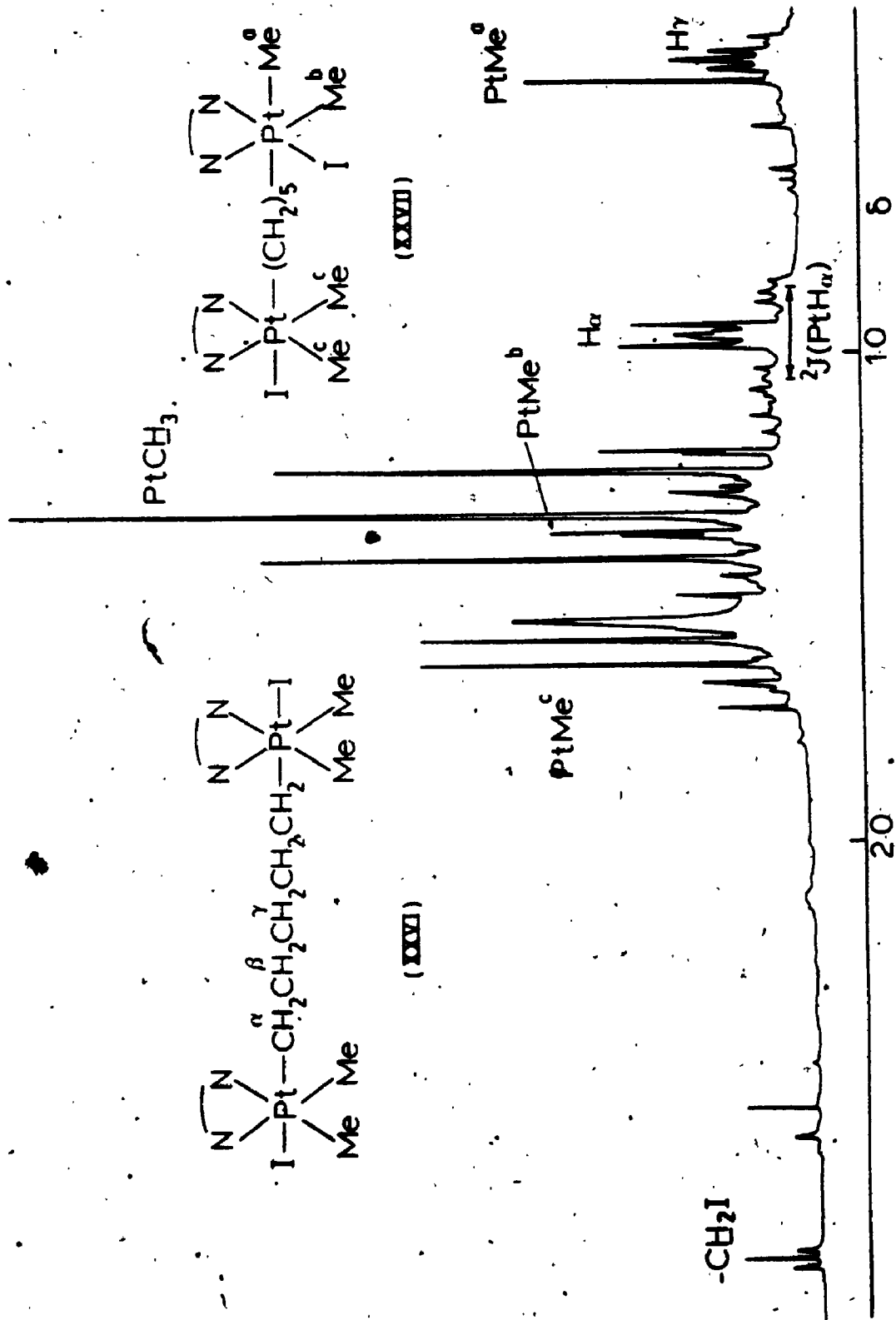


FIGURE 4.17: ^1H NMR Spectrum (400 MHz) of $[\text{Pt}_2\text{I}_2\text{Me}_4\{(\text{CH}_2)_5\}(\text{phen})_2]$ in CD_2Cl_2 .

singlet at 1.60 ppm in the ^1H nmr spectrum. The triplet at 2.85 ppm is due to the protons of the iodomethyl group in (XIX).

It was possible to obtain a ^{13}C nmr spectrum (Table 7.7) of complex (XXVI) and this is shown in Figure 4.18. Due to the low solubility of the complex the spectrum is not very intense. The resonances due to the carbon atoms of the four MePt groups occurs at -5.45 ppm. The signal due to C_α should have ^{195}Pt satellites associated with it. Due to the low signal to noise ratio it is not easy to see these satellites and the assignments given are rather tentative. They have been assigned by comparison with the chemical shift values⁴⁵ of 1,5-diiodopentane and those of complex (XIX).

These binuclear complexes gave elemental analyses consistent with the general formula $[\text{Pt}_2\text{I}_2\text{Me}_4\{(\text{CH}_2)_n\}(\text{phen})_2]$ (Table 7.17).

3.4.2 Pyrolysis of $[\text{Pt}_2\text{I}_2\text{Me}_4\{(\text{CH}_2)_n\}(\text{phen})_2]$ ($n = 3-5$)

Due to the lack of good nmr data for complexes with $n = 3$ and 4, it was decided to analyse the gaseous products produced by pyrolysis of these complexes. It was hoped that analysis of the hydrocarbons produced would give some structural information concerning the complexes.

Analysis was performed using gc/mass spectrometry and the experimental details are presented in section 2.4.2.10 of Chapter 7. The results for each complex are discussed separately.

i) $[\text{Pt}_2\text{I}_2\text{Me}_2\{(\text{CH}_2)_3\}(\text{phen})_2]$

The gc trace of the gaseous products from pyrolysis of (XXIV) is shown in Figure 4.19. The major product was propene with smaller amounts of propane. This was confirmed by injection, into the gc, of a

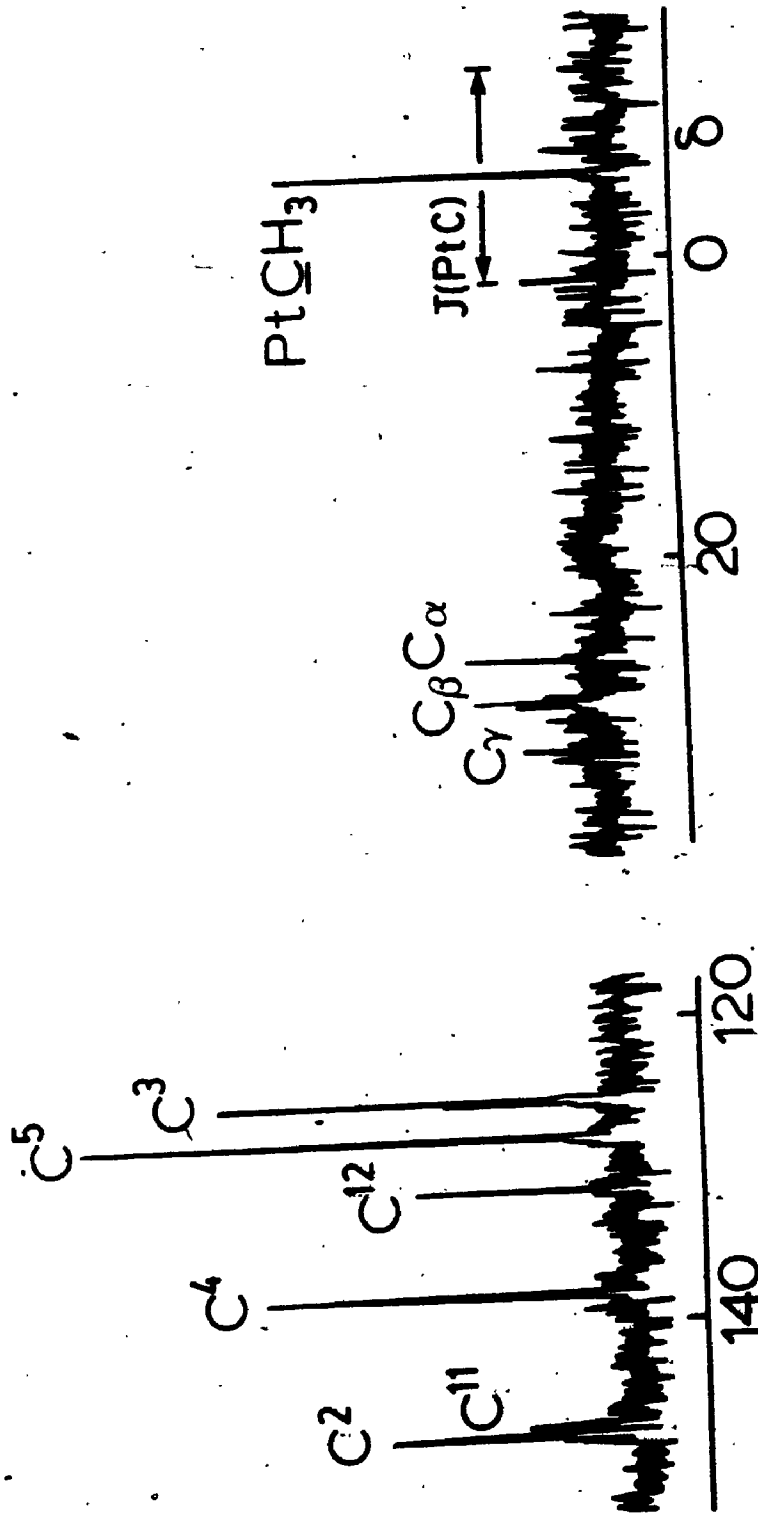


FIGURE 4.18: $^{13}\text{C}\{^1\text{H}\}$ NMR Spectrum (50 MHz) of $[\text{Pt}_2\text{I}_2\text{Me}_4\{(\text{CH}_2)_5\}(\text{phen})_2]$ in CD_2Cl_2 .

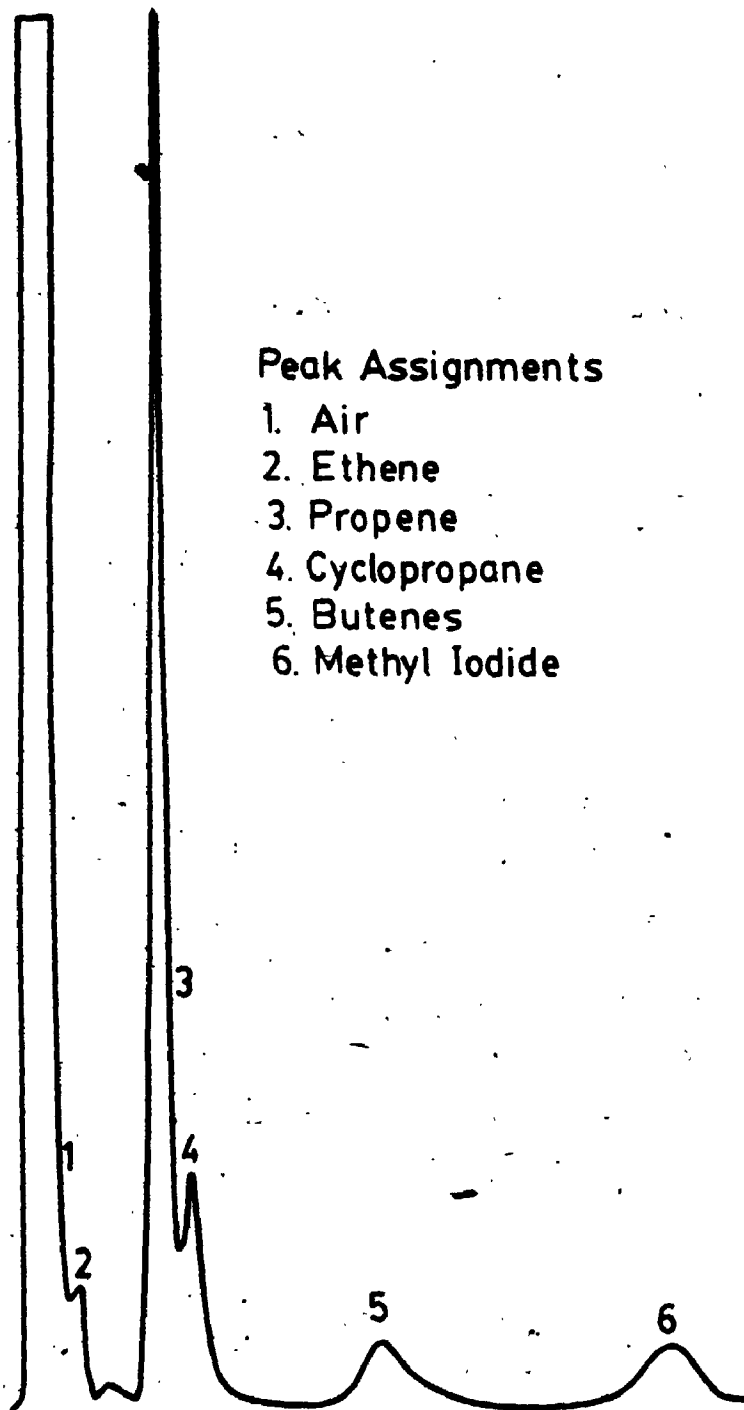
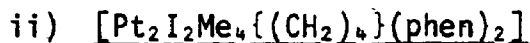


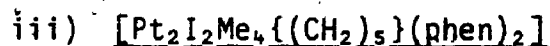
FIGURE 4.19: Gas Chromatography Trace of the Gaseous Products from the Pyrolysis of $[\text{Pt}_2\text{I}_2\text{Me}_4\{(\text{CH}_2)_3(\text{phen})_2\}]$. A Porapak Q Column was used.

mixture of these two hydrocarbons and comparing retention times. The gaseous products responsible for peaks 3 and 4 of Figure 4.19 were analysed by mass spectrometry. The mass spectrum showed a parent ion and fragmentation pattern identical to the published spectrum⁵¹ for propene. This hydrocarbon is presumed to have formed from the μ -hydrocarbyl chain of complex (XXIV).



The gaseous product from pyrolysis of this complex contained small amounts of ethane and ethene (Fig. 4.20), confirmed by their mass spectral patterns,⁵¹ along with larger amounts of methane. The major product was a mixture of butenes. The mass spectra of 1-butene, *cis*-2-butene and *trans*-2-butene are identical and thus they cannot be distinguished by mass spectrometry. Positive identification of butenes was regarded as good evidence for a C_4 carbon backbone in the complex, and no attempt was made to resolve the mixture.

Methyl iodide was also detected and analysed by mass spectrometry. A significant amount of 1-pentene ($m/e = 70$) was detected. The mass spectrum for this molecule is sufficiently different from other C_5H_{10} isomers that a positive identification could be made.



The presence of small traces of ethane and ethene was confirmed by their mass spectra. A larger amount of methane was also detected, confirmed by comparing its retention time with an authentic sample. One of the gaseous fractions gave a parent ion in its mass spectrum at $m/e = 69$, and the fragmentation pattern closely resembled that of 1,3-pentadiene. 1-Pentene was present as one of the fractions, confirmation coming from the presence of a parent ion in its mass spectrum at $m/e = 70$ and a fragmentation pattern identical to that in the literature.⁵¹

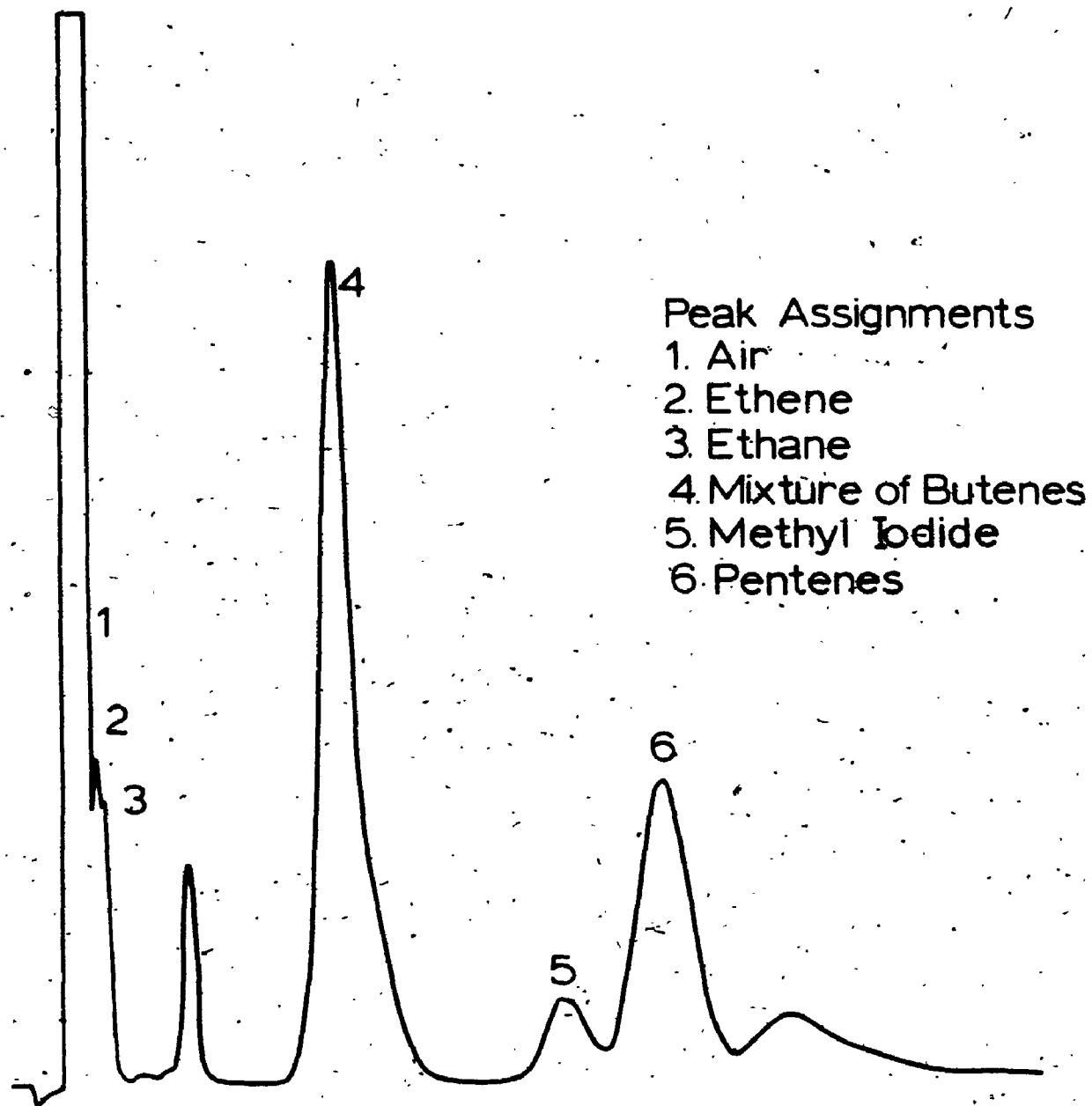


FIGURE 4.20: Gas Chromatography Trace of the Gaseous Products from the Pyrolysis of $[\text{Pt}_2\text{I}_2\text{Me}_4\{(\text{CH}_2)_4\}(\text{phen})_2]$. A Porapak Q Column was used.

The formation of these C₅ hydrocarbons is good evidence for the presence of the μ -hydrocarbyl chain in (XXVI).

3.4.3 Determination of the Second-Order Rate Constant for the Formation of the Binuclear Complexes

Up to the present there has been no data available on the rate of formation of the type of μ -hydrocarbyl complexes discussed here, from the haloalkylmetal precursor. In view of this, the second-order rate constants for the reactions shown in equation 22 were determined.

Experimental details are given in sections 2.4.2.15, 2.4.2.16, and 2.4.2.17 of Chapter 7. The reaction was followed by monitoring the decay of the MLCT band in the uv/visible spectrum due to (II). The absorbance at 472.7 nm (A_t) was recorded as the reaction progressed and a plot of $\log_{10} \frac{(A_t - A_\infty)}{(A_0 - A_\infty)}$ versus time was made for each concentration of the iodoalkylplatinum(IV) complex used. The results are shown in Figure 4.21 for the reaction involving (XIX). From such plots, the pseudo-first-order rate constants (k_{obs}) were determined. A plot of k_{obs} versus concentration of the iodoalkylplatinum(IV) complex produces a straight line, and from the slope of the graph the second-order rate constants (k_2) were determined. These are given in Table 4.3.

3.4.4 Conclusions

The reactions discussed in the previous section follow good second-order kinetics. This is consistent with an S_N2 mechanism operating in the reactions. The trend in the rate constants is also consistent with an S_N2 displacement. The platinum centre of (II) acts as a nucleophilic species, attacking the carbon to which the iodine atom is bonded in the iodoalkylplatinum(IV) complexes. In this way, the iodide

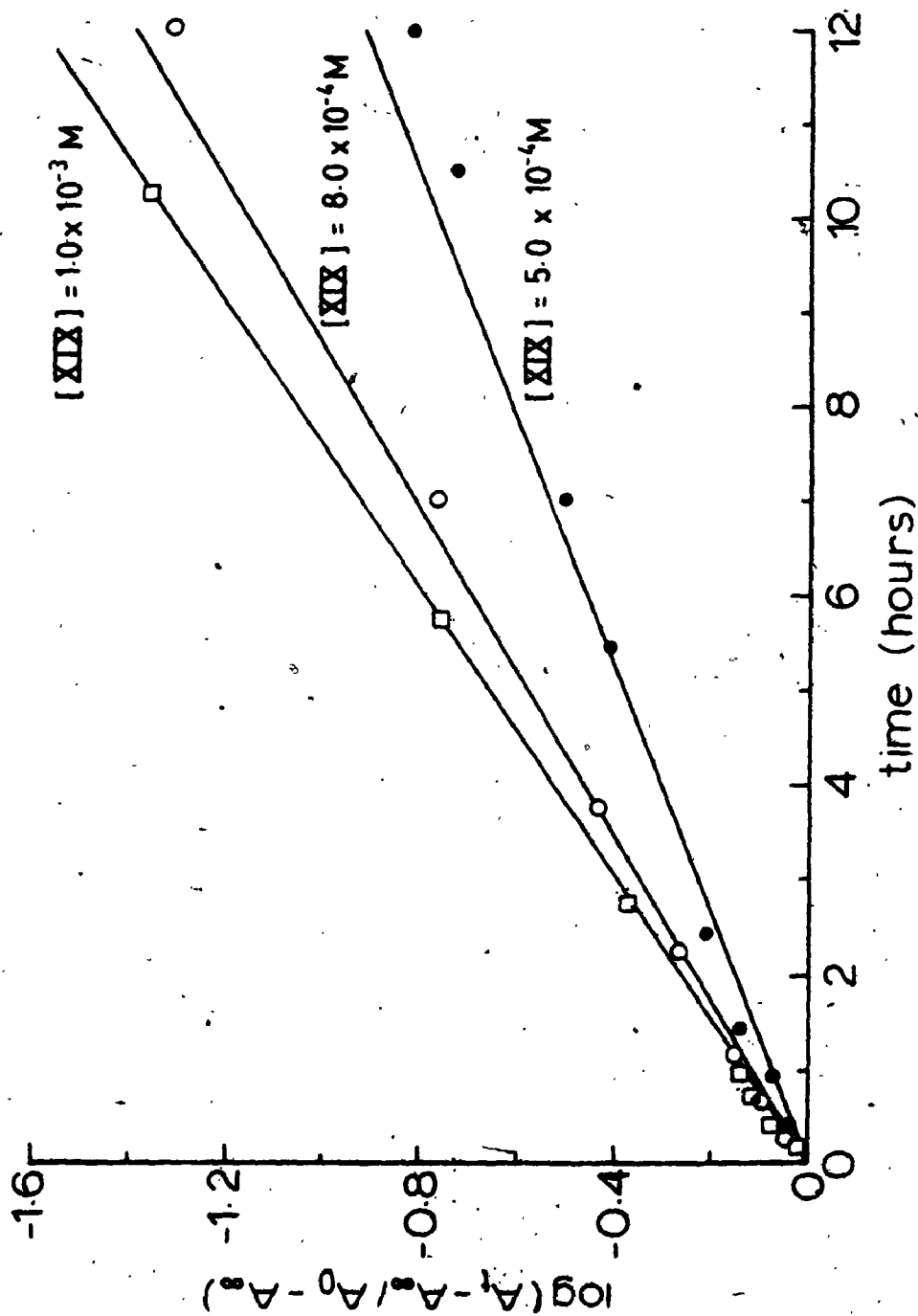


FIGURE 4.21: Plot of $\log \frac{(A_t - A_\infty)}{(A_0 - A_\infty)}$ Versus Time for the Reaction of (II) ($1.0 \times 10^{-4} M$) with $[PtIme_2((CH_2)_5I)(phen)]$ (XIX) in Acetone, at $25^\circ C$ for Varying Concentrations of (XIX).

TABLE 4.3: Second-Order Rate Constants for Reactions of (II), in Acetone, at 25°C

Reagent	$10^3 k_2$ (L mol ⁻¹ S ⁻¹)	Reagent	$10^3 k_2$ (L mol ⁻¹ S ⁻¹)
MeI	69,000		
EtI	69		
ⁿ PrI	34		
ⁿ BuI	39		
CH ₃ (CH ₂) ₄ I	44		
CH ₂ I ₂	<u>a</u>	(XIIIb)	no observed reaction
I(CH ₂) ₂ I	11,700 ^b	(XXIII)	<u>c</u>
I(CH ₂) ₃ I	130	(XVII)	190
I(CH ₂) ₄ I	100	(XVIII)	85
I(CH ₂) ₅ I	84	(XIX)	88

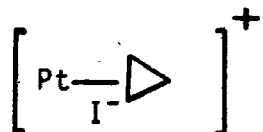
^aVery small in the early stages.

^bRefers to rate of disappearance of band at 472.7 nm in the uv/visible spectrum. Not the overall S_N2 rate constant. See the text for a discussion.

^cNot measured but presumed to be very large.

ion is displaced, with its subsequent coordination to the attacking platinum atom. With the exception of CH_2I_2 and $\text{I}(\text{CH}_2)_2\text{I}$, the data presented in Table 4.3 are second-order rate constants for the reaction of complex (II) with the reagents listed, via an $\text{S}_{\text{N}}2$ mechanism. The discussion that follows deals with the relative rates of these $\text{S}_{\text{N}}2$ reactions.

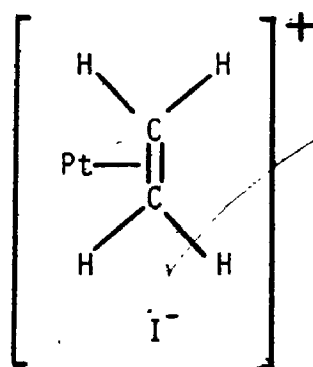
It is clear that for $n = 3$ and 4 ($n =$ number of carbon atoms in the chain) complex (II) reacts more rapidly with the α,ω -diiodoalkanes (even when statistical effects are considered) than with the corresponding primary organic iodides. Of particular interest is the observation that for the reaction of (II) with $[\text{PtIME}_2\{(\text{CH}_2)_n\text{I}\}(\text{phen})]$ ($n = 3-5$) there is a neighbouring group effect. Thus, k_2' for the reaction of (II) with (XVII) is about 50% greater than for the reaction of 1,3-diiodopropane with (II). This corresponds to an increase by a factor of three, if statistical effects are considered, and 5-6 times greater than for the reaction of (II) with *n*-propyl iodide. This activation of the C-I bond in complex (XVII) may occur due to a lowering of the energy of the transition state by contributions from resonance forms such as that shown below, thus making displacement of iodide easier.




Such cyclopropane "edge-complexes" are commonly proposed in platinum complexes.⁵² A similar phenomenon may be important in the Wurtz coupling¹⁸ of 1,3-dihaloalkanes to cyclopropanes using zinc metal through the intermediates $\text{XZnCH}_2\text{CH}_2\text{CH}_2\text{X}$.

Such a neighbouring atom effect is not common in transition-metal complexes. Collman³⁰ has reported a similar effect, but does not give full details for the rate constants.

The rate-constant quoted in Table 4.3 for the reaction of $I(CH_2)_2I$ with (II), is *not* the overall rate constant. The mechanism of this reaction is not fully understood, but it is not S_N2 . The reaction is believed to go *via* the intermediate complex (XXIII) which reacts further, forming the products (XVI) and (XXI). A neighbouring group effect may be operative in complex (XXIII) and a lowering of the energy of the transition state by contribution from resonance forms such as that shown below may account for the rate enhancement.

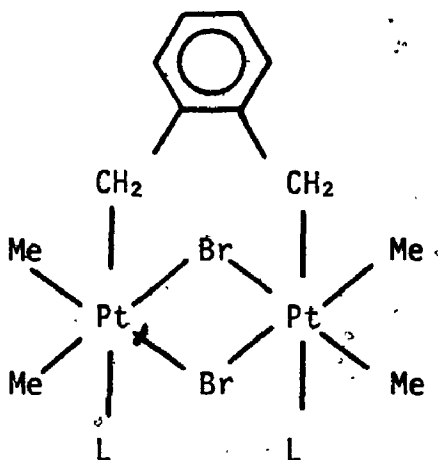


The data presented in this chapter clearly illustrates that the mechanism of oxidative addition of α,ω -diiodohalogenoalkanes to complex (II) varies as a function of the carbon chain-length. An S_N2 mechanism is believed to operate in those cases where the carbon bonded to the iodine atom is not sterically crowded. Such crowding exists for methylene iodide and a radical mechanism is therefore adopted. Steric crowding may partly explain the adoption of a radical mechanism for the reaction of (II) with 1,2-diiodoethane but it is felt that the formation of the stabilised bridged-radical, , is a more important factor in determining the reaction pathway.

3.4.5 Reaction of α,α' -Dibromo-o-xylene with (II)

There has been much interest in the use of the o-xylidene ligand $o-C_6H_4(CH_2)_2$ as a bridging⁵³⁻⁵⁵ or as a chelating ligand.⁵⁶

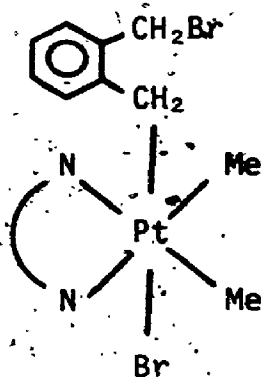
Shaw^{54,55} has oxidatively added α,α' -dibromo-o-xylene to *cis*-[PtMe₂L₂] (L = AsMe₂Ph, or AsMe₂(C₆H₄OMe-2)) to produce bridging complexes as shown below.



In the case where L = AsMe₂(C₆H₄OMe-2) the reaction was faster owing to neighbouring group participation by the *ortho*-methoxy group.

It was decided to investigate the reaction of α,α' -dibromo-o-xylene with (II). The experimental details are given in Section 2.4.1.15 of Chapter 7. Complex (II) was reacted with an excess of α,α' -dibromo-o-xylene, in acetone. The reaction was very fast, and a pale yellow solid was recovered from the solution.

The ¹H nmr spectrum of the product contains a singlet at 1.69 ppm with ¹⁹⁵Pt satellites. This is assigned to the protons of the two MePt groups. A ²J_{PtMe} value of 71 Hz, associated with this signal, indicates that the product is a platinum(IV) complex. The proposed structure is given below.

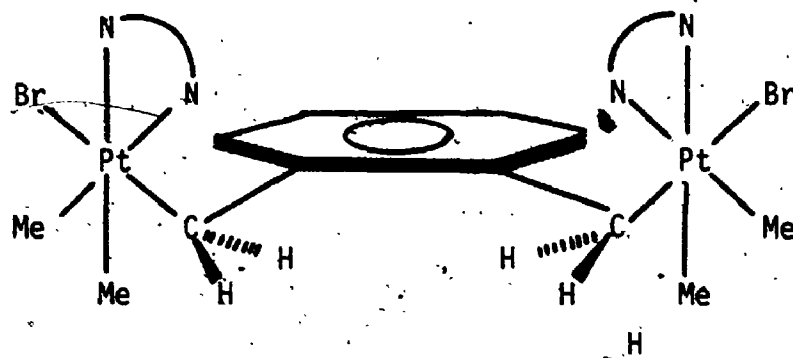


XXVIII

N—N = phen.

The protons of the PtCH₂ group appear as a singlet at 2.99 ppm in the ¹H nmr spectrum with a ²J_{PtMe} value of 94 Hz. Such large coupling was observed in Shaw's bridging-complex.⁵⁴ The protons of the CH₂Br group occur as a singlet at 3.76 ppm. The resonances due to the protons of the xylene ring appear as a complex multiplet and are shifted upfield from those in the free-radical. This is due presumably to their position above the plane of the phenanthroline ring in (XXVIII). The ¹H nmr data for a similar complex, in which 1,10-phenanthroline is replaced by 2,2'-bipyrimidine,⁵⁷ are in excellent agreement with the ¹H nmr data presented here for (XXVIII).

Complex (XXVIII) was reacted with complex (II), in acetone (1:1 mole ratio). The reaction was slow but eventually the orange colour of (II) disappeared with the formation of a pale yellow precipitate. This complex (XXIX) is insoluble in all common organic solvents and no ¹H nmr data could be collected. By analogy with previous work⁵³⁻⁵⁷ it is believed to be the bridging o-xylene complex shown below.



(XXIX)

No mechanistic studies were made for the reactions discussed in this section.

The synthesis of complexes (XXIX), and the μ -polymethylene derivatives $[\text{Pt}_2\text{X}_2\text{Me}_4\{\mu\text{-(CH}_2\text{)}_n\}(\text{phen})_2]$ described above, is significant since these are the first platinum complexes containing μ -hydrocarbyl groups and with no other bridging ligands.

REFERENCES

1. Fischer, F.; Tropsch, H.; *Brennst. Chem.*, 1926, 7, 97.
2. Brady, R.C.; Pettit, R.; *J. Am. Chem. Soc.*, 1980, 102, 6181;
ibid; 1981, 103, 1287.
3. Herrmann, W.A.; *Adv. Organomet. Chem.*, 1982, 20, 159.
4. Holton, J.; Lappert, M.; Pearce, R.; Yarrow, P.I.W.; *Chem. Rev.*,
1983, 83, 135.
5. Chock, P.B.; Halpern, J.; *J. Am. Chem. Soc.*, 1969, 91, 582.
6. Halpern, J.; Maher, J.P.; *J. Am. Chem. Soc.*, 1965, 87, 5361.
7. Scherer, O.J.; Jungmann, H.; *J. Organomet. Chem.*, 1981, 208, 153.
8. Kermode, N.J.; Lappert, M.F.; Skelton, B.W.; White, A.H.; Holton,
J.H.; *J. Chem. Soc. Chem. Comm.*, 1981, 698.
9. Chatt, J.; Head, R.A.; Leigh, G.J.; Pickett, C.J.; *J. Chem. Soc.
Chem. Comm.*, 1977, 299.
10. Takahashi, S.; Suzuki, Y.; Sonogashira, K.; Hagihara, N.; *J. Chem.
Soc. Chem. Comm.*, 1976, 830.
11. Whitesides, G.M.; Young, G.B.; *J. Am. Chem. Soc.*, 1978, 100, 5808.
12. Moss, J.R.; *J. Organometal. Chem.*, 1982, 231, 229.
13. Kuyper, J.; *Inorg. Chem.*, 1978, 17, 77.
14. Moss, J.R.; Spiers, J.C.; *J. Organomet. Chem.*, 1979, 182, C20.
15. Feser, R.; Werner, H.; *Angew. Chem. Int. Ed. Engl.*, 1980, 19, 940.
16. Klein, H.F.; Hammer, R.; *Angew. Chem.*, 1976, 88, 61.
17. Kermode, N.J.; Lappert, M.F.; Skelton, B.W.; White, A.H.; *J.
Organomet. Chem.*, 1982, 228, C71.

18. March, J.; "Advanced Organic Chemistry. Reactions, Mechanisms, Structure". 1968, Chap. 10, McGraw-Hill, New York.
19. Engelter, C.; Moss, J.R.; Niven, M.L.; Nassimbeni, L.R.; Reid, G.; J. Organomet. Chem., 1932, C78.
20. Pejling, S.; Botha, C.; Moss, J.R.; J. Chem. Soc. Dalton Trans., 1983, 1495.
21. Ellis, J.E.; J. Organomet. Chem., 1975, 86, 22.
22. Kaminsky, W.; Sinn, H.J.; Liebigs Ann. Chem., 1975, 424.
23. Sinn, H.J.; Kaminsky, W.; Adv. Organomet. Chem., 1980, 18, 99.
24. Beck, W.; Olgenöller, B.; J. Organomet. Chem., 1977, C45.
25. Olgenöller, B.J.; Beck, W.; Chem. Ber., 1981, 114, 867.
26. King, R.B.; Inorg. Synth., 1963, 2, 531.
27. King, R.B.; J. Am. Chem. Soc., 1963, 85, 1922.
28. King, R.B.; Bisnette, M.B.; J. Organomet. Chem., 1967, 7, 311.
29. Laing, M.; Moss, J.R.; Johnson, J., J. Chem. Soc. Chem. Comm., 1977, 656.
30. Collman, J.P.; MacLaury, M.R.; J. Am. Chem. Soc., 1974, 96, 3019.
31. Bailey, N.A.; Hell, P.L.; Mukhopadhyay, A.; Tabbron, H.E.; Winter, M.J.; J. Chem. Soc. Chem. Comm., 1982, 215.
32. Bailey, N.A.; Hell, P.L.; Manuel, C.P., Mukhopadhyay, A.; Rogers, D.; Tabbron, H.E.; Winter, M.J.; J. Chem. Soc. Dalton Trans., 1983, 2397.
33. Adams, H.; Bailey, N.A.; Winter, M.J.; J. Chem. Soc. Dalton Trans., 1984, 273.
34. Brown, M.P.; Fisher, J.R.; Puddephatt, R.J.; Seddon, K.R.; Inorg. Chem., 1979, 18, 2808.
35. Balch, A.L.; Hunt, C.T.; Lee, C.; Olmstead, M.M.; Farr, J.P.; J. Am. Chem. Soc., 1981, 103, 3764.

36. McKeer, I.R.; Courie, M.; *Inorg. Chim. Acta.*, 1982, 65, L107.
37. Lin, Y.C.; Calabrese, J.C.; Wreford, S.S., *J. Am. Chem. Soc.*, 1983, 105, 1679.
38. Theopold, K.H.; Bergmann, R.G.; *J. Am. Chem. Soc.*, 1980, 102, 5695.
39. Motyl, K.M.; Norton, J.R.; Schauer, C.K.; Anderson, O.P.; *J. Am. Chem. Soc.*, 1982, 104, 7325.
40. Cooke, M.; Forrow, N.J.; Knox, S.A.R.; *J. Chem. Soc. Dalton Trans.*, 1983, 2435.
41. Clegg, D.E.; Hall, J.R.; Swile, G.A., *J. Organomet. Chem.*, 1972, 38, 403.
42. Labinger, J.A.; Osborn, J.A.; Coville, N.J.; *Inorg. Chem.*, 1980, 19, 3236.
43. Cotton, F.A.; Wilkinson, G.; "Advanced Inorganic Chemistry". 1980, 4th Edition, Chap. 28, Wiley-Interscience.
44. Mann, B.E.; Taylor, B.F.; "¹³C NMR Data for Organometallic Compounds". 1981, Chap. 2, Academic Press, London.
45. Stothers, J.B.; "¹³C NMR Spectroscopy". 1972, Chap. 5, Academic Press, New York and London.
46. K6nnecke, A.; Lippmann, E.; Mlochowski, J.; Sliwa, W.; *Org. Mag. Res.*, 1979, 12, 696.
47. Rosenberger, H.; Pettig, M.; Madeji, K.; Pehk, T.; Lippman, E.; *Org. Mag. Res.*, 1970, 2, 329.
48. Chanon, M.; *Bull. Soc. Chim. Fr.*, 1982, II, 197.
49. Hine, J.; *J. Am. Chem. Soc.*, 1950, 72, 2438.
50. Huyser, E.S.; "The Chemistry of the Carbon-Halogen Bond". Patai, S., ed., 1973, Chap. 8, Wiley and Sons, London.
51. Heller, S.R.; Milne, G.W.A., "EPA/NIH Mass Spectral Data Base". 1978, Vol. 1, National Bureau of Standards.

52. Puddephatt, R.J.; *Coord. Chem. Rev.*, 1980, 33, 149.
53. Hersh, W.; Bergman, R.G.; *J. Am. Chem. Soc.*; 1981, 103, 6992.
54. Hutton, A.T.; Shabanzadeh, B.; Shaw, B.L.; *J. Chem. Soc. Chem. Comm.*, 1982, 1345.
55. Constable, A.G.; Langrick, C.R.; Shabanzadeh, B.; Shaw, B.L.; *Inorg. Chim. Acta.*, 1982, 65, L151.
56. Lappert, M.F.; Martin, T.R.; Atwood, J.L.; Hunter, W.E.; *J. Chem. Soc. Chem. Comm.*, 1980, 476.
57. Scott, J.D.; Puddephatt, R.J.; *Inorg. Chim. Acta.*, submitted for publication.
58. Abel, E.W.; Khan, A.K.; Kite, K.; Orrell, K.G.; Sik, V., *J. Chem. Soc. Dalton Trans.*, 1980, 1169.

CHAPTER 5

OXIDATIVE ADDITION OF SECONDARY AND TERTIARY ORGANIC HALIDES TO A DIMETHYLPLATINUM(II) COMPLEX:

1. INTRODUCTION

In Chapters 3 and 4 the reactions of $[\text{PtMe}_2(\text{phen})](\text{II})$ with primary organic halides were discussed. As a natural extension to this, the reaction of (II) with secondary and tertiary organic halides is discussed in this chapter. The oxidative addition of isopropyl iodide and *tert*-butyl iodide to (II) can lead to the formation of the first stable alkylperoxoplatinum(IV) complexes. The x-ray crystal structure of one such peroxoplatinum(IV) complex is presented in this chapter along with details of the mechanism of oxidative addition of ^iPrI and ^tBuI to complex (II).

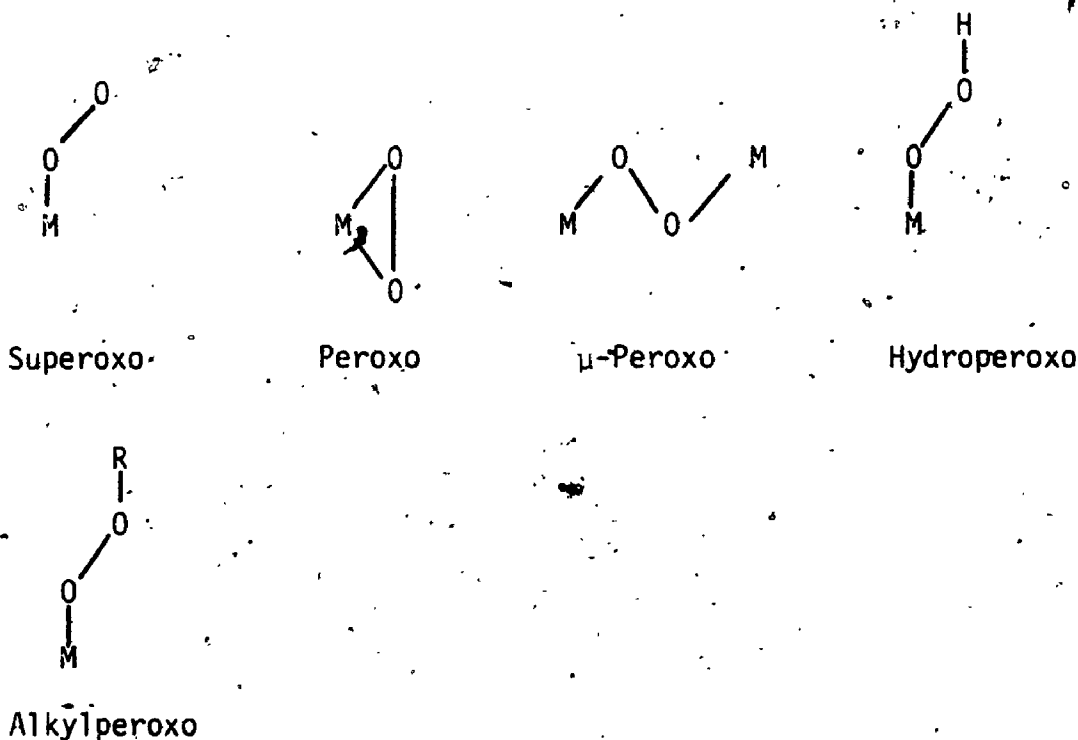
2. LITERATURE SURVEY

Molecular oxygen is one of the most abundant elements on earth and up to now has scarcely been used for the selective oxidative of organic substrates. The oxidation of olefins to ketones or epoxides by use of dioxygen, alkyl peroxides or hydrogen peroxide, in the presence of transition-metal complexes, has been extensively studied. The reaction is believed to proceed *via* the intermediacy of transition-metal peroxides. In order to better understand the mechanism of such metal-catalysed oxidations, there have been many attempts to isolate metal peroxide complexes. This review will deal with the metal-catalysed oxidation of

olefins and the isolation of transition-metal alkylperoxo complexes.

2.1 Oxygen-Transfer Reactions Using Transition-Metal Complexes

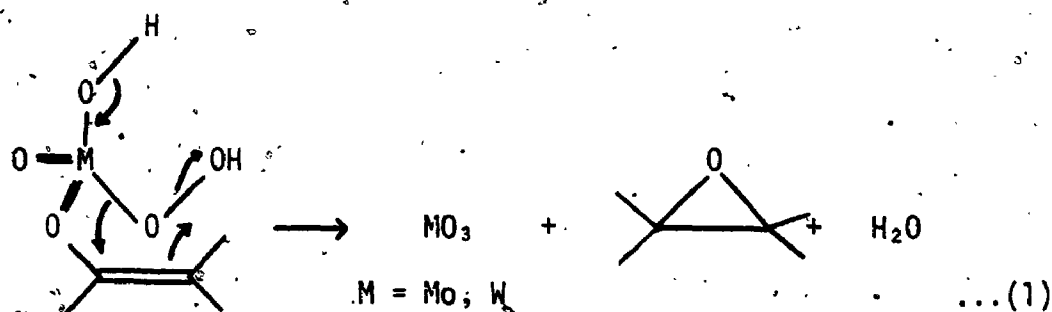
A number of reviews¹⁻⁶ have appeared dealing with transition-metal dioxygen complexes and oxygen-transfer from transition-metal peroxo complexes. Scheme 1 represents the different oxygenated species which may form when O_2 , H_2O_2 , or $ROOH$ react with a metal centre.



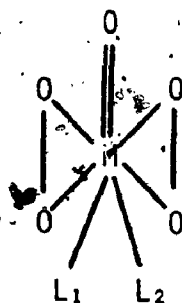
SCHEME 1

Possible Bonding Modes in Metal Peroxo Complexes

The synthesis of glycols by reaction of olefins with hydrogen peroxide, in the presence of certain transition-metal catalysts (e.g. OsO_4 , MoO_3 , V_2O_5) was first reported by Milas,⁷⁻⁸ *et al.* in the 1930s. Many of these reactions proceed *via* epoxides that undergo subsequent hydrolysis to produce the glycol. A possible mechanism for epoxide formation is shown in equation 1.



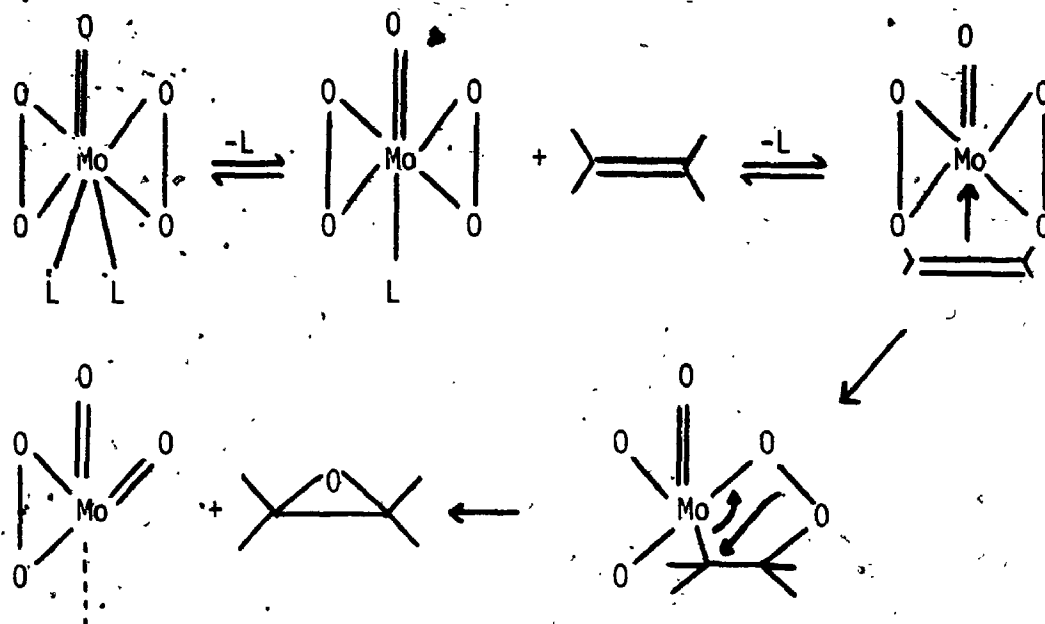
Mimoun and co-workers⁹ have investigated the use of covalent metal peroxides of molybdenum(VI) and tungsten(VI) as epoxidising agents. The structure of these complexes is shown below.



$L_1, L_2 =$ Dimethylformamide, dimethylacetamide or hexamethylphosphoric triamide

$M = Mo, W$

The epoxidation of olefins is stereospecific (*cis*-olefins give *cis*-epoxides) and the reactivity was found to increase with their nucleophilicity. Sharpless used ¹⁸O labelling experiments¹⁰ to prove the peroxidic origin of the transferred oxygen. Mimoun concludes that the olefin coordinates to the metal centre and epoxidation occurs *via* an intramolecular 1,3-dipolar mechanism illustrated in Scheme 2.

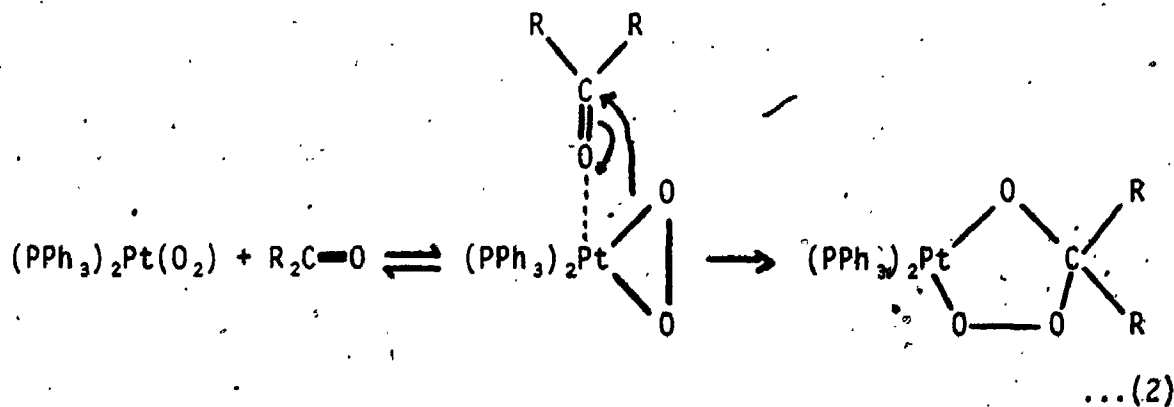


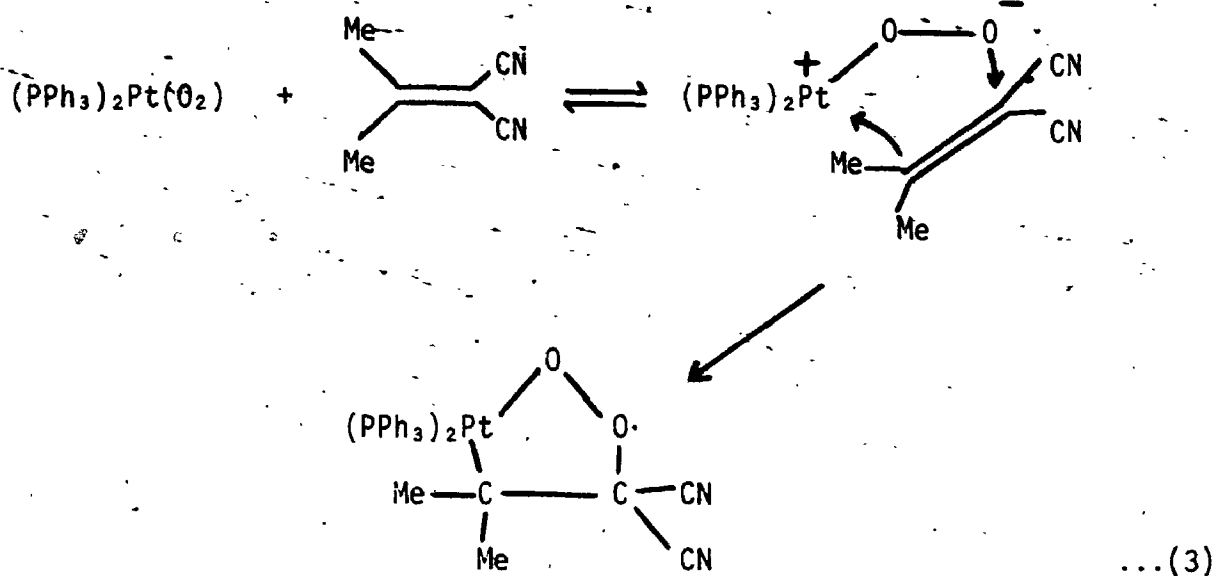
SCHEME 2

Epoxidation of Olefins by Peroxomolybdenum Complexes

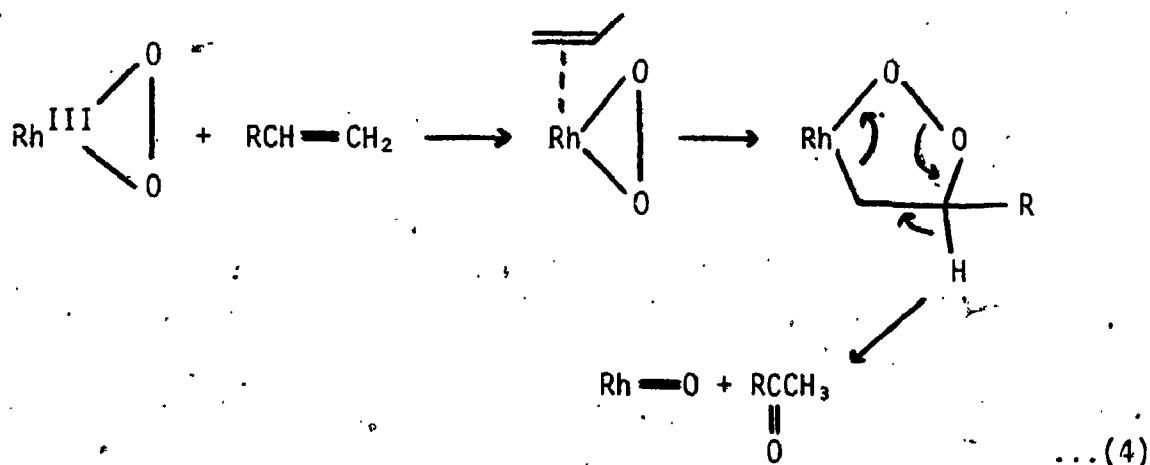
These reactions are not catalytic.

Peroxo complexes of Group VIII transition-metals (eg. Ni, Pd, Pt, Ir) do not readily transfer oxygen to olefins, although stable five-membered peroxo metallocyclic adducts have been isolated^{11,12} with aldehydes, ketones and activated electrophilic olefins (see equations 2 and 3).

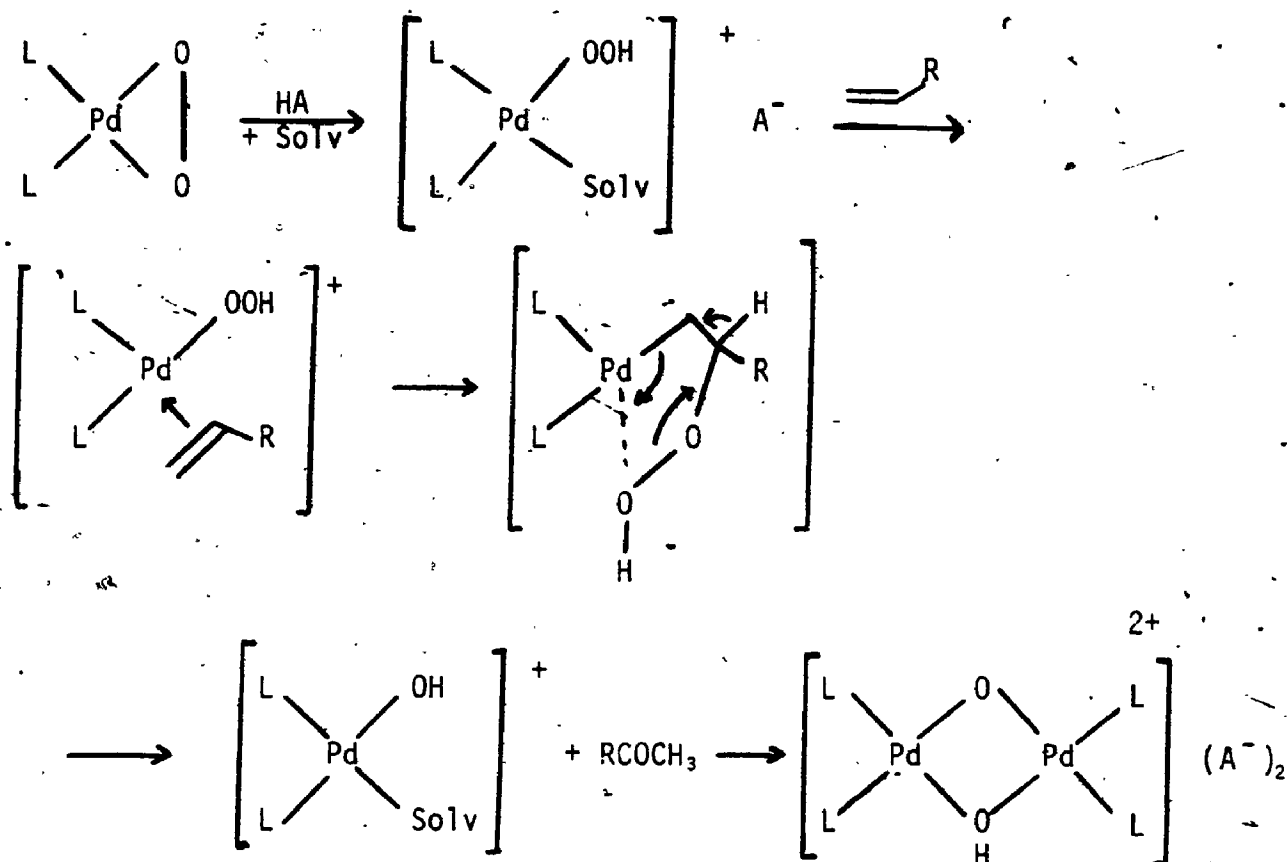




Activation of dioxygen by transition-metal complexes leading to oxidation of unactivated olefins has been observed^{13,14} only for a few rhodium complexes. A $\text{RhCl}_3/\text{Cu}(\text{ClO}_4)_2$ mixture catalyses the oxidation of terminal olefins, by molecular oxygen,¹⁴ to methyl ketones. The reaction is believed to involve activation of dioxygen and oxygen-transfer (equation 4).

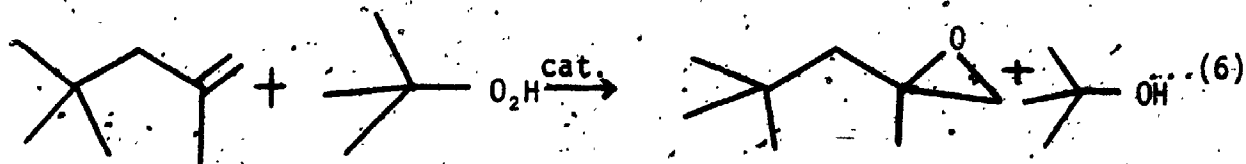


Oxygen-transfer, from palladium hydroperoxo complexes, to terminal olefins has been successfully achieved.¹⁵ The success of this technique is due to the formation of a vacant site for coordination of the olefin. This is illustrated in equation 5.

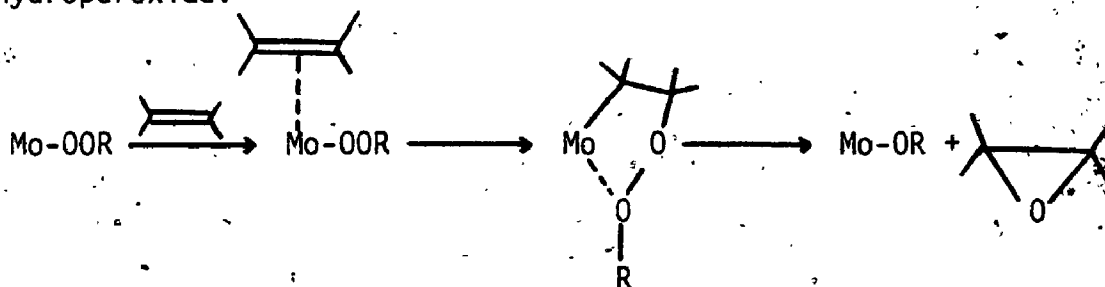


L = PPh₃, Solv = CH₂Cl₂, A⁻ = CH₃SO₃⁻, BF₄⁻. (5)

A further source of oxygen for epoxidation reactions is organic hydroperoxides. Hawkins¹⁶ was the first person to report a metal-catalysed epoxidation of olefins with an organic hydroperoxide. He reported that cyclohexene oxide was obtained, in moderate yield, by treating cyclohexene with cumene hydroperoxide, in the presence of vanadium pentoxide. Brill and Indicator, whilst studying the reaction of *tert*-butyl hydroperoxide with olefins, discovered the catalytic epoxidation of 2,4,4-trimethylpent-1-ene, in the presence of small amounts of molybdenum acetylacetonates (equation 6).



Halcon¹⁷ have developed the large scale production of propylene oxide from the epoxidation of propene. The process involves the use of *tert*-butyl hydroperoxide in the presence of a molybdenum catalyst. Many characteristics of this reaction are similar to those of epoxidation of olefins by peroxomolybdenum complexes, ie. high stereoselectivity (with retention of configuration), increasing reactivity with increasing nucleophilicity of the olefin and strong inhibition by coordinating σ -donor solvents and ligands. Scheme 3 shows the proposed mechanism for this epoxidation. Oxygen-transfer is believed⁵ to occur from the alkylperoxy molybdenum complex obtained by displacement of a ligand on Mo^{VI} by hydroperoxide.



SCHEME 3

Proposed Mechanism for the Molybdenum Hydroperoxide Catalyzed Epoxidation of Olefins

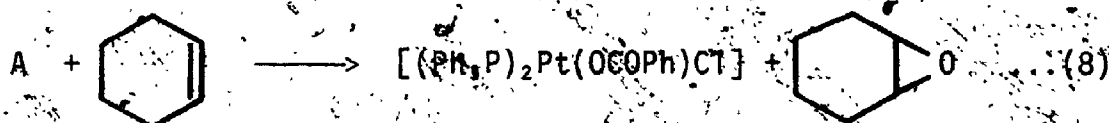
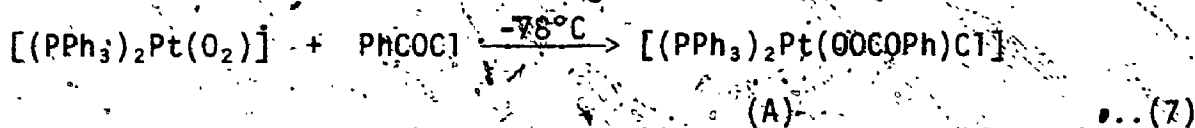
2.2 Isolated Transition-Metal Peroxo Complexes

Stable metal peroxo complexes of the type $M \begin{matrix} O \\ \diagdown \\ | \\ \diagup \\ O \end{matrix}$ are quite common, whereas stable hydroperoxo and particularly alkylperoxo complexes are less common.

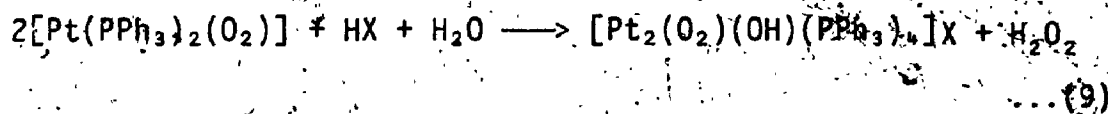
This section will review some of the metal peroxo complexes that have been isolated and for which x-ray crystal structures have been determined. Emphasis will be placed on platinum peroxo complexes.

Oxygen reacts rapidly with a benzene solution of $[Pt(PPh_3)_4]$ to yield the 1:1 adduct, $[(PPh_3)_2Pt(O_2)]$,^{18,19} and two equivalents of

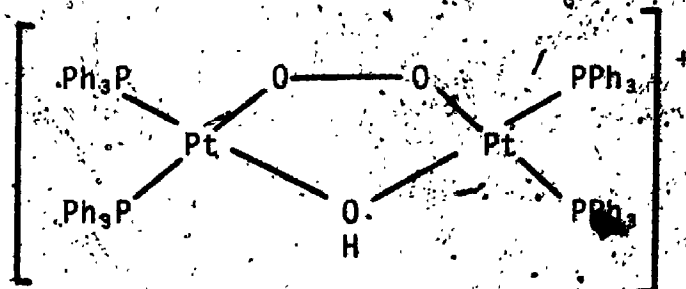
triphenylphosphine oxide. The x-ray crystal structure has been reported²⁰ and the dioxygen ligand is almost coplanar with the two phosphine ligands. Equations 2 and 3 illustrate the reaction of this complex with ketones and an activated olefin. This peroxy complex has not been observed to transfer oxygen to organic substrates. However, if it is reacted with norbornene or cyclohexene, in the presence of the electrophilic benzoyl chloride,²¹ the olefins are epoxidised. This is shown in equations 7 and 8:



When an ethanolic solution of HX (X is a poor nucleophile such as NO_3^- , ClO_4^- , or BF_4^-) is added to a CH_2Cl_2 solution of $[(PPh_3)_2Pt(O_2)]$ the following reaction takes place:²³

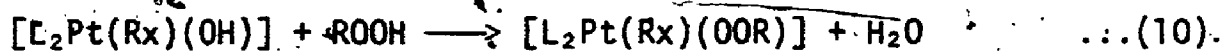


The dimeric nature of this peroxy bridged cation:



has been confirmed by a single-crystal x-ray analysis of the perchlorate derivative.²² The x-ray crystal structure of the platinum peroxymetallacycle shown in equation 3 has also been reported.²⁴

Strukul and co-workers^{25,26} have devised a fairly general route for the formation of platinum(II) hydroperoxo and alkylperoxo complexes. The key reaction is shown in equation 10.



L = diphos, diphoe, 2PPh₃

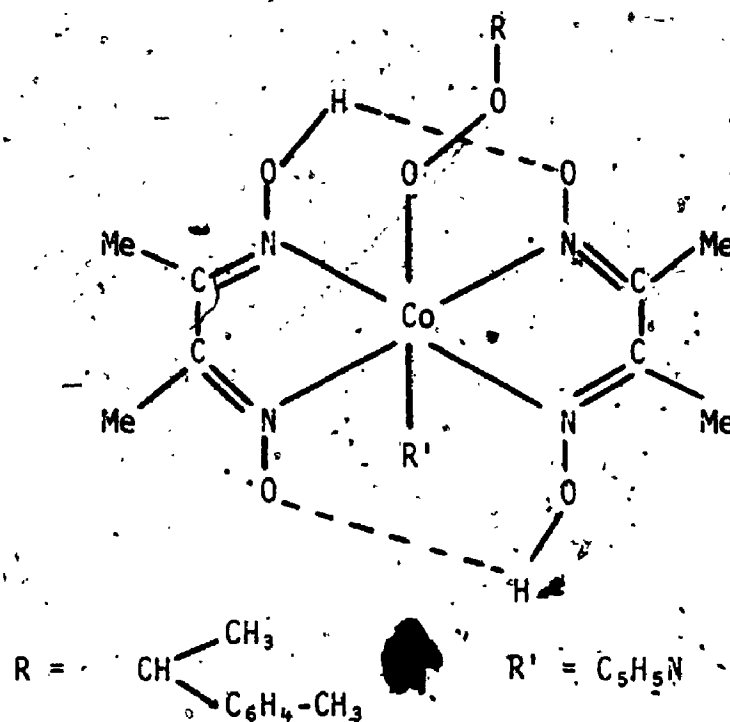
Rx = CF₃, CH₂CN, CH₂CF₃

R = H, ^tBu

When H₂O₂ was used, no reaction occurred for Rx = CH₂CN or CH₂CF₃. The crystal structure of one such complex; *trans*-[(PPh₃)₂Pt(Ph)(OO^tBu)], was later reported by Strukul.²⁷ This is the first structural characterisation of a d⁸ metal complex containing a nonbridging, end-bonded alkylperoxo moiety. An earlier report²⁸ does exist in which the crystal structure of a palladium (d⁸) alkylperoxo complex is given. The peroxo ligands bridge two palladium atoms in the complex [(CCl₃CO₂)Pd(OO^tBu)]₂. Complexes such as these were found to be highly efficient reagents for the selective, stoichiometric oxidation of terminal olefins to methyl ketones, and catalysts for the ketonisation of terminal olefins by *tert*-butyl hydroperoxide. The first Group VIII alkylperoxo complexes to be isolated were by Haszeldine and co-workers.^{29,30} For example when the reaction of an excess of ^tBuOOH with *trans*-[IrX(CO)₂]₂ (X = Cl, Br; L = PPh₃, AsPh₃) is carried out in toluene solution the diperoxo complexes [IrX(OO^tBu)₂(CO)₂L₂] are formed in yields of 25-40%.

The first x-ray crystal structure of a transition-metal alkylperoxo complex was performed by Chiaroni and Pascard-Billy.³¹ The structure is that of an alkylperoxycobaloxime prepared by Giannotti and co-workers.^{32,33} The complexes were prepared by the photochemical

insertion of dioxygen into a cobalt-carbon bond. The x-ray crystal structure in question was of the complex shown below.



The dioxygen insertion is believed to go *via* a five coordinate cobalt complex, produced by dissociation of the base, pyridine.³⁴ Giannotti has also published the x-ray crystal structure of an analogous cumyl peroxide-(pyridine)cobaloxime.³⁵

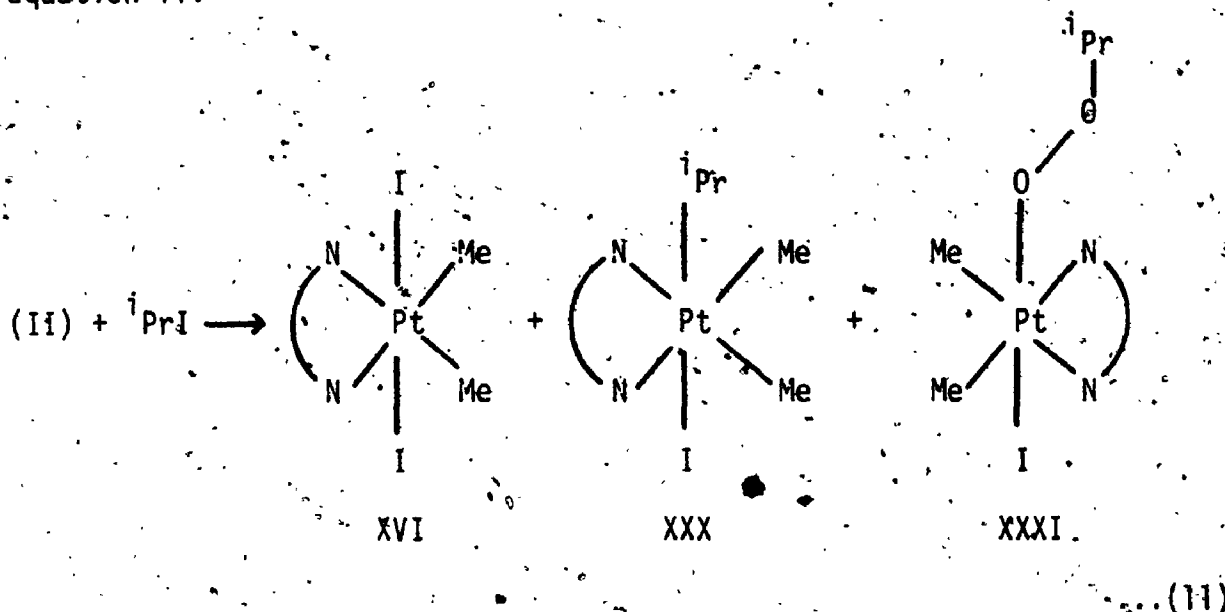
3. RESULTS AND DISCUSSIONS

This section will deal with the products from the reaction of isopropyl iodide and *tert*-butyl iodide with complex (II), their characterisation, and the mechanism of the reactions. The section will be sub-divided into the results of the work with isopropyl iodide and those for the work with *tert*-butyl iodide. A short, final section discusses the reaction of isopropyl bromide with complex (II). All experimental details are found in Section 2.5 of Chapter 7.

3.1 Results from Reaction of ^1PrI with (II)

3.1.1 Products from the Reaction of (II) with ^1PrI

The reaction of (II), in acetone, with isopropyl iodide generally gave a mixture of products. This new reaction is shown in equation 11.



Complex (XXXI) can be separated from complexes (XVI) and (XXX) by column chromatography (see Section 2.5.1.4 of Chapter 7). Small traces of another platinum(IV) complex were sometimes observed, and the complex is believed to be $[\text{Pt}(\text{OH})\text{Me}_2(^1\text{Pr})(\text{phen})]$ (XXXII).

3.1.2 Characterisation of Complexes (XVI), (XXX)-(XXXII)

The complexes were characterised by their ^1H nmr and ^{13}C nmr spectra and by performing several control experiments.

f). ^1H and ^{13}C nmr Spectroscopy

Complex (XVI) was easily identified by comparing its ^1H nmr spectrum with that of an authentic sample.

The high field region of the ^1H nmr spectrum of complex (XXX) is shown in Figure 5.1. The signal at 1.58 ppm is assigned to the protons

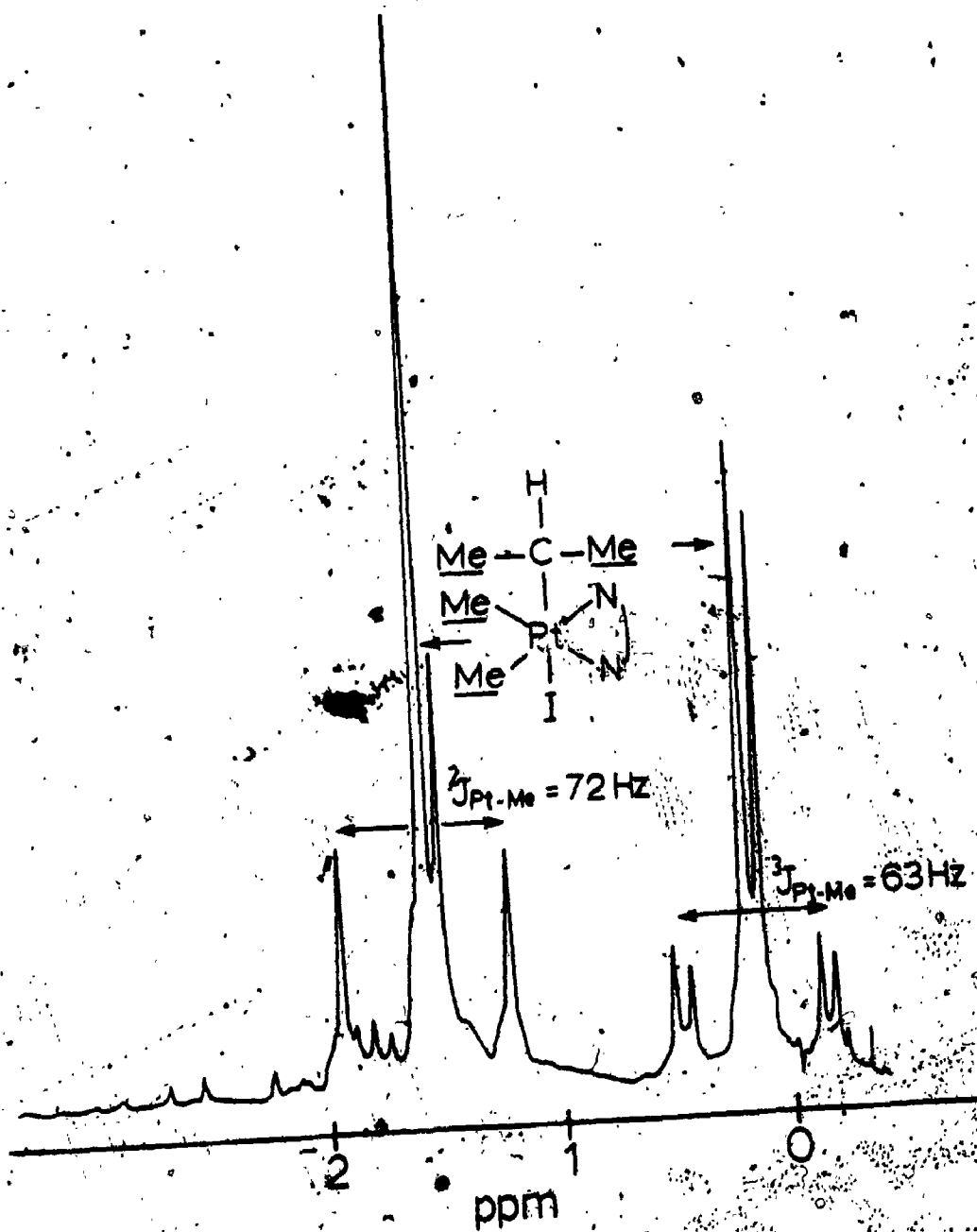


FIGURE 5.1: 1H NMR Spectrum (100 MHz) of $[PtMe_2(1-Py-phen)]$ in CD_2Cl_2 .

of the MePt groups. The observation of only one such signal is clear indication that the complex contains a plane of symmetry bisecting the PtMe_2 angle. The methyl groups of the isopropyl ligand appear as a doublet at 0.16 ppm, with ^{195}Pt satellites. The remaining proton of the isopropyl group couples to these protons and appears as a septet (somewhat obscured) at 1.81 ppm.

Figure 5.2 shows the high field region of the ^1H nmr spectrum of complex (XXXI). The signal due to the MePt groups occurs at 2.03 ppm. The doublet at 0.31 ppm is assigned to the methyl groups of the isopropylperoxy ligand. They are deshielded relative to those of complex (XXX) due to the presence of the peroxy group. Similarly, the remaining proton of the isopropylperoxy ligand is deshielded and occurs as a septet at 3.10 ppm. Full ^1H nmr data for complexes (XXX) and (XXXI) are given in Tables 7.9 and 7.11. The bipy analogue of complex (XXXI) was also synthesised and its ^1H nmr data are presented in Table 7.11.

Figure 5.3 shows the high field region of the $^{13}\text{C}\{^1\text{H}\}$ nmr spectrum of complex (XXX). The assignments are indicated on the spectrum. The $J_{\text{Pt}(\text{CH})}$ coupling could not be measured due to the low signal to noise ratio. The ^{13}C nmr spectral data for complexes (XXX) and (XXXI) are given in Tables 7.10 and 7.12.

ii) Reaction Performed Using Acetone- d_6 As Solvent

The formation of an isopropylperoxoplatinum(IV) complex in the reaction of (I) with isopropyl iodide was not anticipated. The source of the isopropylperoxy ligand was initially thought to be due to some sort of rearrangement of the solvent, acetone. However, when the reaction was performed in acetone- d_6 and the ^1H nmr spectrum of the products was run, the doublet at 0.31 ppm, due to the methyl groups of the isopropylperoxy ligand of (XXXI), was still observed.

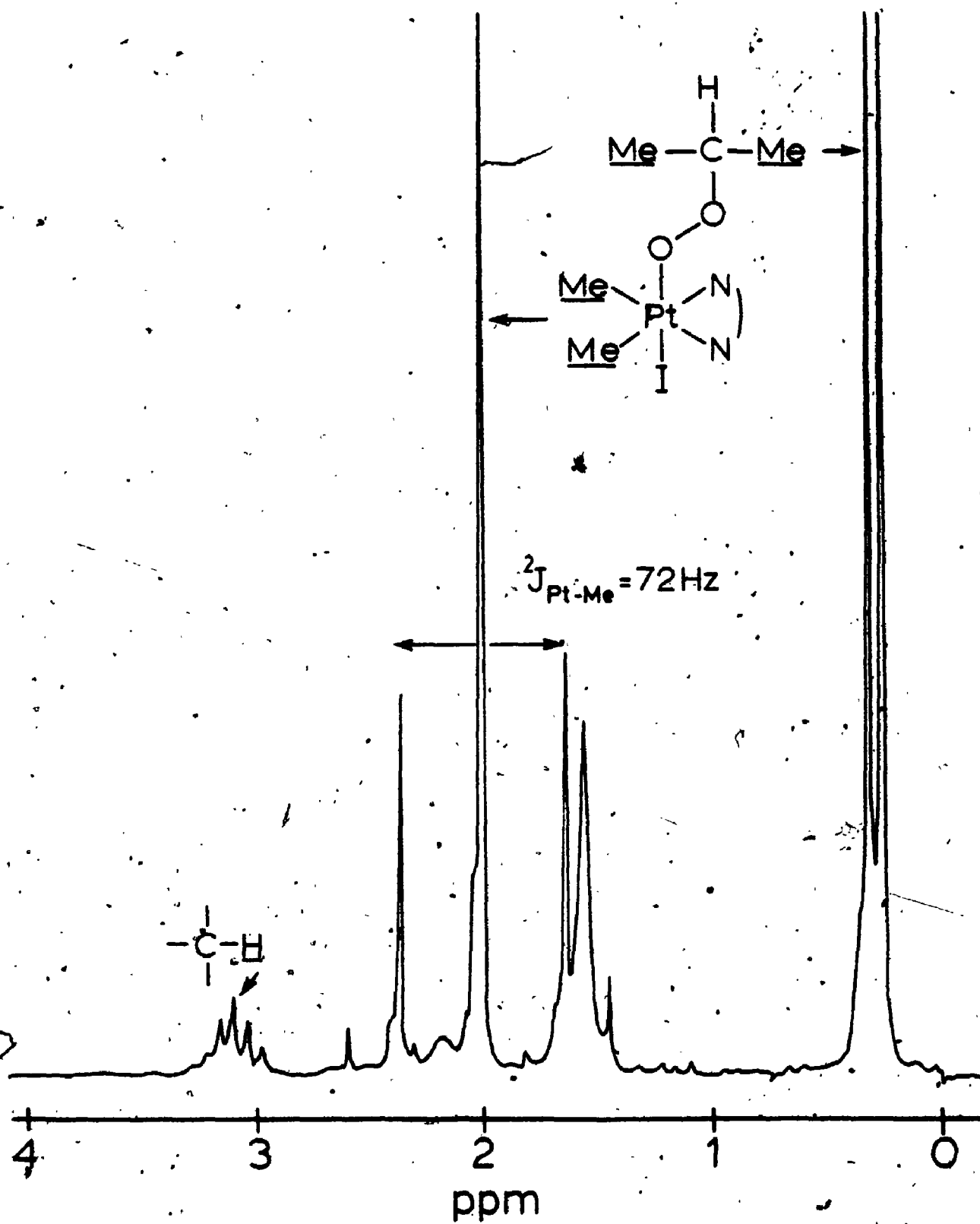


FIGURE 5.2: ^1H NMR Spectrum (100 MHz) of $[\text{PtMe}_2(\text{1PrOO})(\text{phen})]$ in CD_2Cl_2 .

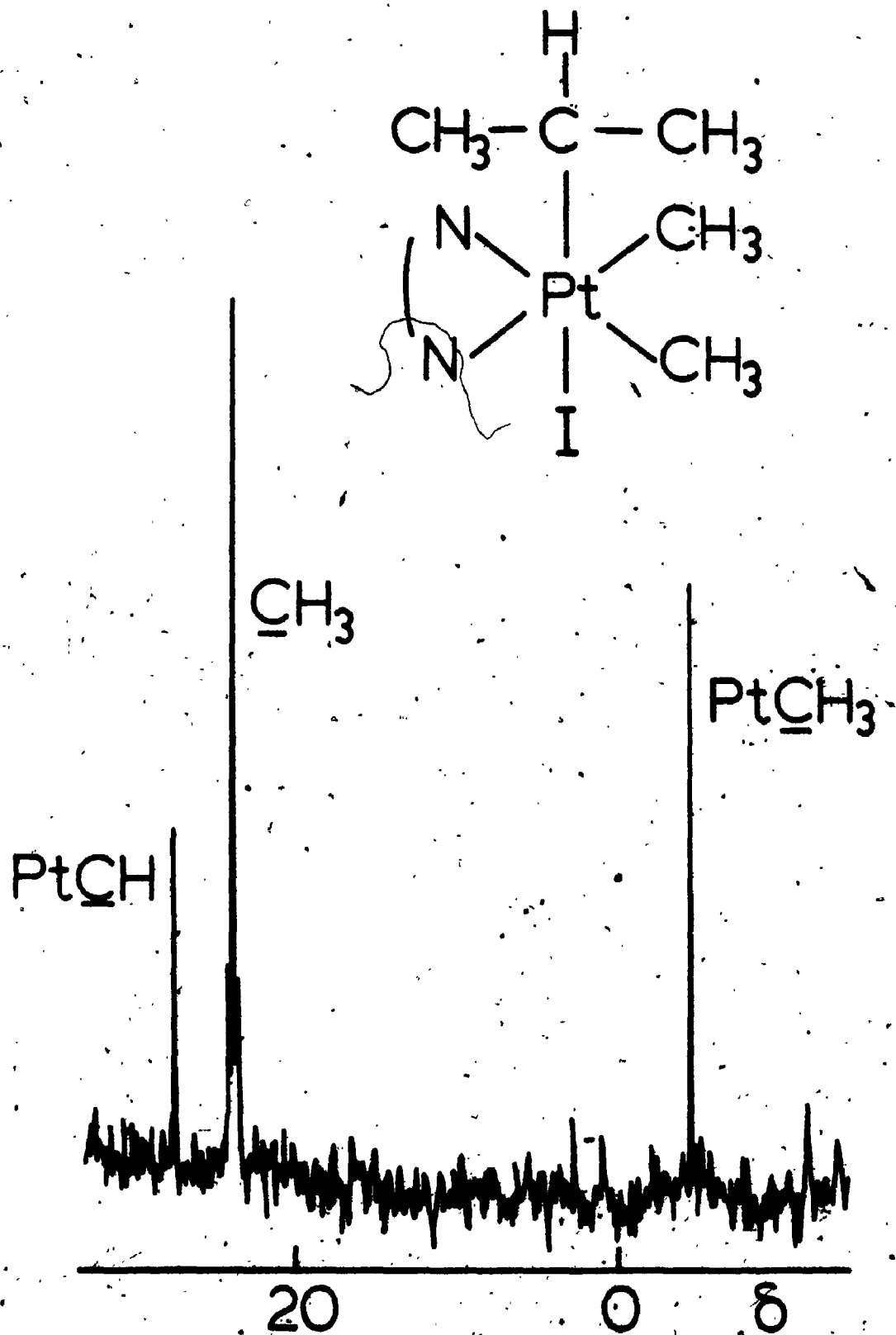


FIGURE 5.3: ^{13}C (1H) NMR Spectrum (50 MHz) of $[PtIme_2(^1Pr)(phen)]$ in CD_2Cl_2 .

iii) Reaction Performed in Acetone, Saturated with Oxygen

The reaction was performed using acetone, saturated with oxygen, as the solvent. In this case the major product (90%) was the isopropylperoxoplatinum(IV) complex (XXXI). The reaction was repeated using oxygen-free acetone as solvent. In this case the only product was complex (XXX).

The isopropylperoxo complex is quite clearly formed from the oxygen dissolved in the solvent.

iv) Qualitative Test for the Peroxide Group in Complex (XXXI)

The reaction between acidified sodium iodide and complex (XXXI) produced elemental iodine. To test for liberated iodine a small amount of $\text{Na}_2\text{S}_2\text{O}_3$ was added to the reaction mixture. The brown colour due to iodine was immediately discharged.

v) Pyrolysis of Complex (XXXI)

A small sample of complex (XXXI) was placed in the reaction vessel shown in Figure 7.1 of Chapter 7. The gaseous products formed by pyrolysis of complex (XXXI) were analysed by gas chromatography (see Section 2.5.2.4 of Chapter 7). By comparison with the retention time of an authentic sample, acetone was shown to be produced.

vi) Reaction Performed Using an Acetone/Water Mixture as Solvent

Complex (XXXII), is believed to have the formula $[\text{Pt}(\text{OH})\text{Me}_2(\text{Pr})\text{-}(\text{phen})]$, and its formation is believed to involve water present in the solvent, acetone. A reaction was therefore performed using a degassed solvent mixture of acetone and water (2:1 by volume). Analysis of the ^1H nmr spectrum of the product mixture showed an increase, by a factor of four, in the amount of complex (XXXII) relative to complex (XXX). The formation of (XXXII) in the degassed solvent confirms that it is not

formed from the intermediate ($^1\text{PrOO}$) radical.

3.1.3 X-ray Crystal Structure of $[\text{PtI}_2\text{Me}_2(^1\text{PrOO})(\text{phen})]$

Due to the novel nature of the title compound, and the lack of x-ray data for alkylperoxometal complexes, the x-ray crystal structure was determined. Figure 5.4 shows the ORTEP drawing of the molecule, and the structural parameters are given in Table 5.1. The x-ray crystal structure was performed using MoK_α radiation at a wavelength of $\lambda = 0.71069 \text{ \AA}$. The crystal belongs to the $P2_1/m$ space group. The structure was determined by Dr. G. Ferguson at the University of Guelph, Guelph, Ontario.

The Pt-I distance (2.624 \AA) is significantly shorter than the terminal $\text{Pt}^{\text{IV}}\text{-I}$ bonds in $[\text{PtI}_2\text{Me}_2(\text{N}\widehat{\text{N}})]^{36}$ (2.651 and 2.647 \AA ; $\text{N}\widehat{\text{N}} = \text{bis}(1\text{-pyrazolyl})\text{methane}$), $[\text{Pt}(\text{acac})_2\text{I}_2]^{37}$ (2.667 \AA ; $\text{acac} = \text{acetylacetonato}$), $[\text{PtI}_5(\text{phen})]$ and $[\text{PtI}_6(\text{phen})]$ (range $2.662\text{-}2.669 \text{ \AA}$).³⁸ Likewise this bond distance is shorter than the sum of the covalent radii.³⁹ This may be due to the low *trans*-influence of the peroxo ligand. The Pt-C bond distances are in the usual range,³⁶ and agree with the sum of the covalent radii.³⁹ The same is true of the Pt-N bond distances.

The Pt-O distance is much shorter than those in the trimethyl-4,6(dioxonyl)platinum(IV) dimer⁴⁰ and in the μ -ethylenediamine-bis-[trimethyl(acetylacetonato)]platinum(IV) complex⁴¹ (2.17 \AA), where the very strong *trans*-influence exerted by the methyl groups opposite the Pt-O bonds can be held responsible for the long Pt-O bonds.

The Pt-O(1) line has an angle of 5.3° to the normal of the $[\text{PtMe}_2(\text{phen})]$ plane, pushing the isopropylperoxo ligand away from the 1,0-phenanthroline ligand. The small torsion angle $\text{N}(1)\text{Pt-O}(1)\text{O}(2)$ (16.1°) as opposed to the torsion angle $\text{N}(10)\text{Pt-O}(1)\text{O}(2)$ (61.0°) places

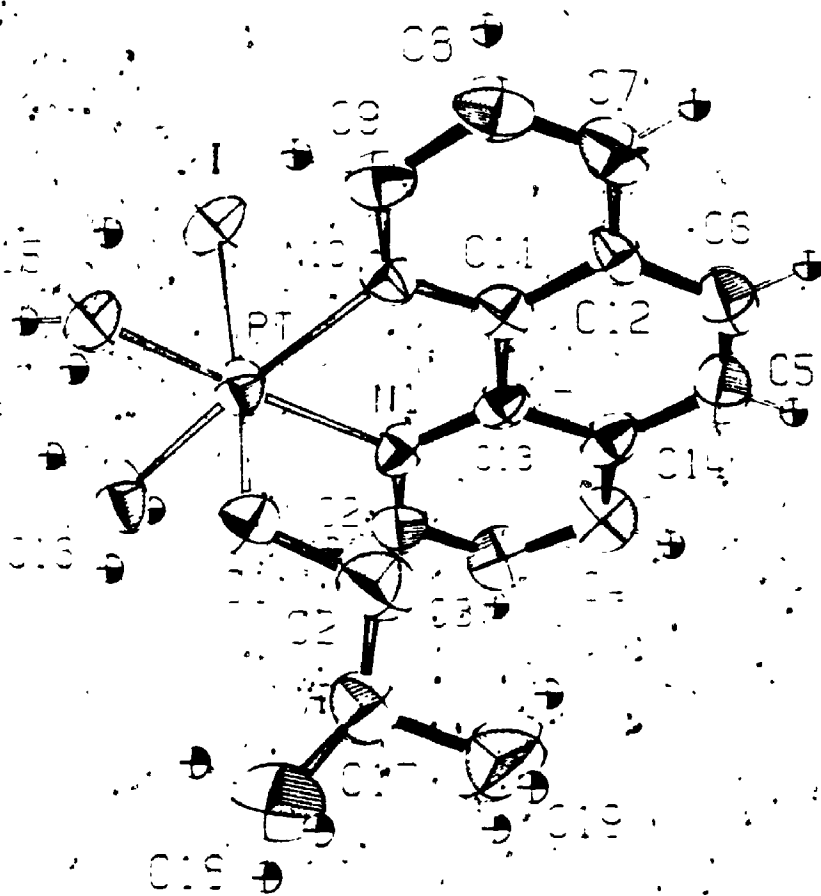
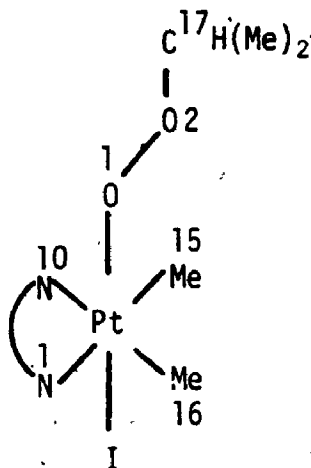


FIGURE 5.4: ORTEP Drawing of the Molecule
[PtIme₂(¹PrOQ)(phen)]

TABLE 5.1: Structural Parameters of the Molecule^a

Bond Distances (Å)

Pt-I	2.624 (1)
Pt-O (1)	2.032 (6)
Pt-C (15)	2.067 (8)
P-C (16)	2.048 (9)
Pt-N (1)	2.175 (7)
Pt-N (10)	2.164 (7)
O (1) - O (2)	1.465 (9)

Bond Angles (°)

I-Pt-N (1)	91.2 (2)
I-Pt-N (10)	89.1 (2)
I-Pt-O (1)	174.6 (2)
I-Pt-C (16)	93.0 (3)
I-Pt-C (15)	90.6 (3)
N-Pt-N	77.0 (3)
N (1)-Pt-C (16)	98.4 (3)
N (2)-Pt-C (15)	98.0 (3)
Pt-O(1)-O(2)	110.2 (4)
O (1)-O (2)-C (17)	107.9 (7)

^aFor the numbering of the atoms see Figure 5.4.

the isopropylperoxo ligand closer to N(1). This is shown in Figure 5.5. Very few x-ray crystal structures of transition-metal peroxo complexes have been determined.^{22,27,28,31,35} The O(1)-O(2) bond distance in complex (XXXI) is 1.465(9) Å. This is close to the value determined by Chiaroni³¹ and Giannotti³⁵ for alkylperoxocobalt(III) complexes (1.455(3) Å). The O-O bond distance of 1.547 Å in the peroxo-bridged platinum complex $[\text{Pt}_2(\mu\text{-O}_2)(\text{OH})(\text{PPh}_3)_4][\text{ClO}_4]^{22}$ is considerably longer than in complex (XXXI). This is presumably due to the constraints of the bridged bonding mode.

The x-ray crystal structure of complex (XXXI) is the first for a peroxoplatinum(IV) complex.

3.1.4 Kinetic and Mechanistic Studies

A series of experiments was performed in order to establish the reaction mechanism for the reaction between (II) and isopropyl iodide. The results of these experiments are discussed in this section and the experimental details are in Section 2.5.2.1 of Chapter 7.

i) UV/visible Spectrum

The uv/visible spectrum of the reaction mixture (300-600 nm) was recorded as the reaction between $[\text{PtMe}_2(\text{phen})]$ and ^1PrI proceeded. A typical spectrum is shown in Figure 5.6. The MLCT band, at 473 nm, due to complex (II) disappears as the reaction proceeds.

ii) Determination of the Rate Constant for the Reaction between II and ^1PrI

The rate of reaction of (II) with isopropyl iodide, in acetone, was determined by monitoring the decay of the MLCT band due to (II), as the reaction progressed. The concentration of isopropyl iodide was in large excess over that of complex (II). The absorbance (A_t) was recorded

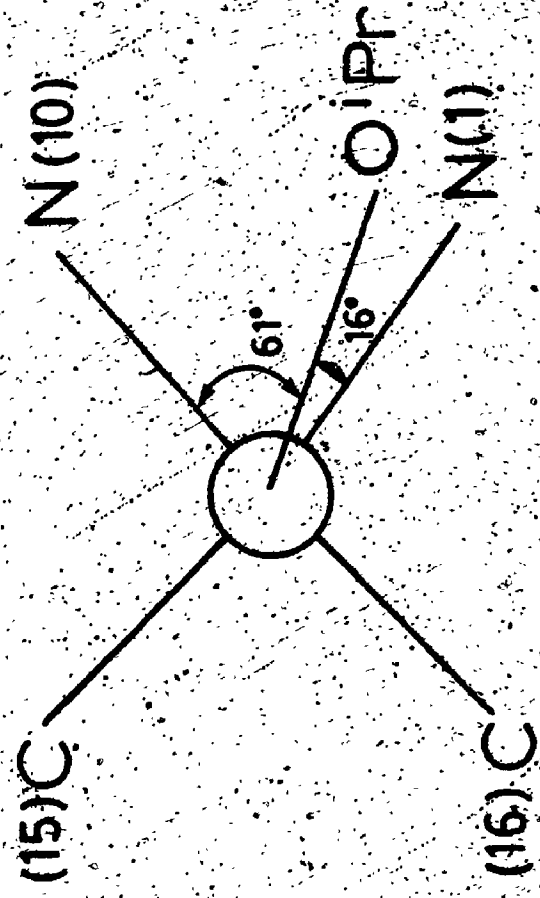


Figure 5.5
Newman Projection of the Molecule [PtMe₂(IPrO)(phen)]
Viewed Along the O(1)-Pt Bond.

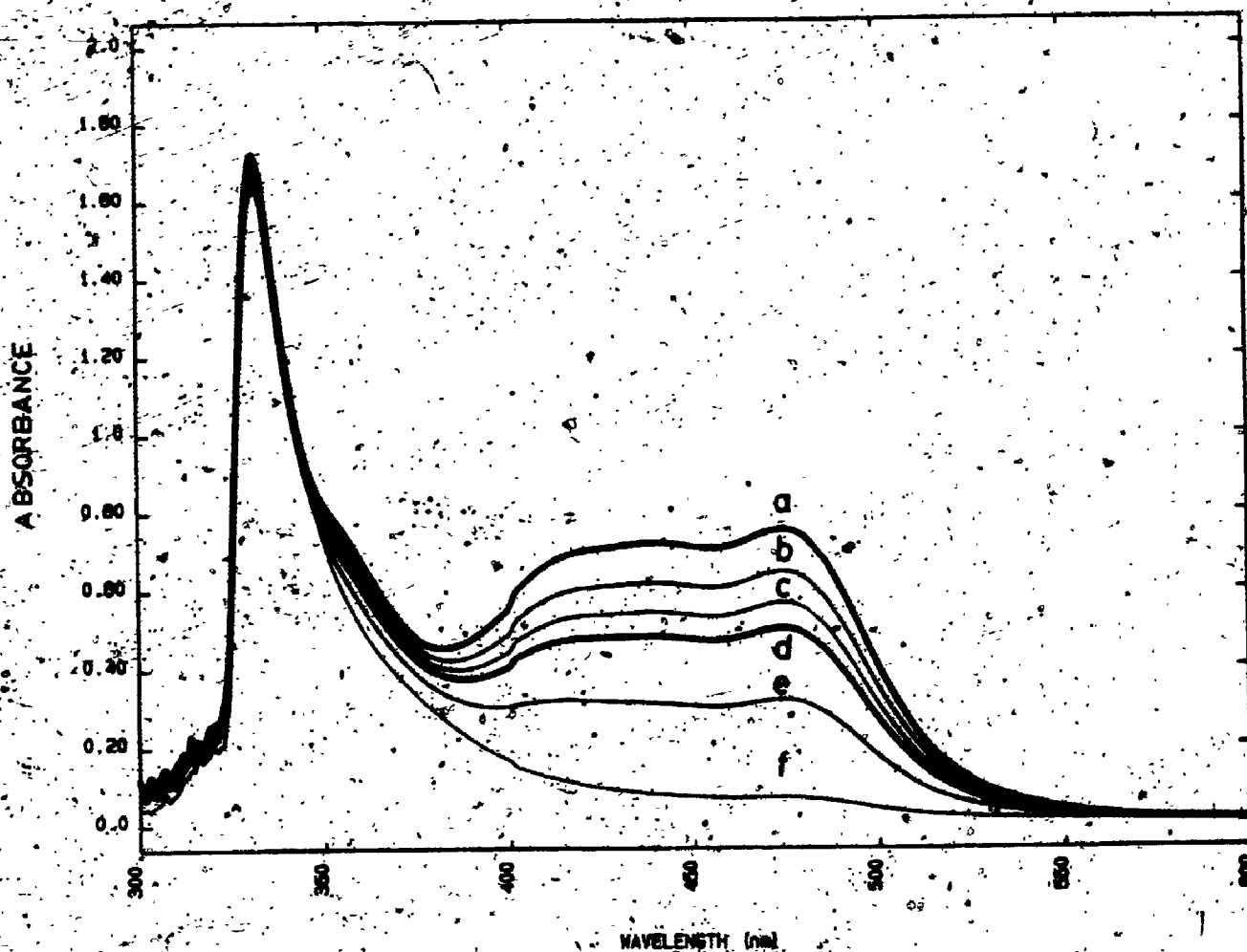
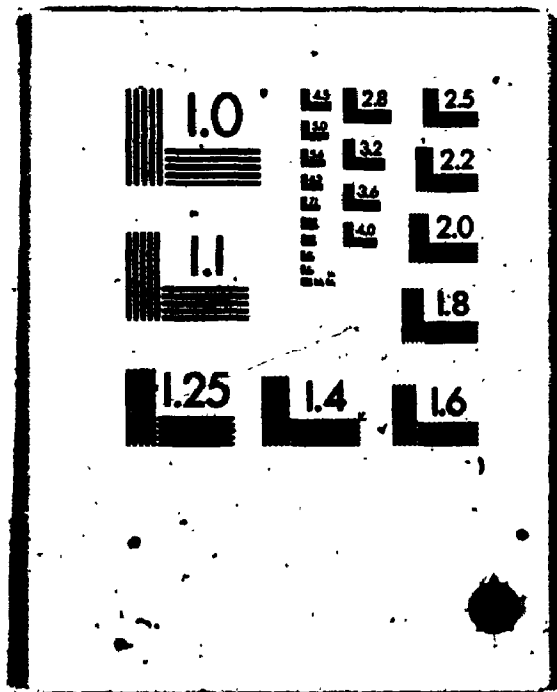


FIGURE 5.6: Change in the UV/Visible Spectrum for the Reaction between (II) and PrI. a) $t = 0$; b) $t = 5$ min; c) $t = 10$ min; d) $t = 15$ min; e) $t = 25$ min; f) $t = 60$ min.

3



at regular intervals and a plot of $\log (A_t - A_\infty)$ versus time was made for each concentration of the isopropyl iodide used. The result for one such experiment is shown in Figure 5.7. The plot is linear for about the first 40% of the reaction after which an acceleration of the reaction rate is observed. A similar result was observed in each of the kinetic plots, as the concentration of the isopropyl iodide was varied. Clearly, the reaction does not follow good overall second-order kinetics. From the slope of plots such as that shown in Figure 5.7 the pseudo-first-order rate constant (k_{obs}) were obtained for each concentration of ^iPrI . If k_{obs} is plotted against the concentration of ^iPrI an overall second-order rate constant of $3.18 \times 10^{-4} \text{ M}^{-1} \text{ S}^{-1}$ was obtained. The solvent, acetone, was not degassed for this experiment. However, in a control experiment using degassed acetone, similar plots as in Figure 5.7 were obtained yielding an overall rate-constant which was in good experimental agreement with the value given above. This implies that the oxygen is not involved in the rate-determining step for the reaction. It should be noted, however, that in other similar kinetic experiments reproducible results were not always obtained. This is an indication of the involvement of free-radicals in the reaction. Furthermore the kinetic experiments were done in the dark.

iii) First-Order Dependence of $[\text{PtMe}_2(\text{phen})]$ for the Reaction of (II) with ^iPrI

The reaction between (II) and isopropyl iodide, in acetone, was monitored by following the decay of the MLCT band (473 nm), due to (II) as the reaction progressed. Several runs were made keeping the concentration of isopropyl iodide constant, whilst varying the concentration of (II). The absorbance (A_t) was recorded as the reaction progressed and a plot of $\log (A_t - A_\infty)$ versus time was made. These plots

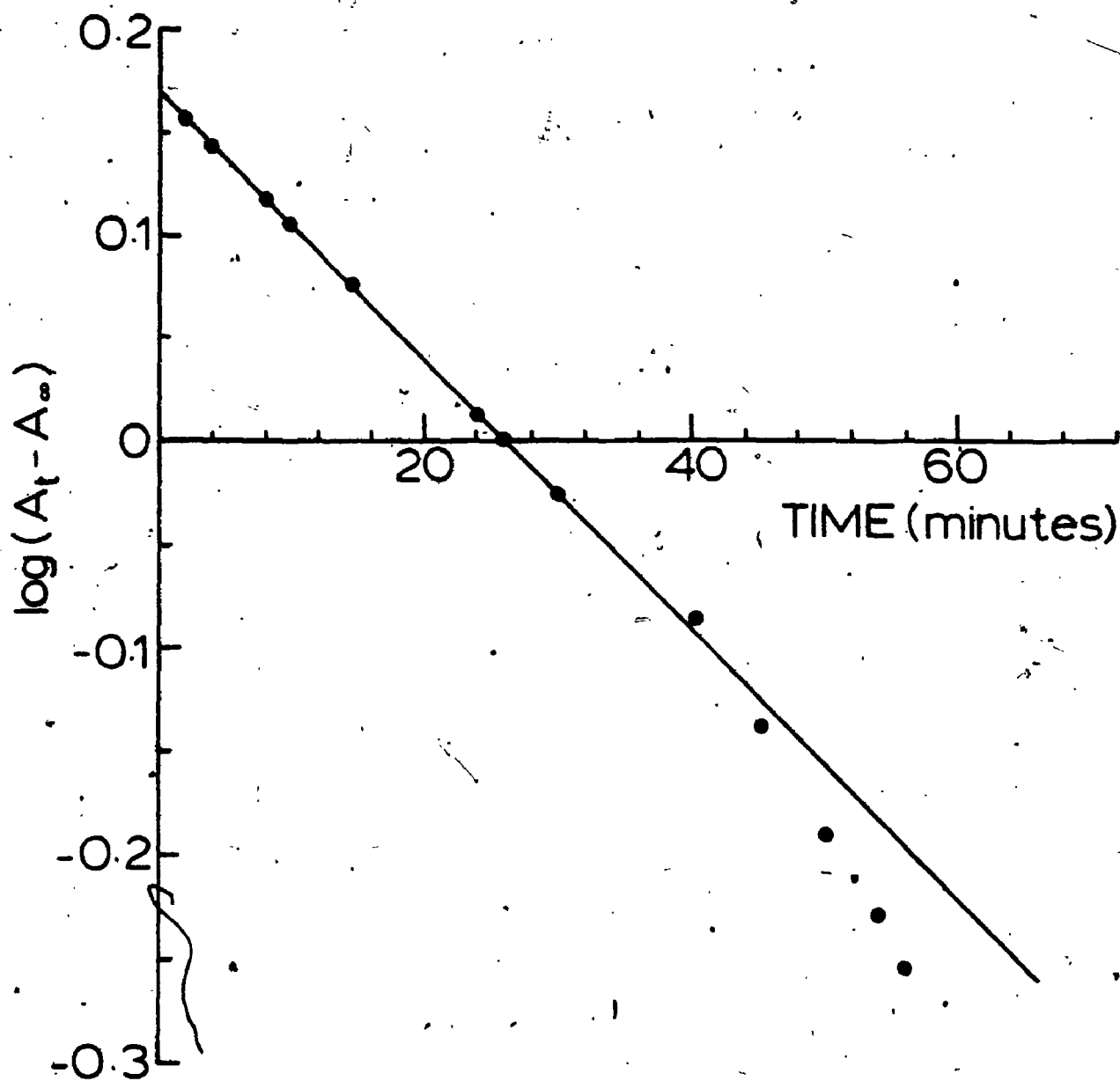


FIGURE 5.7: Plot of $\log(A_t - A_\infty)$ Versus Time for the Reaction between (II) (5.0×10^{-4} M) and ^1PrI (7.5×10^{-1} M) in Acetone at 25°C .

are shown in Figure 5.8. In the linear portion of the plots, the slopes are equal, implying a first-order dependence on the concentration of $[\text{PtMe}_2(\text{phen})]$. From the slope of these lines, an overall rate-constant of $2.93 \times 10^{-4} \text{ M}^{-1} \text{ S}^{-1}$ was obtained. This is in good agreement for the value determined in the previous section. Once again, an acceleration in the rate is observed in the later stages of the reaction. These kinetic experiments were done in the dark.

iv) The Effect of Irradiating the Reaction Mixture

The intermediacy of free-radicals was suspected in the reaction between (II) and isopropyl iodide, and the reaction was believed to be photoinitiated. To confirm this a sample of the reaction mixture was irradiated from above, whilst monitoring the decay of the MLCT band at 473 nm. The results are shown in Figure 5.9. On irradiating the sample a dramatic rate increase was observed. On removing the light source the rate of reaction decreases.

v) The Effect of Galvinoxyl

The reaction under discussion is believed to proceed *via* a free-radical chain mechanism. Radical scavengers such as galvinoxyl have been shown to inhibit such reactions.^{42,43} In the case of the reaction of (II) with isopropyl iodide, the addition of galvinoxyl did not give reproducible results. Galvinoxyl did, on occasion, produce some retardation of the reaction rate, but at other times an acceleration in the rate was observed. However, the use⁴⁴ of 4-methoxy phenol, p-benzoquinone, or hydroquinone as radical inhibitors, did show an inhibition of the photoinitiated reaction. This will be discussed later in this chapter. The failure of galvinoxyl to inhibit some free-radical chain reactions has been observed before.⁴⁵

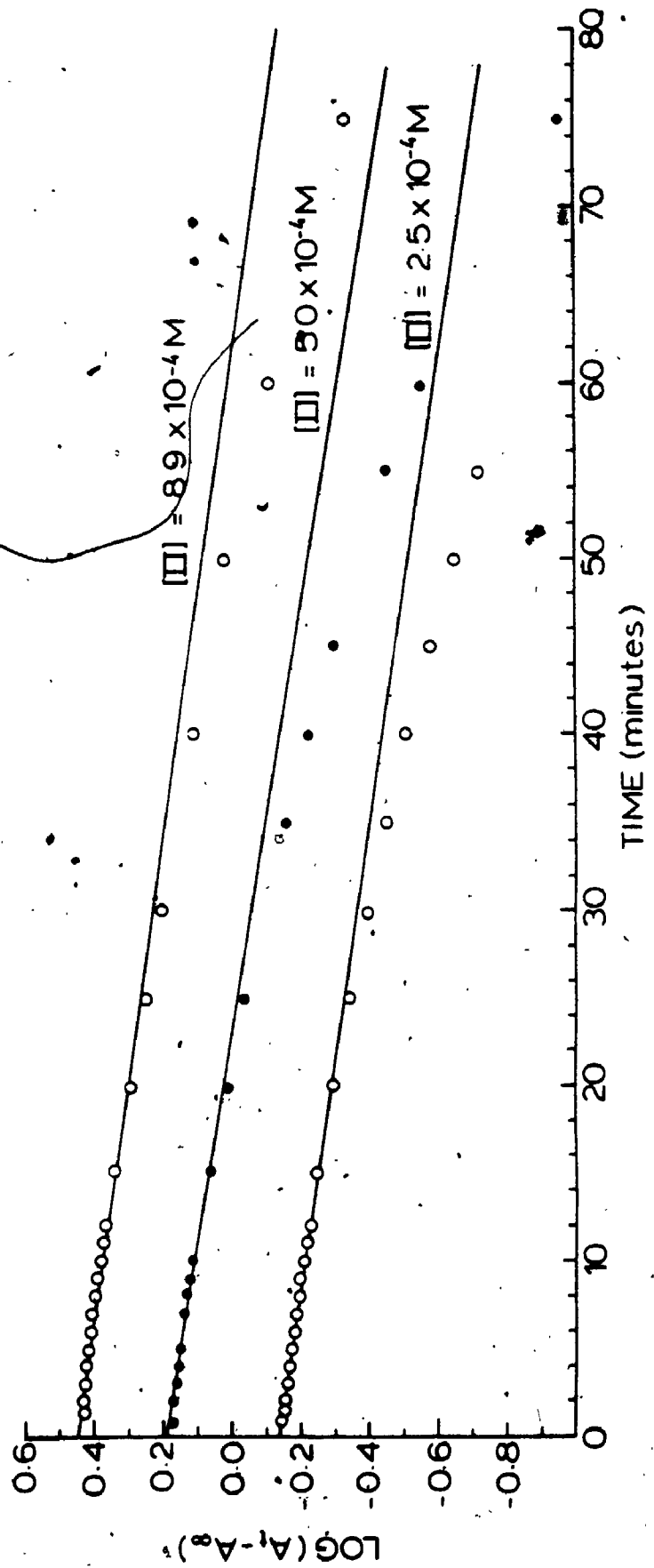


FIGURE 5.8: Plot of $\text{Log}(A_t - A_\infty)$ Versus Time for the Reaction between (II) and $i\text{PrI}$ (1.0 M) in Acetone at 25°C.

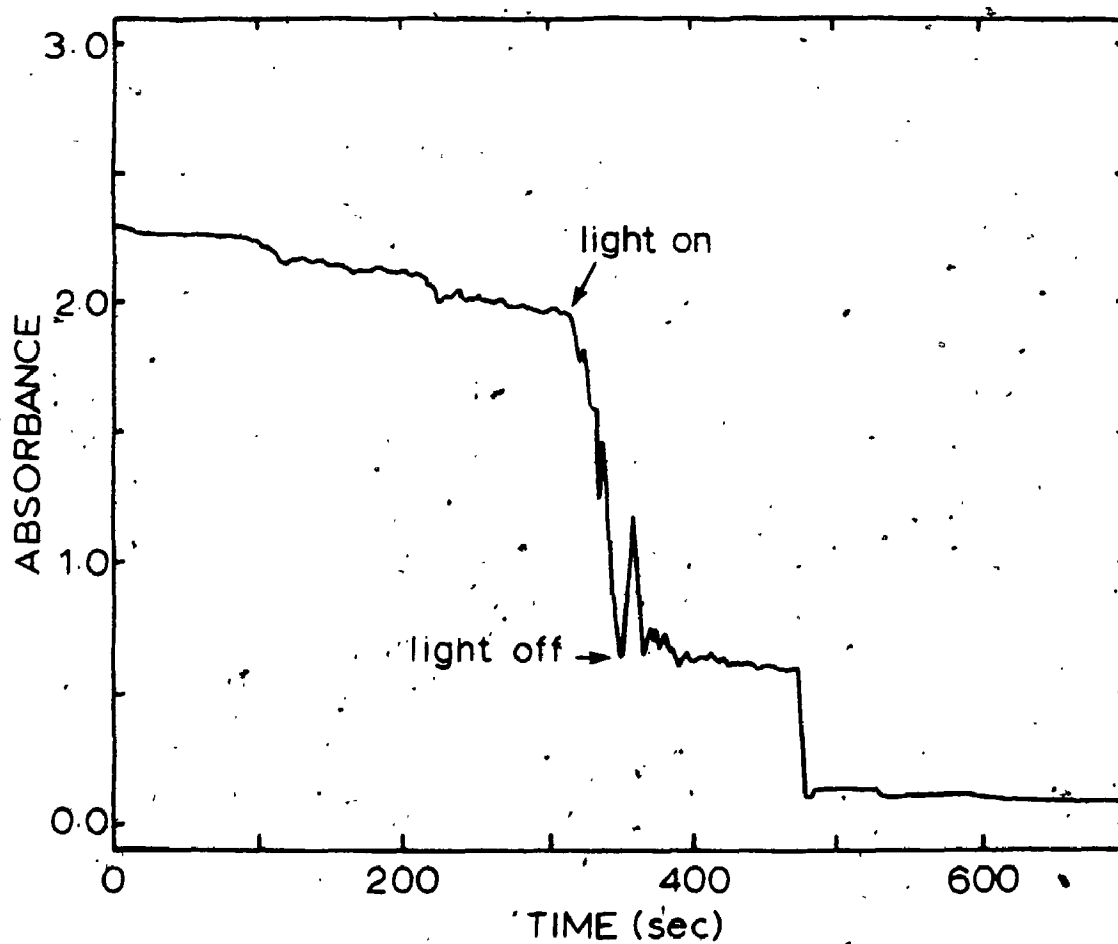


FIGURE 5.9: The Effect of Irradiation on the Reaction between (II) and ^1PrI Followed by Monitoring the Decay of the Band at 473 nm in the UV/Visible Spectrum.

vi) Attempt to Observe CIDNP Effects

The ^1H nmr spectrum of the reaction mixture ((II) and ^1PrI in CD_2Cl_2) was recorded as the reaction proceeded. The sample was irradiated from above by a PRA 200 Watt, high pressure Hg-Xe lamp. Immediately the sample was irradiated the spectrometer field 'lock' was lost. As a result the only signals that could be observed were very broad. On removing the irradiation the field 'lock' returned in a few seconds. No anomalous peak intensities were observed, but the reaction was very much faster when the sample was irradiated. This was shown by the rate of disappearance of the signal due to the MePt group of complex (II).

3.1.5 Product Ratios for Different Reaction Conditions, in the Reaction between (II) and ^1PrI

A series of experiments was performed, under various conditions, for the reaction of (II) with isopropyl iodide in acetone. Details of this work are given in Section 2.5.2.7 of Chapter 7, and the product ratios are given in Table 5.2. These results are discussed below.

3.1.6 Conclusions for the Reaction between (II) and ^1PrI

Judging from the kinetic plots shown in Figures 5.7 and 5.8 the reaction between (II) and isopropyl iodide does not follow second-order kinetics. This therefore eliminates the possibility of an $\text{S}_{\text{N}}2$ type oxidative addition reaction between (II) and ^1PrI . The formation of complex (XVI) is thought to occur *via* a radical non-chain mechanism, as discussed in Chapter 4. The acceleration of the rate of the reaction by irradiation, compared to the rate in diffuse daylight, implies a photo-initiation of the reaction, and the intermediacy of radicals. The

TABLE 5.2: Product Ratio for the Reaction of (II) with Isopropyl Iodide, in Acetone

	Concentration/M			Products %		
	[II]	[¹ PrI]	[O ₂]	(XXX)	(XXXI)	(XVI)
(i)	0.0039	0.6	0 ^a	100	0	0
(ii)	0.004	0.5	0.011 ^b	8	89	3
(iii)	0.015	0.167	0.002 ^b	44	51	5
(iv)	0.0077	0.167	0.002 ^b	34	56	10
(v)	0.0024	0.167	0.002 ^b	0	63	37
(vi)	0.0088	0.33	0.002 ^b	17	58	25
(vii)	0.0088	0.33	0.002 ^{b,e}	15	75	10
(viii)	0.0115	0.165	0.002 ^d	13	49	38
(ix)	0.005	0.80	0.002 ^e	0	84	16
(x)	0.005	0.80	0.002 ^f	35	60	5
(xi)	0.005	0.80	0.002 ^{c,f}	8	67	25
(xii)	0.005	0.80	0.002 ^{c,e}		~100	

^aReaction under N₂. ^bInitial [O₂]; reaction performed in sealed flask. ^c10% mole ratio of galvinoxyl present. ^dAir bubbled through to ensure O₂ saturation throughout the reaction. ^eSample stirred rapidly and irradiated. ^fReaction performed in the dark, with rapid stirring.

The initiation step is presumed to be the same in Schemes 4 and 5. The geminate radical-pair diffuse out of the solvent cage (k_2) and as shown in Scheme 5, the isopropyl radical can react with the oxygen in the solvent or with a molecule of complex (II). The addition of alkyl radicals to molecular oxygen is extremely fast and is probably diffusion controlled^{46,47} in many instances (ie. $k_3 \sim 10^9 \text{ M}^{-1} \text{ S}^{-1}$). For example for the *tert*-butyl radical in cyclohexane a value of $4.93 \times 10^9 \text{ M}^{-1} \text{ S}^{-1}$ has been determined.⁴⁷ A value of similar magnitude can be expected for k_3 in Scheme 5. The rate constant (k_4) for the addition of the isopropyl radical to (II) has been determined (Chapter 6) and is approximately equal to $4.6 \times 10^6 \text{ M}^{-1} \text{ S}^{-1}$. Thus the isopropyl radical shows greater selectivity for addition to molecular oxygen than to (II). This is borne out, in a qualitative fashion, by the data in Table 5.2. In all cases studied, where the solvent was not degassed, the predominant product is the isopropylperoxoplatinum(IV) complex (XXXI).

As the concentration of [II] is increased, the relative amount of products (XXX) and (XXXI), from the chain mechanism, compared to product (XVI), from the non-chain mechanism, is expected to increase. Table 5.2 ((iii)-(v)) shows this to be the case. As pointed out earlier, the photoinitiated oxidative addition reaction between (II) and PrI has been shown to be a free-radical chain mechanism. The reaction does proceed thermally but is slower. The data in Table 5.2 ((ix) and (x)) imply that the thermally initiated reaction ((x)) mechanism is different to the photochemical mechanism. In the thermal reaction (ie, performed in the dark) there is a considerable increase in the amount of (XXX) relative to (XXXI) compared to the photochemical reaction ((ix)). It may be that the thermal reaction proceeds partly via an $\text{S}_{\text{N}}2$ mechanism. The problem of the thermal reaction of isopropyl iodide with (II) will

be discussed in more detail in the conclusion to Chapter 6.

It should again be noted that the galvinoxyl does not inhibit the reaction rate. In the presence of a radical scavenger, one would anticipate a dramatic increase in the amount of (XVI) relative to (XXX) and (XXXI). This is not found to be the case ((vii), (xi)-(xii) in Table 5.2). It is not clear why galvinoxyl fails to inhibit the chain mechanism, but it is known that the galvinoxyl does not react with $[\text{PtMe}_2(\text{phen})]$.

The formation of a transition-metal alkylperoxo complex *via* the mechanism shown in Scheme 5 is believed to be the first of its kind. This complex is stable in solution, showing no decomposition after being in solution for one month.

3.2 Reaction of *tert*-Butyl Iodide with (II)

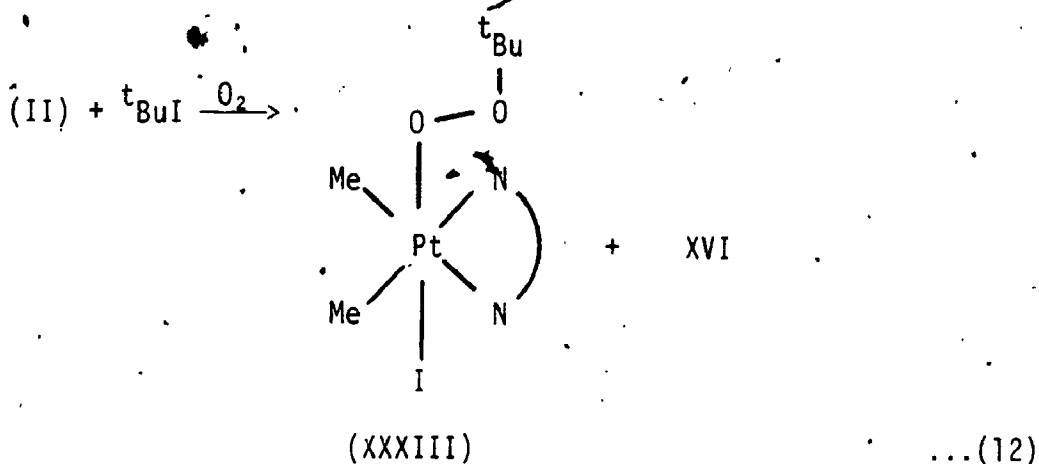
3.2.1 Products from the Reaction

The products obtained from the reaction between (II) and *tert*-butyl iodide were found to be dependent on the solvent and reaction time. Experimental details are given in Section 2.5.1.8 of Chapter 7.

If the reaction is performed in acetone the red-orange colour of the complex (II) fades rapidly with the formation of a yellow solution. If the reaction is stopped at this stage the products isolated are $[\text{PtMe}_2(\text{}^t\text{BuOO})(\text{phen})]$ (XXXIII) and (XVI). If the yellow reaction mixture is left for a short while, a brown colour develops. The product in this case is complex (XVI) along with elemental iodine. None of (XXXIII) was isolated.

In those cases when CH_2Cl_2 was used as solvent, a much larger yield of complex (XXXIII) was obtained and this complex was more stable

in methylene chloride than in acetone. This new reaction is shown in equation 12.



Complex (XXXIII) can be separated from (XVI) by column chromatography as described in Section 2.5.1.3 (Chapter 7).

The reaction of *tert*-butyl hydroperoxide with (II) was investigated. The product was an intractable mixture and was not investigated further.

3.2.2 Characterisation of the Products from the Reaction of (II) with $t\text{BuI}$

Complex (XVI) was easily identified from its ^1H nmr spectral data. The ^1H nmr data for (XXXIII) are given in Table 7.11 of Chapter 7. The signal at 1.92 ppm in the ^1H nmr spectrum is due to the protons of the two MePt groups, with a J_{PtH} coupling (72 Hz) characteristic of a platinum(IV) complex. A very intense singlet occurs, in the spectrum, at 0.26 ppm in the ratio of 3:2 relative to the signal at 1.92 ppm. This is assigned to the protons of the *tert*-butylperoxy ligand. No coupling to ^{195}Pt is observed.

Figure 5.10 shows the high field $^{13}\text{C}\{^1\text{H}\}$ nmr spectrum of (XXXIII). The assignments are shown on the spectrum and confirm the proposed structure.

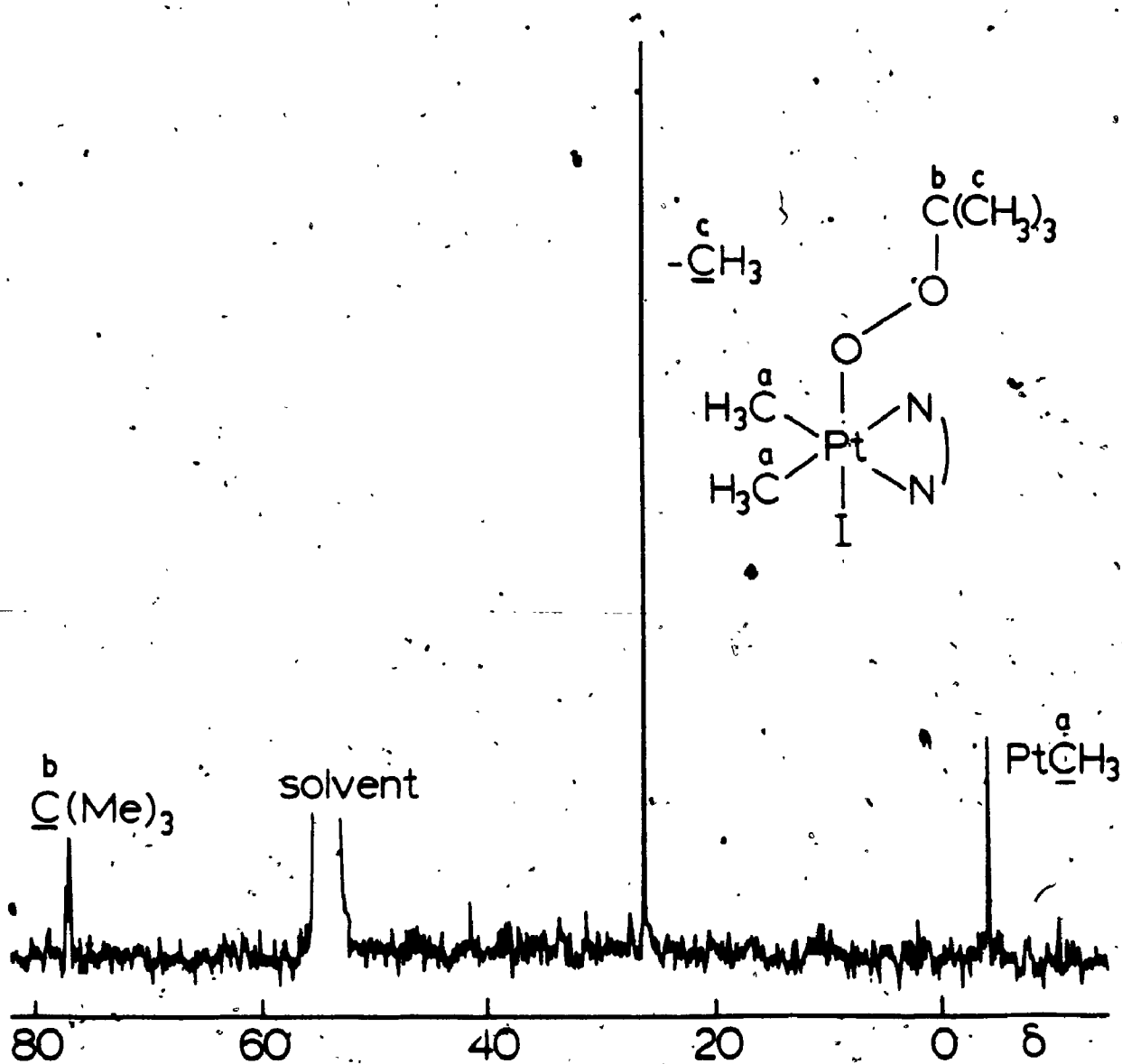


FIGURE 5.10: $^{13}\text{C}\{^1\text{H}\}$ NMR Spectrum (50 MHz) of $[\text{PtMe}_2(\text{tBuCO})(\text{phen})]$ in CD_2Cl_2 .

Elemental analysis of (XXXIII) is consistent with the formula $[\text{Pt}(\text{Me})_2(\text{tBuOO})(\text{phen})]$ (Table 7.18, Chapter 7).

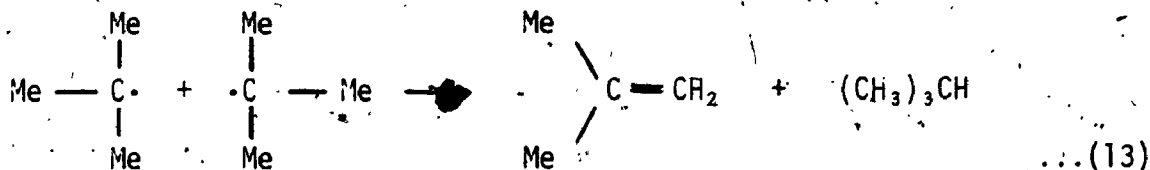
3.2.3 Kinetic and Mechanistic Studies for the Reaction of (II) with tBuI

A series of experiments was performed, aimed at determining the mechanism of this reaction. The results are presented here.

i) Following the Reaction by ^1H NMR Spectroscopy

The reaction between (II) and tBuI in CD_2Cl_2 was monitored by following the ^1H nmr spectrum of the mixture as the reaction progressed.

The spectra indicate that the *tert*-butylperoxoplatinum(IV) is initially formed along with 2-methylpropene (σ , 4.56 ppm, CH ; δ , 1.71 ppm, $(\text{CH}_3)_2$) and 2-methylpropane (δ , 1.56 ppm, CH ; δ , 0.9 ppm, $(\text{CH}_3)_3$). The two latter products are from disproportionation of the *tert*-butyl radical shown in equation 13.



Complex (XVI) was formed in the later stages of the reaction.

In order to confirm that 2-methylpropane and 2-methylpropene were produced due to a reaction involving (II), a control experiment was performed. *tert*-Butyl iodide was left in CD_2Cl_2 for two hours. The ^1H nmr spectrum of the mixture did not show the presence of either of these organic products.

ii) Decomposition of (XXXIII) Monitored by ^1H NMR Spectroscopy

A sample of (XXXIII) (contaminated with (XVI)), was dissolved in acetone- d_6 and the decomposition of the complex was monitored by

recording the ^1H nmr spectrum of the solution at regular intervals. Decomposition of (XXXIII) produced *tert*-butyl alcohol. The platinum product was not identified. There was no growth in the amount of (XVI) due to decomposition of (XXXIII).

iii) Reaction Monitored by UV/Visible Spectrophotometry

To a solution of complex (II) in acetone (not deoxygenated) was added *tert*-butyl iodide. The progress of the reaction was monitored by recording the uv/visible spectrum of the mixture (from 600-325 nm) at regular intervals. The resulting plot of absorbance versus wavelength is shown in Figure 5.11. The reaction proceeds via an intermediate species which absorbs at 435 nm. As this species decays, complex (XVI) is formed, as shown by the growth of the band at 371 (nm), which is characteristic of $[\text{PtI}_2\text{Me}_2(\text{phen})]$. The nature of the intermediate species is not known. It is not believed to be the *tert*-butylperoxoplatinum(IV) complex, (XXXIII), since, by analogy, the reaction of (II) with ^1PrI gave no such uv/visible spectrum (see Figure 5.6). In Chapter 4 it was noted that the reaction between (II) and 1,2-diiodoethane also proceeds via the decay of some intermediate species.

iv) The Effect of Irradiation

To a solution of (II), in acetone, was added ^tBuI . The reaction proceeded, in diffuse daylight, and was monitored by the decay of the MLCT band at 473 nm, due to (II). When the sample was irradiated from above a large increase in reaction rate was observed.

3.3 Reaction of $^1\text{PrBr}$ with (II), in Acetone

3.3.1 Products from the Reaction of $^1\text{PrBr}$ with (II)

Isopropyl bromide reacts very slowly with (II). The product was that of oxidative addition, $[\text{PtBrMe}_2(^1\text{Pr})(\text{phen})]$, (XXXIV). Some

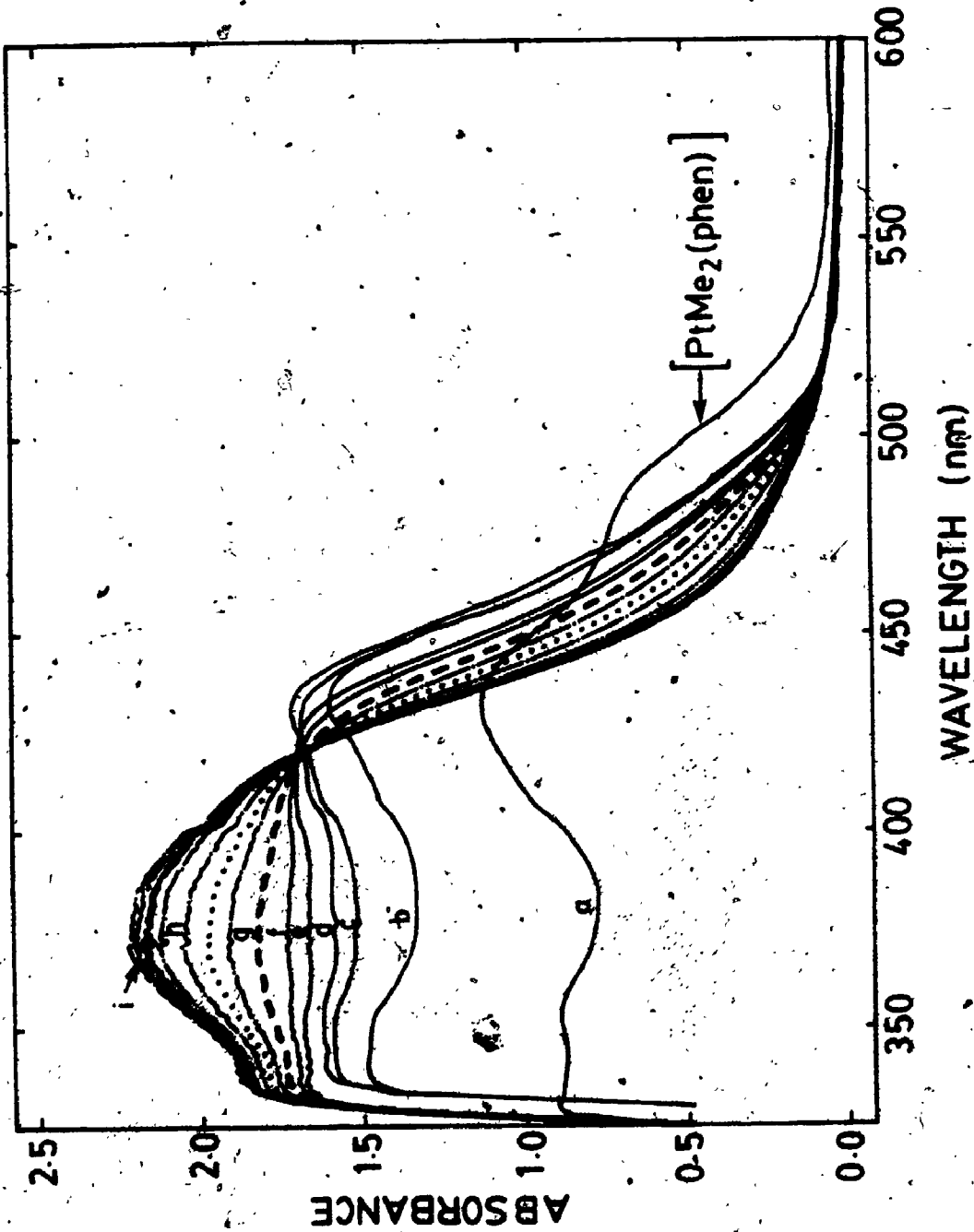


FIGURE 5.11: The Change in the UV/Visible Spectrum during the Reaction between (II) ($7.0 \times 10^{-4} M$) and $tBuI$ ($8.4 \times 10^{-2} M$) in Acetone. a) $t = 0$; b) 20 s; c) $t = 60$ s; d) $t = 80$ s; e) $t = 100$ s; f) $t = 2$ m; g) $t = 5$ m; h) $t = 15$ m; i) $t = 30$ m.

[PtBrMe₂(ⁿPr)(phen)] (XIe) was also formed. The latter complex formed due to the presence of a small amount (< 0.1% molar ratio) of n-propyl bromide as impurity in the isopropyl bromide. This n-propyl bromide could not be completely removed even by a spinning-band distillation of the isopropyl bromide.

It is noteworthy that no isopropylperoxoplatinum(IV) complex was formed. This argues against the intermediacy of radicals in the oxidative addition of isopropyl bromide to (II).

Complexes (XXXIV) and (XIe) were easily characterised by their ¹H nmr spectral data.

3.3.2 Effect of Irradiation on the Reaction between ¹PrBr and (II)

By analogy with the reaction of isopropyl iodide with (II), it was expected that the reaction of isopropyl bromide with (II) could be photoinitiated. However after prolonged irradiation no rate increase was observed. The implication is that this reaction does not involve the intermediacy of radicals and might therefore proceed via an S_N2 mechanism.

3.3.3 Competition Reactions of ⁿPrBr and ¹PrBr with (II)

n-Propyl bromide is known to react with (II) via an S_N2 mechanism. If therefore isopropyl bromide reacts via the same mechanism the product ratio of the reaction (ie, (XIe):(XXXIV)) of a mixture of n-propyl bromide and isopropyl bromide with (II) should be directly proportional to the molar ratio of the mixture of these organic bromides. A series of experiments was therefore performed in which the concentration of (II) was kept constant whilst varying the molar ratio of the two

bromides. The relative amounts of (XIe) and (XXXIV) were determined from the peak heights of the MePt signal of each complex in the ^1H nmr spectrum of the products. Figure 5.12 shows the plot of the relative amounts of (XIe) to (XXXIV) *versus* the molar percentage of n-propyl bromide present in the reaction. A straight line is obtained indicating that the product ratio is directly proportional to the relative rate constants for the reaction of n-propyl bromide and isopropyl bromide with (II). It can therefore be concluded that both organic bromides react with (II) *via* the same mechanism (ie, $\text{S}_{\text{N}}2$).

3.3.4 Determination of the Rate-Constant for the Reaction of a Mixture of $^1\text{PrBr}$ and $^i\text{PrBr}$ with (II)

A series of reactions was performed in which a constant concentration of (II) was reacted with mixtures of a n-propyl bromide and isopropyl bromide. The concentration of isopropyl bromide in these mixtures was also kept constant whilst varying the concentration of n-propyl bromide. The rate of the reaction was measured by monitoring the decay of the MLCT transfer band, in the uv/visible spectrum, due to (II), as the reaction progressed.

For each concentration of n-propyl bromide used a plot was made of $\log^*(A_t - A_\infty)$ *versus* time. A straight line graph resulted in each case. From the slope of these plots the pseudo-first-order rate constants (k_{obs}) were calculated and a plot of k_{obs} *versus* concentration of n-propyl bromide yielded a straight line shown in Figure 5.13. These results are clear indication of a common mechanism for the reaction of n-propyl bromide and isopropyl bromide with (II)

From the slope of the straight line in Figure 5.12 the relative rate constants for the reaction of isopropyl bromide (k_i) and n-propyl

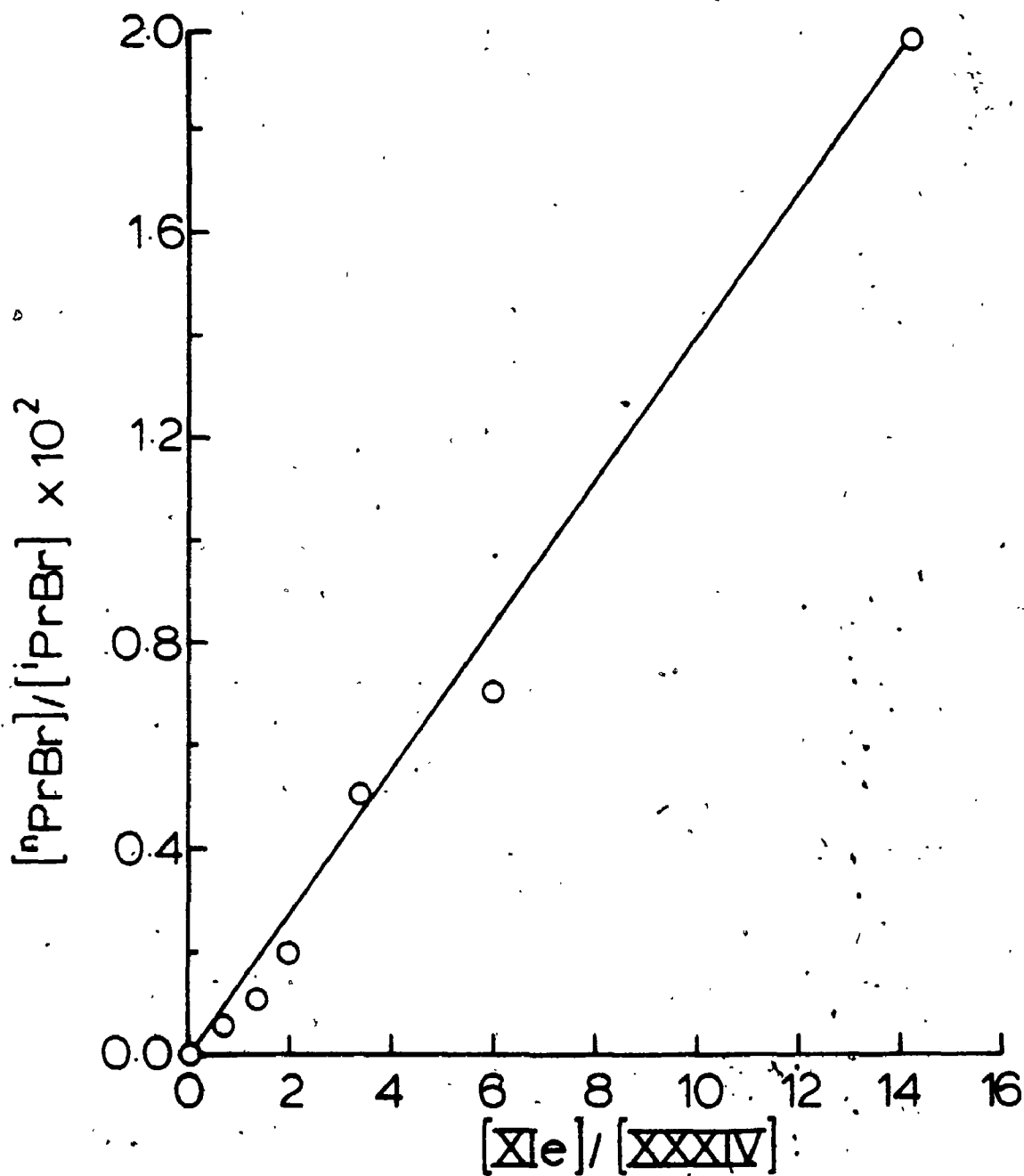


FIGURE 5.12: Plot of Relative Concentrations of $^{119}\text{PrBr}$ and $^{117}\text{PrBr}$ Versus the Relative Concentration of Products in the Reaction of Mixtures of $^{119}\text{PrBr}/^{117}\text{PrBr}$ with (II).

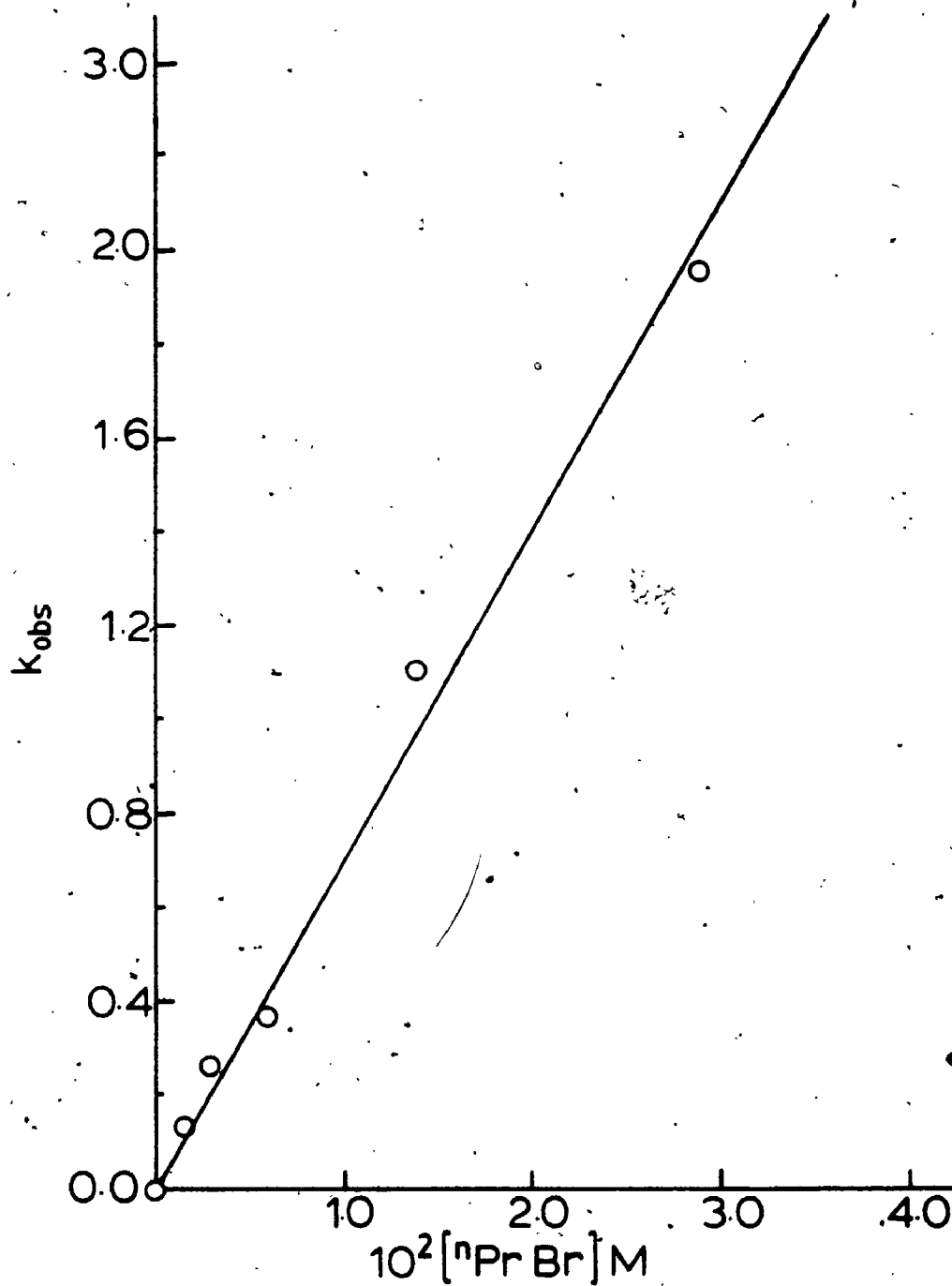


FIGURE 5.13: Plot of the Pseudo-First-Order Rate Constants (k_{obs}) Versus Concentration of $^n\text{PrBr}$ for the Reaction of Mixtures of $^n\text{PrBr}/^i\text{PrBr}$ with (II) at 25°C.

(k_n) with (II) can be calculated. This is illustrated in equations 14 and 15:

$$\frac{k_n [{}^n\text{PrBr}]}{k_i [{}^i\text{PrBr}]} = \frac{[\text{XIe}]}{(\text{XXXIV})} \quad \dots(14)$$

$$\frac{k_i}{k_n} = \frac{[{}^n\text{PrBr}][\text{XXXIV}]}{[{}^i\text{PrBr}][\text{XIe}]} = \text{slope} \quad \dots(15)$$

From this, a value of 1.39×10^{-3} is obtained for k_i/k_n . A plot of $\log(A_t - A_\infty)$ versus time for a reaction of a standard mixture of n-propyl bromide and isopropyl bromide produces a straight line. From the slope of this line a value for the pseudo-first-order rate constant (k_{obs}) can be calculated. This rate constant (k_{obs}) is related to k_i and k_n as shown in equation 16.

$$k_{\text{obs}} = k_i [{}^i\text{PrBr}] + k_n [{}^n\text{PrBr}] \quad \dots(16)$$

For one such kinetic plot a value of $6.0 \times 10^{-6} \text{ S}^{-1}$ was obtained. Using this value the simultaneous equations 17 and 18 can be solved to find k_i and k_n .

$$6.0 \times 10^{-6} = 5.8 \times 10^{-1} (k_i) + 5.8 \times 10^{-3} (k_n) \quad \dots(17)$$

$$\frac{k_i}{k_n} = 1.39 \times 10^{-3} \quad \dots(18)$$

The solution of these equations gave the values $k_i = 12.6 \times 10^{-7} \text{ M}^{-1} \text{ S}^{-1}$, and $k_n = 9.1 \times 10^{-4} \text{ M}^{-1} \text{ S}^{-1}$. The significance of these values is discussed in the next section.

3.4 Conclusions

Although the detailed mechanism of the reaction of *tert*-butyl iodide with (II) is not understood, it is very probable that free-radicals are involved. The detection of 2-methylpropene and 2-methylpropane during the reaction, and the photoinitiated nature of the reaction, point to the intermediacy of free-radicals. An S_N2 mechanism is not expected for the bulky *tert*-butyl iodide. The formation of $[\text{PtIME}_2(\text{}^i\text{PrOO})(\text{phen})]$ and $[\text{PtIME}_2(\text{}^t\text{BuOO})(\text{phen})]$ in the reaction of isopropyl iodide and *tert*-butyl iodide, respectively, with (II) may be used as a criterion for a free-radical mechanism of oxidative addition. This criterion is useful because it can be used quantitatively, but it is limited to systems where the metal complexes are inert to oxygen and where alkylperoxometal derivatives are thermally stable or persist long enough in solution to be detected.

In Chapter 3 the oxidative addition of primary alkyl halides to (II) was discussed. No alkylperoxo-complex was formed in these reactions and this would appear to disprove the intermediacy of free alkyl radicals in this case. In addition, the reactivity series $\text{MeI} \gg \text{EtI} > \text{}^n\text{PrI} \gg \text{}^i\text{PrI}$ is not consistent with a free-radical mechanism for the *n*-alkyl iodides.

In the case of the reaction of isopropyl bromide with (II) the absence of the isopropylperoxoplatinum(IV) complex in the product and the failure to photoinitiate the reaction discounts the intermediacy of radicals in this reaction. It is therefore believed that the oxidative addition of isopropyl bromide to (II) proceeds *via* an S_N2 mechanism. Further support for this conclusion comes from the product analysis and kinetic data for the reaction of mixtures of isopropyl bromide and *n*-propyl bromide with (II).

The photoinitiated reaction of isopropyl iodide with (II) has been demonstrated both here and by co-workers⁴⁴ to be of a free-radical chain type. However, as pointed out earlier (Section 3.1.6), the thermal reaction of isopropyl iodide is not fully understood. The ratio of the second-order rate constants for the reaction of n-propyl iodide and n-propyl bromide with (II) is approximately 7×10^2 . The corresponding ratio for isopropyl iodide and isopropyl bromide is approximately 6×10^2 . This implies that, in the thermally initiated reaction, the isopropyl iodide is expected to react with (II) at least in part *via* an S_N2 mechanism. This problem will be discussed in more detail at the end of the next chapter.

REFERENCES

1. Jones, R.D.; Summerville, D.A.; Basolo, F.; Chem. Rev., 1979, 79, 139.
2. Vaska, L.; Acc. Chem. Res., 1976, 9, 175.
3. Sheldon, R.A.; Aspects Homogeneous Catal., 1981, 4, 3.
4. Martell, A.E.; Pure Appl. Chem., 1983, 55, 125.
5. Mimoun, H.; Angew. Chem. Int. Ed. Engl., 1982, 21, 734.
6. Mimoun, H.; J. Mol. Catal., 1980, 7, 1.
7. Milas, N.; Sussman, S.; J. Am. Chem. Soc., 1936, 58, 1302.
8. Milas, N.; J. Am. Chem. Soc., 1937, 59, 2342.
9. Mimoun, H.; Sérée de Roch, I.; Sajus, L.; Bull. Soc. Chem. France, 1969, 1481.
10. Sharpless, K.B.; Townsend, J.B.; Williams, D.R.; J. Am. Chem. Soc., 1972, 94, 295.
11. Ugo, R.; Conti, F.; Cenini, S.; Mason, R.; Robertson, G.; J. Chem. Soc. Chem. Comm., 1968, 1498.
12. Sheldon, R.A.; Van Doorn, J.A.; J. Organomet. Chem., 1975, 94, 115.
13. Dudley, C.; Read, G.; Tetrahedron Lett., 1972, 5273.
14. Mimoun, H.; Perez-Machirant, M.M.; Sérée de Roch, I.; J. Am. Chem. Soc., 1978, 100, 5437.
15. Igersheim, F.; Mimoun, H.; Nouv. J. Chim., 1980, 4, 711.
16. Hawkins, E.G.E.; J. Chem. Soc., 1950, 2169.
17. Kollar, J.; U.S. Pat., 3350422 and 3351635 (1967).
18. Cook, C.D.; Jauhal, G.S.; Inorg. Nucl. Chem. Letters, 1967, 3, 31.
19. Tokahashi, K.; Sonogashira, K.; Hagihara, N.; J. Chem. Soc. Jap., 1966, 87, 610.

20. Kashiwagi, T.; Yasuoka, N.; Kasai, N.; Kakudo, M.; Takahashi, S.; Hagihari, N.; *J. Chem. Soc. Chem. Comm.*, 1969, 743.
21. Chen, M.J.Y.; Kochi, J.; *J. Chem. Soc. Chem. Comm.*, 1977, 204.
22. Bhaduri, S.; Raithby, P.R.; Zuccaro, C.; Hursthouse, M.R.; Casella, L.; Ugo, R.; *J. Chem. Soc. Chem. Comm.*, 1978, 991.
23. Bhaduri, S.; Casella, L.; Ugo, R.; Raithby, R.; Zuccaro, C.; Hursthouse, M.B.; *J. Chem. Soc. Dalton Trans.*, 1979, 1624.
24. Read, G.; Urgelles, M.; Galas, A.M.R.; Hursthouse, M.B.; *J. Chem. Soc. Dalton Trans.*, 1983, 911.
25. Michelin, R.A.; Ros, R.; Strukul, G.; *Inorg. Chim. Acta*, 1979, 37, L491.
26. Strukul, G.; Ros, R.; Michelin, R.A.; *Inorg. Chem.*, 1982, 21, 495.
27. Strukul, G.; Michelin, R.A.; Orbell, J.D.; Randaccio, L.; *Inorg. Chem.*, 1983, 22, 3706.
28. Mimoun, H.; Charpentier, R.; Mitschler, A.; Fischer, J.; Weiss, R.; *J. Am. Chem. Soc.*, 1980, 102, 1047.
29. Both, B.L.; Haszeldine, R.N.; Neuss, G.R.H.; *J. Chem. Soc. Chem. Comm.*, 1972, 1074.
30. Booth, B.L.; Haszeldine, R.N.; Neuss, G.R.H.; *J. Chem. Soc. Dalton Trans.*, 1982, 37.
31. Chiaroni, A.; Pascard-Billy, C.; *Bull. Soc. Chim. Fr.*, 1973, 781.
32. Duong, K.N.V.; Fontaine, C.; Giannotti, C.; Gaudemer, A.; *Tetrahedron Lett.*, 1971, 17, 1187.
33. Fontaine, C.; Duong, K.N.V.; Merienne, C.; Gaudemer, A.; Giannotti, C.; *J. Organomet. Chem.*, 1972, 38, 167.
34. Giannotti, C.; Fontaine, C.; Septe, B.; *J. Organomet. Chem.*, 1974, 71, 107.

35. Giannotti, C.; Fontaine, C.; Chiaroni, A.; Riche, C.; *J. Organomet. Chem.*, 1976, 113, 57.
36. Clark, H.C.; Ferguson, G.; Jain, V.K.; Parvez, M.; *Organometallics*, 1983, 2, 806.
37. Cook, P.M.; Dahl, L.F.; Hopgood, D.; Jenkins, R.A.; *J. Chem. Soc. Dalton Trans.*, 1973, 294.
38. Buse, K.; Keller, H.; Pritzkow, H.; *Inorg. Chem.*, 1977, 16, 1072.
39. Pauling, L.; "The Nature of the Chemical Bond". 1960, 3rd ed. Ithaca: Cornell University Press.
40. Swallow, A.G.; Truter, M.R.; *Proc. Roy. Soc.*, 1960, A, 254, 205.
41. Robson, A.; Truter, M.R., *J. Chem. Soc.*, 1965, 630.
42. Hall, T.L.; Lappert, M.F.; Lednor, P.W.; *J. Chem. Soc. Dalton Trans.*, 1980, 1448.
43. Labinger, J. A.; Osborn, J.A.; Coville, N.J.; *Inorg. Chem.*, 1980, 19, 3236.
44. Hill, R.; Ph.D. Thesis: University of Western Ontario. 1984.
45. Chanon, M.; *Bull. Soc. Chim. France*, 1982, 7-8, 197.
46. Ingold, K.U.; *Acc. Chem. Res.*, 1969, 2, 1.
47. Maillard, B.; Ingold, K.U.; Scaiano, J.C.; *J. Am. Chem. Soc.*, 1983, 105, 5095.

CHAPTER 6

RADICAL TRAPPING BY ALKENES AS A ROUTE TO ORGANOPLATINUM(IV) COMPLEXES AND AS A TEST OF THE MECHANISM OF OXIDATIVE ADDITION

1. INTRODUCTION

The previous chapter dealt with the trapping of isopropyl and *tert*-butyl radicals by dioxygen, with subsequent formation of alkylperoxo-platinum(IV) complexes. The trapping of alkyl radicals by alkenes during oxidative addition has been used as a mechanistic test in several instances, but the method has not been used quantitatively nor has it yielded useful organometallic products.¹⁻⁴ This chapter reports results which show the potential of trapping alkyl radicals by α,β -unsaturated olefins for both synthetic and mechanistic applications.

The work will be divided into the results using isopropyl iodide and those using *tert*-butyl iodide.

2. RESULTS FOR THE REACTION OF ^iPrI WITH (II) IN THE PRESENCE OF α,β -UNSATURATED OLEFINS

Unless otherwise stated, all the reactions in this chapter were performed using distilled alkenes, in diffuse daylight and in deoxygenated solvent. Experimental details are given in Section 2.6.1 of Chapter 7. In the reaction between isopropyl iodide and $[\text{PtMe}_2(\text{phen})]$ (II), in acetone, and in the presence of excess of α,β -unsaturated alkenes, new products were formed in high yield according to equation 1.

In this case the radical is trapped by boron as the oxygen-centred resonance form to give an enolate derivative. The spectroscopic data for complexes (XXXV) leave no doubt that the softer platinum centre traps the carbon-centred radicals to form the α -substituted alkylplatinum(IV) derivatives.

2.2 Characterisation of Complexes (XXXV)

The elemental analysis presented in Table 7.18 of Chapter 7 is consistent with the general formula $[\text{Pt}(\text{Me})_2\{\text{CH}(\text{X})\text{CH}_2^*\text{Pr}\}(\text{phen})]$ for complexes (XXXV). The high field region of the ^1H nmr spectrum of (XXXVa) is shown in Figure 6.1, with the Newman Projection of the molecule viewed along the $(\text{CN})\text{C}-\text{CH}_2$ bond. The carbon atom marked with an asterisk is asymmetric. As a result of this the MePt groups are nonequivalent. They are diastereotopic as are the protons H_β and H_γ . Singlets due to the protons of the two MePt groups occur at 1.70 ppm and 1.78 ppm.

The signal due to H_α appears as a doublet of doublets centred at 2.26 ppm with a $^2J_{\text{PtH}}$ value of 92 Hz. The vicinal coupling $^3J_{\text{H}\alpha\beta}$ should be greater⁸ than the vicinal coupling $^3J_{\text{H}\alpha\gamma}$ and this is indeed the case (13 Hz and 4 Hz respectively). These values were used to assign the signals for H_β (0.08 ppm) and H_γ (0.65 ppm). The methyl groups of the isopropyl moiety are also diastereotopic. Each methyl group appears as a doublet, one at 0.40 ppm, the other at 0.70 ppm. The signal due to proton H_C is assigned to the unresolved signal at 1.43 ppm. The $^{13}\text{C}\{^1\text{H}\}$ nmr spectrum of complex (XXXVa) is shown in Figure 6.2. The signals due to the nonequivalent PtCH₃ groups are seen at high field. The rest of the assignments are marked on Figure 6.2. These assignments were confirmed by a 2-D heteronuclear $^1\text{H}-^{13}\text{C}$ chemical shift correlated experiment. The result of this experiment is shown in Figure 6.3 and confirms the assignments discussed above.

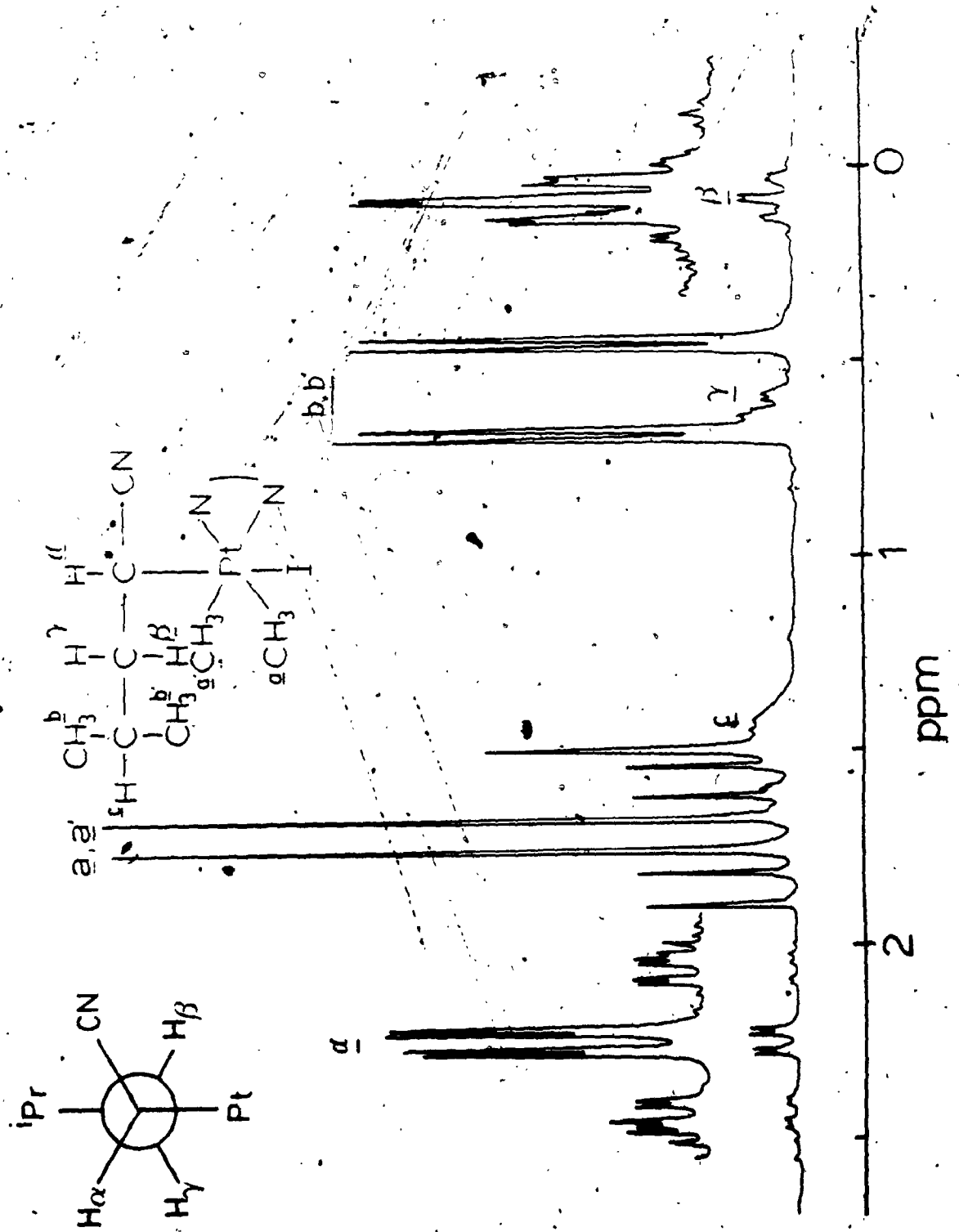


FIGURE 6.1: The ¹H NMR Spectrum (400 MHz) of [PtIme₂(CHCNCH₂¹Pr)(phen)].

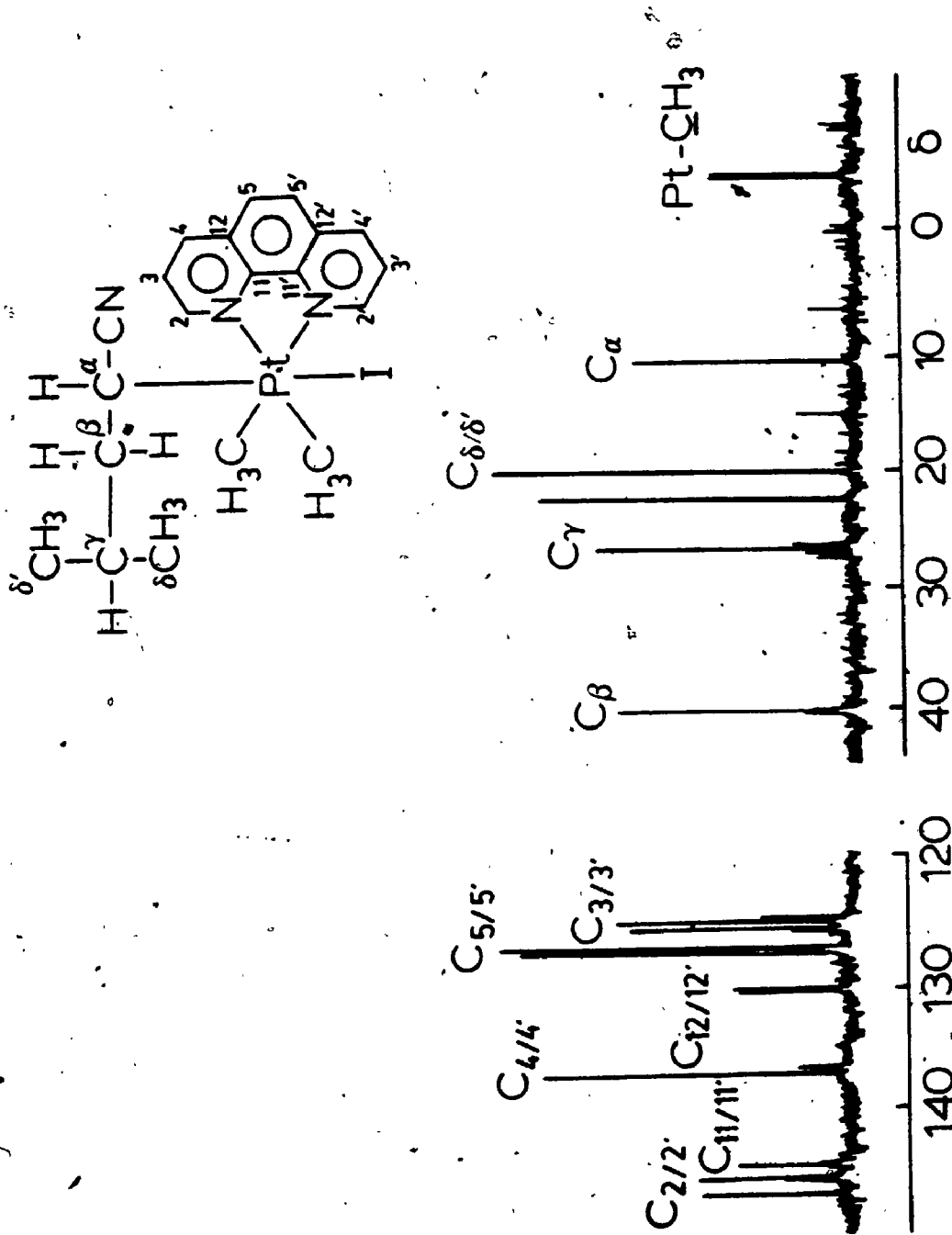


FIGURE 6.2: $^{13}C\{^1H\}$ NMR Spectrum (50 MHz) of $[PtIme_2(CHCNCH_2^1Pr)(phen)]$. Solvent CD₂Cl₂.

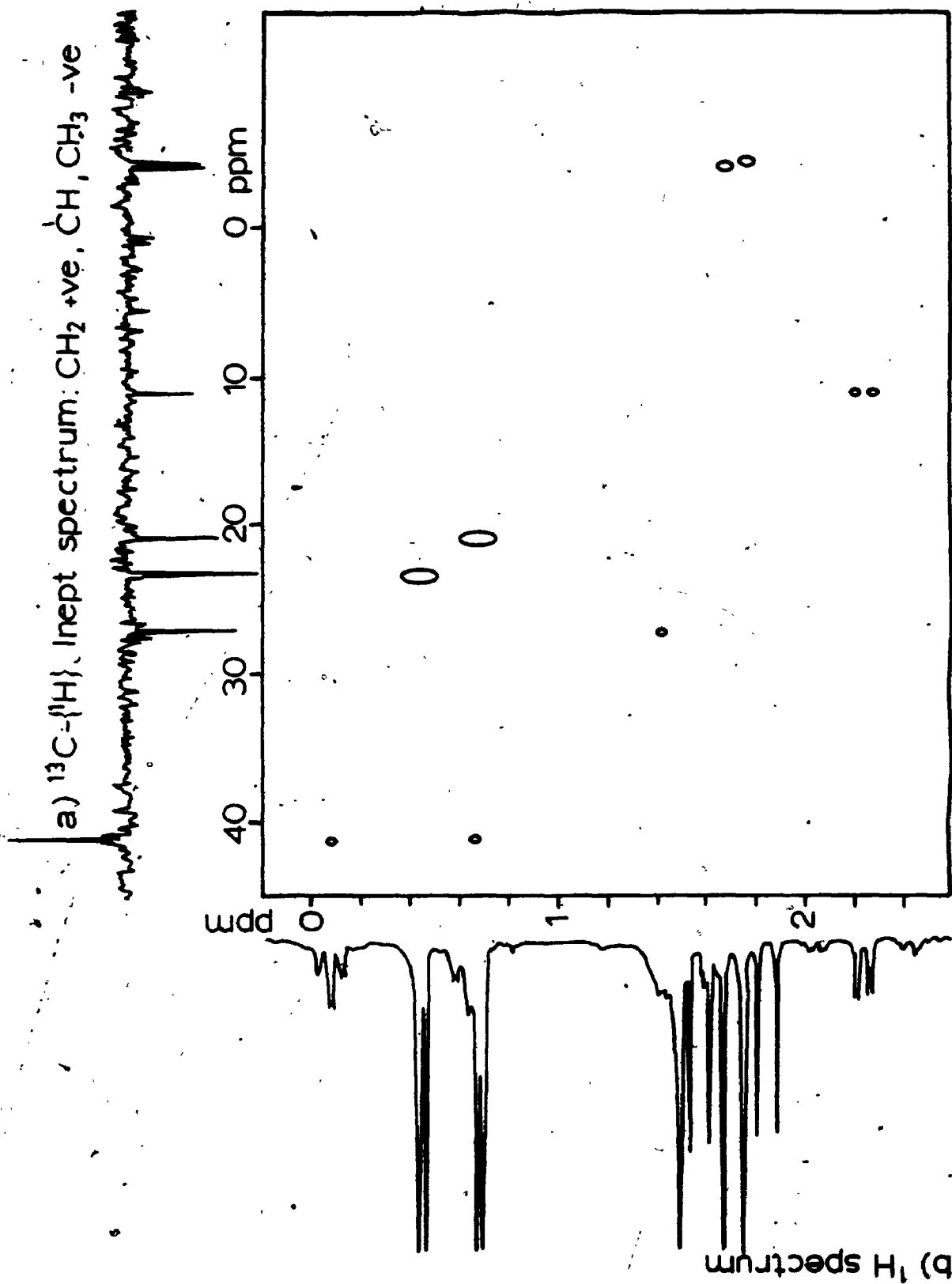


FIGURE 6.3: 2-D Heteronuclear $^1\text{H}\text{-}^{13}\text{C}$ Chemical Shift Correlated NMR of $[\text{Pt}(\text{Me})_2(\text{CHCNCH}_2^i\text{Pr})(\text{phen})]$.

The ^1H nmr spectra of complexes (XXXVb) and (XXXVc) contain the same basic characteristics as that for (XXXVa) and the data are presented in Table 7.13 of Chapter 7. The $^{13}\text{C}\{^1\text{H}\}$ nmr spectra of these complexes were also obtained (Table 7.14 of Chapter 7) and, to confirm the assignments of Table 7.14, the INEPT experiment was performed for each of them. In this way complexes (XXXV) were unambiguously characterised.

The presence of the group X in complexes (XXXV) was further confirmed from their infra-red spectra [(XXXVa) $\nu_{\text{C}\equiv\text{N}}$, 2200 cm^{-1} ; (XXXVb) $\nu_{\text{C}=\text{O}}$, 1650 cm^{-1} ; (XXXVc) $\nu_{\text{C}=\text{O}}$, 1665 cm^{-1}].

2.3 Kinetic Studies for the Reaction of $i\text{-PrI}$ with (II) in the Presence of Acrylonitrile

i) The Effect of Radical Scavengers

The reaction of isopropyl iodide with (II) in the presence of the α,β -unsaturated olefins is believed to proceed *via* a free-radical chain mechanism. If this is so the reaction should be inhibited by radical scavengers. The reaction was performed, in diffuse daylight, in the presence of the radical scavenger 4-methoxyphenol and in the absence of the scavenger. The reagent concentrations used were identical for both experiments. The reaction was followed by monitoring the decay of the MLCT band at 473 nm, due to (II), as the reaction progressed. The results are shown in Figure 6.4. It is evident that the radical scavenger inhibits the reaction. Similar experiments with galvinoxyl did not give reproducible results. These results, and those for the photo-initiated reaction of isopropyl iodide with (II)⁹ only, indicate that the reaction under discussion does proceed *via* a free-radical chain mechanism.

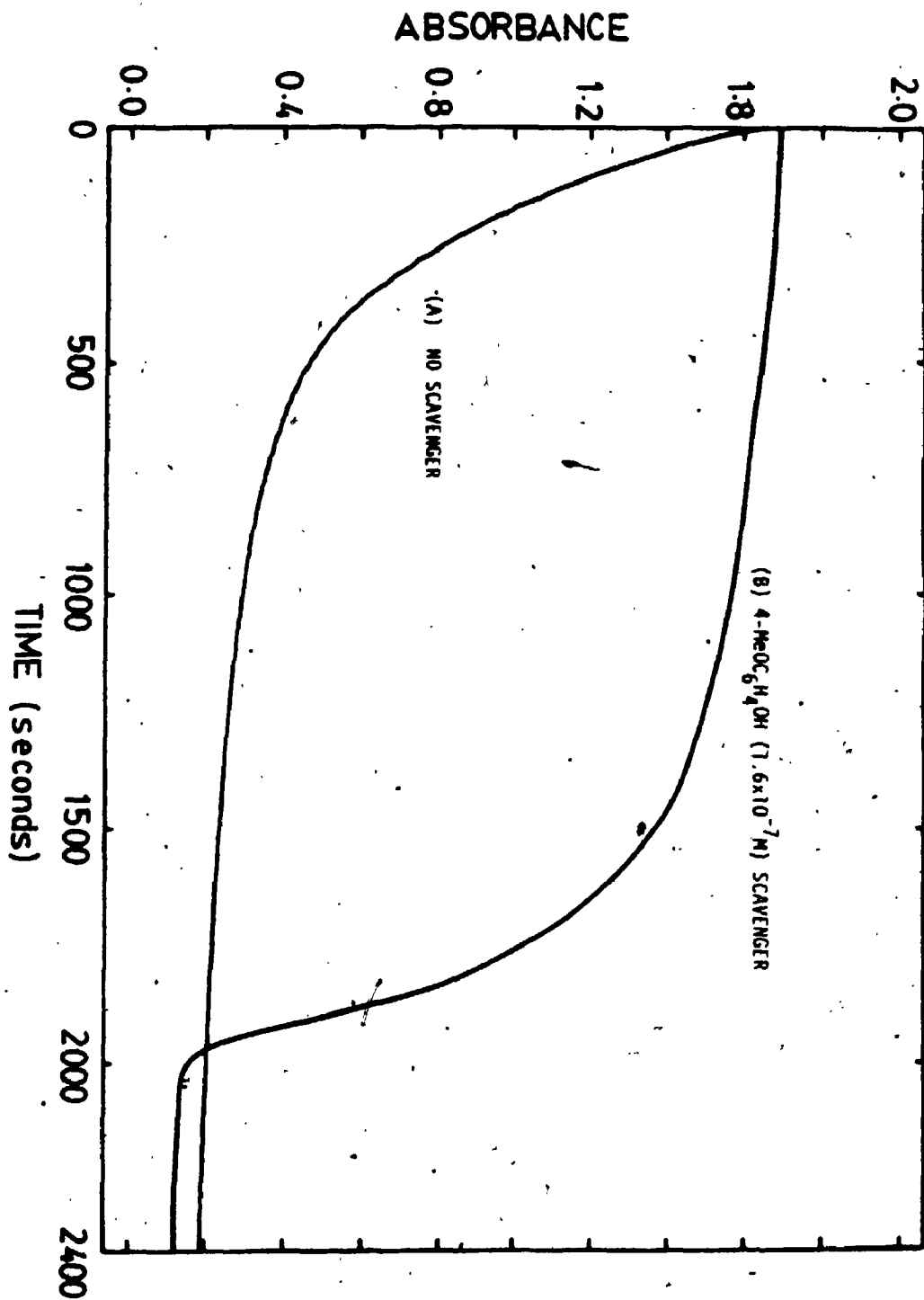


FIGURE 6.4: Plot of Absorbance Versus Time (λ , 473 nm) for the Reaction of (II) with ^tPrI and CH₂CHCN in Acetone at 21°C.

ii) Kinetic Studies Performed in the Dark for the Reaction of ^1PrI with (II) in the Presence of Acrylonitrile

The thermal reaction of isopropyl iodide with (II), in the presence of acrylonitrile, was investigated by following the reaction in the dark. This was achieved by monitoring the decay of the MLCT band at 473 nm, due to (II), as the reaction progressed. Several runs were performed, keeping the concentration of isopropyl iodide and (II) constant, whilst varying the concentration of acrylonitrile. The absorbance (A_t) was measured at regular intervals and a plot of $\log(A_t - A_\infty)$ versus time was made for each concentration of acrylonitrile. The result for one such plot is shown in Figure 6.5. The plot is not linear but the slope was calculated using the linear portion of the graph. If the rate determining step of the reaction involves only (II) and isopropyl iodide, and is independent of the alkene concentration, the plots of $\log(A_t - A_\infty)$ versus time (as in Figure 6.5) should have the same slope. This was found to be the case and a pseudo-first-order rate constant (k_{obs}) was calculated. Knowing k_{obs} , and the concentration of isopropyl iodide, an average overall second-order rate constant of $3.1 \times 10^4 \text{ M}^{-1} \text{ S}^{-1}$ was calculated. This value agrees well with the overall rate constant determined for the reaction of isopropyl iodide with (II) in the dark (see Section 3.1.4(ii) of Chapter 5).

2.4 Product Ratio, (XXXVa) to (XXX), in the Reaction of ^1PrI and (II) in the Presence of Varying Concentrations of Acrylonitrile

The photoinitiated reaction of isopropyl iodide with (II) in the presence of α,β -unsaturated olefins, is believed to occur largely by a free-radical chain mechanism. Scheme 1 shows this mechanism for acrylonitrile.

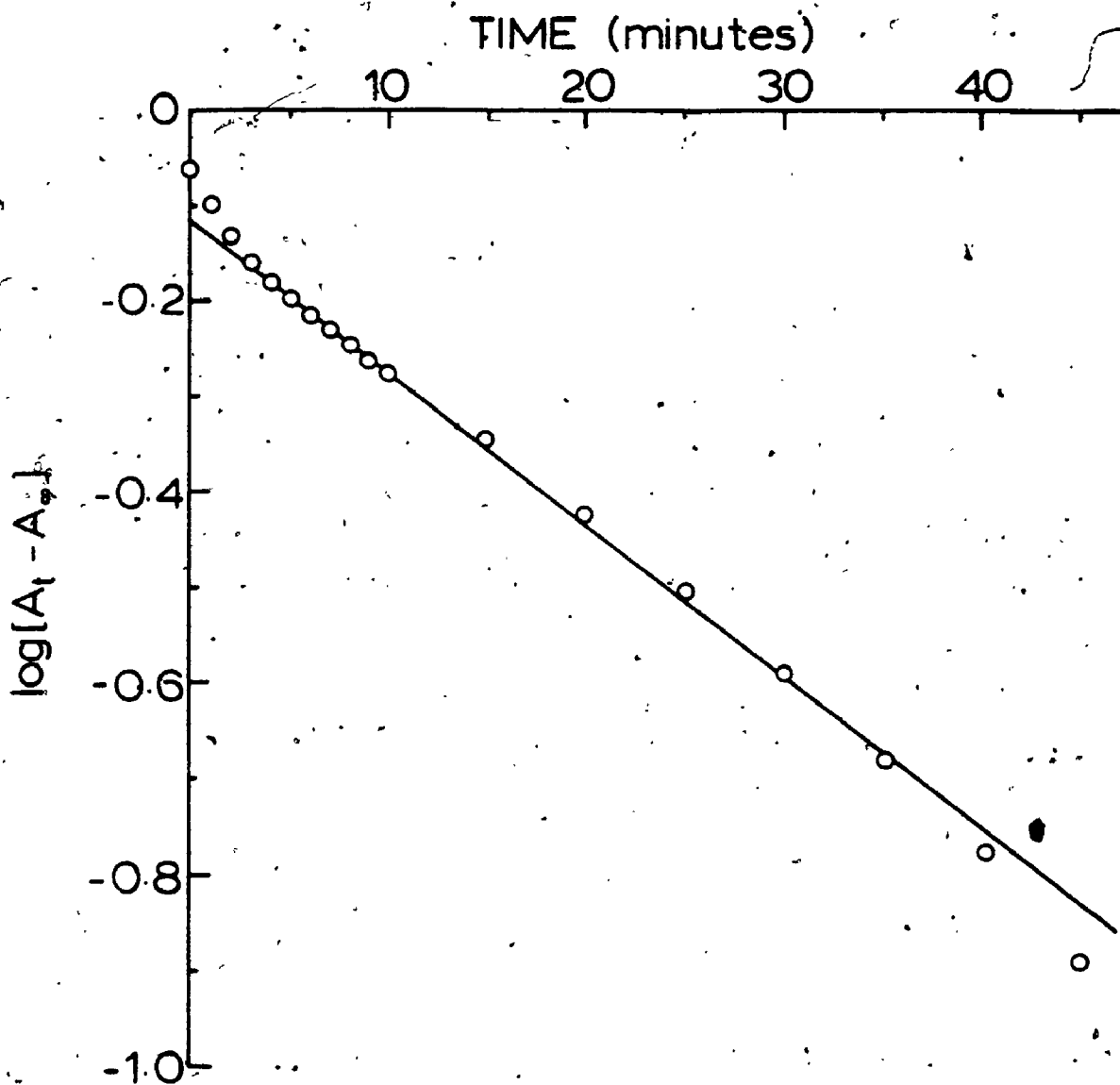
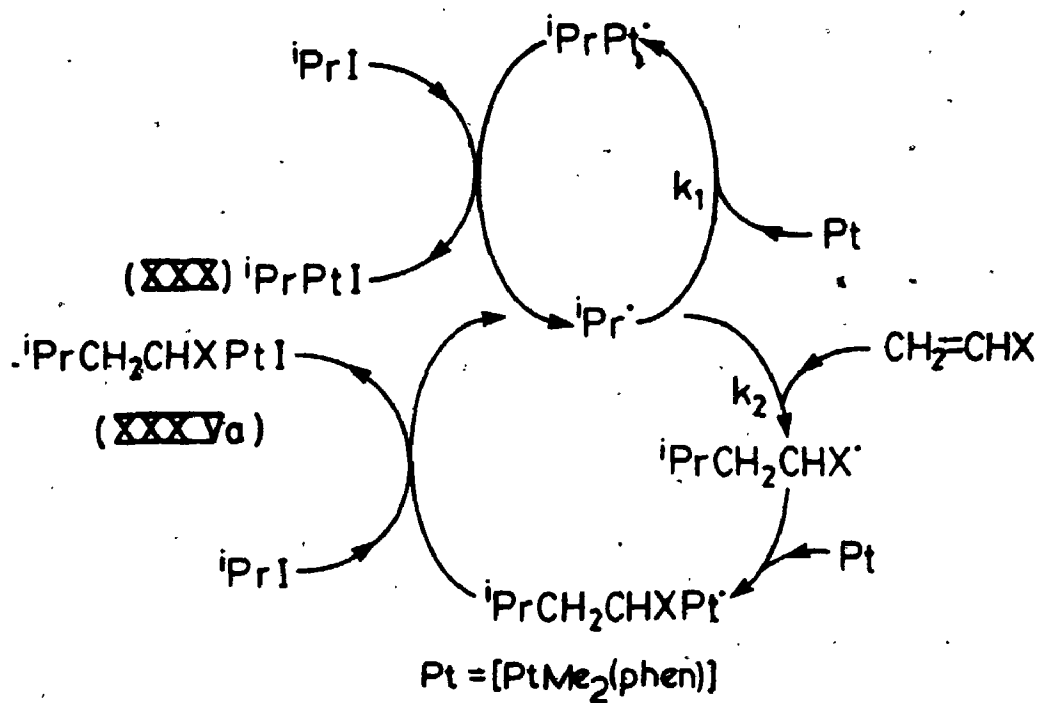


FIGURE 6.5: A Plot of $\text{Log } (A_t - A_\infty)$ Versus Time for the Reaction of $(\text{II})^t$ (5.0×10^{-4} M) with $i\text{PrI}$ (2.0 M) and CHCNCH_2 (1.0 M) in Acetone at 25°C .



Scheme 1

Mechanism of the reaction $\text{PtMe}_2(\text{phen}) + \text{iPrI} + \text{CH}_2=\text{CHCN}$

The scheme indicates that $[\text{PtMe}_2(\text{phen})]$ and $\text{CH}_2 = \text{CHCN}$ compete for the isopropyl radicals, and thus the product ratio $(\text{XXX})/(\text{XXXVa})$ can be equated to $k_1[\text{PtMe}_2(\text{phen})]/k_2[\text{CH}_2 = \text{CHCN}]$. To confirm this, a series of experiments was performed (in diffuse daylight) in which the concentration of isopropyl iodide was kept constant, whilst varying the relative concentrations of (II) and acrylonitrile. The relative amounts of (XXX) and (XXXVa) were determined by calculating the relative intensities of the high field doublets in the ^1H nmr spectrum of the product due to the isopropyl groups of (XXX) and (XXXVa) respectively. The results of this work are shown in Table 6.1. Decreasing the concentration of (II), or increasing that of acrylonitrile, should increase the molar percentage of (XXXVa) produced. This is borne out by the data in Table 6.1 ((i)-(ix)). One reaction was performed in the dark producing 100% complex (XXXVa). This will be discussed in the next section.

The rate constant¹⁰ for the radical addition, $\text{Et}\cdot + \text{CH}_2 = \text{CHCN}$, is equal to $2 \times 10^5 \text{ M}^{-1} \text{ S}^{-1}$. This figure was calculated for different experimental conditions to those used here, but it can be used as an estimate for the value k_2 in Scheme 1. Thus from the relative concentrations of (II) and CH_2CHCN , and the product ratios for the reaction (Table 6.1), a mean value of $k_1/k_2 \approx 20 \pm 10$ was calculated. It follows therefore that $k_1 \approx 4 \times 10^6 \text{ M}^{-1} \text{ S}^{-1}$. This value is in good agreement with that estimated by a co-worker⁹ using a completely different method. This appears to be the first estimate of a rate constant for attack of a radical at a diamagnetic transition-metal centre, and shows that such additions can be very rapid. Similar rate constants have been determined for $\text{S}_{\text{H}}2$ reactions of main-group metal

TABLE 6.1: Products Formed from the Reaction of (II) with ^1PrI (0.4 M) and $\text{CH}_2 = \text{CHCN}$ in Acetone at 20°C

	10 ($\text{PtMe}_2(\text{phen})$), M	$[\text{CH}_2 = \text{CHCN}]$, M	Molar % of (XXX)
i)	4.2	0.12	29.4
ii)	3.2	0.12	20.8
iii)	2.1	0.12	17.5
iv)	4.2	0.40	11.6
v)	4.2	0.20	17.8
vi)	4.2	0.10	28.6
vii)	4.2	0.06	37.0
viii)	4.2	0.02	50.0
ix)	4.2	1.8	0
x)	4.2^{a}	1.7	0

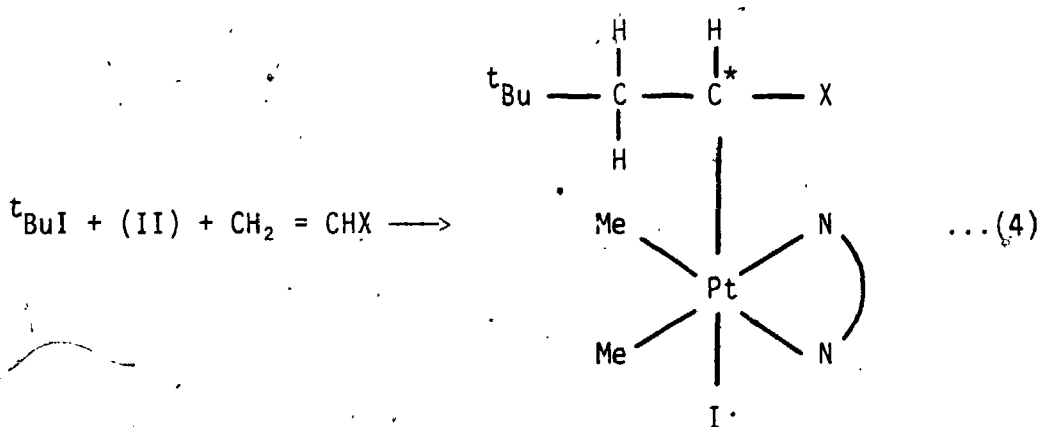
^aReaction performed in the dark.

alkyls, in which radical addition at the metal centre is probably rate determining.¹¹ In principle a similar experiment at high alkene concentration, measuring the relative yields of (XXXVa) and poly(alkene), could give the relative rate constants for attack of $[RCH_2CHX]^\cdot$ at platinum or alkene. Attempts were made, but reproducible results could not be obtained.

3. Results for the Reaction of $t\text{BuI}$ with (II) in the Presence of Alkene

3.1 Products from the Reaction

The reaction of *tert*-butyl iodide with (II) in the presence of alkene, was attempted under various conditions. For the reaction performed in deoxygenated methylene chloride and in the dark the major product was that shown in equation 4.



XXXVI a) $X = \text{C}(=\text{O})\text{H}$

b) $X = \text{CN}$

Small traces of the complex $[\text{PtI}_2\text{Me}_2(\text{phen})]$ (XVI) were observed. For the reaction performed in acetone and in diffuse light the amount of (XVI) increased relative to complexes (XXXVI).

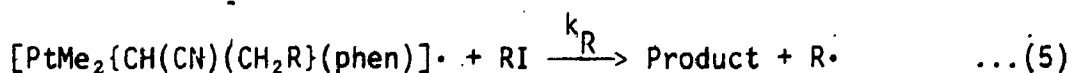
Complexes (XXXVI) were isolated as pale yellow solids, and the complexes are stable in methylene chloride solution.

3.2 Characterisation of Complexes (XXXVI)

Figure 6.6 shows the high field region of the ^1H nmr spectrum of complex (XXXVIb). The spectrum contains two equally intense singlets at 1.68 ppm and 1.76 ppm, each with ^{195}Pt satellites ($J_{\text{PtH}} = 71.5$ Hz). These are assigned to the protons of the two MePt groups. The methyl groups are diastereotopic, due to the presence of an asymmetric carbon in the molecule (marked with an asterisk in equation 4). The $^2J_{\text{PtMe}}$ value is consistent with a platinum(IV) complex. The very intense singlet at 0.67 ppm is obviously due to the protons of the *tert*-butyl moiety. Full ^1H nmr and ^{13}C nmr spectral data for complexes (XXXVI) are given in Tables 7.13 and 7.14 of Chapter 7. The ^{13}C nmr spectral assignments were confirmed by performing the INEPT experiment for these complexes.

3.3 Competition Reaction of ^tBuI and ^iPrI with (II) in the Presence of Acrylonitrile

In this competition experiment, complex (II) was treated with mixtures of isopropyl iodide and *tert*-butyl iodide, in the presence of high acrylonitrile concentration. The reaction was performed in diffuse light and under these conditions the reaction proceeds *via* a free-radical chain pathway. The product ratio (XXXVIb)/(XXXVa) is determined by the relative rates of the propagation step for ^tBuI and ^iPrI , involving the abstraction of iodine by the five-coordinate platinum(III) species $[\text{PtMe}_2\{\text{CH}(\text{CN})\text{CH}_2\text{R}\}(\text{phen})]^\cdot$ ($\text{R} = ^i\text{Pr}, ^t\text{Bu}$). This is shown below in equation 5.



The product ratio (XXXVIb)/(XXXVa), for these competition reactions, is therefore given by the expression shown below in equation 6.

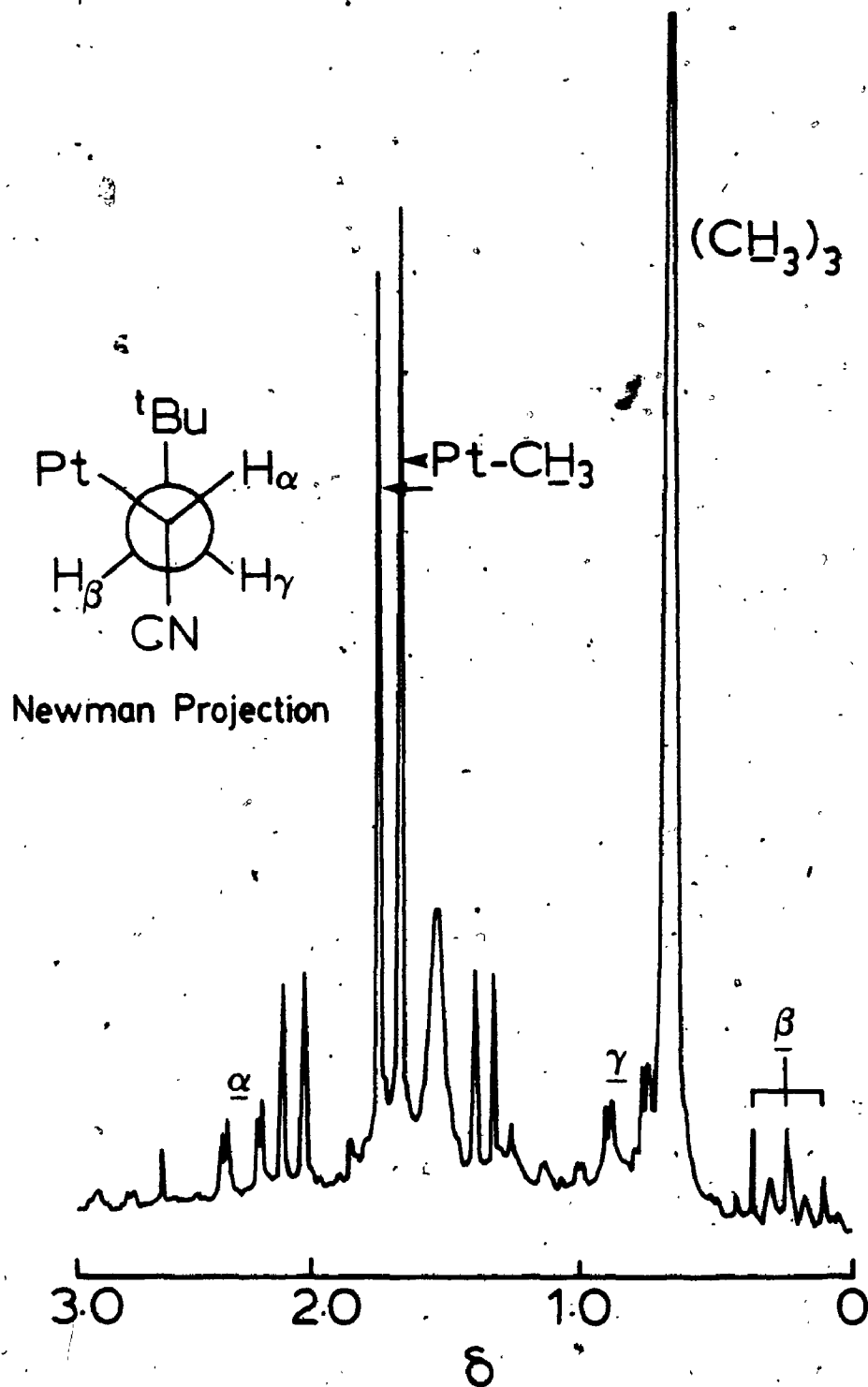


FIGURE 6.6: ^1H NMR Spectrum (100 MHz) of $[\text{PtIme}_2(\text{CHCNCH}_2^t\text{Bu})(\text{phen})]$ in CD_2Cl_2 .

$$\frac{k_t[\text{}^t\text{BuI}]}{k_i[\text{}^i\text{PrI}]} = \frac{[\text{XXXVib}]}{[\text{XXXVa}]} \quad \dots(6)$$

The selectivity for the formation of these two products is given by the relative rate constants k_t/k_i . The product ratio for these competition reactions was determined by measuring the intensity of the singlet due to the *t*-butyl methyl groups of (XXXVib) relative to the doublets due to the isopropyl methyl groups of (XXXVa), in the ^1H nmr spectra of the products. Two such spectra are shown in Figure 6.7. The mean value of k_t/k_i is 1.7 ± 0.2 . Thus abstraction from the *tert*-butyl iodide is faster, as expected from the weaker C-I bond, but the selectivity is low. For example, bromine abstraction by metal radicals gives $k(\text{}^t\text{BuBr})/k(\text{}^i\text{PrBr})$ in the range 2-8 for the reactions¹²⁻¹⁴ of $\text{Bu}_3\text{Sn}\cdot$, Cr(II) , Ag(o) and $[\text{Co}(\text{CN})_5]^{3-}$.

4. GENERAL CONCLUSIONS FOR CHAPTERS 5 AND 6

It is clear that the series of reactions discussed in Chapters 5 and 6 are very closely related. The reaction of (II) with isopropyl iodide and *tert*-butyl iodide in the presence of alkene or dioxygen leads to novel organoplatinum(IV) complexes. The use of such radical trapping molecules as oxygen and α,β -unsaturated olefins serves as a good criterion for the intermediacy of free-radicals in these reactions, and yields novel quantitative data for the interaction of metal centres with radicals.

The data presented in this work clearly point to a free-radical reaction pathway for the photoinitiated reaction between (II) and isopropyl iodide and *tert*-butyl iodide. The formation of $[\text{PtI}_2\text{Me}_2(\text{phen})]$ in these reactions is believed to derive from a competing radical non-chain mechanism.

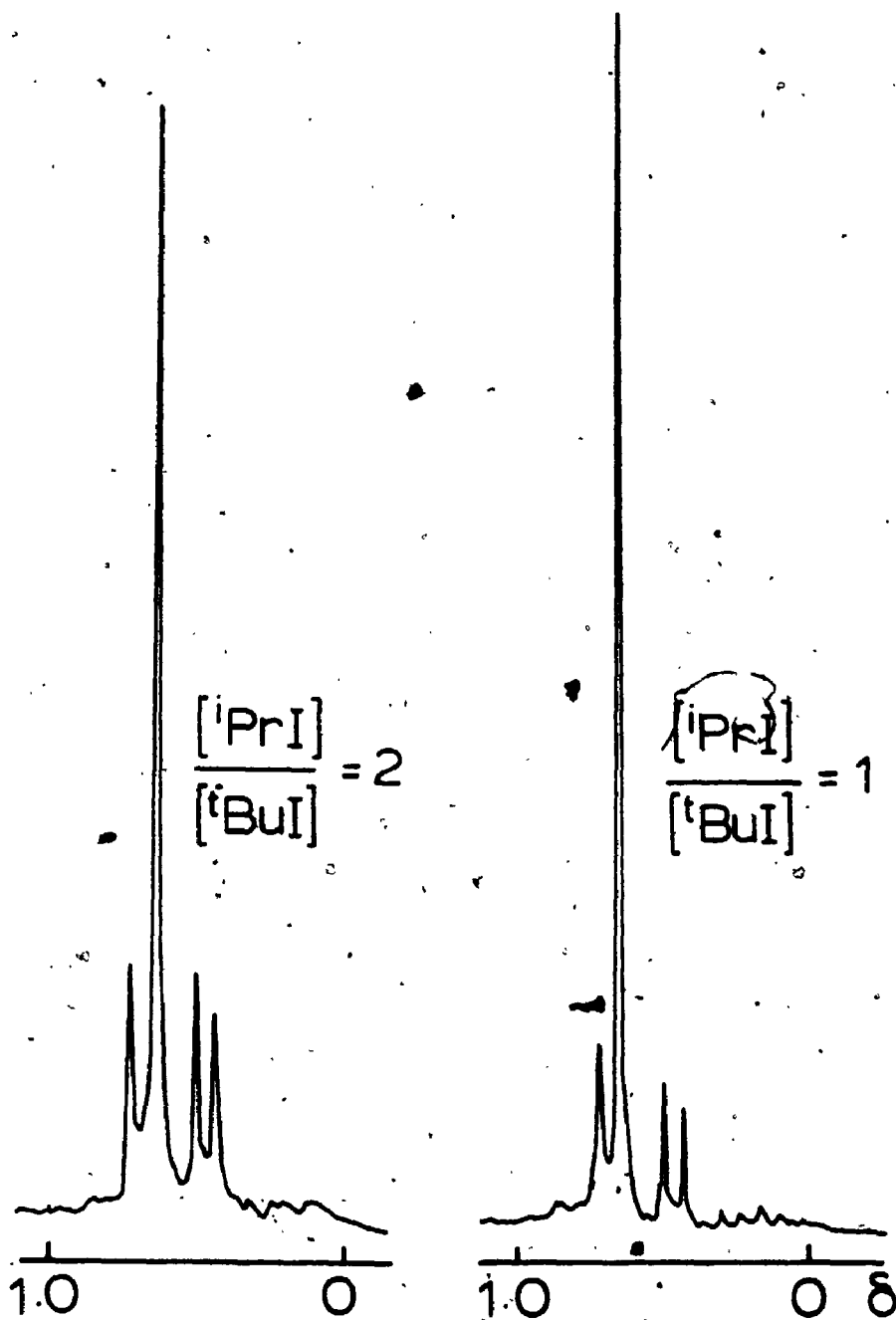
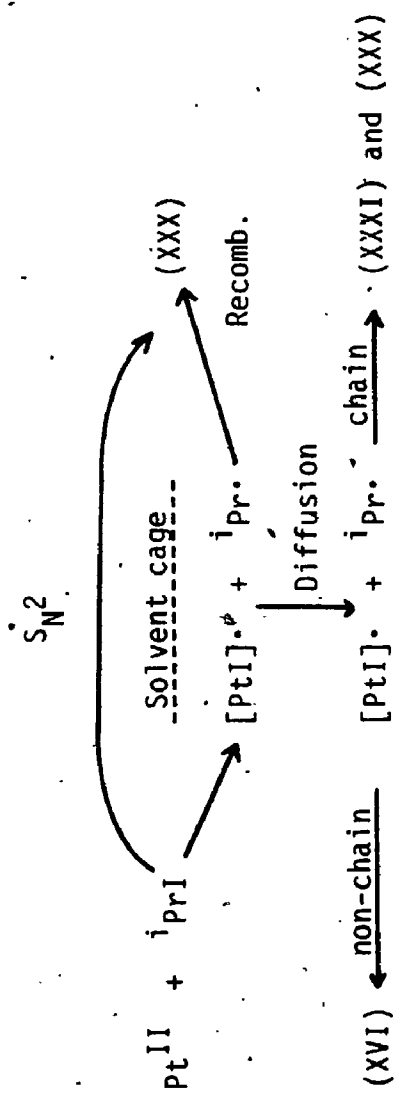


FIGURE 6.7: High Field Region of the ^1H NMR Spectrum (100 MHz) of the Products from the Reaction of (II) with Mixtures of $^i\text{PrI}/^t\text{BuI}$ and CHCNCH_2 :

The thermal reaction of isopropyl iodide with (II) is not fully understood. In Chapter 5 the relative rates, $k(^n\text{PrI})/k(^n\text{PrBr})$ and $k(^i\text{PrI})/k(^i\text{PrBr})$, for the reaction with (II), were found to be in close agreement (7×10^2 and 6×10^2 respectively). This implies that the thermal reaction between isopropyl iodide and (II) could proceed, at least in part, *via* an S_N2 mechanism. The product of such a mechanism would be $[\text{PtIME}_2(^i\text{Pr})(\text{phen})]$, (XXX). This view receives further support from the product analysis in Table 5.2 of Chapter 5. For the reaction performed in the dark (x), there is a significant increase in the amount of (XXX) relative to complexes (XXXI) and (XVI). It does seem reasonable that if the radical pathway is sufficiently retarded then the S_N2 pathway becomes significant. These competing pathways are summarised below in Scheme 2. A similar scheme has been proposed by Osborn.¹⁵ An alternative explanation is that in the thermally initiated reaction, the geminate radical-pair in the solvent cage, undergoes a greater degree of recombination (giving (XXX)), as opposed to diffusion out of the cage, than in the photoinitiated reaction. The photoinitiated radical-pair might be expected to be more energetic than those initiated thermally. Some of this excitation energy could be transformed into translational energy carrying the radicals out of the solvent cage. It should be noted, however, that conflicting data is presented in Table 6.1 of this chapter. In the reaction of ^iPrI with (II), in the presence of a large excess of acrylonitrile, and performed in the dark, the sole product was the radical trap complex (XXXVa). Clearly therefore, the whole reaction has proceeded *via* the free-radical chain mechanism. This may be rationalised in terms of a *very long* chain length for the production of (XXXVa) compared to a far smaller chain length for the formation of the isopropylperoxyplatinum(IV) complex. If this is the case, the S_N2 pathway would be



SCHEME 2

Competing Pathways for the Thermal Reaction of iPrI with (II)

expected to be far more competitive for the reaction in the presence of oxygen, compared to the reaction in the presence of alkene.

The reaction of CH_2I_2 or $\text{I}(\text{CH}_2)_2\text{I}$ with (II), in the presence of alkene, did not yield the radical trapped organoplatinum(IV) complexes, analogous to complexes (XXXV). These reactions are believed to involve free-radicals and, as such, the radical trapped product would be expected. The failure to isolate such products may be due to the instability of the radical $\text{RCH}_2\dot{\text{C}}\text{HX}$ ($\text{R} = \text{CH}_2\text{I}$ or $\text{I}(\text{CH}_2)_2$).

In conclusion, the oxidative addition of alkyl halides to transition-metal centres, in the presence of oxygen or α,β -unsaturated olefins, may yield interesting organometallic products and serve as a probe for the intermediacy of free-radicals in such reactions.

REFERENCES

1. Labinger, J.A.; Osborn, J.A.; Coville, N.J.; *Inorg. Chem.*, 1980, 19, 3236.
2. Lappert, M.F.; Lednor, P.W.; *Adv. Organomet. Chem.*, 1976, 14, 345.
3. Kwiatek, J.; Seyler, J.K.; *J. Organomet. Chem.*, 1965, 3, 421.
4. Halpern, J.; *Pure Appl. Chem.*; 1979, 51, 2171.
5. Eastmond, G.C.; "Comprehensive Chemical Kinetics"; Bamford, C.H.; Tipper, C.F.H.; Eds.; Elsevier: Amsterdam, 1976, Vol. 14a.
6. Kabalka, G.W.; Brown, H.C.; Suzuki, A.; Honma, S.; Arase, A.; Ioth, M.J.; *J. Am. Chem. Soc.*, 1970, 92, 710.
7. Brown, H.C.; Kabalka, G.W.; *J. Am. Chem. Soc.*, 1970, 92, 714.
8. Karplus, M.; *J. Am. Chem. Soc.*, 1963, 85, 2870.
9. Hill, R.; Ph.D. Thesis, 1984, University of Western Ontario.
10. Abell, P.I.; "Comprehensive Chemical Kinetics"; Bamford, C.H.; Tipper, C.F.H.; Eds.; Elsevier: Amsterdam, 1976, Vol. 18, Chap. 3.
11. Davies, A.G.; Roberts, B.P.; "Free Radicals"; Kochi, J.K.; Ed.; Wiley: New York, 1973, Chap. 10.
12. Kuivila, H.G.; *Adv. Organomet. Chem.*, 1964, 1, 47.
13. Tamund, M.; Kochi, J.K.; *J. Am. Chem. Soc.*, 1971, 93, 1483.
14. Halpern, J.; *Ann. N.Y. Acad. Sci.*, 1974, 239, 2.
15. Kramer, A.V.; Osborn, J.A.; *J. Am. Chem. Soc.*, 1974, 96, 7832.

CHAPTER 7
INSTRUMENTATION AND PREPARATIVE WORK

1. INSTRUMENTATION

1.1 Vacuum Line

The vacuum line used throughout this work worked at a pressure of approximately 10^{-3} torr. This was found to be quite sufficient for drying compounds, evaporating and degassing solvents and distilling the α, β -unsaturated olefins.

1.2 Reaction Vessels

All preparative work was done using Quickfit round bottom flasks. The use of grease was normally avoided. Work that was done under N_2 or O_2 was achieved by use of a two-necked round bottom flask with the gas bubbled through the solution using a glass frit. All preparative work was done at room temperature.

1.3 Photolysis

Any preparative work or kinetic experiments that required photolysis were performed using a Cole Parmer Low Noise Illuminator, Model 9741-50 (λ range 400-800 nm).

1.4 Nuclear Magnetic Resonance Spectroscopy

1H nmr spectra were recorded using a Varian XL-100 spectrometer at 100 MHz, and occasionally a Varian T60 operating at 60 MHz.

^{13}C nmr spectra were recorded using a Varian XL-200 spectrometer operating at 50 MHz. In each of the above cases, the chemical shifts, δ , in the deuterated solvents are quoted in ppm from external or internal TMS, using the solvent peak as reference.

The 2-D heteronuclear ^{13}C , ^1H chemical shift correlated experiment discussed in Chapter 5 was performed on a Bruker AM250 spectrometer. The spectra were obtained using a 5 mm $^1\text{H}/^{13}\text{C}$ dual probe.

1.5 Gas-Liquid Chromatography

A Varian Aerograph Series 1400 system was used. The three columns that were variously employed were Molecular Sieve 5A, Porapak Q, and 10% SE-30, each as 6' x 1/8" columns.

1.6 Mass Spectrometry

Mass spectra were recorded on a Varian Mat Bremen Mass Spectrometer Mat 311A, which has a mass range of 0-3000. This was also occasionally used in conjunction with the Gas-Chromatograph discussed above.

1.7 Infra-Red Spectroscopy

A Beckman 4250 instrument was used for all spectra discussed in this work.

Spectra of solid complexes were recorded as either nujol mulls on cesium iodide plates or in the form of cesium iodide pellets. The normal range scanned was 200-4000 cm^{-1} .

1.8 Ultra-violet and Visible Spectroscopy

All the kinetic studies discussed in this work were carried out by the use of UV/visible spectroscopy.

Spectra were recorded using either a Cary 118 spectrophotometer fitted with a thermostated cell compartment or a Hewlett Packard 8450A Diode Array Spectrophotometer. A pair of 1 cm quartz UV cells were used, one of which contained the sample solution, the other the solvent, to compensate for any solvent absorption. The wavelength range normally used was 600-300 nm.

1.9 Quantitative Analysis

The elements normally analysed were carbon, hydrogen and nitrogen. Occasionally analysis was obtained for halogens. This work was done by Guelph Chemical Laboratories, Ontario. The Canadian Microanalytical Service Ltd., Vancouver, was used for any oxygen analysis.

2. PREPARATIVE WORK

2.1 Preparation of General Compounds

The preparation of compounds used generally throughout this work are described in this section.

2.1.1 [PtCl₂(SMe₂)₂]

To distilled water (30 mL) in a round bottom flask (250 mL) was added K₂[PtCl₄] (0.5 g). Once the solid was dissolved dimethyl sulphide (2.5 mL) was added and a reflux condenser attached to the flask. The mixture was stirred for 2 hours during which time a pale

brown slurry forms. This was heated at 80°C for 1 hour. A bright yellow solution of $[\text{PtCl}_2(\text{SMe}_2)_2]$ formed. The solution was allowed to cool to room temperature and then CH_2Cl_2 (120 mL) was added to extract the $[\text{PtCl}_2(\text{SMe}_2)_2]$. The mixture was filtered and the CH_2Cl_2 layer recovered using a separatory funnel. A little anhydrous MgSO_4 was added to help dry the CH_2Cl_2 extract. This solution was again filtered and the solvent removed on the rotary evaporator. The yellow $[\text{PtCl}_2(\text{SMe}_2)_2]$ was now dried on the vacuum line. The complex was characterised by its ^1H nmr spectral parameters. Yield 90%.

2.1.2 $[\text{Pt}_2\text{Me}_4(\mu\text{-SMe}_2)_2]$

The apparatus for this synthesis consisted of a dry two-necked round bottom flask (250 mL) fitted with a dropping funnel and a nitrogen inlet. Methylolithium solution (12.0 mL, 1.3 M in ether) was added dropwise to a suspension of $[\text{PtCl}_2(\text{SMe}_2)_2]$ (0.51 g, mixture of the *cis* and *trans* isomer) prepared as described above. The reaction mixture was under an atmosphere of nitrogen and at 0°C, and was allowed to react for 1 hour, after which it was brought to room temperature. The mixture was then hydrolysed with saturated aqueous ammonium chloride solution (10 mL) and the resultant mixture filtered. The ether layer, containing the desired product was recovered by use of a separating funnel. To this extract was added anhydrous MgSO_4 to dry the sample. The solution was filtered and the ether solvent removed by use of a rotary evaporator. The off-white solid was further dried on the vacuum line. Yield 71%, mp 86°C decomp.

2.1.3 [PtMe₂(bipy)]

This synthesis was performed in a 100 mL round bottom flask. To a solution of [Pt₂Me₄(μ-SMe₂)₂] (0.46 g) in dry benzene (20 mL) was added 2,2'-bipyridine (0.56 g) in dry ether (15 mL). The solution turns an immediate red colour. On cooling to 5°C for 16 hours fine red crystals of the product are formed. The mixture was filtered and the [PtMe₂(bipy)] washed with ether. The solid was dried on the vacuum line. Yield 80%.

2.1.4 [PtMe₂(phen)]

This complex was prepared by the same method as used for [PtMe₂(bipy)]. In this case however 1,10-phenanthroline was added to the [Pt₂Me₄(μ-SMe₂)₂], and a little acetone was used to dissolve it due to its low solubility in ether. The desired product has a red-orange colour.

2.2 Preparative Work and Experimental Details for Reactions of Chapter 2

2.2.1 Preparative Work and Experimental Details for the Work With [PtMe₂bipy]

2.2.1.1 Drying Methanol and Ethanol

To methanol (70 mL under an atmosphere of nitrogen) was added dry magnesium turnings (50 g) and resublimed iodine (0.5 g). The mixture was warmed until hydrogen gas began to evolve, at which time more methanol (900 mL) was added. The mixture was refluxed for half an hour and eventually distilled under nitrogen.

2.2.1.2 [PtMe₂(OMe)(bipy)(OH₂)] [OH]

A sample of [PtMe₂(bipy)] (0.1 g) was placed in a dry round

bottom flask and dry methanol (30 mL) was added. The platinum complex did not readily dissolve but after about 6 hours a yellow solution was produced. The solution was first filtered and then the solvent removed on the rotary evaporator. An oily material was left which was dissolved in a small volume of CH_2Cl_2 (3 mL) and precipitated from this by adding pentane (15 mL). The precipitate was still rather oily in texture and the process of dissolving in CH_2Cl_2 followed by precipitation was repeated until an amorphous pale yellow-brown solid formed. This was dried on the vacuum line. Yield 73%, mp 160°C decomp.

2.2.1.3 $[\text{PtMe}_2(\text{OEt})(\text{bipy})(\text{OH}_2)][\text{OH}]\cdot\text{H}_2\text{O}$

The procedure used here was identical to that for the synthesis of $[\text{PtMe}_2(\text{OMe})(\text{bipy})(\text{OH}_2)][\text{OH}]$ as described above, but using dry ethanol as the solvent.

2.2.1.4 $[\text{PtMe}_2(\text{OH})(\text{bipy})(\text{OH}_2)][\text{OH}]$

To a solution of $[\text{PtMe}_2(\text{bipy})]$ (0.03 g) in acetone (15 mL) was added distilled water (15 mL). The solution turned yellow over a period of several hours. The solvents were removed on the rotary evaporator at a temperature of 50°C . The oily residue was further dried on the vacuum line at about 50°C . The residue was dissolved in a little CH_2Cl_2 and then precipitated by addition of pentane (15 mL). The process of dissolving in CH_2Cl_2 and precipitation was repeated to give an amorphous light brown solid.

2.2.1.5 Reaction of D_2O with $[\text{PtMe}_2(\text{bipy})]$

A solution of $[\text{PtMe}_2(\text{bipy})]$ (0.05 g) in THF (18 mL, dried over CaH_2) was made up. To this was added D_2O (5 mL). The mixture was left for 3 hours after which it was worked up, as described above in the reaction of $[\text{PtMe}_2(\text{bipy})]$ with H_2O .

2.2.1.6 [PtMe₂(OMe)(bipy)(OH₂)] [PF₆]

A solution of [PtMe₂(bipy)] (0.10 g) in methanol (20 mL) was allowed to react for 5 hours. The volume was reduced to about 3 mL and a solution of [NH₄][PF₆] (0.09 g) in methanol (5 mL) was added. The product precipitated as a pale yellow solid. It was filtered off and dried under vacuum. Yield 53%, mp 180°C decomp.

2.2.1.7 [PtMe₂(OMe)(bipy)(OH₂)] [ClO₄] · 2H₂O

A solution of [PtMe₂(bipy)] (0.12 g) in methanol (20 mL) was allowed to react for 16 hours, after which the solvent volume was reduced to about 5 mL. To this was added a solution of 70% HClO₄ (0.1 mL) in methanol (2 mL). The resultant solution was evaporated on the rotary evaporator and then on the vacuum line. The residue was washed with ether several times. Yield 54%, mp 206°C decomp.

2.2.1.8 [PtMe₂(OMe)(bipy)(OH₂)] [BPh₄] · H₂O

A solution of [PtMe₂(bipy)] (0.06 g) in methanol (15 mL) was left to react for several hours, forming the characteristic yellow solution. The solvent volume was reduced to about 3 mL and to this was added a solution of Na[BPh₄] (0.05 g) in methanol (5 mL). The solvent was removed on the vacuum line leaving a yellow solid residue.

2.2.1.9 [PtMe₂(OH)(bipy)(OH₂)] [PF₆]

A solution of [PtMe₂(bipy)] (0.17 g) in acetone (25 mL) and water (25 mL) was allowed to react for 16 hours. The volume of solvent was reduced on the rotary evaporator to about 15 mL. A stoichiometric amount of [NH₄][PF₆] (0.07 g) in a minimum volume of water was added to precipitate the solid as a pale yellow solid. The sample was filtered and the solid dried on the vacuum line. Mp 195°C decomp.

2.2.1.10 Attempted Crystallisation

For each complex described in the above section extensive attempts were made to grow crystals of the products. No success was achieved.

The slow diffusion technique was tried, whereby a saturated solution of the complex was made up in CH_2Cl_2 or acetone and placed in a 10 cm length, 2 mm diameter glass tube. A solvent such as pentane or ether, in which the complex is insoluble, was carefully added onto the surface of the solution. By means of slow diffusion of the two layers it was hoped crystals would form.

An alternative technique was to make up saturated solutions of the complexes and allow slow evaporation of the solvent.

Finally saturated solutions of the complexes were made up. A solvent was then added in which the complex was insoluble, in sufficient volume to reach the threshold of precipitation. The solution was then cooled to -5°C . In all cases, oils or amorphous solids formed rather than simple crystals.

2.2.1.11 Detection of CH_4 by Gas Chromatography in the Reaction between $[\text{PtMe}_2(\text{bipy})]$ and MeOH

For this experiment the Varian Aerograph Series 1400 instrument was used along with a Porapak Q column. The injector was kept at 60°C the current at 125 mA and the detector at 100°C .

The instrument was first calibrated according to the following procedure. 2 mL of methanol were placed in the vessel shown in Fig. 7.1. This was degassed and evacuated on the vacuum line by three cycles of freeze-thawing. To this vessel, varying known volumes of CH_4 gas were introduced. For each known volume of gas in the vessel a 0.05 mL sample was removed by a gas tight syringe and injected into the chromatogram.

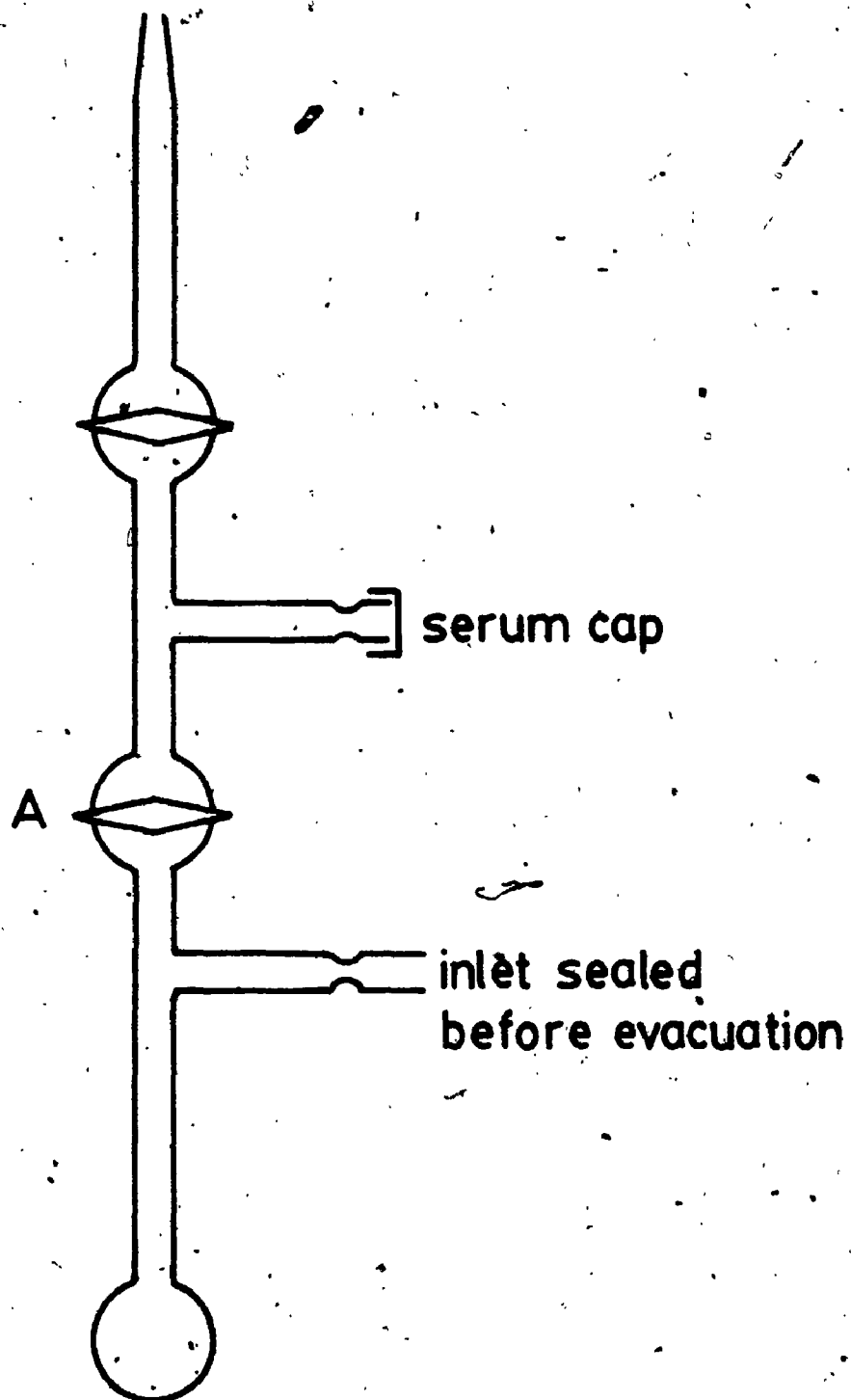


FIGURE 7.1: Apparatus for Collecting Gases for Gas Chromatography Analysis.

In this way the peak height on the chromatogram could be correlated to the volume of CH_4 in the reaction vessel.

The reaction was then carried out in the same reaction vessel using a solution of $[\text{PtMe}_2(\text{bipy})]$ (0.02 g) in methanol (2 mL). Under conditions of STP if the CH_4 were evolved quantitatively from the reaction mixture, a volume of close to 1 mL would be expected for this mass of complex. The identical procedure for degassing and evacuating was used here as in the calibration run. The solution was left to react for 1 day after which time a sample of the gas above this solution (0.05 mL) was injected into the chromatogram. Only trace amounts of CH_4 were detected. In order to allow for any chance of the CH_4 dissolving in the solvent a blank was run. Methanol (2 mL) was added to the clean reaction vessel and after degassing and evacuating a portion of CH_4 (1.0 mL) was introduced into the vessel. From the vessel a sample of gas (0.05 mL) was injected into the chromatogram. The vessel was then left for a day after which a further sample of the gas (0.05 mL) was injected into the chromatogram. There was little change from the initial peak height to that of 1 day later.

2.2.1.12 Detection of C_2H_6 by Gas Chromatography in the Reaction between $[\text{PtMe}_2(\text{bipy})]$ and EtOH

The same procedure as above was used. In this case again small traces of CH_4 were detected but no C_2H_6 .

2.2.1.13 Conductivity Measurements for Reaction between $[\text{PtMe}_2(\text{bipy})]$ and Methanol

A 0.001 M solution of $[\text{PtMe}_2(\text{bipy})]$ in methanol was made up and the conductivity of the solution was followed using an Industrial Instruments Conductivity Bridge, Model RC-18, to a limiting value of

$$\Lambda_M = 76.5 \text{ cm}^2 \Omega^{-1} \text{ mol}^{-1}$$

2.2.2 Preparative Work and Experimental Details for the Work with $[\text{PtMe}_2(\text{phen})]$

Much of the preparative details in this section are the same as those described above for the preparative work using $[\text{PtMe}_2(\text{bipy})]$ and so details given in this section will be more terse.

2.2.2.1 $[\text{PtMe}_2(\text{OMe})(\text{phen})(\text{OH}_2)][\text{OH}]$

To a dry round bottom flask (100 mL) containing $[\text{PtMe}_2(\text{phen})]$ (0.1 g) was added some dry methanol (30 mL). The sample was stirred for about 10 hours after which time a yellow solution had formed. The solvent was removed on the rotary evaporator and the oily residue dissolved in CH_2Cl_2 (3 mL). The product was precipitated out as a pale brown solid by the addition of pentane (20 mL). The solid was dried on the vacuum line. Yield 72%, mp 140°C decomp.

2.2.2.2 $[\text{PtMe}_2(\text{OEt})(\text{phen})(\text{OH}_2)][\text{OH}]\cdot\text{H}_2\text{O}$

The same procedure as above was used, using $[\text{PtMe}_2(\text{phen})]$ (0.1 g) and dry ethanol (30 mL). The isolation of the product was performed by the same technique as above.

2.2.2.3 $[\text{PtMe}_2(\text{O}^i\text{Pr})(\text{phen})(\text{OH}_2)][\text{OH}]$

A solution of $[\text{PtMe}_2(\text{phen})]$ (0.13 g) in an isopropanol/acetone mixture (70 mL, 2:1 by volume) was left to react for 3 days. The acetone was required to aid with the solubility of the $[\text{PtMe}_2(\text{phen})]$. The solution slowly turned yellow and the solvent was removed on the rotary evaporator. A brown solid remains which was dissolved in a little CH_2Cl_2 (3 mL) and precipitated by the addition of pentane (20 mL). The solid was dried on the vacuum line. Yield 74%, mp 70°C decomp.

2.2.2.4 Reaction of $t\text{BuOH}$ with $[\text{PtMe}_2(\text{phen})]$

To a mixture of acetone (30 mL) and tertiary butyl alcohol (25 mL) was added $[\text{PtMe}_2(\text{phen})]$ (0.1 g). The round bottom flask was

fitted with a reflux condenser and the solution heated, at 50°C, for 10 days. A yellow solution was produced along with signs of decomposition products. The solution was filtered and the solvent reduced in volume by heating at 50°C on the rotary evaporator and finally on the vacuum line. The oily residue was dissolved in a little CH₂Cl₂ and precipitated by addition of pentane (20 mL).

2.2.2.5 Reaction of PhCH₂OH with [PtMe₂(phen)]

A solution of [PtMe₂(phen)] (0.1 g) was made up in acetone (20 mL). To this solution was added benzyl alcohol (20 mL). The reaction mixture was left to react for 8 days. The solution was heated on the rotary evaporator, at 60°C, to reduce the volume and then on the vacuum line. An oily residue was left to which was added ether (20 mL). This produced some solid complex which was dried on the vacuum line.

2.2.2.6 [PtMe₂(OH)(phen)(OH₂)] [OH]

To a solution of [PtMe₂(phen)] (0.05 g) in acetone (20 mL) was added distilled water (15 mL). The mixture was allowed to stand for 5 hours, after which time the solvents were removed on the rotary evaporator at 70°C. An oily residue remained which was worked up with CH₂Cl₂ and pentane to produce a pale brown solid. Yield 80%, mp 130°C decomp.

2.2.2.7 [PtMe₂(OMe)Cl(phen)]

A solution of [PtMe₂(phen)] (0.08 g) in methanol (35 mL) was allowed to react for 10 hours. To this was added HCl in ether (0.32 mL, 0.63 M, a 1:1 mol. ratio). This was left to react for 20 minutes after which the solvent was removed under vacuum leaving an oily residue. As much as possible was dissolved in CH₂Cl₂ and precipitated with pentane (20 mL). The cream coloured solid was dried on the vacuum line.

2.2.2.8 Gas Chromatography on Gaseous Products of Reaction between MeOH and [PtMe₂(phen)]

A Varian Aerograph 1400 g.c. was used for this work. The injector was kept at 60°C. Methanol (3 mL) was introduced into the reaction vessel shown in Fig. 7.1 along with [PtMe₂(phen)] (0.02 g). The sample was degassed by three cycles of freezing and thawing and finally the vessel was evacuated. The reaction mixture was left to stand for 1 day. A sample of the gas above the solution was removed using a gas syringe and introduced into the chromatogram, fitted with a Porapak Q column. A small peak, with a retention time corresponding to methane, was observed.

A second sample of the gaseous product was injected into the instrument now fitted with a Molecular Sieve 5A column. The chromatogram showed a peak corresponding to hydrogen.

2.2.2.9 ²H nmr of Sample from Reaction between CH₃OD and [PtMe₂(phen)]

A small volume (5 mL) of fresh CH₃OD was placed in a dry round bottom flask (10 mL). To this was added [PtMe₂(phen)] (0.05 g) and the solution kept under an atmosphere of nitrogen. The solution turned yellow after 10 hours and the solvent was removed under vacuum leaving an oily residue. This was dissolved in dry CH₂Cl₂ (2 mL) and the solid precipitated by addition of dry benzene (15 mL). The solid was dried and dissolved in dry CH₂Cl₂ (0.04 g, dried over P₂O₅ and distilled on the vacuum line). The ²H nmr of the sample showed no signal other than that of the internal reference, CDCl₃.

2.2.2.10 Potentiometric Titration of [PtMe₂(OEt)(phen)-(OH₂)] [OH] with HCl

A Sargent-Welch pH 6000 meter was used for this experiment. Ethanol (25 mL) was pipetted into a conical flask. To this was added

[PtMe₂(phen)] (0.1092 g) and the solution was left to react for 1 day. An aqueous solution of HCl (0.02 M) was made up using a standard sample of HCl (0.10 M).

The HCl solution was added, from a burette, to the [PtMe₂(OEt)-(phen)(OH₂)] [OH] solution, and the pH recorded after each addition. A plot was made of pH of the solution versus the volume of acid added. The experiment was repeated using 0.1058 g of [PtMe₂(phen)] in 25 mL of ethanol.

A blank titration of pure ethanol against the 0.02 M HCl was performed. The change in pH was recorded and compared to the above results. The type of pH changes in the two titrations were clearly completely different.

2.2.2.11 Calculation of the Molar Extinction Coefficient of [PtMe₂(phen)] in Acetone

A solution of [PtMe₂(phen)] (0.0041 g) in acetone (100 mL, 1.01 x 10⁻⁴ M) was made up. A sample of the solution was transferred to a 1 cm. quartz cuvette which was then placed in the thermostatically controlled (21°C) sample holder of a Cary 118 spectrophotometer. A reference cell of acetone was also used. Absorbance values were recorded for the bands at 473 nm, 438 nm, 420.5 nm, 354.5 nm, and 326 nm. The values are shown below:

$$\begin{aligned}\epsilon_{473} &= 3600 \text{ l mol}^{-1} \text{ cm}^{-1} \\ \epsilon_{438} &= 3540 \text{ l mol}^{-1} \text{ cm}^{-1} \\ \epsilon_{420} &= 3420 \text{ l mol}^{-1} \text{ cm}^{-1} \\ \epsilon_{354} &= 2970 \text{ l mol}^{-1} \text{ cm}^{-1} \\ \epsilon_{326} &= 3660 \text{ l mol}^{-1} \text{ cm}^{-1}\end{aligned}$$

2.2.2.12 Kinetic Measurements for the Reaction between [PtMe₂(phen)] and MeOH, and EtOH

A 0.0001 M solution of [PtMe₂(phen)] was made up by dissolving 0.0041 g of the complex in 100 mL of methanol. A portion of the solution was transferred to a 1 cm quartz cuvette held in the cell compartment of a Cary 118 spectrophotometer, at 21°C. The absorbance at 415.5 nm was recorded at different time intervals. The reaction took about 1-1/2 hours to go to completion, and was monitored over at least four half-lives.

The same technique was used for the reaction between ethanol and [PtMe₂(phen)]. A plot was made of $\log_{10} (A_t - A_\infty)$ versus time.

2.2.2.13 Reaction of D₂O with [PtMe₂(phen)]

A solution of [PtMe₂(phen)] (0.05 g) in THF (18 mL, dried over CaH₂) was made up. To this was added D₂O (5 mL). The mixture was left for 3 hours after which it was worked up, as described above in the reaction of [PtMe₂(phen)] with H₂O.

2.3 Preparative Work and Experimental Details for Work in Chapter 3

The preparative technique used in this section is the same for all complexes.

2.3.1 [PtIme₃(phen)]

To an orange-red solution of [PtMe₂(phen)] (0.08 g) in acetone (20 mL) was added excess MeI (0.5 mL). The solution immediately turned a very pale yellow. The solvent was removed under vacuum and the pale yellow solid was redissolved in a small volume of CH₂Cl₂. On addition of pentane (20 mL) the product was precipitated and dried under vacuum. Yield 84%, mp 284°C.

2.3.2 [PtI Me₂(Et)(phen)]

The addition of EtI (0.20 mL) to a solution of [PtMe₂(phen)] (0.07 g) in acetone (20 mL) produced a rapid colour change to pale yellow. The solid product was recovered using the normal procedure. Yield 78%.

2.3.3 [PtBr Me₂(Et)(phen)]

An excess of EtBr (0.14 mL) was added to a solution of [PtMe₂(phen)] (0.1 g) in acetone (20 mL). The reaction mixture was left to stand for about 15 hours. Some signs of decomposition were observed and so the solution was filtered. The product was recovered in the normal way. Yield 78%, mp 269°C decomp.

2.3.4 [PtI Me₂(ⁿPr)(phen)]

To a solution of [PtMe₂(phen)] (0.07 g) in acetone (20 mL) was added an excess (0.20 mL) of 1-iodopropane. After several minutes the solution was pale yellow and the solid product was recovered from this solution by the normal procedure.

2.3.5 [PtBr Me₂(ⁿPr)(phen)]

An excess of 1-bromopropane (1.0 mL) was added to a solution of [PtMe₂(phen)] (0.14 g) in acetone (20 mL). The reaction mixture was left to stand for about 3 hours after which time the solution was yellow. The solid product was recovered in the usual way. Yield 82%, mp 268°C decomp.

2.3.6 [PtI Me₂(ⁿBu)(phen)]

An excess of 1-iodobutane (0.1 mL) was added to a solution containing [PtMe₂(phen)] (0.14 g) in acetone (20 mL). The solution was left to stand for 1 hour by which time it was a yellow colour. The solid product was isolated using described techniques. Yield 74%, mp 130°C.

2.3.7 Preparation of $\overline{\text{CH}_2\text{CH}_2\text{CH}}\text{-CH}_2\text{Br}$

The method used here was that described in the literature. A solution of cyclopropylcarbinol (7.2 g) in anhydrous ether (30 mL), was made up and placed in a two necked round bottom flask (100 mL). The solution was cooled by a Dry Ice-acetone mixture and N₂ gas passed through the flask. To this solution was slowly added phosphorus tribromide (3.5 mL) and the mixture was allowed to come to room temperature overnight. Water (5 mL) was added, the ether layer separated, washed with anhydrous NaHCO₃ and dried over Drierite. The sample was fractionally distilled.

2.3.8 [PtBr Me₂($\overline{\text{CH}_2\text{-CHCH}_2\text{CH}_2}$)(phen)]

To a solution containing [PtMe₂(phen)] (0.08 g) in acetone (20 mL) was added an excess of cyclopropylcarbinyl bromide (0.25 mL). The solution was left to stand for several hours and the pale yellow solid was recovered from the solution by the technique already described.

2.3.9 [PtI Me₂(CH₃-(CH₂)₄)(phen)]

An excess of 1-iodopentane (1 mL) was added to a solution containing [PtMe₂(phen)] (0.08 g) in acetone (20 mL). The solution

rapidly turned yellow and the solid product was extracted as described above.

2.3.10 [PtI(Me₂)(CH₃-(CH₂)₆)(phen)]

To a solution containing [PtMe₂(phen)] (0.09 g) in acetone (20 mL) was added 1-iodoheptane (0.1 mL). The solution was yellow in colour after 1 hour. The solid product was recovered using described techniques. Yield 79%, mp 210°C.

2.3.11 Kinetics for the Reaction of MeI with [PtMe₂(phen)]

Due to this reaction being very rapid, the fast-scanning Hewlett Packard 8450A instrument was used. A solution of [PtMe₂(phen)] (0.0122 g) in acetone (100 mL, 3×10^{-4} M) was made up in a volumetric flask. A portion (3 mL) of this solution was transferred by pipette into a 1 cm quartz cuvette. Next a solution of MeI (0.1121 mL) in acetone (100 mL, 1.8×10^{-2} M) was made up in a volumetric flask. A portion (0.25 mL) of this solution was transferred, using a glass syringe, into the cuvette of [PtMe₂(phen)]. The two solutions were rapidly stirred and immediately placed in the cell compartment of the instrument. A solvent cell was also used. The absorbance reading at 472.7 nm was recorded at regular time intervals. The reaction was monitored over at least four half-lives and took about 1/2 hour to reach the A_{∞} value. The experiment was repeated several times, keeping the concentration of the [PtMe₂(phen)] constant but varying the concentration of MeI.

2.3.12 Kinetics of the Reaction between $[\text{PtMe}_2(\text{phen})]$ and $\text{C}_2\text{H}_5\text{I}$, $\text{C}_3\text{H}_7\text{I}$, $\text{C}_4\text{H}_9\text{I}$, and $\text{C}_5\text{H}_{11}\text{I}$

The same technique was used for each of these primary organic iodides and thus they will be treated together in this section.

A solution of EtI (1.56 g) in acetone (100 mL, 1.0×10^{-1} M) was made up in a volumetric flask. A sample (30 mL) of this solution was pipetted into a conical flask containing $[\text{PtMe}_2(\text{phen})]$ (0.008 g) in acetone (10 mL). The two solutions were thoroughly mixed and a sample quickly transferred to a 1 cm quartz cuvette which was placed in the cell compartment of the thermostatically controlled (25°C) Cary 118 spectrophotometer. A solvent reference cell was used. The absorbance at 472.7 nm was recorded at regular time intervals. The reaction was monitored through five half-lives, and a plot of $\log_{10} (A_t - A_\infty)$ versus time was made. The process was repeated adding 20 mL of the EtI solution to 20 mL of the complex solution (0.008 g present), 10 mL of the EtI solution to 30 mL of the complex solution (0.008 g present) and finally 5 mL of the EtI solution to 35 mL of the complex solution (0.008 g present). In this way the initial $[\text{PtMe}_2(\text{phen})]$ concentration was kept constant (5.0×10^{-4} M). The same procedure was used for the other three organic iodides. In order to decrease the reaction time for the 1-iodopropane and 1-iodobutane the initial concentration of their solutions was increased to 2.0×10^{-1} M and 4.0×10^{-1} M respectively.

2.4 Preparative Work and Experimental Details for the Work in Chapter 4

2.4.1 Simple Preparative Work

2.4.1.1 $[\text{PtI}_2\text{Me}_2(\text{phen})]$

To a solution of $[\text{PtMe}_2(\text{phen})]$ (0.13 g) in acetone (20 mL) was

added a very slight excess of iodine in acetone (0.056 g). The intense colour of the iodine immediately disappeared and the solvent was removed on the rotary evaporator. The brown solid was washed with CCl_4 to remove any excess iodine and dried on the vacuum line. Yield 84%, mp 330°C decomp.

2.4.1.2 [PtClMe₂(CH₂Cl)(phen)]

A solution of [PtMe₂(phen)] (0.07 g) in CH_2Cl_2 (20 mL) was left to react for 1 day. The orange solution turns to a pale yellow. The volume of solvent was reduced to about 3 mL and pentane (20 mL) was added to precipitate the solid product. The sample was dried on the vacuum line. A mixture of *cis* and *trans* isomers was produced.

2.4.1.3 [PtClMe₂(CD₂Cl)(phen)]

A solution of [PtMe₂(phen)] (0.03 g) in CD_2Cl_2 (4 mL) was left to react till a pale yellow solution was formed. The solid was recovered by precipitation using pentane (15 mL). A mixture of *cis* and *trans* isomers was produced.

2.4.1.4 [PtBrMe₂(CH₂Br)(phen)]

To a solution of [PtMe₂(phen)] (0.08 g) in acetone (8 mL) was added CH_2Br_2 (1.0 mL) and the reaction mixture left to stand for 4 hours. The solid product was recovered by reducing the volume of solvent on the rotary evaporator and precipitating the solid by addition of pentane (15 mL). A mixture of the *cis* and *trans* isomers is formed. Yield 75%.

2.4.1.5 Reaction between CH_2ClI and [PtMe₂(phen)]

To a solution of [PtMe₂(phen)] (0.114 g) in acetone (20 mL), was added CH_2ClI (0.02 mL, a 1:1 mole ratio). After about 15 minutes a yellow solution developed and a little precipitate formed. The solution was filtered. The solvent was removed from the filtrate on the rotary

evaporator, and the solid remaining was redissolved in CH_2Cl_2 (3 mL). On addition of pentane (15 mL) the solid precipitated out, and was dried under vacuum. Mp 160°C .

The experiment was repeated but this time an excess of CH_2ClI (0.2 mL), was added. Again the solution went yellow and there was some precipitate.

2.4.1.6 Reaction between $[\text{PtMe}_2(\text{phen})]$ and CH_2ClBr

To a solution of $[\text{PtMe}_2(\text{phen})]$ (0.103 g) in acetone (20 mL) was added an excess of CH_2ClBr (1.25 mL). The reaction went to completion in 4 hours. The solvent was removed and the solid redissolved in a little CH_2Cl_2 from which it was precipitated by the addition of pentane (20 mL). The solid was dried under vacuum.

2.4.1.7 Reaction between $\text{I}(\text{CH}_2)_2\text{I}$ and $[\text{PtMe}_2(\text{phen})]$

The 1,2-diiodoethane was recrystallised from carbon tetrachloride before use.

To a solution of $[\text{PtMe}_2(\text{phen})]$ (0.2 g) in acetone (20 mL) was added a solution of $\text{I}(\text{CH}_2)_2\text{I}$ (0.14 g) in acetone (10 mL). A brown precipitate forms after a few minutes. The reaction mixture was left to stand for 1/2 hour and then filtered. The solvent was removed from the filtrate. The solid residue and the precipitate were dried under vacuum.

2.4.1.8 Reaction between $\text{Br}(\text{CH}_2)_2\text{Br}$ and $[\text{PtMe}_2(\text{phen})]$

To a solution of $[\text{PtMe}_2(\text{phen})]$ (0.09 g) in acetone (20 mL) was added an excess of 1,2-dibromoethane (0.25 mL). A pale yellow precipitate forms after 20 minutes. The solution was filtered and the precipitate washed with ether, and dried under vacuum (mp 280°C decomp). The solvent was removed from the filtrate using the rotary evaporator and the solid residue was dried on the vacuum line.

2.4.1.9 [PtMe₂(CH₂CH₂CH₂I)(phen)]

To a solution of [PtMe₂(phen)] (0.09 g) in acetone (30 mL) was added a large excess of 1,3-diiodopropane (1.0 mL). The reaction was left to stand for 2 hours after which time a yellow solution had developed and no precipitate was formed. The solvent was removed and the product dissolved in a little CH₂Cl₂ and recovered by precipitation using pentane (20 mL). Yield 81%, mp 335°C decomp.

2.4.1.10 [PtMe₂{(CH₂)₄I}(phen)]

To a solution of [PtMe₂(phen)] (0.04 g) in acetone (20 mL) was added 1,4-diiodobutane (0.02 mL). The colour changed to yellow very rapidly and a precipitate of [Pt₂I₂Me₄{(CH₂)₄}(phen)₂] formed. The solution was filtered and the solvent removed on the rotary evaporator. The solid from the filtrate was redissolved in CH₂Cl₂ (3 mL) and precipitated with pentane (15 mL).

2.4.1.11 [PtMe₂{(CH₂)₅I}(phen)]

To a solution of [PtMe₂(phen)] (0.09 g) in acetone (20 mL) was added an excess of 1,5-diiodopentane (0.3 mL). The reaction mixture was left to stand for 2 hours after which time a yellow solution had developed. There was no sign of a precipitate and the solid product was recovered in the way already described. Yield 84%, mp 212°C.

2.4.1.12 [Pt₂I₂Me₄{(CH₂)₃}(phen)₂]

A solution of [PtMe₂(phen)] (0.019 g) in acetone (15 mL) was made up. To this was added a solution of [PtMe₂{(CH₂)₃I}(phen)] (0.032 g) in acetone (25 mL, a 1:1 mole ratio). The reaction solution was left to stand for a day, after which time some precipitate had formed and a pale yellow solution. The solution was filtered and the solid was recovered from the filtrate solution by evaporation of the

solvent. This solid product and the precipitate were dried under vacuum and both were found to be the desired binuclear complex. Mp 195°C decomp.

2.4.1.13 [Pt₂I₂Me₄{(CH₂)₄}(phen)₂]

A solution of [PtMe₂(phen)] (0.011 g) in acetone (25 mL) was prepared. To this was added a solution of [PtIME₂{(CH₂)₄I}(phen)] (0.006 g) in acetone (20 mL, 1:1 mole ratio). The reaction solution was left to stand for 1 day after which a yellow solution had developed. There were signs of precipitate and the solution was filtered. The solvent was removed under vacuum. Yield 85%, mp 269°C.

2.4.1.14 [Pt₂I₂Me₄{(CH₂)₅}(phen)₂]

A solution of [PtMe₂(phen)] (0.021 g) in acetone (20 mL) was made up. To this was added a solution of [PtIME₂{(CH₂)₅I}(phen)] (0.039 g) in acetone (20 mL). The solution was left to react for 1 day during which time a yellow solution developed. The solvent volume was reduced on the rotary evaporator and pentane (15 mL) added to precipitate the solid product. Yield 89%, mp 195°C decomp.

2.4.1.15 [PtBrMe₂(C₈H₈Br)(phen)]

A solution of [PtMe₂(phen)] (0.044 g) in acetone (25 mL) was prepared. To this was added a solution of α,α'-dibromo-o-xylene (0.06 g) in acetone (15 mL). The work was done in the fume-hood due to the lachrymatory nature of the organic ligand.

A reaction occurs immediately on addition of the two solutions and the solution turns yellow. The solvent was removed on the rotary evaporator and washed with ether to remove any excess α,α'-dibromo-o-xylene. The solid product was redissolved in CH₂Cl₂ (3 mL) and precipitated from the solution with pentane (15 mL). Yield 60%, mp 280°C decomp.

2.4.1.16 Reaction of $[\text{PtMe}_2(\text{phen})]$ with $[\text{PtBrMe}_2(\text{C}_6\text{H}_5\text{Br})(\text{phen})]$

To a solution of $[\text{PtMe}_2(\text{phen})]$ (0.012 g) in acetone (20 mL) was added a solution of $[\text{PtBrMe}_2(\text{C}_6\text{H}_5\text{Br})(\text{phen})]$ (0.019 g) in acetone (15 mL, 1:1 mole ratio). The solution was allowed to stand for 3 days in which time a yellow, opaque solution formed. The solvent was removed under vacuum.

2.4.2 Other Experimental Procedures from Chapter 4

2.4.2.1 Reaction of CH_2I_2 with $[\text{PtMe}_2(\text{phen})]$ followed on the Varian T60 NMR Instrument

To a solution of $[\text{PtMe}_2(\text{phen})]$ (0.015 g) in CH_2Cl_2 (1 mL) in an nmr tube was added CH_2I_2 (0.003 mL, 1:1 mole ratio). The solution was shaken vigorously and placed in the probe of a Varian T60 nmr spectrometer. The probe was at ambient temperature. Nmr spectra were taken at regular intervals over a period of about 15 minutes and finally after about 2 hours. The *cis* isomer forms initially but with time the *trans* isomer forms with gradual disappearance of the *cis* product. There is only a small amount of the iodine product $[\text{PtI}_2\text{Me}_2(\text{phen})]$.

2.4.2.2 Following the Effect of Galvinoxyl in the Reaction of CH_2I_2 with $[\text{PtMe}_2(\text{phen})]$, by Use of NMR

The conditions for this experiment were identical to those described in Section 2.4.2.1. In this case however a 6% molar amount (0.001 g) of galvinoxyl was added to the solution of $[\text{PtMe}_2(\text{phen})]$ before the addition of CH_2I_2 . Spectra were recorded over a period of 15 minutes and finally after 14 hours. The reaction was slower than the one described in Section 2.4.2.1 but again the *cis* isomer forms before the *trans*.

2.4.2.3 Reaction of CH_2I_2 with $[\text{PtMe}_2(\text{phen})]$ in the Presence of Galvinoxyl and Diffuse Light

To a solution of $[\text{PtMe}_2(\text{phen})]$ (0.035 g, 0.0058 M) in acetone (15 mL) was added galvinoxyl (0.002 g, 5% molar amount). To this solution was added CH_2I_2 (0.007 mL, 0.0058 M). The reaction solution was left to stand for 1 hour in diffuse daylight, after which time the solvent was removed on the rotary evaporator and the residue redissolved in CH_2Cl_2 (3 mL) and precipitated with pentane (15 mL). The major product was $[\text{PtI}_2\text{Me}_2(\text{phen})]$ with some of the *cis* and *trans* isomers of $[\text{PtIME}_2(\text{CH}_2\text{I})(\text{phen})]$.

2.4.2.4 $[\text{PtMe}_2(\text{phen})]$ with Excess CH_2I_2 in the Dark and in Diffuse Daylight

Two solutions of $[\text{PtMe}_2(\text{phen})]$ (0.10 g) in acetone (30 mL) were made up, in round bottom flasks (100 mL). One of the solutions was left in diffuse daylight and CH_2I_2 (0.5 mL) was added. The reaction went to completion immediately and the solid was removed immediately by the technique previously described. The flask containing the second solution was wrapped in aluminium foil and placed in a dark cupboard. To this solution was added CH_2I_2 (0.5 mL) and it was left to react for 20 minutes. The solid was removed using the described procedure.

2.4.2.5 Reaction between a 1:1 Mole Ratio of CH_2I_2 and $[\text{PtMe}_2(\text{phen})]$ in the Dark and in Diffuse Daylight

Two solutions of $[\text{PtMe}_2(\text{phen})]$ (0.038 g) in acetone (10 mL) were made up in round bottom flasks (50 mL). To one flask in diffuse daylight was added CH_2I_2 (0.007 mL). A reaction occurred immediately. The solution was left to stand for 20 minutes before removing the solid product by the previously described technique. The second flask was wrapped in aluminium foil and placed in a dark cupboard. To this was

added CH_2I_2 (0.007 mL) and the solution left to stand for 20 minutes. After this time it had changed to yellow and the solid product was removed in the usual way.

2.4.2.6 Reaction between a 1:1 Mole Ratio of CH_2I_2 and $[\text{PtMe}_2(\text{phen})]$ in CH_2Cl_2

To a solution of $[\text{PtMe}_2(\text{phen})]$ (0.035 g) in CH_2Cl_2 (10 mL) was added CH_2I_2 (0.009 mL). The solution was left to stand in diffuse daylight and the reaction was completed in four minutes. The solid product was removed by reducing the volume of solvent on the rotary evaporator and adding pentane (15 mL) to precipitate the solid. It was dried under vacuum.

2.4.2.7 Isomerisation of $\text{cis}-[\text{PtIME}_2(\text{CH}_2\text{I})(\text{phen})]$ in Presence of LiCl

To a solution of $\text{cis}-[\text{PtIME}_2(\text{CH}_2\text{I})(\text{phen})]$ (0.017 g) in an acetone $d_6/\text{CD}_2\text{Cl}_2$ solvent mixture (3 mL) was added a solution of LiCl (0.0016 g, 1:1 mole ratio) in acetone d_6 (1 mL). The *cis* isomer did have traces of the *trans* isomer present at the start. The solutions were mixed in an nmr tube and the reaction was followed on the Varian XL-100 nmr instrument over a period of five days.

2.4.2.8 Analysis of the Gaseous Products from the Reaction between $\text{I}(\text{CH}_2)_2\text{I}$ and $[\text{PtMe}_2(\text{phen})]$, Using Gas Chromatography

A solution of $[\text{PtMe}_2(\text{phen})]$ (0.04 g) in CH_2Cl_2 (3 mL) was placed in the apparatus shown in Fig. 7.1. The solution was frozen by use of a liquid nitrogen Dewar. A sample of $\text{I}(\text{CH}_2)_2\text{I}$ (0.028 g, 1:1 mole ratio) in CH_2Cl_2 (1 mL) was now introduced into the vessel which was then sealed with a serum cap. The reaction vessel was evacuated whilst the contents were still frozen and then sealed off by closing tap A. The mixture was allowed to return to room temperature and left to react for

1 hour. A brown precipitate forms in the vessel. Using a gas-tight syringe (1 mL) a sample of the gas was removed from the vessel and injected into the Varian Aerograph 1400 gas chromatograph operating at 50°C and fitted with a Porapak Q column. The gas chromatogram showed a large air peak, two small peaks (probably CH₄ and C₂H₆) and one large peak. A sample of pure ethene gas was injected into the gc instrument and its retention time corresponded to that of the large peak from the sample gas. Using a gas-tight syringe (1 mL) a small volume of pure ethene gas (0.1 mL) was injected through the serum cap into the reaction vessel. From the reaction vessel a sample of the gas was again removed and injected into the gc. The peak, thought to be due to ethene, increased in height dramatically.

2.4.2.9 Analysis of the Gaseous Products from Pyrolysis of [Pt₂I₂Me₄{(CH₂)₂}(phen)₂] Using Gas Chromatography

A sample of [Pt₂I₂Me₄{(CH₂)₂}(phen)₂] (0.03 g) was placed in the reaction vessel shown in Fig. 7.1. The vessel was sealed with a serum cap and evacuated on the vacuum line. The sample was heated until it melted, and charred. Using a gas-tight syringe (1 mL) a sample of the gaseous product was removed from the vessel and injected into a Varian Aerograph gc fitted with a Porapak Q column. The instrument was at 60°C. The gas chromatogram showed the presence of large amounts of CH₄, C₂H₄ and smaller traces of two other gases. This was verified by the injection of authentic samples of CH₄ and C₂H₄ into the instrument. The presence of CH₄ in the gaseous product was further proved by injection of the product gases into a Molecular Sieve 5A column. A large peak corresponding to that for an authentic CH₄ sample was observed.

2.4.2.10 Analysis of Gaseous Products from Pyrolysis of $[\text{Pt}_2\text{I}_2\text{Me}_4\{(\text{CH}_2)_3\}(\text{phen})_2]$, Using Mass Spectrometry and Gas Chromatography

The same procedure as described in the previous section was used to pyrolyse the sample. The gaseous product was analysed by injection of a sample into the Varian Aerograph 1400 gc. The gases detected were ethene, propylene, cyclopropane and butenes. This was verified by injection of authentic samples of these gases into the gc and comparing retention times. The gaseous products were also analysed by a mass spectral analysis. This was achieved by separation of the products using the Varian Aerograph gc followed by analysis of each gas using the Varian Mat Bremen Mass Spectrometer MAT 311A. A temperature program was used ranging from 20-150°C and set at 15°C min⁻¹.

2.4.2.11 Analysis of the Gaseous Products from Pyrolysis of $[\text{Pt}_2\text{I}_2\text{Me}_4\{(\text{CH}_2)_4\}(\text{phen})_2]$, Using Mass Spectrometry and Gas Chromatography

The same procedure as described in the previous section was used.

2.4.2.12 Analysis of the Gaseous Products from Pyrolysis of $[\text{Pt}_2\text{I}_2\text{Me}_4\{(\text{CH}_2)_5\}(\text{phen})_2]$, Using Mass Spectrometry and Gas Chromatography

The same procedure as described in Section 2.4.2.10 was used.

2.4.2.13 Kinetic Studies of the Reaction between CH_2I_2 and $[\text{PtMe}_2(\text{phen})]$, Using UV/Visible Spectroscopy

A series of kinetic experiments were performed for this reaction, and each of them will be discussed in this section.

A Hewlett Packard 8450A Diode Array Spectrophotometer was used in this study, and irradiation of any sample solutions was done using a Cole Parmer Low Noise Illuminator, Model 9741-50.

i) Change of Absorbance with Time

A solution of $[\text{PtMe}_2(\text{phen})]$ (5 mL, 5.0×10^{-4} M) in acetone, was

added to a solution of CH_2I_2 (5 mL, 4.0×10^{-2} M) and the resultant solution was thoroughly mixed. A sample of the reaction solution was quickly transferred to a 1 cm quartz cuvette and placed in the cell compartment of the spectrophotometer. A reference cell containing solvent was also used. The absorbance readings at 472.7 nm were recorded over a period of 5 minutes. The results show an induction period for the reaction.

ii) Irradiation of the Sample Solution

The same volumes and concentrations of solutions as described above were used. The cuvette containing the reaction solution was placed in the cell compartment and a series of scans were made from 600 to 325 nm. After 15 minutes the sample was irradiated, from above, for a period of 5 seconds and the absorbance recorded from 600 to 325 nm immediately afterwards. A dramatic reduction in absorbance was noted.

In order to observe the effect, on the early stages of the reaction, of irradiating the sample, a further experiment was carried out. To a solution of $[\text{PtMe}_2(\text{phen})]$ in acetone (4 mL, 1.5×10^{-3} M) was added a solution of CH_2I_2 (1 mL, 5.0×10^{-2} M) in acetone. The mixture was mixed thoroughly and quickly placed in a 1 cm quartz cuvette in the cell compartment of the spectrophotometer. A reference cell was again used. The sample was irradiated, from above, whilst absorbance readings were taken at 472.7 nm. The reaction went to completion in about 1 minute. This exact procedure was repeated, without irradiation and went to completion in just over two minutes with a longer induction period.

iii) Reaction Performed in the Presence of Galvinoxyl

A solution of $[\text{PtMe}_2(\text{phen})]$ in acetone (2.0 mL, 5.0×10^{-4} M) was transferred to a 1 cm quartz cuvette. To this was added a solution

of CH_2I_2 (1.0 mL, 4.0×10^{-3} M) in acetone. The cuvette was then placed in the cell compartment of the spectrophotometer. Absorbance readings were taken at 472.7 nm. The reaction became very fast after about 3-1/2 minutes at which time a solution of galvinoxyl (0.25 mL, 10% molar ratio with respect to $[\text{PtMe}_2(\text{phen})]$) was added. The reaction rate decreased noticeably, but not dramatically.

2.4.2.14 Kinetics for the Formation of $[\text{PtIme}_2\{(\text{CH}_2)_n\text{I}\}(\text{phen})]$ ($n = 3, 4, 5$)

This work was performed using the Cary 118 spectrophotometer. A solution of $\text{I}(\text{CH}_2)_3\text{I}$ (1.0×10^{-3} M) in acetone was made up in a volumetric flask (100 mL). A sample of this solution (30.0 mL) was pipetted into a conical flask containing a solution of $[\text{PtMe}_2(\text{phen})]$ (0.008 g) in acetone (10.0 mL). The two solutions were thoroughly mixed and a sample quickly transferred to a 1 cm quartz cuvette, which was placed in the thermostatically controlled (25°C) cell compartment of the spectrophotometer. A solvent reference cell was used. The absorbance reading at 472.7 nm was recorded at regular time intervals. The reaction was monitored through four half-lives, and a plot of $\log_{10}(A_t - A_\infty)$ versus time was made. A series of experiments was performed using the same concentration of $[\text{PtMe}_2(\text{phen})]$ but varying the concentration of $\text{I}(\text{CH}_2)_3\text{I}$.

The identical procedure and concentrations were used for following the kinetics for the formation of $[\text{PtIme}_2\{(\text{CH}_2)_4\text{I}\}(\text{phen})]$ and $[\text{PtIme}_2\{(\text{CH}_2)_5\text{I}\}(\text{phen})]$.

2.4.2.15 Kinetics for the Formation of $[\text{Pt}_2\text{I}_2\text{Me}_4\{(\text{CH}_2)_3\}(\text{phen})_2]$

This work was performed on the Cary 118 spectrophotometer. A solution of $[\text{PtIme}_2\{(\text{CH}_2)_3\text{I}\}(\text{phen})]$ (0.056 g) was made up in acetone

(30.0 mL, 2.66×10^{-3} M). A portion of this (10.0 mL) was pipetted into a conical flask and to it was added a solution of $[\text{PtMe}_2(\text{phen})]$ (10.0 mL, 1.0×10^{-4} M). The solutions were thoroughly mixed and a sample transferred to a 1 cm quartz cuvette in the thermostatically controlled cell compartment (25°C) of the spectrophotometer. The absorbance at 472.7 nm was followed with time, and over three half-lives. A plot of $\log_{10} (A_t - A_\infty)$ against time was made. The procedure was repeated keeping the concentration of $[\text{PtMe}_2(\text{phen})]$ constant but varying the concentration of $[\text{PtIME}_2\{(\text{CH}_2)_3\text{I}\}(\text{phen})]$.

2.4.2.16. Kinetics for the Formation of $[\text{Pt}_2\text{I}_2\text{Me}_4\{(\text{CH}_2)_4\}(\text{phen})_2]$

This work was performed on the Cary 118 spectrophotometer. A solution of $[\text{PtIME}_2\{(\text{CH}_2)_4\text{I}\}(\text{phen})_2]$ (0.029 g) was made up in acetone (20 mL, 2.0×10^{-3} M). A portion of this (5.0 mL) was pipetted into a conical flask and to it was added acetone (5.0 mL). A solution of $[\text{PtMe}_2(\text{phen})]$ in acetone (10.0 mL, 1.0×10^{-4} M) was added to this solution and a portion of this reaction mixture transferred to a 1 cm quartz cuvette in the thermostatically controlled (25°C) compartment of the spectrophotometer. The procedure was repeated, keeping the concentration of $[\text{PtMe}_2(\text{phen})]$ constant, but varying the concentration of $[\text{PtIME}_2\{(\text{CH}_2)_4\text{I}\}(\text{phen})]$.

2.4.2.17. Kinetics for the Formation of $[\text{Pt}_2\text{I}_2\text{Me}_4\{(\text{CH}_2)_5\}(\text{phen})_2]$

The procedure used here was identical to that described in Section 2.4.2.15. The initial concentration of $[\text{PtIME}_2\{(\text{CH}_2)_5\text{I}\}(\text{phen})]$ was 2.0×10^{-3} M and that of $[\text{PtMe}_2(\text{phen})]$, 2.0×10^{-4} M.

2.4.2.18 The Effects of Irradiation and Galvinoxyl on the Rate of Reaction between $I(CH_2)_3I$ and $[PtMe_2(phen)]$

The Hewlett Packard 8450A Diode Array Spectrophotometer was used for this work and irradiation was performed using a Cole Parmer Low Noise Illuminator.

A series of experiments were performed under this heading and each will be described in this section.

i) Irradiation of the Reaction Sample

A solution of $[PtMe_2(phen)]$ (1.5 mL, 1.5×10^{-3} M) in acetone, and a solution of $I(CH_2)_3I$ (1.5 mL, 2.5×10^{-2} M) were mixed thoroughly in a 1 cm quartz cuvette and quickly placed in the cell compartment of the spectrophotometer. The absorbance was measured at 472.7 nm and the sample was kept in the dark initially. After 1 minute the sample was irradiated for a period of 3 minutes, whilst simultaneously measuring the absorbance. There appears to be no change in the rate of reaction.

ii) The Effect of Galvinoxyl

A solution of $[PtMe_2(phen)]$ (1.5 mL, 1.5×10^{-3} M) in acetone, and a solution of $I(CH_2)_3I$ (1.5 mL, 1.0×10^{-3} M) in acetone, were mixed thoroughly in a 1 cm quartz cuvette and quickly placed in the cell compartment of the spectrophotometer. The absorbance was measured at 472.7 nm, in diffuse daylight. After 100 seconds, a solution of galvinoxyl in acetone (0.1 mL, 4% mole ratio with respect to Pt(II) complex) was added and the mixture thoroughly stirred. No change in rate of reaction was observed.

In order to observe the behaviour of the $I(CH_2)_3I$ with galvinoxyl, a solution of these two together in acetone was made up and the UV/visible spectrum was run from 600 to 325 nm. There were two

λ_{max} , one at 396 nm and 578 nm, both due to the galvinoxyl. On irradiating the sample for several minutes no change was observed.

2.4.2.19. UV/Visible Spectrum for Reaction between $I(CH_2)_5I$ and $[PtMe_2(phen)]$

To a solution of $[PtMe_2(phen)]$ (5.0 mL, 5.0×10^{-4} M) was added $I(CH_2)_5I$ (0.15 mL, producing 2.0×10^{-1} M solution) and the reaction mixture was quickly transferred to a 1 cm quartz cuvette in the cell compartment of the Hewlett Packard Spectrophotometer. Several plots of absorbance versus λ were made from 600 to 325 nm.

2.4.2.20 Reaction between $I(CH_2)_2I$ and $[PtMe_2(phen)]$ followed by UV/Visible Spectroscopy

The Hewlett Packard Spectrophotometer was used for this study along with the Cole Parmer Illuminator. A series of experiments were carried out, which are discussed in this section.

i) Repeated Scans (600-325 nm) of the Reaction Mixture

A solution of $[PtMe_2(phen)]$ in acetone (4.0 mL, 5.0×10^{-4} M) was transferred to a 1 cm quartz cuvette. To this solution was added a solution of $I(CH_2)_2I$ in acetone (0.5 mL, approx. 1:1 mole ratio). The cuvette was quickly transferred to the cell compartment of the spectrophotometer and a series of scans were made of absorbance versus λ (600-325 nm) over a period of 35 minutes. A very intense band (off scale) developed as soon as the solutions had been mixed, centred at approximately 400 nm.

The spectrum of the final product (diluted to bring band on scale) shows a strong band at 350 nm.

The spectrum of the $I(CH_2)_2I$ solution was recorded from 600 to 325 nm and shows a weak band at 370 nm.

ii) UV/Visible Spectrum of $[PtI_2Me_2(phen)]$

A solution of $[PtI_2Me_2(phen)]$ (1.0×10^{-3} M) was placed in a

1 cm quartz cuvette in the cell compartment of the spectrophotometer. The UV/visible spectrum (λ 600-325 nm) shows a λ_{max} at 366 nm with a shoulder at approximately 350 nm.

iii) Irradiation of the Reaction Sample

To a solution of $[\text{PtMe}_2(\text{phen})]$ in acetone (5.0 mL, 1.5×10^{-3} M) was added a solution of $\text{I}(\text{CH}_2)_2\text{I}$ in acetone (5.0 mL, 9.0×10^{-3} M). A sample was quickly transferred to a 1 cm quartz cuvette in the cell compartment of the spectrophotometer. The absorbance at 472.7 nm was followed with time, initially in diffuse daylight. After 2 minutes the sample was irradiated from above for a period of 1 minute. A rapid fall in absorbance was observed. When the illuminator was removed the decay of the absorbance reading levelled off dramatically. The process was repeated after 4 minutes (irradiating for 1 minute) and after 9 minutes (irradiating for 1 minute). The same result was observed as described above.

iv) The Effect of Galvinoxyl

A reaction solution identical to the one in the previous section (iii) was made up and placed in the cell compartment of the spectrophotometer. The sample was irradiated in the initial part of the reaction for 1 minute and again after 3 minutes in order to produce a fast rate. The galvinoxyl solution (0.5 mL, 10% molar ratio with respect to $\text{Pt}(\text{II})$ complex) was added after 250 seconds. The plot levels off very dramatically.

2.4.2.21 Isomerisation of the Products in the Reaction between $[\text{PtMe}_2(\text{phen})]$ and CH_2ClBr

A solution of the reaction product (0.02 g) in CDCl_3 (0.75 mL) was made up and transferred to an nmr tube. The tube was placed in the probe of a Varian T60 nmr instrument and spectra were recorded over a period of 1 day.

2.5 Preparative Work and Experimental Details of the Work in Chapter 5

2.5.1 Simple Preparative Work

The 2-iodopropane used in this work was purchased from Aldrich Chemical Company, Inc. It was quoted as 97% pure. It was further purified by means of a spinning band distillation. The ethyl iodide present, after distillation, was estimated at less than 0.5%. Unless otherwise stated all the work was done in diffuse daylight and at room temperature.

2.5.1.1 [PtMe₂(¹Pr)(phen)]

A two necked round bottom flask (100 mL) was fitted with a glass frit bubbler and an outlet tap. Dry acetone (50 mL, stored over Molecular Sieve) was transferred into the flask and nitrogen gas was bubbled through for 45 minutes. A sample of [PtMe₂(phen)] (0.078 g) was added to the acetone and was dissolved by use of a magnetic stirrer. To this mixture was added 2-iodopropane (3.0 mL). Nitrogen gas was bubbled through the reaction solution throughout the experiment. The solution was left to stand for 40 minutes till it was yellow in colour. The volume of solvent was reduced on the rotary evaporator and pentane (20 mL) was added to precipitate the solid product, which was dried under vacuum. Yield 84%, mp 196°C.

2.5.1.2 [PtMe₂(¹Pr)(bipy)]

The apparatus and procedure described in the previous section was used in this synthesis. A solution of [PtMe₂(bipy)] (0.042 g) in dry acetone (35 mL) was left to react for 20 minutes, till a yellow solution was produced. The solid product was removed as described in the previous section, and dried under vacuum. Yield 85%.

2.5.1.3 $[\text{PtI Me}_2(^1\text{PrOO})(\text{bipy})]$

A solution of $[\text{PtMe}_2(\text{bipy})]$ (0.0382 g, 4.8×10^{-3} M) was made up in acetone (40 mL) in a quickfit round bottom flask (100 mL) fitted with a non-greased stopper. To this was added an excess of ^1PrI (0.67 mL). The reaction solution was left to stand for 12 hours by which time it was a pale yellow. The solvent volume was reduced on the rotary evaporator and the solid product precipitated by addition of pentane (20 mL). The solid was dried under vacuum. The product was contaminated with $[\text{PtI}_2\text{Me}_2(\text{bipy})]$ (50%).

2.5.1.4 $[\text{PtI Me}_2(^1\text{PrOO})(\text{phen})]$

A variety of conditions and concentrations were used in preparing samples of this complex. Three of those techniques will be discussed here.

i) A solution of $[\text{PtMe}_2(\text{phen})]$ (0.13 g) in acetone (30 mL) was made up in a quickfit round bottom flask (100 mL). To this was added ^1PrI (4 mL) and a non-greased stopper was used to seal the flask. The solution was left to stand for 1-1/2 hours after which time there was a sudden colour change to yellow. The volume of solvent was reduced and the solid was precipitated by addition of pentane (30 mL). The solid was dried under vacuum. The ^1H nmr spectrum of the sample showed the presence of $[\text{PtI Me}_2(^1\text{Pr})(\text{phen})]$ (15% mole ratio).

The sample was purified by means of column chromatography. A column was packed with a CHCl_3 /silica gel 60 slurry and a small layer of sand was deposited on the top of the silica gel. A concentrated solution of the reaction product (0.08 g) was made up in CHCl_3 (4 mL). A small volume of this solution (1 mL) was transferred to the column. The column was eluted with a mixture of acetone and methylene chloride (1:10

by volume). A pale yellow band was observed moving down the column. This fraction was found (by ^1H nmr) to contain $[\text{Pt}(\text{Me}_2(^i\text{Pr})(\text{phen}))]$ and some $[\text{PtI}_2\text{Me}_2(\text{phen})]$ (approx. 1:1 mole ratio). It appears that some decomposition occurred on the column producing the latter complex. A second fraction was collected by eluting with pure acetone. This fraction was found (by ^1H nmr) to be the desired $[\text{Pt}(\text{Me}_2(^i\text{PrOO})(\text{phen}))]$. A small trace (less than 10% mole ratio) of a new Pt(IV) complex was present as a contaminant. It is believed that this was formed on the column and is postulated to be $[\text{Pt}(\text{OH})\text{Me}_2(^i\text{Pr})(\text{phen})]$. This sample of the isopropylperoxo complex was sent for elemental analysis.

ii) A solution of $[\text{PtMe}_2(\text{phen})]$ (0.049 g) in acetone (25 mL, 4.8×10^{-3} M) was made up in a round bottom flask (100 mL). To this was added an excess of ^iPrI (2.0 mL). The flask was left open to the atmosphere and the solution was stirred very vigorously by means of a magnetic stirrer. This was to ensure a constant supply of air to the solution. The solution went yellow after 1 hour. The solvent volume was reduced (3 mL) and the product was precipitated by the addition of pentane (20 mL). The sample was dried under vacuum. A trace amount of $[\text{PtI}_2\text{Me}_2(\text{phen})]$ (5% molar ratio) was present, as shown by the ^1H nmr spectrum.

iii) A solution of $[\text{PtMe}_2(\text{phen})]$ (0.049 g) in acetone (25 mL, 4.8×10^{-3} M) was made up in a round bottom flask (100 mL). To this was added ^iPrI (2.0 mL) and the solution was irradiated by means of a Cole Parmer Illuminator, positioned in the neck of the flask. The reaction solution was stirred vigorously by means of a magnetic stirrer, and the reaction went to completion in five minutes. The solid product was recovered by the technique already described. The product was contaminated with $[\text{PtI}_2\text{Me}_2(\text{phen})]$ (approx. 15% molar ratio).

2.5.1.5 [PtBrMe₂(¹Pr)(phen)]

A great amount of problem was encountered in isolating a pure sample of this complex due to the presence of a small percentage of 1-bromopropane in the 2-bromopropane. The 2-bromopropane was purified using a spinning band distillation technique. The 1-bromopropane was estimated by gas chromatography to be present, after distillation, in less than a 0.1% molar ratio. Two preparative procedures are described below.

i) To a solution of [PtMe₂(phen)] (0.064 g) in acetone (30 mL) was added freshly distilled ¹PrBr (2.0 mL). The solution was refluxed for 2 hours after which time no reaction was apparent. The solution was left to stand for 2 weeks after which time the solvent was removed on the rotary evaporator and the solid residue redissolved in a little CH₂Cl₂ (4 mL). The solid was precipitated by addition of pentane (20 mL). The solid was dried under vacuum. Mp 230-237°C.

ii) To a solution of [PtMe₂(phen)] (0.14 g) in acetone (30 mL) was added freshly distilled ¹PrBr. The solution was left to stand for 2-1/2 weeks. Some decomposition appeared to have occurred so the solution was filtered. The solvent was reduced in volume and the solid product recovered in the usual manner. The ¹H nmr spectrum showed the presence of the [PtBrMe₂(¹Pr)(phen)] complex and [PtMe₂(phen)] in a 50% molar ratio.

2.5.1.6 Reaction between [PtIME₂(¹Pr)(phen)] and Ag₂O

In an aqueous solution of KOH (5 mL, 0.1 M) was added an aqueous solution of AgNO₃ (5 mL, 0.1 M). A reddish-brown precipitate of Ag₂O formed and the solution was filtered to recover the Ag₂O. A solution of [PtIME₂(¹Pr)(phen)] (15 mL, 6 x 10⁻³ M) in acetone, was added an excess

of the solid Ag_2O . The mixture was stirred for 1/2 hour after which time it was filtered to remove unreacted Ag_2O . The solvent was removed on the rotary evaporator and the residual solid redissolved in CH_2Cl_2 . It was precipitated from solution by addition of pentane (15 mL) and dried under vacuum.

2.5.1.7 Reaction between ${}^t\text{BuOOH}$ and $[\text{PtMe}_2(\text{phen})]$

To a solution of $[\text{PtMe}_2(\text{phen})]$ (0.06 g) in acetone (20 mL) was added ${}^t\text{BuOOH}$ (0.25 mL). The solution went yellow in 10 minutes. The solvent was reduced in volume by use of the rotary evaporator and the solid was precipitated by addition of pentane (20 mL). The product was dried under vacuum.

2.5.1.8 $[\text{PtIme}_2({}^t\text{BuOO})(\text{phen})]$

A series of reactions were carried out with ${}^t\text{BuI}$, using a variety of experimental conditions. These will be discussed in this section.

The ${}^t\text{BuI}$ was washed, before use, with a saturated solution of $\text{Na}_2\text{S}_2\text{O}_3$. The iodine-free ${}^t\text{BuI}$ was then dried over anhydrous MgSO_4 , and stored at -5°C in the dark.

i) To a solution of $[\text{PtMe}_2(\text{phen})]$ (0.06 g) in acetone (30 mL) was added ${}^t\text{BuI}$ (0.2 mL). The reaction was done in diffuse daylight. The colour changes quite rapidly and once it had become yellow the solvent volume was quickly reduced on the rotary evaporator and some solid precipitated by the addition of pentane (20 mL). It is important to stop the reaction at the yellow stage because if left to react the product is $[\text{PtI}_2\text{Me}_2(\text{phen})]$. The solid product was dried under vacuum. The ${}^1\text{H}$ nmr spectrum of the product showed the presence of $[\text{PtI}_2\text{Me}_2(\text{phen})]$ and $[\text{PtIme}_2({}^t\text{BuOO})(\text{phen})]$ (1:1 molar ratio).

ii) To a solution of $[\text{PtMe}_2(\text{phen})]$ (0.1 g) in CH_2Cl_2 (10 mL) was added $t\text{-BuI}$ (0.1 mL). The reaction was carried out in a dark cupboard, and the reaction vessel was wrapped in aluminium foil. The reaction solution was left to stand for three hours and then the solvent volume was reduced (3 mL) and the solid sample precipitated using pentane (20 mL). The ^1H nmr spectrum showed the presence of a mixture of $[\text{PtI}_2\text{Me}_2(\text{phen})]$ and $[\text{PtIME}_2(t\text{-BuOO})(\text{phen})\text{I}]$ (approx. 1:1 mole ratio).

iii) A solution of $[\text{PtMe}_2(\text{phen})]$ (0.073 g) in CH_2Cl_2 (20 mL) was prepared in a two necked round bottom flask (100 mL). Using a glass frit, oxygen was bubbled through the solution. The apparatus was fitted with a tap outlet and completely wrapped in aluminium foil. After 20 minutes a sample of $t\text{-BuI}$ (0.15 mL) was added and the solution left to react for 2 hours, after which time the solvent volume was reduced (3 mL) and the solid precipitated by addition of pentane (30 mL). The solid was dried under vacuum. The ^1H nmr spectrum showed that $[\text{PtIME}_2(t\text{-BuOO})(\text{phen})]$ was the major product with some of the diiodide complex (about 30%) present.

The sample was purified by means of column chromatography. A saturated solution (2 mL) of the product was made up in CHCl_3 , and transferred to the top of a column packed with a CHCl_3 /silica gel 60 slurry. The column was eluted with CH_2Cl_2 and the fraction collected was found to be the diiodide complex. The column was then eluted with acetone and the fraction collected was almost 100% $[\text{PtIME}_2(t\text{-BuOO})(\text{phen})]$. Mp 208°C .

iv) A solution of $[\text{PtMe}_2(\text{phen})]$ (0.089 g) in CH_2Cl_2 (20 mL) was prepared in a round bottom flask (100 mL). To this solution was added $t\text{-BuI}$ (0.2 mL) and a non-greased stopper was placed in the neck of

the flask. The solution was left to react for 1-1/2 hours after which time the solid product was precipitated in the usual manner and dried under vacuum. The ^1H nmr spectrum showed the main product to be $[\text{PtIME}_2(\text{}^t\text{BuOO})(\text{phen})]$ with a small amount of the diiodide complex (approx. 10%).

2.5.2 Experimental Procedures from Chapter 5

2.5.2.1 Reaction between ^1PrI and $[\text{PtMe}_2(\text{phen})]$ in Acetone- d_6

To a solution of $[\text{PtMe}_2(\text{phen})]$ (0.016 g) in acetone- d_6 (4 mL) was added ^1PrI (0.5 mL). The solution was left to react for 1/2 hour in diffuse daylight. A small amount of precipitate was produced. The solid product was recovered by precipitation, using pentane (15 mL). The sample was dried under vacuum, and was found by ^1H nmr to consist mainly of the Pt(IV) peroxo complex, with some of the diiodide complex (approx. 20%).

2.5.2.2 Reaction between $[\text{PtMe}_2(\text{phen})]$ and ^1PrI in a Solvent Mixture of Water and Acetone

i) To a solution of $[\text{PtMe}_2(\text{phen})]$ (0.07 g) in an acetone/water mixture (25 mL, 2:1 by volume) was added ^1PrI (1.0 mL). The reaction solution was left to stand for 45 minutes in diffuse daylight. The solution turned yellow and the acetone was removed on the rotary evaporator. The product was extracted from the water by means of CH_2Cl_2 (10 mL). The CH_2Cl_2 solution was dried over anhydrous MgSO_4 , filtered, and the solid product was recovered by reduction of the solvent volume followed by the addition of pentane (15 mL) producing a pale yellow precipitate. The solid was dried under vacuum and was shown by ^1H nmr to contain $[\text{PtIME}_2(\text{}^1\text{PrOO})(\text{phen})]$, $[\text{PtIME}_2(\text{}^1\text{Pr})(\text{phen})]$, $[\text{PtI}_2\text{Me}_2(\text{phen})]$ and the postulated $[\text{Pt}(\text{OH})\text{Me}_2(\text{}^1\text{Pr})(\text{phen})]$ in the ratio 1:0.85:0.16:0.16.

ii) An acetone/water solution (50 mL, 4:1 by volume) was placed in a two necked round bottom flask (100 mL), fitted with a glass frit bubbler and a tap outlet. Nitrogen gas was bubbled through the mixture for 30 minutes after which time a sample of $[\text{PtMe}_2(\text{phen})]$ (0.08 g) was dissolved in the solvent. To this solution was added ^iPrI (3.0 mL) and the reaction solution was left to stand, in diffuse daylight, for 2 hours. Nitrogen gas was bubbled through the solution during the reaction period. The solid product was recovered using the same technique as described in part (i) of this section. The product was shown by ^1H nmr to contain $[\text{PtIME}_2(^i\text{Pr})(\text{phen})]$, $[\text{Pt}(\text{OH})\text{Me}_2(^i\text{Pr})(\text{phen})]$ and $[\text{PtI}_2\text{Me}_2(\text{phen})]$ in the ratio 1:0.2:0.05.

2.5.2.3 Crystallisation of $[\text{PtIME}_2(^i\text{PrOO})(\text{phen})]$

A saturated solution of $[\text{PtIME}_2(^i\text{PrOO})(\text{phen})]$ (0.05 g) in CH_2Cl_2 (5 mL) was made up and filtered before use. Half the solution was placed in a 10 cm length, 2 mm diameter glass tube, and the other half into a similar tube. Ether was carefully added to the surface of the solution in one tube and hexane to the other tube. The tubes were cork sealed and kept at -5°C for five days, after which time crystals had formed. The solvent was decanted and the crystals dried under vacuum. A sample of these crystals was sent away for an X-ray crystallographic determination.

2.5.2.4 Pyrolysis of $[\text{PtIME}_2(^i\text{PrOO})(\text{phen})]$ and Analysis of Products by Gas Chromatography

A sample of $[\text{PtIME}_2(^i\text{PrOO})(\text{phen})]$ (0.03 g) was placed in the apparatus shown in Fig. 7.1. The apparatus was sealed with a rubber serum cap and evacuated using the vacuum line. The sample was heated by means of a bunsen flame till it melted and charred. A Varian Aerograph Series 1400 gas chromatogram was used for this work, fitted with a 10%

SE-30, column held at 70°C. A gaseous sample was removed from the pyrolysis vessel, using a gas-tight syringe (1 mL) and injected into the gc (injection port at 70°C). Three peaks were observed, the central one being the most intense. A mixture of acetone/isopropanol (2:1 by volume) was made up and a small sample (1 µL) was injected into the gc. The components have almost identical retention times but were just resolvable. A small volume of acetone (2 µL), was injected into the reaction vessel, through the serum cap. A sample of the gas, now in the vessel, was removed and injected into the gc. The intensity of the central peak increased dramatically, indicating that the pyrolysis had produced acetone.

2.5.2.5. Reaction between ^1PrI and $[\text{PtMe}_2(\text{phen})]$ in THF

Two solutions were made up of $[\text{PtMe}_2(\text{phen})]$ (0.039 g), one in acetone (50 mL) and one in THF (50 mL). Nitrogen gas had been bubbled through the solvents prior to their use. To each solution was added ^1PrI (1.0 mL) and the solutions were left to react, in diffuse daylight, for 1 hour. The solvents were removed on the rotary evaporator and the solid residue redissolved in CH_2Cl_2 (3 mL). The solid was recovered by addition of pentane (20 mL). The solvents had not been thoroughly degassed, as some $[\text{PtIME}_2(^1\text{PrOO})(\text{phen})]$ was formed. The ratio of $[\text{PtIME}_2(^1\text{Pr})(\text{phen})]$, $[\text{PtIME}_2(^1\text{PrOO})(\text{phen})]$ and $[\text{PtI}_2\text{Me}_2(\text{phen})]$ in THF was 1:0.64:0.32, and in acetone was 1:0.76:0.20.

2.5.2.6. Attempt to Observe C.I.D.N.P. Effects in the Reaction between ^1PrI and $[\text{PtMe}_2(\text{phen})]$

A solution of $[\text{PtMe}_2(\text{phen})]$ (0.02 g) was made up in CD_2Cl_2 (0.75 mL). This solution was transferred to a 506 PP nmr tube, and the sample placed in the probe of a Varian XL-100 nmr machine. The sample was photolysed from above using a P.R.A. 200 Watt, high pressure Hg-Xe

lamp. Immediately the sample was photolysed the deuterium lock was lost and only broad signals were observed. On removal of the lamp the lock returned in a matter of several seconds. The reaction was slow in the dark and repeated scans from 0 to 3 ppm failed to show any anomalous peak intensities. The photolysis was shown to clearly speed up the reaction but no spectral details could be recorded during photolysis. The major product was $[\text{PtIME}_2(^1\text{Pr})(\text{phen})]$ along with some $[\text{PtI}_2\text{Me}_2(\text{phen})]$ (30%) and a very small trace of $[\text{PtIME}(^1\text{PrOO})(\text{phen})]$:

2.5.2.7 Investigation of the Product Ratios in the Reaction between ^1PrI and $[\text{PtMe}_2(\text{phen})]$ with Variation of Concentration of Reagents

A series of synthetic experiments were performed in order to correlate product ratios with concentration of reagents and experimental conditions. In this way, insight into the reaction mechanism might be gained. The work will be sub-divided according to the experimental conditions.

i) Work Done in Stoppered Flask and in Diffuse Daylight

Solutions of $[\text{PtMe}_2(\text{phen})]$ of varying concentrations were made up in quickfit round bottom flasks (100 mL). Acetone was used as solvent. To these solutions was added a measured amount of ^1PrI , and a non-greased stopper was used to seal the flask. The solutions were left to stand until their colour changed from orange to yellow. Galvinoxyl (10% molar ratio, with respect to Pt(II)) was added to two of the solutions. This produced a mauve colour which persists throughout the reaction. One of these two solutions was left in diffuse daylight, whilst the other was stored in a dark cupboard. The solvent was removed on the rotary evaporator, and the solid residue was redissolved in CH_2Cl_2 (3 mL). On addition of pentane (20 mL) the solid precipitated and was

dried under vacuum. The percentage present of each platinum(IV) complex was evaluated from the ^1H nmr spectra.

ii) Work Done in Open Flask and with Rapid Stirring of Reaction Solution

A series of solutions of $[\text{PtMe}_2(\text{phen})]$ were made up in acetone, and with varying concentrations. The solutions were in unstoppered round bottom flasks (100 mL) and all were stirred vigorously throughout the reaction period, by means of a magnetic stirrer.

To each solution was added ^1PrI . Four of the reaction vessels were left in diffuse daylight (one of which contained a 10% molar ratio amount of galvinoxyl). Two of the solutions (one of which contained a 12% molar ratio of galvinoxyl) were irradiated, from above, using a Cole Parmer Illuminator, and finally one solution was kept in a dark cupboard. The solid product was recovered, in each case, by the method described in the previous section.

iii) Work Done with Constant Air Flow through the Reaction Solution

A solution of $[\text{PtMe}_2(\text{phen})]$ (0.093 g) in acetone (20 mL, 1.15×10^{-2} M) was made up in a two necked round bottom flask, fitted with a glass frit bubbler and a tap outlet. To this was added ^1PrI (0.33 mL, 1.65×10^{-1} M), and air was bubbled through the solution. The solid product was recovered by means of the technique previously described.

2.5.2.8 Qualitative Test for the Peroxide Linkage in $[\text{PtIME}_2(^1\text{PrOO})(\text{phen})]$

A solution of $[\text{PtMe}_2(^1\text{PrOO})(\text{phen})]$ (0.03 g) was made up in a degassed solvent mixture of acetone/acetic acid (10 mL). A small volume of distilled water was degassed by bubbling through nitrogen gas, and using this a saturated solution of NaI was prepared. This solution (5 mL) was added to the solution of the Pt(IV) complex. Initially there was no

change but after 10 minutes a light brown colouration appeared. A few drops of an aqueous solution of $\text{Na}_2\text{S}_2\text{O}_3$ were added and the mixture became clear.

2.5.2.9 Reaction between $t\text{BuI}$ and $[\text{PtMe}_2(\text{phen})]$ Followed by ^1H NMR

A solution of $[\text{PtMe}_2(\text{phen})]$ (0.02 g) was made up in CD_2Cl_2 (0.75 mL), and was transferred to an nmr tube. Some freshly cleaned $t\text{BuI}$ (3 μL) was added to the solution and the mixture thoroughly mixed. The tube was placed in the probe (50°C) of the XL-100 nmr instrument. A series of scans were taken over a period of 1-1/2 hours, during which time the solution was occasionally held in diffuse daylight to induce reaction. On completion of the reaction the solvent was removed under vacuum, the solid residue redissolved in CD_2Cl_2 and the ^1H nmr recorded.

2.5.2.10 Decomposition of $[\text{PtIME}_2(t\text{BuOO})(\text{phen})]$ in Solution, Followed by ^1H NMR

A solution of $[\text{PtIME}_2(t\text{BuOO})(\text{phen})]$ (0.02g) contaminated with $[\text{PtIME}_2(\text{phen})\text{I}]$ was made up in acetone- d_6 (0.75 mL), transferred to an nmr tube and placed in the probe of an XL-100 nmr instrument. The relative peak heights of the Pt-Me signal, for each of the Pt(IV) complexes, were measured relative to the acetone- d_6 signal at 2.04 ppm. Several spectra were recorded over a period of 20 hours and the relative peak heights measured in each case. Finally a small sample of $t\text{BuOH}$ (2 μL) was added to the solution and the ^1H nmr spectrum recorded.

2.5.2.11 Kinetics of the Reaction between $i\text{PrI}$ and $[\text{PtMe}_2(\text{phen})]$

A series of experiments were performed, on the Cary 118 and the Hewlett Packard Diode Array Spectrophotometers, and these will be described in this section.

i) Determination of the Rate Constant for the Reaction

A solution of $[\text{PtMe}_2(\text{phen})]$ (0.008 g) in acetone (39.0 mL, 5.0×10^{-4} M) was made up and to this was added ^1PrI (1.0 mL). The solution was thoroughly shaken and a sample of it transferred to a 1 cm quartz cuvette which was quickly placed in the thermostatically controlled (25°C) compartment of a Cary 118 Spectrophotometer. The absorbance at 472.7 nm was monitored with time. The reaction was followed over five half-lives. The experiment was repeated several times using the same mass of $[\text{PtMe}_2(\text{phen})]$ (0.008 g) in a total of 40 mL of solvent, but varying the concentration of ^1PrI . A similar series of experiments were performed using degassed acetone. This was done by bubbling N_2 gas through the acetone for 40 minutes.

ii) Effect of Galvinoxyl on the Reaction Rate

A solution of $[\text{PtMe}_2(\text{phen})]$ (0.008 g) was made up in acetone (36 mL) and to it was added ^1PrI (4.0 mL). A portion of the sample was transferred to a 1 cm quartz cuvette and placed in the cell compartment of the Cary 118 instrument. The absorbance was monitored at 472.7 nm with time and when the reaction rate was increasing noticeably a small volume of galvinoxyl solution in acetone (0.1 mL, 5% molar ratio with respect to Pt(II)) was added. This was repeated for a degassed sample of the reaction solution.

A similar experiment was performed only in this case the galvinoxyl was present at the start of the reaction. A solution of $[\text{PtMe}_2(\text{phen})]$ (0.008 g) was made up in degassed acetone (36 mL) and to it was added some galvinoxyl (0.001 g, approx. 10% molar ratio with respect to Pt(II)). To this solution was added ^1PrI (4.0 mL) and a portion of the resulting solution quickly transferred to a 1 cm quartz

cuvette. This was placed in the cell compartment of the Cary 118 Spectrophotometer and the absorbance of 472.7 nm recorded with time.

iii) Experiment to Show 1st Order Dependence of the Concentration of $[PtMe_2(phen)]$ on the Reaction Rate

A solution of $[PtMe_2(phen)]$ (0.028 g) in acetone (70.0 mL) was made up. A portion of this solution (10.0 mL) was pipetted into acetone (26.0 mL) and to it was added 1PrI (4.0 mL). A portion was put in a 1 cm quartz cell and the absorbance at 472.7 nm was measured with time on the Cary 118 instrument.

The work was repeated keeping the concentration of 1PrI constant, but varying the concentration of the $[PtMe_2(phen)]$.

iv) Irradiation of the Reaction Solution

A solution of $[PtMe_2(phen)]$ (3.0×10^{-4} M) was made up in acetone and to a sample of it in a 1 cm quartz cuvette was added 1PrI (0.25 mL of a 4.5 M solution). Several spectra of the solution were recorded between 600 and 300 nm. The sample was then irradiated from above using a Cole Parmer Illuminator and the spectrum recorded whilst the light was shining.

The experiment was also performed by monitoring the absorbance at 472.7 nm whilst periodically irradiating the sample.

A further extension of this work was to irradiate the sample and add a portion of galvinoxyl (4% molar ratio with respect to Pt(II)) once the reaction was proceeding at a fast rate.

2.5.2.12 Irradiation of the Reaction between 1PrBr and $[PtMe_2(phen)]$, Followed by UV/Visible Spectroscopy

A solution of $[PtMe_2(phen)]$ (2.7×10^{-4} M) was made up in acetone and a sample (2.0 mL) transferred to a 1 cm quartz cuvette. To this was added 1PrBr (2.3 mL, 4.6 M) and the UV/visible spectrum was

recorded periodically from 600 to 325 nm. The Hewlett Packard Diode Array instrument was used. After 10 minutes the sample was irradiated from above, using a Cole Parmer Illuminator, for a period of 30 minutes and the spectrum recorded.

2.5.2.13 Kinetic Experiments for the Reaction between ^tBuI and $[\text{PtMe}_2(\text{phen})]$

This work was done using the Hewlett Packard Diode Array Spectrophotometer, and in diffuse daylight unless otherwise stated.

i) Following the Reaction by Means of the UV/Visible Spectrum of the Reaction Mixture

A solution of $[\text{PtMe}_2(\text{phen})]$ was made up in acetone (5.0×10^{-4} M). To a sample (5.0 mL) of this was added a solution of freshly cleaned ^tBuI (5.0 mL, 1.0×10^{-2} M) in acetone. A sample of the reaction solution was quickly transferred to a 1 cm quartz cuvette held in the cell compartment of the Diode Array Spectrophotometer. A series of scans from 600 to 325 nm were made over a period of 20 minutes and the spectrum of the final product was recorded.

ii) Irradiation of the Reaction Mixture

To an acetone solution of $[\text{PtMe}_2(\text{phen})]$ (1.5 mL, 1.5×10^{-3} M), in a 1 cm quartz cell, was added a ^tBuI acetone solution (1.5 mL, 8.4×10^{-3} M). The cell was quickly placed in the cell compartment and the absorbance at 472.7 nm recorded with time. After 4 minutes the sample was irradiated from above for 1 minute. The process was repeated a short while later and at this point a solution of galvinoxyl (0.25 mL, 4% molar ratio with respect to Pt(II)) was added. The sample continued to be irradiated. The UV/visible spectrum of the product was recorded.

iii) Growth of the Peak at 371 nm

To a solution of $[\text{PtMe}_2(\text{phen})]$ (1.0 mL, 1.4×10^{-3} M) in

acetone, was added a solution of t -BuI (2.0 mL, 8.4×10^{-2} M) in acetone. The resultant solution was transferred to a 1 cm quartz cuvette and spectra (600-325 nm) recorded periodically and the absorbance at 371 nm noted accurately.

2.6 Preparative Work and Experimental Details of the Work in Chapter 6

The α,β -unsaturated olefins used in this work were purified by distillation on the vacuum line, and all work was done in diffuse daylight, unless otherwise stated.

2.6.1 Preparative Work

2.6.1.1 [PtMe₂{CH(CHO)CH₂¹Pr}(phen)]

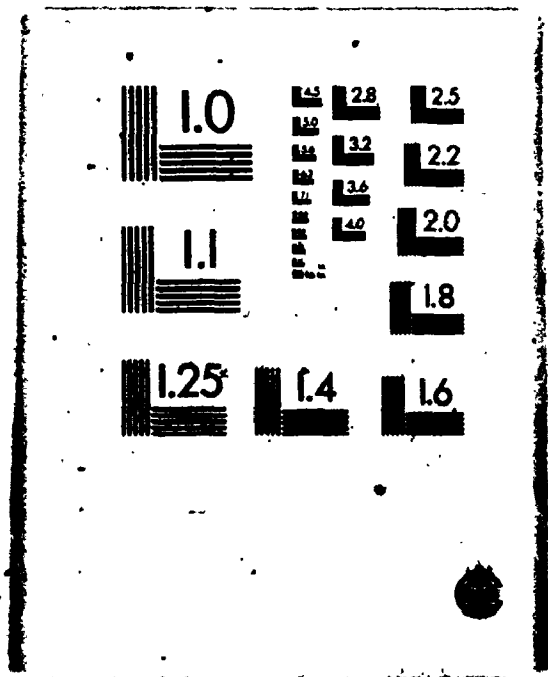
A portion of acetone (30 mL) was degassed on the vacuum line by three cycles of freeze/thawing. After this the acetone (25 mL) was quickly transferred to a two necked round bottom flask which was fitted with a glass frit bubbler, a tap outlet and contained a sample of [PtMe₂(phen)] (0.058 g). Nitrogen gas was bubbled through the solution for 10 minutes after which time some acrolein (2 mL) was added, followed by ¹PrI (1 mL).

Nitrogen was bubbled through during the reaction. The solution turned yellow in 15 minutes. The solvent was removed under vacuum and the solid residue redissolved in CH₂Cl₂ (3 mL). The solid was recovered by precipitation using pentane (20 mL) and dried on the vacuum line. Yield 70%, mp 195-198°C. The same procedure was used for all the preparative work in this section.

2.6.1.2 [PtMe₂{CH(CN)CH₂¹Pr}(phen)]

A solution of [PtMe₂(phen)] (0.043 g), in degassed acetone

4 4
OF / DE



(25 mL), was made up and to it was added a sample of acrylonitrile (3 mL), followed by ^1PrI (1 mL). The reaction was done under N_2 . The solution turned yellow in about 1 hour and the solid product was recovered in the usual way.

2.6.1.3 $[\text{PtIME}_2\{\text{CH}(\text{COMe})\text{CH}_2^1\text{Pr}\}(\text{phen})]$

A solution of $[\text{PtMe}_2(\text{phen})]$ (0.106 g) in degassed acetone (3.5 mL), was made up and to it was added methyl vinyl ketone (2.5 mL) followed by ^1PrI (0.75 mL). The reaction was done under nitrogen and took about 40 minutes to go to completion. The solid product was recovered in the usual manner. It was found by ^1H nmr to contain predominantly the desired product along with small traces of polymer, $[\text{PtIME}_2(^1\text{Pr})(\text{phen})]$, $[\text{PtI}_2\text{Me}_2(\text{phen})]$ and $[\text{PtIME}_2(\text{Et})(\text{phen})]$. The latter was formed due to the presence of a small percentage of EtI in the ^1PrI .

The product was dissolved in a small volume of CHCl_3 (2 mL) in a glass vial and some pentane was carefully applied on top of the solution. This was left for several days at -5°C when crystalline material formed. This was found by ^1H nmr to be predominantly the impurities, leaving the mother liquor enriched in the desired product. The solid product was recovered from the mother liquor by addition of pentane (10 mL) and dried under vacuum.

2.6.1.4 Reaction between ^1PrI , Styrene and $[\text{PtMe}_2(\text{phen})]$

A solution of $[\text{PtMe}_2(\text{phen})]$ (0.043 g) in degassed acetone (25 mL) was made up and to it was added styrene (3 mL) followed by ^1PrI (1 mL). The reaction was done under N_2 and the solid product recovered by the usual method. The ^1H nmr showed the presence of mainly polystyrene (confirmed with an authentic sample), unreacted styrene, $[\text{PtIME}_2(^1\text{Pr})(\text{phen})]$ and a small trace of $[\text{PtI}_2\text{Me}_2(\text{phen})]$.

2.6.1.5 Reaction between Methyl Methacrylate ^1PrI and $[\text{PtMe}_2(\text{phen})]$

A solution of $[\text{PtMe}_2(\text{phen})]$ (0.042 g) was made up in degassed acetone (25 mL) and to it was added methyl methacrylate (3 mL) followed by ^1PrI (1 mL). The reaction was done under N_2 and took 5 hours to go to completion. The solid product was recovered in the usual way and the ^1H nmr showed it to contain predominantly polymethyl methacrylate (confirmed by comparison with authentic sample) along with traces of $[\text{PtIME}_2(^1\text{Pr})(\text{phen})]$.

2.6.1.6 $[\text{PtIME}_2\{\text{CH}(\text{CN})\text{CH}_2^t\text{Bu}\}(\text{phen})]$

A solution of $[\text{PtMe}_2(\text{phen})]$ (0.09 g) in degassed CH_2Cl_2 (10 mL) was prepared and to it was added acrylonitrile (2.5 mL) followed by ^tBuI (0.2 mL). The reaction was done under N_2 , and in the dark and took 1 hour to go to completion. The sample was recovered by the usual technique and dried under vacuum. Yield 78%, mp 246°C .

2.6.1.7 $[\text{PtIME}_2\{\text{CH}(\text{CHO})\text{CH}_2^t\text{Bu}\}(\text{phen})]$

A solution of $[\text{PtMe}_2(\text{phen})]$ (0.09 g) in degassed CH_2Cl_2 (10 mL) was prepared and to it was added acrolein (2.5 mL) followed by ^tBuI (0.2 mL). The reaction was done under N_2 , in the dark, and went to completion in 1/2 hour. The solid was recovered in the usual manner. Yield 80%.

2.6.1.8 Reaction between $\text{CH}_2\text{CH}(\text{CN})$ and $[\text{PtMe}_2(\text{phen})]$

To a solution of $[\text{PtMe}_2(\text{phen})]$ (0.08 g) in degassed acetone (35 mL) was added $\text{CH}_2\text{CH}(\text{CN})$ (7 mL). The solution became yellow in about 5 hours. The solid was recovered in the usual manner. It was found to be very insoluble in the common solvents.

2.6.2 Other Experimental Details of the Work in Chapter 6

2.6.2.1 Competition Experiment for the Reaction of $t\text{BuI}$ and $i\text{PrI}$, in the Presence of $\text{CH}_2\text{CH}(\text{CN})_2$, with $[\text{PtMe}_2(\text{phen})]$

A solution of $[\text{PtMe}_2(\text{phen})]$ (0.035 g) in degassed CH_2Cl_2 (25 mL) was prepared and to it was added acrylonitrile (1.15 mL). Nitrogen gas was now bubbled through the solution for 10 minutes after which a mixture of $i\text{PrI}$ and $t\text{BuI}$ (1.0 mL, 1:1 ratio by volume) was added and the solution was left to react in diffuse daylight and under N_2 . On completion of the reaction the solid product was recovered by the technique already described and the sample analysed by ^1H nmr.

Two more reactions were performed varying only the relative amounts of $t\text{BuI}$ and $i\text{PrI}$.

2.6.2.2 Competition Reaction between $[\text{PtMe}_2(\text{phen})]$ and Methyl Vinyl Ketone for $i\text{Pr}$ Radicals

A sample of acetone (45 mL) was degassed by a thaw/freeze cycle on the vacuum line and to it was added $[\text{PtMe}_2(\text{phen})]$ (0.081 g) and $\text{CH}_2\text{CHC}(\text{O})\text{Me}$ (0.4 mL). Nitrogen gas was bubbled through the solution and $i\text{PrI}$ (2 mL) was added. On completion of the reaction the solid product was recovered in the usual way, dried under vacuum, and analysed by ^1H nmr.

The procedure was repeated twice more, varying the concentration of each reagent.

2.6.2.3 Reaction of CH_2I_2 , and $[\text{PtMe}_2(\text{phen})]$ in the Presence of Acrolein

To a solution of $[\text{PtMe}_2(\text{phen})]$ (0.045 g) in acetone (25 mL, not degassed) was added acrolein (2.3 mL) followed by CH_2I_2 (0.5 mL). The solution immediately turned yellow and the solvent was removed on the rotary evaporator. The solid residue was redissolved in CH_2Cl_2 and

precipitated by the addition of pentane (20 mL). The solid was dried under vacuum.

2.6.2.4 Reaction of CH_2I_2 and $[\text{PtMe}_2(\text{phen})]$ in the Presence of Acrylonitrile

To a solution of $[\text{PtMe}_2(\text{phen})]$ (0.058 g) in acetone (30 mL, not degassed) was added acrylonitrile (5 mL) followed by CH_2I_2 (0.2 mL). The solution immediately turned yellow and somewhat cloudy. The solid product was isolated as described in the previous section and dried under vacuum.

A similar reaction was performed in CD_2Cl_2 . To a solution of $[\text{PtMe}_2(\text{phen})]$ (0.021 g) in CD_2Cl_2 (1 mL, not degassed) was added acrylonitrile (0.25 mL) followed by CH_2I_2 . A small amount of white precipitate formed and after 3 days the mother liquor was removed and analysed by ^1H nmr.

2.6.2.5 Reaction of $\text{I}(\text{CH}_2)_2\text{I}$ and $[\text{PtMe}_2(\text{phen})]$ in the Presence of Acrylonitrile

To a solution of $[\text{PtMe}_2(\text{phen})]$ (0.043 g) in acetone (30 mL, not degassed) was added acrylonitrile (3 mL) followed by freshly purified $\text{I}(\text{CH}_2)_2\text{I}$ (0.3 g). The reaction solution was left to stand for 1 hour during which time a red-brown precipitate (presumably $[\text{Pt}_2\text{I}_2\text{Me}_4\{(\text{CH}_2)_2\}(\text{phen})_2]$) had formed. The solution was filtered and the solid product in the filtrate recovered as previously described.

2.6.2.6 Ratio of the Products Formed by the Reaction of $[\text{PtMe}_2(\text{phen})]$ with ^1PrI and $\text{CH}_2\text{CH}(\text{CN})$

To a solution of $[\text{PtMe}_2(\text{phen})]$ (0.043 g) in degassed acetone (25 mL, 4.2×10^{-3} M) was added acrylonitrile (0.33 mL) followed by ^1PrI (1.0 mL). The reaction was done under N_2 , and went to completion in 1 hour. The solid product was isolated as previously described and analysed by ^1H nmr. A series of similar experiments was performed

varying only the concentration of the acrylonitrile.

A further two experiments were performed this time in the dark, using in the one case distilled acrylonitrile and in the other undistilled acrylonitrile. The solid products were analysed by ^1H nmr.

2.6.2.7 Kinetics of the Reaction between ^1PrI , $[\text{PtMe}_2(\text{phen})]$ and $\text{CH}_2\text{CH}(\text{CN})$

This work was performed on the Hewlett Packard 8450A Diode Array Spectrophotometer. A series of experiments was performed under differing conditions and these will be described in this section.

i) Determination of Rate Constant for Reaction in the Dark

To a solution of $[\text{PtMe}_2(\text{phen})]$ (0.008 g) in acetone (35 mL) was added acrylonitrile (1.0 mL) and the sample was degassed by a series of freeze/thaw cycles on the vacuum line. The solution was stored under nitrogen gas and an aliquot (5.0 mL) was transferred to a 1 cm quartz cuvette, and sealed with a serum cap. Nitrogen gas was bubbled through the solution in the cuvette by means of a syringe needle and finally a sample of ^1PrI (1.0 mL) was introduced through the syringe needle (in the dark). The cuvette was placed in the cell compartment of the UV/visible spectrophotometer and the decay of the band at 472.7 nm was monitored with time.

This procedure was repeated using the same concentrations of $[\text{PtMe}_2(\text{phen})]$, and ^1PrI but varying that of $\text{CH}_2\text{CH}(\text{CN})$.

ii) Addition of Radical Inhibitor, in Diffuse Daylight

To a solution of $[\text{PtMe}_2(\text{phen})]$ (0.004 g) in degassed acetone (20.0 mL, 5.0×10^{-4} M) was added $\text{CH}_2\text{CH}(\text{CN})$ (0.8 mL, undistilled). The acrylonitrile contained a small percentage (approx. 1%) of the radical inhibitor 4-methoxyphenol. A sample of the solution (5.0 mL) was transferred to a 1 cm quartz cuvette and sealed with a serum cap and N_2

bubbled through for 5 minutes. To this was added ^1PrI (0.10 ml) and the absorbance was followed at 472.7 nm with time (in diffuse daylight). The experiment was repeated in order to confirm the observation.

A similar experiment was performed, using distilled acrylonitrile and in the presence of galvinoxyl (20% molar ratio with respect to the Pt(II)).

A reaction was performed without the presence of the radical scavengers.

TABLE 7.1: ^1H NMR Data for Complexes in Chapter 2

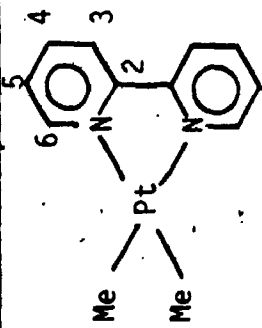
Complex ^a	PtMe δ /ppm.	$^2\text{J}(\text{PtH})/\text{Hz}$	PtOR ^b δ /ppm	J/Hz	N^{C} δ /ppm	J/Hz
	1.14	86			9.28(H_6) ^d	5.2($\text{J}_{5,6}$), 1.5($\text{J}_{4,6}$)
					7.52(H_5)	7.2($\text{J}_{4,5}$), 1.5($\text{J}_{3,4}$)
					8.02(H_4)	7.7($\text{J}_{3,4}$)
					8.06(H_3)	
$[\text{PtMe}_2(\text{OMe})(\text{bipy})(\text{OH}_2)]^+$	1.71	73	2.75	41.0(J_{PtH})	9.04(H_6) ^e	5.0($\text{J}_{5,6}$)
					7.67(H_5)	8.0($\text{J}_{4,5}$) 1.3($\text{J}_{3,5}$)
					8.06(H_4)	7.5($\text{J}_{3,4}$)
					8.20(H_3)	
$[\text{PtMe}_2(\text{OEt})(\text{bipy})(\text{OH}_2)]^+$	1.80	72.5	2.90(CH_2)	14(J_{PtH})	9.03(H_6) ^f	5($\text{J}_{6,6}$) 1.5($\text{J}_{4,6}$)
			0.74(CH_3)	7(J_{HH})	7.67(H_5)	8($\text{J}_{4,5}$) 1.3($\text{J}_{3,5}$)
					8.05(H_4)	8($\text{J}_{3,4}$)
					8.20(H_3)	
$[\text{PtMe}_2(\text{O}^i\text{Pr})(\text{bipy})(\text{OH}_2)]^+$	1.82	73	2.84(CH)		9.04(H_6) ^g	5($\text{J}_{5,6}$)
			0.60(CH_3)	6(J_{HH})	7.64(H_5)	7($\text{J}_{4,5}$)
					8.05(H_4)	7($\text{J}_{3,4}$)
					8.19(H_3)	

TABLE 7.1: ¹H NMR Data for Complexes in Chapter 2

Complex ^a	PtMe δ/ppm	2J(PtH)/Hz	PtOR ^b δ/ppm	J/Hz	N ^c δ/ppm	J/Hz
[PtMe ₂ (OH)(bipy)(OH ₂)] ⁺	1.84	70			9.02(H ₆) ^h	5.5(J _{5,6}) 1.5(J _{4,6})
					7.90(H ₅)	8.0(J _{4,5}) 1.5(J _{3,5})
					8.34(H ₄)	8.1(J _{3,4})
					8.72(H ₃)	
	1.15	86.5			9.51(H ₂) ⁱ	5.2(J _{2,3})
					7.82(H ₃)	8.0(J _{3,4})
					8.63(H ₄)	1.3(J _{2,4})
					7.92(H ₅)	
[PtMe ₂ (OMe)(phen)(OH ₂)] ⁺	1.80	72.5	2.65	40(J _{PtH})	9.32(H ₂) ^j	5.0(J _{2,3})
					8.03(H ₃)	8.0(J _{3,4})
					8.62(H ₄)	1.8(J _{2,4})
					8.07(H ₅)	
[PtMe ₂ (OEt)(phen)(OH ₂)] ⁺	1.79	73	2.85(CH ₂)	21(J _{PtH})	9.30(H ₂) ^k	5(J _{2,3})
			0.59(CH ₃)	7(J _{HH})	8.01(H ₃)	7(J _{3,4})
					8.60(H ₄)	2(J _{2,4})
					8.06(H ₅)	

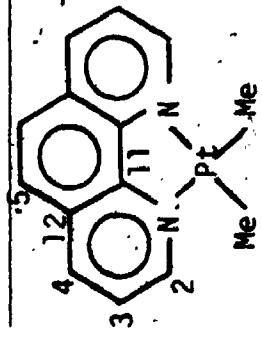


TABLE 7.1: ¹H NMR Data for Complexes in Chapter 2

Complex ^a	PtMe δ/ppm	² J(PtH)/Hz	PtOR ^b δ/ppm	J/Hz	N ^c δ/ppm	J/Hz
[PtMe ₂ (O ⁱ Pr)(phen)(OH ₂)] ⁺	1.84	73	2.89(CH) 0.48(CH ₃)	40(J _{PtH}) 6(J _{HH})	9.32(H ₂) ⁻ , 8.0(H ₃), 8.51(H ₄), 7.98(H ₅)	5(J _{2,3}) 8(J _{3,4}) 1.5(J _{2,4})
[PtMe ₂ (OH)(phen)(OH ₂)] ⁺	1.73	72.5			9.30(H ₂) 8.0(H ₃) 8.61(H ₄) 8.05(H ₅)	
[PtMe ₂ (OMe)Cl(phen)-J]	2.03	71	2.40	58(J _{PtH})	9.40(H ₂) ^m , 8.28(H ₃) ⁿ , 8.99(H ₄), 8.33(H ₅)	5(J _{2,3}) 8(J _{3,4}) 1.5(J _{2,4})

^a¹H nmr Data, in CDCl₃, for: [Pt₂Me₄(μ-SMe₂)₂], δ(MePt) 0.63, ²J(PtH) 85, δ(MeS) 2.75, ³J(PtH) 20 (1:8:18:8:1 quintet); *cis*-[PtCl₂(SMe₂)₂], δ(MeS) 2.55, ³J(PtH) 50; *trans*-[PtCl₂(SMe₂)₂]; δ(MeS) 2.44, ³J(PtH) 40. ^bR = H, Me, Et or ⁱPr. ^cN = bipy or phen, solvent CD₂Cl₂. ^dJ(PtH) 22. ^eJ(PtH) 12. ^fJ(PtH) 13. ^gJ(PtH) 16. ^hJ(PtH) 16. ⁱJ(PtH) 12. ^jJ(PtH) 15. ^kJ(PtH) 16. ^mJ(PtH) 12.

TABLE 7.2: ^{13}C - $\{^1\text{H}\}$ NMR Data for Complexes in Chapter 2

Complex ^a	PtMe	$^1\text{J}(\text{PtC})/\text{Hz}$		PtOR ^b	$^1\text{J}(\text{PtC})/\text{Hz}$		δ/ppm	$\text{N} \text{ } ^{13}\text{C}$	δ/ppm	$\text{J}(\text{PtC})/\text{Hz}$
	δ/ppm			δ/ppm						
$[\text{PtMe}_2(\text{OMe})(\text{bipy})(\text{OH}_2)]^+$	-2.30	701		57.32		$18(^2\text{J}_{\text{PtC}})$	147.6 (C ₆)		10.8	
							126.8 (C _{5'})		12	
							139.1 (C ₄)		-	
							123.4 (C ₃)		-	
							155.0 (C ₂)		8	
$[\text{PtMe}_2(\text{QEt})(\text{bipy})(\text{OH}_2)]^+$	-2.60	700		64.0 (CH ₂ O)		$15(^2\text{J}_{\text{PtC}})$	126.8 (C ₅)			
				19.7 (CH ₃ >C)		$43(^3\text{J}_{\text{PtC}})$	139.6 (C ₄)			
							124.0 (C ₃)			
							153.3 (C ₂)			
$[\text{PtMe}_2(\text{OMe})(\text{phen})(\text{OH}_2)]^+$	-2.58	696		57.07		$24(^2\text{J}_{\text{PtC}})$	131.26 (C ₁₂)			
							146.66 (C ₁₁)			
							127.65 (C ₅)			
							138.24 (C ₄)			
							125.46 (C ₃)			
							147.15 (C ₂)			

TABLE 7.2: $^{13}\text{C}\{-^1\text{H}\}$ NMR Data for Complexes in Chapter 2

Complex ^a	PtMe δ/ppm	$\text{J}(\text{PtC})/\text{Hz}$	PtOR ^b δ/ppm	J/Hz	$\overline{\text{N}}^{\text{c}}$ δ/ppm	$\text{J}(\text{PtC})/\text{Hz}$
[PtMe ₂ (OEt)(phen)(OH ₂)] ⁺	-2.30	696	64.03 (CH ₂ -O)	16 (² J _{PtC})	131.14 (C ₁₂)	
			19.73 (CH ₃ -C)	36 (³ J _{PtC})	147.23 (C ₁₁)	
					127.62 (C ₅)	
					138.23 (C ₄)	
					125.39 (C ₃)	
[PtMe ₂ (O ⁱ Pr)(phen)(OH ₂)] ⁺	-2.89	720	68.65 (C-O)		131.39 (C ₁₂)	
			27.39 (CH ₃ -C)	24 (³ J _{PtC})	147.08 (C ₁₁)	
					127.90 (C ₅)	
					138.60 (C ₄)	
					125.53 (C ₃)	
				147.116 (C ₂)		

^aSolvent CD₂Cl₂.^bR = Me, Et, or ⁱPr.^cN = bipy, or phen.

TABLE 7.3: ^1H NMR Data for Complexes in Chapter 3

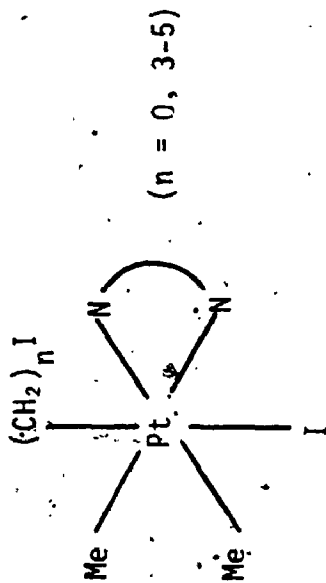
Complex ^a	PtMe δ/ppm	$^2\text{J}(\text{PtH})/\text{Hz}$	PtR ^b δ/ppm	J/Hz	N N^c δ/ppm	J/Hz
[PtMe ₃ (phen)]	1.63	71.5	0.65	73 ($^2\text{J}_{\text{PtH}}$)	9.32 (H ₂) ^d 7.92 (H ₃) 8.60 (H ₄) 8.08 (H ₅)	5.0 (J _{2,3}) 8.0 (J _{3,4}) 1.5 (J _{2,4})
[PtMe ₂ (Et)(phen)]	1.63	71.5	-0.11 (CH ₃) 1.48 (CH ₂)	68.41 ($^3\text{J}_{\text{PtH}}$) 72.0 ($^2\text{J}_{\text{PtH}}$)	9.25 (H ₂) ^e 7.87 (H ₃) 8.50 (H ₄) 7.97 (H ₅)	4.98 (J _{2,3}) 8.19 (J _{3,4}) 1.43 (J _{2,4})
[PtMe ₂ (ⁿ Pr)(phen)]	1.60	72.5	0.43 (CH ₃ , broad) 1.4 (Pt-CH ₂)		9.27 (H ₂) ^f 7.97 (H ₃) 8.60 (H ₄) 8.06 (H ₅)	5.09 (J _{2,3}) 8.0 (J _{3,4}) 1.4 (J _{2,4})
[PtMe ₂ (ⁿ Bu)(phen)]	1.63	71.4	0.43 (CH ₃) 0.87 (CH ₂ CH ₂)	7.1 ($^3\text{J}_{\text{HH}}$)	9.26 (H ₂) ^g 7.89 (H ₃) 8.51 (H ₄) 7.97 (H ₅)	5.09 (J _{2,3}) 8.19 (J _{3,4}) 1.4 (J _{2,4})
[PtBrMe ₂ (Et)(phen)]	1.47	71.1	0.04 (CH ₃)	65.4 ($^3\text{J}_{\text{PtH}}$) 7.6 ($^3\text{J}_{\text{HH}}$)	9.22 (H ₂) ^h 7.96 (H ₃) 8.58 (H ₄) 8.02 (H ₅)	5.05 (J _{2,3}) 8.0 (J _{3,4}) 1.2 (J _{2,4})

TABLE 7.3: $^1\text{H-NMR}$ Data for Complexes in Chapter 3

Complex ^a	PtMe		PtR ^b		N ^c	
	δ/ppm	$^2J(\text{PtH})/\text{Hz}$	δ/ppm	J/Hz	δ/ppm	J/Hz
[PtBrMe ₂ (ⁿ Pr)(phen)]	1.47	71.0	0.50	(CH ₃ , broad)	9.22 (H ₂) ^d	5.0 (J _{2,3})
					7.96 (H ₃)	8.0 (J _{3,4})
					8.58 (H ₄)	1.5 (J _{2,4})
					8.04 (H ₅)	
[PtI Me ₂ {(CH ₂) ₄ CH ₃ }(phen)]	1.60	71.5	0.48	(CH ₃ , broad)	9.26 (H ₂)	
					7.90 (H ₃)	
					8.51 (H ₄)	
					7.98 (H ₅)	
[Pt(CH ₂ CHCH ₂ CH ₂)Me ₂ (phen)Br]	1.66	71.5	1.36	(PtCH ₂ , d)	9.41 (H ₂)	5.0 ^e (J _{2,3})
					7.89 (H ₃)	8.0 (J _{3,4})
			-0.57	CH ₂ CH ₂ CH (broad)	8.51 (H ₄)	1.5 (J _{2,4})
			-0.80		7.96 (H ₅)	

^aSolvent, CD₂Cl₂.^bR = Me, Et, ⁿPr, ⁿBu, (CH₂)₄CH₃, CH₂-CHCH₂CH₂.^cN = phen.^dJ(PtH) 18.^eJ(PtH) 18.^fJ(PtH) 17.^gJ(PtH) 18:5.^hJ(PtH) 17.ⁱJ(PtH) 18.

TABLE 7.4: ^1H NMR Data for Complexes in Chapter 4 of General Structure



Complex ^a	Pt-Me δ /ppm	$^2J(\text{PtH})/\text{Hz}$	$(\text{CH}_2)_n$ δ /ppm	J/Hz	$\overline{N} \overline{b}$ δ /ppm	J/Hz
$[\text{PtI}_2\text{Me}_2(\text{phen})]$	2.53	74.0			9.25 (H_2) ^c	5.0 ($J_{2,3}$)
					8.01 (H_3)	8.0 ($J_{3,4}$)
					8.58 (H_4)	1.6 ($J_{2,4}$)
					8.10 (H_5)	
<i>trans</i> - $[\text{PtI}(\text{Me}_2\{(\text{CH}_2)_3\text{I}\})-$ $(\text{phen})]$ ^d	1.61	71	2.73 (CH_2I)	7 ($^3J_{\text{HH}}$)	9.25 (H_2) ^e	5.0 ($J_{2,3}$)
			0.4 (H) _{α}		7.99 (H_3)	8.5 ($J_{3,4}$)
					8.62 (H_4)	
					8.09 (H_5)	1.6 ($\text{H}_{2,4}$)
<i>cis</i> - $[\text{PtI}(\text{Me}_2\{(\text{CH}_2)_3\text{I}\})-$ $(\text{phen})]$	1.63 (<i>trans</i> to N)	72	3.41 (CH_2I) ^f			
	0.65 (<i>trans</i> to I)	72				

TABLE 7.4: ^1H NMR Data for Complexes in Chapter 4
of General ...

Complex ^a	Pt-Me δ /ppm	$^2J(\text{PtH})/\text{Hz}$	$(\text{CH}_2)_n$ δ /ppm	J/Hz	$\sum N^b$ δ /ppm	J/Hz
<i>trans</i> -[PtIME ₂ {(CH ₂) ₄ I}-(phen)]	1.64	71.5	2.92 (CH ₂ I)	6.5 ($^3J_{\text{HH}}$)	9.27 (H ₂) ^f	6.0 (J _{2,3})
				0.87 (H _{α})	7.91 (H ₃)	8.5 (H _{3,4})
					8.51 (H ₄)	1.7 (J _{2,4})
					7.99 (H ₅)	
<i>cis</i> -[PtIME ₂ {(CH ₂) ₄ I}-(phen)] ^g	1.66 (<i>trans</i> to N) 0.59 (<i>trans</i> to I)	72 73	3.35 (CH ₂ I)	6.5 ($^3J_{\text{HH}}$)		
<i>trans</i> -[PtIME ₂ {(CH ₂) ₅ I}-(phen)]	1.60	71.5	2.90 (CH ₂ I)	6.9 ($^3J_{\text{HH}}$)	9.25 (H ₂) ^h	6.0 (J _{2,3})
				1.45 (H _{α})	7.92 (H ₃)	8.0 (J _{3,4})
				0.40 (H _{β})	8.51 (H ₄)	1.7 (J _{2,4})
				0.99 (H _{γ})	8.0 (H ₅)	
				1.39 (H _{δ})		
<i>cis</i> -[PtIME ₂ {(CH ₂) ₅ I}-(phen)]	1.62 (<i>trans</i> to N) 0.65 (<i>trans</i> to I)	71.5 74	3.22 (CH ₂ I)			

TABLE 7.4: ^1H NMR Data for Complexes in Chapter 4
of General

Complex ^a	Pt-Me δ/ppm	$^2\text{J}(\text{PtH})/\text{Hz}$	$(\text{CH}_2)_n$ δ/ppm	J/Hz	$\overline{\text{N}}^b$ δ/ppm	J/Hz
<i>trans</i> -[Pt(Me) ₂ (CH ₂) ₃ I]- (bipy)]	1.51	71.5	3.19 (CH ₂ I)	7.25 ($^3\text{J}_{\text{HH}}$)	8.07 (H ₃) ⁱ	
					8.24 (H ₄)	
					7.68 (H ₅)	
					9.01 (H ₆)	

^aSolvent, CD₂Cl₂.

^b $\overline{\text{N}}$ = phen or bipy.

^cJ(PtH) 18.

^dNotation for carbon chain: Pt-CH₂ ^{α} -CH₂ ^{β} -CH₂I

^eJ(PtH) 20.

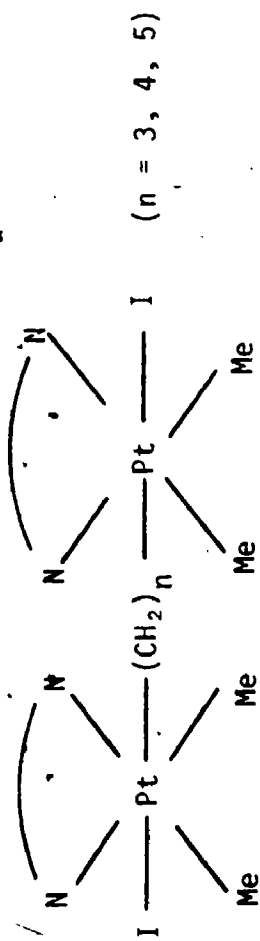
^fJ(PtH) 18.

^gSpectrum run on Bruker WH400.

^hJ(PtH) 17.

ⁱpoor resolution.

TABLE 7.5: ^1H NMR Data for Complexes in Chapter 4 with General Structure



Complex	Pt/Ie δ/ppm	$^2J(\text{PtH})/\text{Hz}$	$(\text{CH}_2)_n^a$ δ/ppm	J/Hz	N^b δ/ppm	J/Hz
<i>trans/trans</i> - $[\text{Pt}_2\text{I}_2\text{Me}_4-$ $\{(\text{CH}_2)_3\}(\text{phen})_2]$ <u>c</u>	1.22	72	Not assigned			
<i>trans/trans</i> - $[\text{Pt}_2\text{I}_2\text{Me}_4-$ $\{(\text{CH}_2)_4\}(\text{phen})_2]$ <u>d</u>	1.58	72	Not assigned			
<i>trans/trans</i> - $[\text{Pt}_2\text{I}_2\text{Me}_4-$ $\{(\text{CH}_2)_5\}(\text{phen})_2]$ <u>f</u>	1.34	70	0.96 (H_α) -0.07 (H_β) 0.4 (H_γ)	64 ($^2J_{\text{PtH}}$) ^g	9.02 (H_2) ^g 7.84 (H_3) 8.49 (H_4) 7.98 (H_5)	5.0 ($J_{2,3}$) 8.5 ($J_{3,4}$) 1.0 ($J_{2,4}$)

TABLE 7.5: ^1H NMR Data for Complexes in Chapter 4
with General Structure ...

Complex	PtMe δ/ppm	$^2\text{J}(\text{PtH})/\text{Hz}$	$(\text{CH}_2)_n^a$ δ/ppm	N N^b δ/ppm	J/Hz	J/Hz
<i>cis/trans</i> - $[\text{Pt}_2\text{I}_2\text{Me}_4-$ $\{(\text{CH}_2)_5\}(\text{phen})_2]$	1.36 (<i>trans</i> to N)	72				
	0.45 (<i>cis</i> to N)	73				
	1.64 ^h	66				

^aNomenclature for carbon chain Pt-($\text{CH}_2-\overset{\alpha}{\text{C}}\text{H}_2-\overset{\beta}{\text{C}}\text{H}_2$)-Pt.

^b $\text{N N} = \text{phen}$.

^cSolvent, D.M.F.-*d*₇.

^dSolvent, acetone-*d*₆.

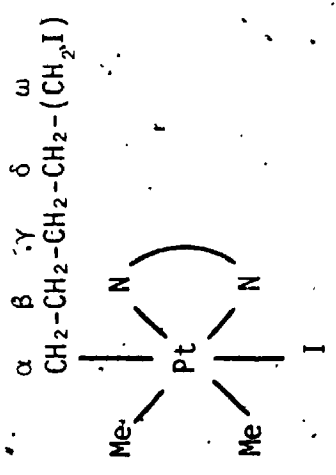
^eJ(PtH) 18.

^fSolvent, CD_2Cl_2 ; spectrum run on Bruker WH400.

^gJ(PtH) 18.

^hTwo peaks due to non-equivalent in plane Me groups. Probably superimposed.

TABLE 7.6: $^{13}\text{C}\{^1\text{H}\}$ NMR Data^a for Complex with Structure

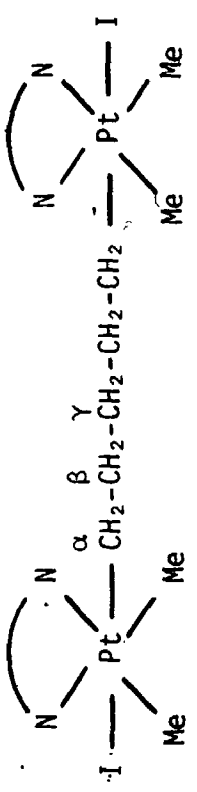


Pt-Me	$^1\text{J(PtC)}/\text{Hz}$	(CH ₂)	J/Hz	δ/ppm	δ/ppm
-5.41	695.8	26.14 (C _α)	662.8 ($^1\text{J}_{\text{PtC}}$)	131.61 (C ₁₂)	
		31.67 (C _β)	87.6 ($^2\text{J}_{\text{PtC}}$)	147.53 (C ₁₁)	
		33.39 (C _γ)	70 ($^3\text{J}_{\text{PtC}}$)	128.126 (C ₅)	
		29.07 (C _δ)	28.7 ($^4\text{J}_{\text{PtC}}$)	138.33 (C ₄)	
		7.34 (C _ω)		125.75 (C ₃)	
				147.67 (C ₂)	

^aSolvent, CD₂Cl₂.

^b $\overline{\text{N-N}}$ = phen.

TABLE 7.7: $^{13}\text{C}\{^1\text{H}\}$ NMR Data^a for the Binuclear Complex



Pt-Me δ/ppm	$^1\text{J}(\text{PtC})/\text{Hz}$	(CH_2) δ/ppm	J/Hz	$\overline{\text{N N}}^b$
-5.45	700	26.403 (C_α)	670 ($^1\text{J}_{\text{PtC}}$)	131.54 (C_{12})
		29.18 (C_β)		146.76 (C_{11})
		30.53 (C_γ)		128.097 (C_5)
				138.25 (C_4)
				125.622 (C_3)
				147.56 (C_2)

^aSolvent, CD_2Cl_2 .

^b $\overline{\text{N N}}$ = phen.

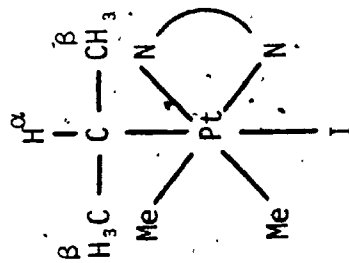
TABLE 7.8: ^1H NMR Data for Complexes in Chapter 4 of General Formula $[\text{PtXMe}_2\{(\text{CH}_2)_X\}(\text{phen})]^{a,d}$

Complex ^b	Pt-Me δ/ppm	$^2J(\text{PtH})/\text{Hz}$	CH_2X δ/ppm	J/Hz	$\text{N}^{c,e}$ δ/ppm	J/Hz
<i>trans</i> -[PtI ₂ (CH ₂ I)(phen)]	1.68	70.5	2.86	40 ($^2J_{\text{PtH}}$)	9.18 (H ₂) ^d	5.0 ($J_{2,3}$)
					8.05 (H ₃)	8.0 ($J_{3,4}$)
					8.63 (H ₄)	1.3 ($J_{2,4}$)
					8.11 (H ₅)	
<i>cis</i> -[PtI ₂ (CH ₂ I)(phen)]	1.80 (<i>trans</i> to N)	72	4.50	80 ($^2J_{\text{PtH}}$)		
					0.84 (<i>trans</i> to N)	26 ($^2J_{\text{PtH}}$)
<i>trans</i> -[PtClMe ₂ (CD ₂ Cl)(phen)]	1.47	70			9.06 (H ₂)	5.0 ($J_{2,3}$)
					7.90 (H ₃)	8.1 ($J_{3,4}$)
<i>cis</i> -[PtClMe ₂ (CD ₂ Cl)(phen)]	1.56 (<i>trans</i> to N)	69			8.50 (H ₄)	1.0 ($J_{2,4}$)
			0.72 (<i>trans</i> to Cl)	74	7.94 (H ₅)	
<i>trans</i> -[PtBrMe ₂ (CH ₂ Br)(phen)]	1.70	68	3.50	43.25 ($^2J_{\text{PtH}}$)	8.97 (H ₂)	5.0 ($J_{2,3}$)
					7.78 (H ₃)	8.0 ($J_{3,4}$)
					8.41 (H ₄)	1.5 ($J_{2,4}$)
					7.85 (H ₅)	

TABLE 7.8: ^1H NMR Data for Complexes in Chapter 4 ...

Complex ^b	Pt-Me δ/ppm	$^2\text{J}(\text{PtH})/\text{Hz}$	CH_2X δ/ppm	$\widehat{\text{N}}\widehat{\text{C}}$ δ/ppm	J/Hz
$\text{cis}[\text{PtBrMe}_2(\text{CH}_2\text{Cl})(\text{phen})]$	1.65, 0.81	70 73.5	5.13 4.51		$^2\text{J}_{\text{PtH}}$ $^2\text{J}_{\text{PtH}}$

^aX = Cl, Br, I.^bSolvent, CDCl_3 . *cis* and *trans* refer to mode of addition. $\widehat{\text{N}}\widehat{\text{C}}$ = phen.^d $\text{J}(\text{PtH})$ -20.

TABLE 7.9: ^1H NMR Data^a for Complex with Structure:

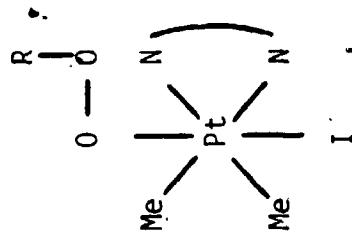
Pt-Me δ /ppm	$^2\text{J}(\text{PtH})/\text{Hz}$	(CH^α) δ /ppm	J/Hz	(CH^β) δ /ppm	J/Hz	$\overline{\text{N N}}^b$ δ /ppm	J/Hz
1.58	72	1.81	6.4 ($^3\text{J}_{\text{HH}}$)	0.16	63. ($^3\text{J}_{\text{PtH}}$)	9.32 (H_2) ^c	5.0 ($\text{J}_{2,3}$)
					6:5 ($^3\text{J}_{\text{HH}}$)	8.0 (H_3)	8.1 ($\text{J}_{3,4}$)
						8.64 (H_4)	
						8.08 (H_5)	1.0 ($\text{J}_{2,4}$)

^aSolvent CD_2Cl_2 .^b $\overline{\text{N N}}$ = phen.^c $\text{J}(\text{PtH})$ 15.

TABLE 7.10: $^{13}\text{C}\{^1\text{H}\}$ NMR Data for $[\text{Pt}(\text{Me})_2\{(\text{CH}_3)_2\text{CH}\}(\text{phen})]$

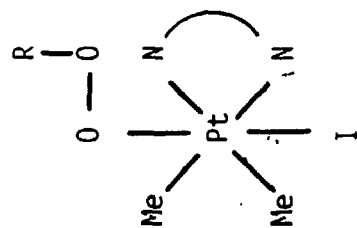
PtMe^{a} δ/ppm	$^1\text{J}(\text{PtC})/\text{Hz}$	(CH) δ/ppm	J/Hz	(CH) δ/ppm	$^2\text{J}(\text{PtC})/\text{Hz}$	$\bar{\text{N}}^{\text{b}}$ δ/ppm	$\text{J}(\text{PtC})/\text{Hz}$
-3.48	730	28.12	not obs.	24.47	32	131.55 (C ₁₂)	
						146.86 (C ₁₁)	
						128.03 (C ₅)	
						138.21 (C ₃)	
						125.64 (C ₃)	~ 20
						148.08 (C ₂)	~ 20

^aSolvent CD_2Cl_2 .^b $\bar{\text{N}}$ = phen.

TABLE 7.11: ^1H NMR Data for Complexes with the Structure:

Complex	PtMe δ/ppm	$^2J(\text{PtH})/\text{Hz}$	$\nu(\text{OOR})^a$ δ/ppm	J/Hz	$\overline{\text{N N}}^b$ δ/ppm	J/Hz
[PtMe ₂ (¹ PrOO)(phen)] ^c	2.03	72	3.10 (CH)	6(³ J _{HH})	9.40 (H ₂) ^d	5.0 (J _{2,3})
					8.03 (H ₃)	8.0 (J _{3,4})
					8.60 (H ₄)	
			0.31 {C(CH ₃) ₂ }		8.08 (H ₅)	1.2 (J _{2,3,4})
[PtMe ₂ (¹ PrOO)(bipy)] ^e	1.83	72	3.22 (CH)	6(³ J _{HH})	8.97 (H ₆)	5.1 (J _{5,6})
					7.65 (H ₅)	1.5 (J _{4,5})
					8.04 (H ₄)	7.0 (J _{4,5})
			0.51 {C(CH ₃) ₂ }		8.24 (H ₃)	
[PtMe ₂ (^t BuOO)(phen)] ^f	1.92	72	0.26 {C(CH ₃) ₃ }		9.32 (H ₂)	5.0 (J _{2,3})
					8.0 (H ₃)	8.0 (J _{3,4})
					8.58 (H ₄)	1.5 (J _{2,3,4})
					8.05 (H ₅)	

^aR = ⁱPr or ^tBu.^cSolvent CD₂Cl₂.^eSolvent CDCl₃.^dJ(PtH) 18.^fSolvent CD₂Cl₂.^bN N = phen or bipy.

TABLE 7.12: $^{13}\text{C}\{^1\text{H}\}$ NMR Data for Complexes with Structure

Complex	PtMe δ/ppm	$^1\text{J}(\text{PtC})/\text{Hz}$	δ/ppm (OOR) ^a	J/Hz	$\overline{\text{N}}^{\text{b}}$ δ/ppm
$[\text{PtIME}_2(^i\text{PrOO})(\text{phen})]_{\text{C}}$	-4.61	~ 600	19.88 (CH ₃) 75.39 (CH)	~ 150	131.36 (C ₁₂) 147.18 (C ₁₁) 127.99 (C ₅) 138.65 (C ₄) 125.00 (C ₃) 147.52 (C ₂)
$[\text{PtIME}_2(^t\text{BuOO})(\text{phen})]_{\text{d}}$	-4.17	630	26.04 (CH ₃) 76.40 (C(CH ₃) ₃)		130.98 (C ₁₂) 145.70 (C ₁₁) 127.78 (C ₅) 138.50 (C ₄) 125.39 (C ₃) 147.50 (C ₂)

^aR = ⁱPr or ^tBu.^cSolvent CD₂Cl₂.^b $\overline{\text{N}}$ = phen.^dSolvent CD₂Cl₂.

TABLE 7.13: ^1H NMR Data for Complexes with Structure

Complex	PtMe		R		X		H _a , B, Y		N N	
	δ/ppm	$^2J(\text{PtH})/\text{Hz}$	δ/ppm	J/Hz	δ/ppm	J/Hz	δ/ppm	J/Hz	δ/ppm	J/Hz
[PtMe ₂ (CH(CN)CH ₂ ^b Pr)(phen)] ^d	1.68	71	0.40	(CH ₃) ₆ (² J _{HH})			2.26	(H _a) ₁₃ (³ J _{H_aH_b})	9.26	(H ₂) ^e
	1.75	72.5	0.70	(CH ₂) ₂ (³ J _{HH})					9.16	(H ₂ ')
			1.43	(CH) ₂ (³ J _{HH})			0.08	(H _B) ₉₂ (² J _{PtH})	7.96	(H ₃)
[PtMe ₂ (CH(CHO)CH ₂ ^d Pr)(phen)] ^d	1.82	71	0.49	(CH ₃) ₆ (³ J _{HH})	8.76	(CHO)			9.17	(H ₂) ^f
	1.88	72	0.64	(CH ₃) ₆ (³ J _{HH})			2.95	(H _a) ₃ (³ J _{MeH_a})	not res.	(H ₂) ^g
			1.17	(CH) ₂ ^e					8.59	(H ₃) ^g
									8.49	(H ₃ ')
									8.01	(H ₃)

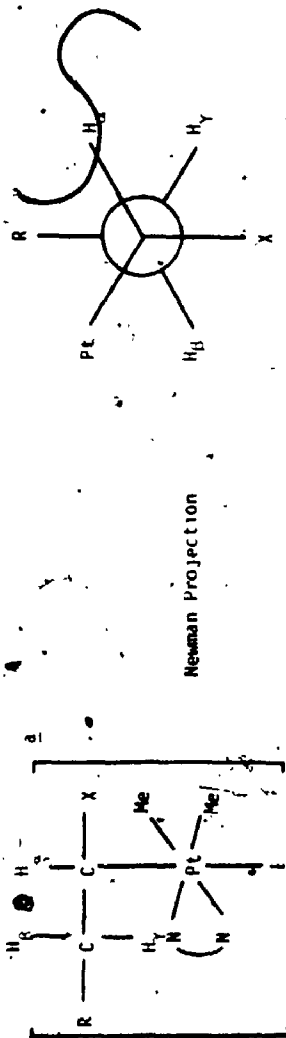


TABLE 7.13: ¹H NMR Data for Complexes with ...

Complex	PtMe δ/ppm	² J(PtH)/Hz	R δ/ppm	X δ/ppm	J/Hz	H _a , β, γ δ/ppm	J/Hz	N, M δ/ppm
[PtMe ₂ (CH(COMe)CH ₂ ^b Pr)- (phen)] ^d	1.74	70	0.52 (CH ₃)	1.40 (COCH ₃)	6.0 (³ J _{HH})	2.94 (H _α)		complex pat. (H ₂)
	1.85	70.5	0.67 (CH ₃)		6.0 (³ J _{HH})			not res. (H ₃) 8.52 (H _α) ^l 8.44 (H _α) ^l 7.97 (H ₃)
[PtMe ₂ (CH(CN)CH ₂ ^b Bu)- (phen)] ^d	1.68	70.5	0.67 (CH ₃)			3.25 (H _α), 2 (³ J _{H_αH_β})}		7.26 (H ₂) ^k , 8.0 (H ₃ , ^l)
	1.76	71.0				12.5 (³ J _{H_αH_β}) 96 (²J_{PtH_α})}}		9.20 (H ₂) ^l 8.02 (H ₃)
[PtMe ₂ (CH(CMO)CH ₂ ^b Bu)- (phen)] ^d	1.81	71.5		8.55 ^o (CHO)		0.23 (H _β) 13 (² J _{H_βH_α})}		8.66 (H ₂)
	1.76	71.5	0.57 (CH ₃)			0.83 (H _γ) 48 (³ J _{PtH})		8.12 (H ₃) 8.06 (H ₃) ^o

^aX = CH, CHO, or C(-O)Me, R = ^bPr or ^cBu. ^dSolvent, CDCl₃. Spectrum run on Bruker AM250 instrument. ^eTwo doublet of doublet patterns. ^fSolvent, CDCl₃. Remaining spectra were run on Varian XL-100 instrument. ^gTentative assignment, due to poor resolution. ^hJ(PtH) 17. ⁱTwo doublet of doublet patterns. ^jSolvent, CDCl₃. ^kTwo doublet of doublet patterns. ^lSolvent, CD₂Cl₂. ^mTwo doublet of doublet patterns, J(PtH) 16. ⁿJ(PtH) 16. ^oSolvent, CD₂Cl₂. ^pTentative assignment due to complex aromatic patterns. ^qRest of aromatic region is very complex.

TABLE 7.14: $^{13}\text{C}\{^1\text{H}\}$ NMR of Complexes with ...

Complex	δ/ppm	Pt-Me $J(\text{PtC})/\text{Hz}$	δ/ppm	R	$J(\text{PtC})/\text{Hz}$	δ/ppm	$\text{C}_{\text{CH}_2\text{CH}_3}$ $J(\text{PtC})/\text{Hz}$	δ/ppm	X	$J(\text{PtC})/\text{Hz}$	δ/ppm	$^n\text{M}^d$ $J(\text{PtC})/\text{Hz}$	
[Pt(Me) ₂ {CH(CH ₃)CH ₂ Pr}(phen)]	-3.81	647.9	27.88 (CH)	66.6 (¹ J _{PtC})	43.94 (C _α)	553.6 (¹ J _{PtC})	202.32	50	(² J _{PtC})	131.58 (C _{1,2,3,4}) ^e	131.78	146.42 (C _{1,2,3,4}) ^e	
	-6.24	638.9	21.57 (CH ₂)		37.49 (C _β)	33.3 (² J _{PtC})				146.64 (C _{3,5,5'}) ^e	128.08 (C _{3,5,5'}) ^e	128.15	
			23.45 (CH ₃)								138.69 (C _{6,6,6'}) ^e	138.76	125.54 (C _{3,5,5'}) ^e
											125.93	148.05 (C _{2,2'}) ^e	148.36
[Pt(Me) ₂ {CH ₂ (CHO)CH ₂ ^t Bu}(phen)] ^e	-3.47	650.5	30.74 (C(CH ₂)) ₂ ^e		42.74 (C _α)	543	201.81	60.2	(² J _{PtC})	131.52 (C _{1,2,3,4}) ^e	131.68	147.95 (C _{1,2,3,4}) ^e	
	-5.44	652.0	29.64 (CH ₂)		42.17 (C _β)	34.8 (² J _{PtC})				147.99	128.11	128.06 (C _{3,5,5'}) ^e	
											138.66 (C _{6,6,6'}) ^e	138.79	125.45 (C _{3,5,5'}) ^e
											125.92 (C _{3,5,5'}) ^e	148.05 (C _{2,2'}) ^e	148.42

^tR = ^tPr or ^tBu; X = CH, CHO or C(-O)Me.^dn M = phen.^eSolvent, CCl₄.^eRemaining spectra were run in CD₂Cl₂.^e500pt satellites too weak to observe.

TABLE 7.15: Elemental Analysis for Complexes in Chapter 2

Complex	Percentage Composition ^a					
	C.	H.	N.	O.	F.	P.
[PtMe ₂ (OMe)(bipy)(OH ₂)] [OH]	35.1 (34.9)	4.3 (4.5)	5.7 (6.3)			
[PtMe ₂ (OEt)(bipy)(OH ₂)] [OH] · H ₂ O	34.7 (35.1)	4.6 (5.0)	5.9 (5.9)			
[PtMe ₂ (O ⁱ Pr)(bipy)(OH ₂)] [OH]	37.5 (37.9)	5.1 (5.1)	5.4 (5.9)			
[PtMe ₂ (OMe)(phen)(OH ₂)] [OH]	38.0 (38.2)	4.3 (4.2)	5.7 (5.9)			
[PtMe ₂ (OEt)(phen)(OH ₂)] [OH] · H ₂ O	38.0 (38.9)	4.2 (4.6)	5.4 (5.7)	11.3 (11.3)		
[PtMe ₂ (O ⁱ Pr)(phen)(OH ₂)] [OH] ^b	40.0 (39.9)	4.6 (4.6)	5.7 (5.8)			
[PtMe ₂ (OH)(phen)(OH ₂)] [OH]	37.8 (36.8)	3.7 (3.9)	5.6 (6.1)	10.8 (10.5)		
[PtMe ₂ (OH)(bipy)(OH ₂)] [OH]	32.9 (33.3)	4.3 (4.2)	6.2 (6.5)			
[PtMe ₂ (OMe)(bipy)(OH ₂)] [PF ₆]	26.5 (27.1)	3.4 (3.3)	4.7 (4.9)		18.5 (19.8)	
[PtMe ₂ (OMe)(bipy)(OH ₂)] [BPh ₄]	58.0 (59.6)	4.9 (5.2)	3.8 (3.8)			
[PtMe ₂ (OMe)(bipy)(OH ₂)] [ClO ₄] · 2H ₂ O	26.8 (27.7)	3.5 (3.55)	5.1 (5.0)			
[PtMe ₂ (OH)(bipy)(OH ₂)] [PF ₆]	26.4 (25.7)	3.3 (3.0)	5.0 (5.0)			5.35 (5.5)
[PtMe ₂ (OMe)Cl(phen)]	37.7 (38.2)	3.9 (3.6)	5.7 (5.9)			

^aCalculated percentages in parentheses.

TABLE 7.16: Elemental Analysis for Complexes in Chapter 3

Complex	Percentage Composition ^a				\bar{x}^b
	C	H	N		
[PtI Me ₃ (phen)]	32.9 (32.91)	3.2 (3.1)	5.0 (5.1)		21.8 (23.2)
[PtI Me ₂ (phen)Et]	33.8 (34.2)	3.1 (3.4)	4.94 (4.99)		22.9 (22.6)
[PtBr Me ₂ (phen)Et]	37.2 (37.4)	3.7 (3.69)	5.8 (5.5)		15.2 (15.6)
[PtBr Me ₂ (phen) ⁿ Pr]	38.5 (38.6)	4.1 (3.97)	5.35 (5.30)		
[PtI Me ₂ (phen){(CH ₂) ₃ Me}]	36.4 (36.7)	3.8 (3.9)	4.9 (4.8)		21.7 (21.6)

^aCalculated percentages in parentheses.

^b \bar{x} = Br or I.

TABLE 7.17: Elemental Analysis for Complexes in Chapter 4

Complex	Percentage Composition ^a			
	C.	H.	N.	X. ^b
[PtI ₂ Me ₂ (phen)]	25.44 (25.49)	2.1 (2.1)	3.95 (4.25)	
[PtBrMe ₂ (CH ₂ Br)(phen)]	34.1 (31.1)	2.72 (2.76)	3.83 (4.83)	27.41 (27.64)
[PtI ₂ Me ₂ (CH ₂ I)(phen)]	28.2 (26.8)	2.2 (2.4)	4.0 (4.16)	33.4 (37.8) ^c
[PtI ₂ Me ₂ {(CH ₂) ₃ I}(phen)]	29.1 (29.1)	2.80 (2.85)	4.24 (3.99)	36.1 (36.2)
[PtI ₂ Me ₂ {(CH ₂) ₄ I}(bipy)]	26.7 (26.6)	2.44 (2.95)	4.1 (4.1)	20.91 (37.51) [*]
[PtI ₂ Me ₂ {(CH ₂) ₄ I}(phen)]	28.4 (30.2)	3.16 (3.08)	3.3 (3.9)	35.8 (35.5)
[PtI ₂ Me ₂ {(CH ₂) ₅ I}(phen)]	31.3 (31.3)	3.3 (3.3)	3.8 (3.8)	26.6 (34.9) [*]
[Pt ₂ Br ₂ Me ₄ {(CH ₂) ₂ }(phen) ₂]	35.84 (36.07)	3.20 (3.21)	5.61 (5.61)	16.89 (16.03) [*]
[Pt ₂ I ₂ Me ₄ {(CH ₂) ₂ }(phen) ₂]	33.4 (32.8)	2.92 (2.97)	5.1 (5.1)	18.22 (23.5) [*]
[Pt ₂ I ₂ Me ₄ {(CH ₂) ₃ }(phen) ₂]	33.4 (33.6)	2.9 (3.1)	5.2 (5.1)	22.80 (22.97)
[Pt ₂ I ₂ Me ₄ {(CH ₂) ₃ }(bipy) ₂]	30.9 (30.6)	3.38 (3.21)	5.2 (5.3)	18.76 (23.99) [*]
[Pt ₂ I ₂ Me ₄ {(CH ₂) ₄ }(phen) ₂]	33.5 (34.3)	3.4 (3.2)	4.6 (5.0)	
[Pt ₂ I ₂ Me ₄ {(CH ₂) ₅ }(phen)]	34.9 (34.9)	3.5 (3.4)	4.8 (4.9)	22.8 (22.4)

^aCalculated percentages in parentheses.^bX = Br or I.^cInterference from Pt was encountered for the halogen analysis and particularly with those marked *.

TABLE 7.18: Elemental Analysis for Complexes in Chapters 5 and 6

Complex	Percentage Composition ^a		
	C	H	N
[PtIme ₂ (ⁱ Pr)(phen)]	35.3 (35.5)	3.5 (3.7)	5.9 (4.9)
[PtBrMe ₂ (ⁱ Pr)(phen)]	38.69 (38.64)	4.1 (3.98)	5.3 (5.2)
[PtIme ₂ (ⁱ PrOO)(phen)]	34.21 (33.61)	3.26 (3.46)	4.57 (4.61)
[PtIme ₂ (^t BuOO)(phen)]	34.7 (34.8)	3.6 (3.7)	4.4 (4.5)
[PtIme ₂ {CH(CH ₃)CH ₂ ⁱ Pr}(phen)]	38.0 (38.0)	3.88 (3.96)	4.58 (4.44)
[PtIme ₂ {CH(COMe)CH ₂ ⁱ Pr}(phen)]	39.0 (39.0)	4.13 (4.19)	4.34 (4.42)
[PtIme ₂ {CH(CN)CH ₂ ⁱ Pr}(phen)]	35.7 (38.2)	3.7 (3.8)	6.1 (6.7)
[PtIme ₂ {CH(CH ₃)CH ₂ ^t Bu}(phen)]	37.6 (38.5)	3.8 (4.2)	4.2 (4.3)
[PtIme ₂ {CH(CN)CH ₂ ^t Bu}(phen)]	37.0 (39.1)	3.6 (4.0)	6.0 (6.5)

^aCalculated percentages in parentheses

TABLE 7.19: Mass Spectral Data

Complex	M/e	Assignment ^a
[PtI Me ₂ {(CH ₂) ₄ I}(phen)]	685	{P-2Me}
	659	{P-(CH ₂) ₄ }
	588	{P-I}
	558	{P-2Me-I}
	532	{P-(CH ₂) ₄ -I}
	517	{P-(CH ₂) ₄ -I-Me}
[PtI Me ₂ {(CH ₂) ₂ CH ₃ }(phen)]	546	{P-(CH ₂) ₂ -Me}
	531	{P-(CH ₂) ₃ -Me}
	517	{P-(CH ₂) ₃ -2Me}
	461	{P-I}
[Pt ₂ I ₂ Me ₄ {(CH ₂) ₃ }(phen) ₂]	659	{PtI ₂ Me ₂ (phen)}
	629	{PtI ₂ (phen)}
	574	{PtI ₂ Me ₂ {(CH ₂) ₃ }(phen)}
[PtI Me ₂ {(CH ₂) ₅ I}(phen)]	517	{P-(CH ₂) ₅ -I-Me}
	502	{P-(CH ₂) ₅ -2Me-I}
	475	{P-2I}
	460	{P-2I-Me}
	445	{P-2I-2Me}
[PtMe ₂ (OMe)(phen)(OH ₂)] ⁺	454	{P}
[PtCl Me ₂ (OMe)(phen)]	471	{P}
	456	{P-Me}
	440	{P-MeO}
	425	{P-Me-MeO}
	420	{P-Me-Cl}
	410	{P-2Me-MeO}

^a

P = Molecular ion.

END

2	6	10	3	18	5
---	---	----	---	----	---

FIN